POLITECNICO DI MILANO
DEPARTMENT of ELECTRONICS, INFORMATION AND BIOENGINEERING
MASTER DEGREE IN BIOENGINEERING

Development and validation of a culture chamber for neurophysiological trials on iPS neuron-like cells

Supervisor

Prof. Alessandra Pedrocchi

Tutors:

Prof. Andrea Menegon,
Eng. Alice Geminiani

Master degree thesis of

Giovanni Palazzo

Matr. # 851229

Academic Year 2016-2017

Ringraziamenti

Questa tesi è la prosecuzione di un lavoro di sviluppo di una tecnologia che ha richiesto l'approfondimento di diversi campi dell'Ingegneria Biomedica e della neurobiologia.

Desidero ringraziare la professoressa Alessandra Pedrocchi che mi ha introdotto all'affascinante mondo del neuroimaging e mi ha dato l'opportunità di cimentarmi in questo progetto multidisciplinare.

Sul fronte della neurofisiologia, desidero ringraziare primo tra tutti il dottor Andrea Menegon, per la sua pazienza e disponibilità, nonché per aver messo a disposizione le numerose risorse del Centro di Imaging Sperimentale. Ad al dottor Menegon va anche il merito di avermi fornito tutti gli strumenti di interpretazione dei dati biologici.

Ringrazio inoltre la mia tutor, l'ing. Alice Geminiani, la quale mi ha seguito costantemente sotto tutti gli aspetti di questo lavoro: dal recupero della strumentazione necessaria, fino all'ultima fase di revisione dell'elaborato. Ad Alice va anche la mia riconoscenza per avermi aiutato nella cura di progetti scaturiti dal lavoro di tesi. Ringrazio l'ing. Giulia Regalia, per la sua disponibilità e tempestività nel fornirmi chiarimenti approfonditi, e l'ing. Giovanni Sala che mi ha affiancato nella prima parte del progetto.

Grazie a Silvia per il suo supporto tecnico nella fase di progettazione grafica.

Concludendo, tengo particolarmente a ringraziare l'intero team del CIS: Alessia, Amleto, Andrea, Cecilia, Davide, Dimitra, Eugenia, Ilaria, Marco, Matteo, Paola, Tiziana ed in particolare Nausicaa. Grazie per avermi assistito, per avermi trasmesso entusiasmo e per avermi fatto sentire parte integrante di un affiatato gruppo di ricerca.

Contents

ABSTRACT

Recording neural activity from *in-vitro* cultures is fundamental for investigating single neuron, network dynamics as well as effects of pharmacological treatments. The traditional intracellular electrophysiology measurement system, i.e. Patch Clamp, allows detailed studies of neuronal activities, but has some drawbacks: invasiveness, poor spatial resolution and the intrinsic biophysical and mechanical instability that does not allow experiments lasting more than few hours. On the other hand, when recording from a neuronal culture, Multi Electrode Array (MEA) systems represent a valid alternative for the study of network dynamics[1]. They are based on substrate-integrated matrices of electrodes for recording extracellular activity, as a voltage difference between the extracellular environment and a reference electrode.

Environmental conditions play a fundamental role in electrophysiology, and their effect is increased considering long-term studies. For this reason, if MEA technology is applied to the study of chronic events, it is mandatory an environment of culture which parameters are constantly monitored and controlled. Several studies have shown that temperature influences basic neuronal properties such as single ion channel conductance[2], [3]. Another crucial aspect is the condition of the medium where the cells are grown, specifically its pH[4]. One of the most effective methods to keep culture pH in optimal ranges is controlling CO_2 concentration inside the sample, as done by cell culture incubators[4], [5]. Finally, for culture survival and electrophysiological activity stationary, osmolarity is fundamental[6], [7]. Standard cell culture conditions result in an increase of extracellular salt concentration over time, and thus hyperosmolarity, due to medium evaporation[4], [6]. Evaporation can be avoided by the presence of an atmosphere saturated with water vapour (i.e. relative humidity equal to 100%), the absence of air ventilation in contact with the medium and of temperature gradient between the medium and the surrounding atmosphere[7].

All the perturbations described above represent the main reason why standard MEA acquisitions outside cell incubators are performed on a short time interval (e.g. 10-30 minutes), thus preserving data reliability, and reproducibility. Whereas this represents a powerful and effective method for temporally restricted studies (e.g. acute effect of a drug), it is a problem for acquisitions that require an extended period. Until now, few solutions have been proposed to tackle this issue. For example, studies of network development typically sample the state of a culture once every few days[8], [9]. Studies of chronic pharmacological treatments measure the network activity after some hours or days of incubation after the drug delivery[10]. However, unavoidably all those approaches bring with them serious risks, such as culture infection, lost in data continuity, missing information. Then, it seems that the most reliable way to preserve environmental conditions and simultaneously get continuous data for an extended period is to perform recordings directly inside an environment with controlled parameters[8], [10]. This eventually leads to the diffusion of commercial climate-controlled chambers for prolonged microscopy investigations outside a cell incubator (e.g. Ibidi GmbH, Okolab srl). Even this approach presents tricky aspects: in some studies, MEA signals must be acquired from the recording device partially put inside the incubator[7].

Based on the described issues, a proposed solution is to implement a bench-top system, which allows to perform acquisitions in an environmental controlled space, while integrating multiple MEA platforms. Many solutions are available on the market: most of MEA acquisition boards are equipped with a heated-plate below the MEA to avoid thermal shock to the cells, controlled via an electronic feedback loop. In order to compensate for medium evaporation and thus stabilize osmolarity, it is common to use custom-designed caps, including connection to tubes for medium perfusion[4], [7], [11]. However, closed caps/chambers over the MEA require moving the cap and directly pipetting in the medium, thus exposing culture medium to lab air. This is an issue especially for chronic pharmacological experiments, where a binding requirement is that the operation of drug stimulation does not expose cells to infection risk, which would induce artefactual activity throughout the chronic experiment. Alternatively to cap-shaped solutions fitted with the MEA housing of commercial pre-amplifiers, few custom-designed stand-alone chambers have been introduced[5]. Being independent on the MEA head-stage, the temperature in such chambers can be maintained with heaters integrated in the top or surrounding the chamber, allowing higher temperature spatial homogeneity. Finally, since most of the setups

are designed for single MEA experiments, they may not be practical and easy to handle if used to record simultaneously from more than one MEA chip, which is fundamental to shorten experimental time and improve comparability of data from different cultures[10]. For instance, small chambers/caps each confined around each MEA would require the reproduction of the desired gaseous atmosphere confined over each chip[12][13]. Alternatively, setups resorting to medium perfusion would require the constant connection of perfusion equipment to each MEA[5], [14]. These arrangements likely complicate the experimental operations and hinder accessibility and handiness of the setup especially in case of multiple MEAs.

Within this framework, in the present work we describe the assembly and validation of a bench-top multi-MEA recording and cell-culturing chamber developed to overcome the limits of previous solutions[13]. While a first prototype has provided an exemplary prolonged uninterrupted recording of one culture on MEA, its reproducibility and applicability in different scenarios (e.g., different cultures, experimenters, etc.) still need to be assessed[15]. Validation and testing in multiple conditions are mandatory to transform a research experimental prototype into a validated prototype applicable in a reproducible way to multiple setups, which can be used also by other laboratories. To this aim, here we describe: (1) the assembly and validation of the multi-MEA recording system coupled to the chamber, (2) the test of the control system that regulates environmental parameters through a set of sensors and feedback controllers, and (3) neurophysiological experiments conducted on multiple cell cultures (e.g. hippocampal neurons, iPS neuron-like cells), aimed at extrapolating meaningful features, describing the behaviour of cells inside the bench-top chamber[10], [14], [16].

II. MATERIALS AND METHODS

A. Setup Description

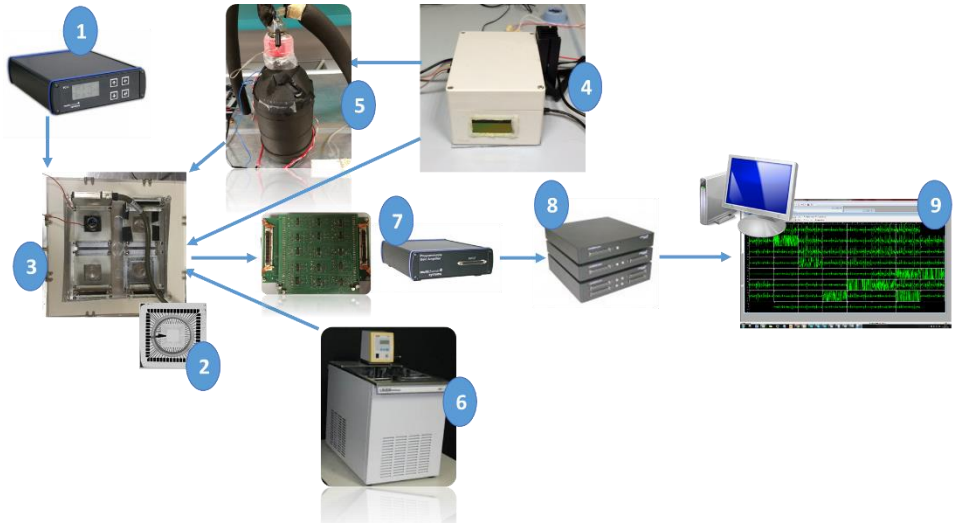

Figure 1 Custom setup:
(1) TC02 thermal controller;
(2) MEA chip;
(3) Culture chamber;
(4) Control Unit;
(5) Air perfusion system;
(6) Thermostat;
(7) Filter Amplifiers (FA);
(8) Data acquisition systems;
(9) MC_Rack platform.

The custom setup developed here includes: (1) TC02 thermal controller (from MCS, Multichannel Systems GmbH); (2) MEA chip; (3) Culture chamber & Pre-amplification boards; (4) Control Unit: environmental parameters controller; (5) Air perfusion system; (6) Thermostat: water-flow based temperature controller; (7) Filter Amplifiers (FA): FA64 (MCS), Custom and PGA: 64-channel filter amplifier (MCS), with programmable gain and filter settings; (8) Data acquisition systems (analog/digital board converting analog signals in digital data streams in real time: USB-ME128-System and USB-ME64-System (MCS); (9) MC_Rack software platform for data visualization and analysis. The chamber is composed of plates made of Poly-Methil-methacrylate (PMMA) and has been sized in order to house 4 MEAs simultaneously. The compartments on the top plate are designed for multiple tools insertion (injection inlets, sensors box, etc.). Fixed to the top of the chamber, there is a set of four acquisition boards[11]. Each of them is composed of an array of 60 golden pins, which transfer the signal to a pre-amplifier system. According to different needs, amplifiers with different gains have been developed[11].

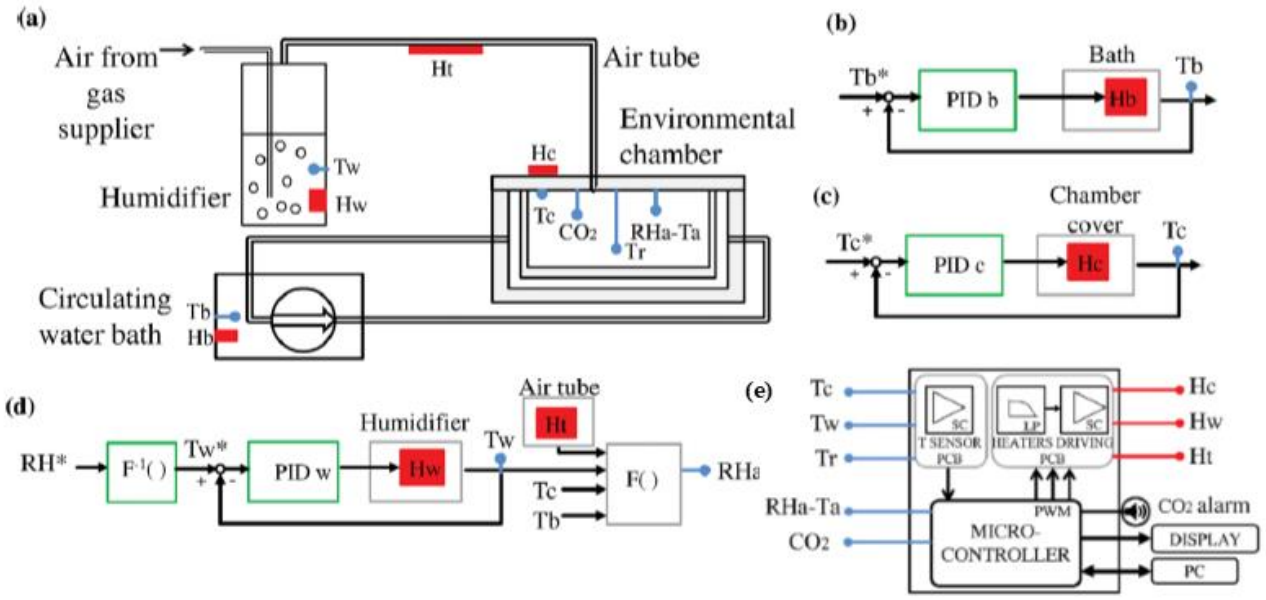

Figure 2 Environmental Control System Scheme:

a) Schematic representation of the enhanced environment control equipment coupled to the chamber. Blue points: sensors; red rectangles: heating elements.

b) Scheme of the control of the temperature in the bath, Tb, and the chamber cover, Tc. Tb*, Tr*=set points. The parameters tuned to obtain the desired temperature profile relate to the external controller (green block).

c) Scheme of the feedback control of the inner top plate temperature (Tc). Tc*=set point. This system prevents the formation of moisture on the top-plate through a heated wire (Hc).

d) Control scheme to obtain the desired RH level in the chamber (RHa). A heated wire (Hw) controlled by a PID sytem (in green) and a heated wire inside the air tube (Ht) bring the humidified aire to the desired temperature.

e) Scheme of the control unit coupled to the chamber, containing custom PCB for temperature signal processing, a microcontroller and a PCB that drives heating elements (Hc, Hw, Ht) through pulse-width modulated (PWM) signals.

Adapted from [11] (Regalia et al., 2016)

The environmental parameters controller must maintain specific values in temperature, relative humidity and CO_2 concentration inside the bioreactor, in order to assure cells survival. In case of hippocampal neurons, used during trials in this work, literature suggests optimal range of values: temperature: 36–38°C, Relative Humidity (RH) >90%, CO_2: 4.5–5% [9]. Fig.2 shows a scheme of the whole system, indicating the position of each sensor (in blue) and actuator (in red) integrated in the setup. To reproduce a high and stable RH in the chamber, a humidifying and heating module has been devised. A 10L/150bar cylinder flows a mixture of gas (11.99% O_2-5.04% CO_2) with a pressure equal to approximately 180mmHg inside a bottle filled with 450ml sterilized *Salf* water, by means of a rigid tube. This bottle contains a heater (Hb) regulated by a PID controller. This setup becomes a custom air humidifier, which delivers the air stream to the chamber through a thermally insulated silicone tube heated with a bounded Nickel–Chrome wire. The humidifier water temperature [Tw] is measured by an immersion Pt100 thermoresistance [Tw] and regulated by a Nickel-Chrome heater (Hw) according to a PID control loop.

Two other heat sources are exploited: heated water filling the cavity between the internal and external box, circulated and tempered by a commercial pump (E360, Lauda GmbH) equipped with a Pt100 probe [Tb], and a Nickel–Chrome wire (Hc) coupled to the chamber top plate. This wire is connected to MCS TC02 thermal controller, which allows to regulate the temperature of the top plate thanks to a miniaturized Pt100 probe below the top plate [Tc]. This helps also to avoid moisture deposition beneath the top plate, which would contaminate the cell cultures. A miniaturized digital RH and temperature sensor [RHa and Ta] is integrated in the chamber (SHT75, Sensirion Inc.). RHa depends on the value of Tb, Tc, Tw, and the power delivered to the air tube heater [Ht] [block F()]. A miniaturized digital infrared CO_2 sensor (COZIR Probe, Gas Sensing Solutions Ltd.), CO_2 in *Fig.2*, monitors the CO_2 level. The custom-built control unit (Fig.1) houses a microcontroller (Arduino Due board, Arduino) and a custom printed circuit. The microcontroller reads the inputs from the sensors, displays the environmental parameters, and provides control outputs that drive the heaters and a miniaturized

loud speaker for CO_2 level alarm. Through USB communication, environmental parameters are logged to a computer for real-time remote monitoring.

B. Validation of the environment control system

Once each sensor has been set, a long-time test (about 26h) on the three main environmental parameters has been carried out. For each one, minimum value, maximum value, mean and Standard Deviation (SD) of the full measurements are computed. Then, in these stabilized conditions, we tested the maintenance of the medium in which the cells studied have to be plunged in order to supply them nutrients.

C. Validation of the MEA recording system

To check the quality of the MEA signals through the entire acquisition pathway, a series of tests have been conducted on the chamber. The custom pre-amplification boards used are indicated with their gain (eg. 46, 92). A one or five-minute-long recording for all the four boards, once with a MEA-SG, signal generator (60MEA-Signal Generator, sold by Multi Channel System GmbH) and then with a chip filled with a physiological solution (PBS). Then, the same recordings have been repeated with a commercial pre-amplifier, in order to obtain a benchmark useful for a comparison (Fig. 3). After the acquisitions, the signal generated were analysed. In detail, for what concerns the tests performed with the signal generator, a quantitative signal analysis was performed in MATLAB R2016b through an ad-hoc feature extraction algorithm[14]. After digital signal filtering (300 Hz-3kHz, Butterworth 2nd order), the SNR of firing electrodes was computed as the ratio of the peak-to-peak amplitudes of spikes by the standard deviation of signal computed over the first 500ms. It is also useful to extract a truth table regarding fake spikes correctly detected, to do a comparison between the two setups in specificity and sensitivity. It is then possible to extrapolate statistical measures of the performance of a binary classification test (classification function).

Once all the necessary data were obtained, we compared the benchmark signal and those produced by the custom set-up. The qualitative part of the analysis was done directly thanks to MC_Rack replay mode. Specifically, qualitative analysis focused on comparison between benchmark and custom set-up in terms of noise band amplitude, spike amplitude and parameters extracted. The second testing part involved a MEA chip filled with Phosphate-buffered saline (PBS). The recordings were acquired in an incubator-like environment, in order to check how the humidity, temperature and CO_2 influence the electrodes' behaviour.

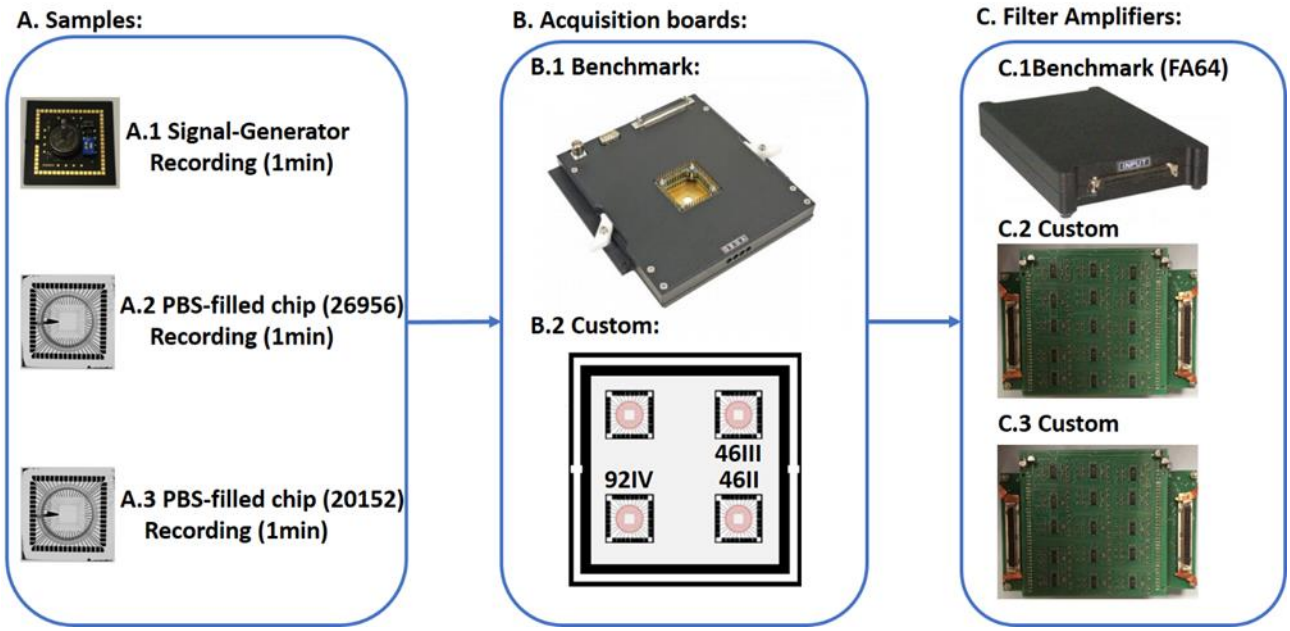

Figure 3 Scheme resuming acquisition protocol for the validation of parallel acquisition. In the first panel (A) is described the equipment used for validating the setup. The second panel (B) shows the commercial pre-amplification board (Benchmark) and the custom culture chamber with the three boards used, each one indicated with its gain (eg. 46, 92). The third panel (C) shows the Benchmark and the custom Filter Amplifiers (FA) used in this work.

D. Neurophysiological trials

The cells chosen for the neurophysiological trials are hippocampal neurons from mouse prenatal embryos (E18), widely used in MEA recordings[13], [17]. Animal handling have been performed in accordance with San Raffaele Scientific Institute guidelines and with an approved IACUC protocol number 694. The acquisitions have been repeated at 12 days *in-vitro* (DIV) and 18 DIV. In order to isolate and study how each one of the variability factors influences the analysis of neuronal activity, several acquisition protocols have been developed and applied during physiological trials. First, the benchmark acquisitions are performed. One of the main aims of benchmark recordings is monitoring cultures activity during different days *in-vitro* and setting a standard for the custom registrations in the same time window. In order to compare benchmark and custom setups, multiple acquisitions of chips have been performed in parallel. A pre-processing performed with MC_Rack is carried out. One of its tools consists in customizing the spike detection selecting the factor for which multiplying the standard deviation (SD) for thresholding, depending on the distribution of noise. This represents a useful tool in case of spurious spikes that are not biological. To isolate and study this computational variability factor we analysed the recordings on a single chip and in the same time interval with the benchmark system and a custom board. Then, using MC_Rack, we analysed the data using the same thresholds except the SD. The timestamps so obtained have been used in the MATLAB algorithm for features parameter extraction. Another test was performed to compare cells activity at different DIVs. For a better comprehension of the network activity, once spike detection is applied to the all MEA channels, a picture of the spatio-temporal distribution of spiking neuronal activity throughout the experiment can be observed in raster plots.

III. RESULTS

A. Setup validation

The environmental parameters measured during the long acquisition (about 26 hours) are reported in Table I. It is possible to appreciate a very low variance of all values throughout the acquisition, assuring a suitable environment for cells even in case of long-term experiments. We monitored an evaporation rate less than 15% per day. This quite high value is probably due to a non-optimal sealing of the inlets. Anyway, we have decided to overcome this issue with the adoption of improved PDMS caps, which have guaranteed an optimal sealing during biological trials.

Regarding the test conducted with the MEA-SG, it is possible to appreciate the similarities between the benchmark and the custom system, both in terms of spike detection parameters (Table II) and signal amplitude and shape (Fig.4-5). Compared to the benchmark system, all the three boards show a constant and predictable behaviour. In detail, board with higher amplification factor seems to exhibit a slightly higher number of artefacts that is possible to identify even on the signal averaged in the Power Spectral Density (PSD) analysis. Besides, it is possible to note same amount of background noise, and the same shape of spikes generated by the MEA-SG. However, there are some differences among the various couplings, like an interference on ground pin, which seems to record the signal coming from the other channels, albeit at reduced amplitudes. In general, a uniform presence of peaks in the PSD can be seen around the same frequencies (10^3Hz). The amplitude variability depends on the board-FA couplings and the scalability ratio performed by MC_Rack. There are not channels that are constantly unusable, in terms of large noise or no signal. The disturbances found during the test acquisitions on some channels are transitory.

Table I ENVIRONMENTAL PARAMETER ANALYSIS

	Min	***Max***	***Mean± SD***
T [°C]	36,65	36,98	36,81±0,08
CO_2 %	4,78	5,67	5,23 ± 0,23
Rh %	97,87	98,91	98,25 ± 0,25

Table II MEA-SG TEST: SPIKE DETECTION PARAMETERS

	TPR	***SPC***	***PPV***	***ACC***	***AR***	***AS***	***SW***	***NE***	***SNR***
Benchmark	0,9	1	1	0,97	0,001	8,3	0,001	1,3	4,2
Custom	0,9	0,97	0,96	0,94	0,3	9,5	0,001	1.1	6,3

Comparison in terms of classification functions and spike detection parameters between two explicative acquisitions of benchmark and custom setup, using signal generator. True Positive Rate(TPR): Sensitivity; SPC: Specificity; Positive Predictive Value (PPV): Precision; ACC: Accuracy; AR: Amplitude Rate; AS: Amplitude Ratio; SW: Spike Width; NE: Noise Esteem; SNR: Signal to Noise Ratio.

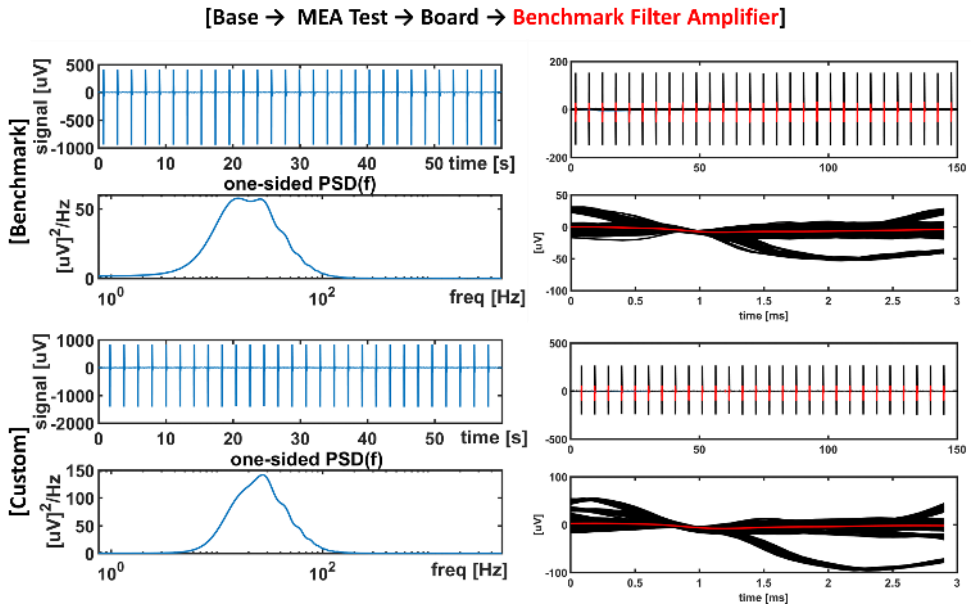

Figure 4 Comparison between PSD and spike waveforms of Benchmark (top panel) and Custom (bottom panel) system with a commercial FA, using signal generator. The first row shows averaged signal (left) and spikes detected in red (right). The second row shows PSD (left) and spike waveforms (right). Waveforms detected as spikes (EPSP) are highlighted in red over signal representations.

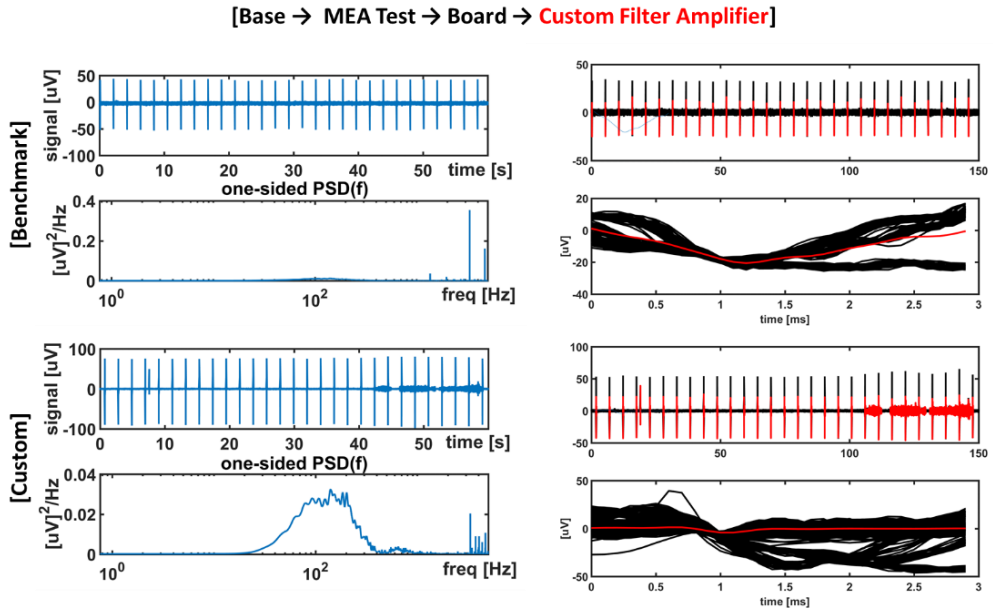

Figure 5 Comparison between PSD and spike waveforms of Benchmark (top panel) and Custom (bottom panel) system with a custom FA (right block), using signal generator. The first row shows averaged signal (left) and spikes detected in red (right). The second row shows PSD (left) and spike waveforms (right). Waveforms detected as spikes (EPSP) are highlighted in red over signal representations.

B. Neurophysiological trials

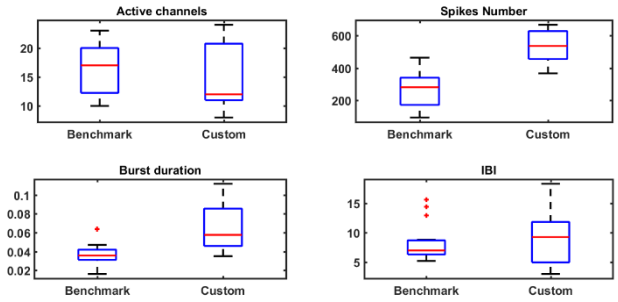

Figure 6 12 DIV. Box plots representing meaningful spiking and bursting features (IBI: Inter Burst Frequencies). Population of 15 samples corresponding to bins (1 bin = 1 minute).

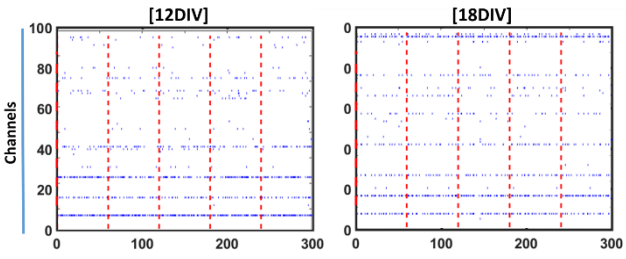

Figure 7 Raster plots representing spike events and thus mean firing rate at 12 and 18 DIV, in 5 minutes acquisition. Time expressend in seconds on x-axis, board channels on vertical axis.

We report some meaningful features extracted during neurophysiological trials on hippocampal neurons from mouse prenatal embryos (E18). During all the recordings, the benchtop setup used has proved capable of performing multiple acquisitions at the same time with good performances, and the boards did not present any form of interaction among them. This parallel approach has been made possible thanks to the use of three Filter Amplifiers simultaneously. Each of them has been proved couplable with any pre-amplification board. Environmental factors, such as humidity or temperature, does not influence drastically any component of the electronic acquisition chain put into the bioreactor.

For a comparison between custom and benchmark setup, we report some meaningful spiking and bursting features that preserve their statistical values in both systems. We report box plots, of the same culture, representing the feature values measured in each minute for an acquisition of 15 minutes (Fig.6). It is possible to appreciate few outliers, most of them in the representation of Inter Burst Frequencies. Regarding the median, shifting between benchmark and custom setups, it is reasonable to assert that there is an influent impact of the culture behaviour in the comparison. According to the literature, in fact, 12 DIV is a common time step for the onset of recordable spiking activity[17]. However, it is possible to note an oscillating electrophysiological behaviour of the firing cells, resulting in a higher variability of parameters measured with the custom setup. Anyway, the range in which most of the values lies is the same in both cases.

In Fig.7 it is possible to observe a picture of the spatio-temporal distribution of spiking neuronal activity throughout the experiment, referred to as raster plot. Each plot is 5-minute-long (time scale depicted on vertical axes), and the single 1-minute-long bins are indicated with red dashed vertical lines. On horizontal axes, the board channels are depicted. The acquisitions are performed after 12 and 18 DIV. It is possible to note a high activity in the first rows (corresponding to channles from 12 to 40), which is constant along all the acquisition. The activity is reduced at 18 DIV, alternating firing and silent periods.

To conclude, we report *p-values*, obtained with Wilcoxon non-parametric test, for a robust statistical analysis. The first regard two DIV acquisitions, the second Benchmark and Custom setup, with a comparison among four meaningful features. For the comparison between different DIVs, it is possible to note $p>0.05$ for all the features selected, except for the Burst Duration. This means a smaller variation in terms of medians for the features selected, except for burst duration, which results having a median value higher at 18 DIV. Regarding the comparisons among different custom boards, Wilcoxon test suggests different median values among different custom boards.

Variability in the spiking activity identified in two acquisitions performed in a restricted time window, even if considering one single chip with the same cell-culture, can be ascribed to four main classes of variability factors. Biological variability factors enclose all changings due to intrinsic electrophysiological activity of the neuron. Environmental factors influence neuron activity: as demonstrated in several studies, even small changes in CO_2 concentration, temperature, humidity, pH and so on alter the neuron's behaviour[1], [2].

Hardware-related factors include all the differences in terms of electronic devices that affect spiking and bursting activity. Computational variability factors take into account all the editable thresholds and settings chosen during analysis. All these elements can explain the observed network's behaviour. First, referring to biological variability factor, the neuronal network could have behaved differently during two recordings, even if the time interval is short. Regarding environmental variability, a controlled environment, with ideal parameters set, could allow the cells to increase their activity. About hardware-related variability factor, a higher gain of the first stage of pre-amplifier in the custom board could compromise its sensitivity to electrophysiological activity, which is a good point unless different hypersensitive electrodes record the same neuron spiking, altering and making an overestimation of the spiking activity.

We report a clear example of computational variability factor. As stated, it is possible to customize the spike detection selecting the factor for which multiplying the standard deviation (5*SD or 7*SD). However, studying spiking and bursting activity parameters extrapolated with these two different values has shown that adopting a higher factor compromises the sensitivity of the spike detection. It is clearly possible to appreciate an invariance in spike detection using the benchmark system in the two cases. This is because a thinner noise bandwidth is revealed, in particular during the first 500ms, when the algorithm computes the standard deviation for the detection. On the contrary, on the test conducted with a custom board there is a drastic reduction in terms of spike detection. Although the noise amplitude lies on an acceptable range (minus than ±20µV), it is higher than the benchmark one, so the spike amplitudes are not high enough to constitute a sufficient deviation from the white-noise bandwidth. This drawback is reflected also in the raster plots, where the mean firing rate gets a significant reduction.

Regarding the acquisitions on hiPS cells in their first stage of development, we first performed an acquisition with the MEA Benchmark setup. A detection of the poor and low-amplitude activity has been made possible only thanks to the reduced noise band of the MCS benchmark setup. With the adoption of the custom pre-amplification board, the slight neurophysiological activity was covered by the noise bandwidth, preventing the possibility of quantitative analysis. For what concerns the acquisitions performed in an advanced growth state, the benchtop system has proved to be capable of monitoring neurophysiological activity in iPS neuron-like cells. The difference showed in the results between spikes number detected by the benchmark board and the ones detected by the custom system are due to the deterioration state of the cell culture. This suggest an improvement required with the maintenance protocol, for instance regarding the medium change.

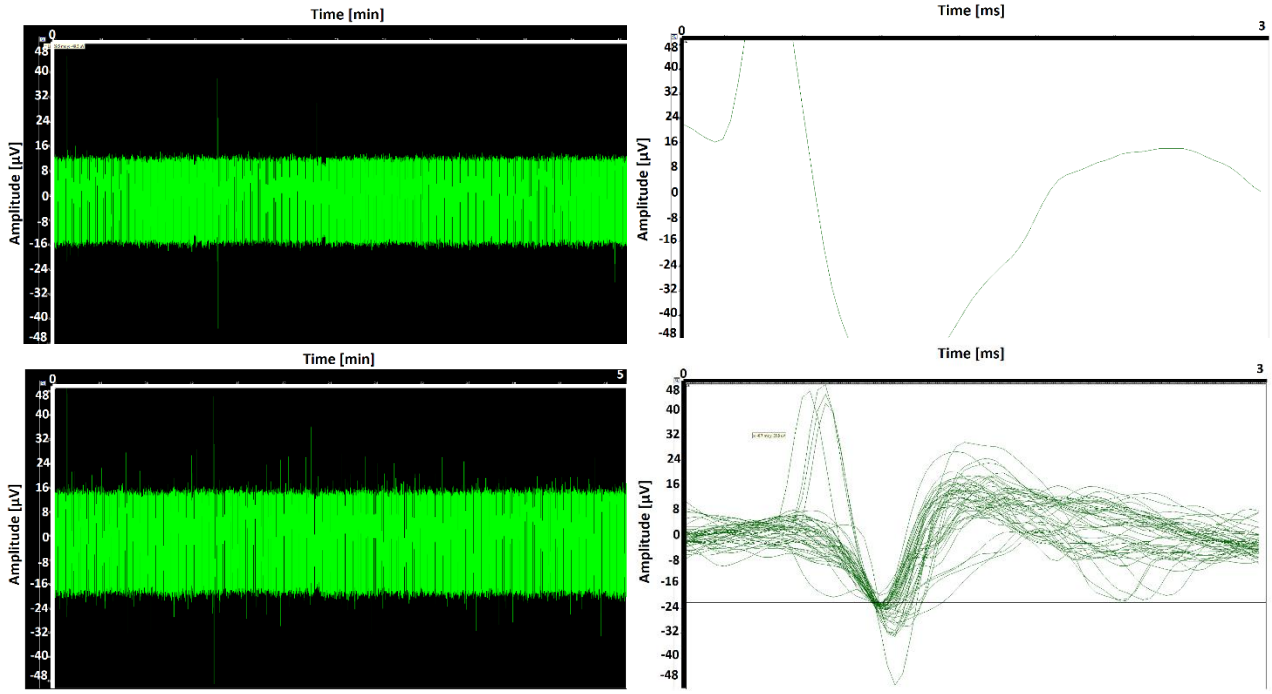

Figure 8 Sperimental (custom) setup. Upper panles: Channel 66 activity monitored during acquisition of hiPSc culture (14DIV). Lower panles: Channel 36 activity monitored during acquisition of hiPSc culture (25DIV). Longterm-signal window (left), Waveform detected window (right). From MC_Rack analysis.

IV. CONCLUSIONS

In this work, we have improved and validated a bench-top system, which integrates an environmental control monitoring system and a multi-MEA recording system, effectively enhancing its performance and improving its capability to perform multiple acquisitions in parallel (i.e. multi-MEA format). This kind of approach has been made possible thanks to the use of three Filter Amplifiers simultaneously. Each of them has been proved combinable with any pre-amplification board, even if some couplings have been proved to act better in acquiring signals.

After the validation of the acquisition system and the environmental control system, the trial conducted on the hippocampal cells has highlighted several advantages of the personalized bench-top system. The setup, preventing unnecessary movements from incubators to acquisition system, strongly reduces detrimental perturbations of neuronal activities. Besides, meaningful information about neuronal network activity has been extrapolated, turning to be helpful to define protocols for efficient biological and pharmacological studies. We also identified some interesting variability factors, that affects cellular activity analysis.

The approach with the MEA Benchmark setup proved the need of improvements for this kind of technology in monitoring hiPSc activity in their first stage of development. With the acquisitions performed in an advanced growth state, the benchtop system has proved to be capable of monitoring neurophysiological activity in iPS neuron-like cells. The difference shown in the results between spikes number detected by the benchmark board and the ones detected by the custom system are due to the deterioration state of the cell culture. This suggest an improvement required with the maintenance protocol, for instance regarding the medium change.

Regarding the first part of neuron-like cells differentiation, a detection of the poor and low-amplitude activity has been made possible only thanks to the reduced noise band of the MCS Benchmark setup. Moreover, the protocol adopted for the differentiation of hiPSc requires a different O_2 concentration respect to the one adopted during classical neurophysiological trials. For this reason, if the custom MEA bench-top system needs to be used in monitoring this first step in neurons development, it should be calibrated properly, both installing cylinders with a different O_2 concentration and setting the PID system in order to reach desired values. Then, this calibration needs to be changed when the neurons switch to the second stage of maturation.

We have also defined some critical points that could compromise the quality of recordings, as well as the stability of the internal environment of the bioreactor, identifying outlooks for better implementations.

One of these problems is represented by non-uniform heating of the culture chamber top-plate, leading to moisture making beneath the top-plate that could in turn contaminate the cultures. To partially overcome thisissue, on the top-plate of the second prototype chamber a wire made of the same material used in the first prototype has been installed. This configuration presents a more organized distribution respect to the previous one, as well as a better adherence to the top-plate thanks to a heat-resistance tape.

The question of multiple sources recorded at the same time has been dealt using different Filter Amplifiers and performing multiple registrations from a PC. This approach, although capable of performing simultaneous recordings without compromising PC performance in terms of speed, could generate some issues that compromise the signal quality. One of them is the use of multiple Filter Amplifiers, which represents unavoidably a hardware-related variability factor described in results. Working with parallel and long-time acquisitions, another critical aspect is the big amount of data produced, increasing the computational resources needed for acquisition and analysis.

In conclusion, MEAs are a widely used technology in several studies and constitute an establishment of experimental tools promoting a better understanding of the way the Nervous System processes information in physiological and pathological conditions. Through a series of validation tests and multiple biological trials, this work highlights some fundamental aspects that must be taken into account during both system development and data analysis, in order to get the most reliable representation of cellular electrophysiological features.

SOMMARIO

La registrazione dell'attività neurale da colture *in-vitro* è fondamentale per lo studio del singolo neurone, delle dinamiche di rete e degli effetti dei trattamenti farmacologici. Il tradizionale sistema di misurazione elettrofisiologico intracellulare, la tecnica Patch Clamp, consente studi dettagliati delle attività neuronali, ma presenta alcuni inconvenienti: invasività, scarsa risoluzione spaziale e intrinseca instabilità biofisica e meccanica che non consente esperimenti della durata di più di poche ore. D'altra parte, quando si registra da una coltura neuronale, i sistemi Multi Electrode Array (MEA) rappresentano un'alternativa valida per lo studio delle dinamiche di rete[1]. Si basano su matrici di elettrodi integrate per registrare l'attività extracellulare. La misura ottenuta è una differenza di tensione tra l'ambiente extracellulare ed un elettrodo di riferimento.

Le condizioni ambientali giocano un ruolo fondamentale nello studio dei meccanismi elettrofisiologici, ed il loro impatto si intensifica se si considerano studi di durata prolungata. Per questo motivo, se la tecnologia MEA viene applicata allo studio di eventi cronici, è obbligatorio che l'ambiente di cultura mantenga dei parametri ambientali costantemente monitorati e regolati. Diversi studi hanno dimostrato che la temperatura influenza le proprietà neuronali di base come la conduttanza del singolo canale ionico, la resistenza di membrana, l'ampiezza del potenziale d'azione, la durata e la velocità di propagazione del potenziale d'azione e la trasmissione sinaptica[2], [3]. Un altro aspetto cruciale è la condizione del terreno in cui vengono coltivate le cellule, in particolare il suo pH[3], [4]. Uno dei metodi più efficaci per mantenere il pH della coltura in intervalli ottimali è il controllo della concentrazione di CO_2 all'interno del campione, come nel caso degli incubatori di colture cellulari[4], [5]. Infine, per la sopravvivenza della coltura e l'attività elettrofisiologica stazionaria, l'osmolarità è fondamentale[6], [7]. Le condizioni standard di coltura cellulare determinano un aumento nel tempo della concentrazione extracellulare di sali, e quindi dell'iperosmolarità, a causa dell'evaporazione del terreno di coltura[4], [6]. Essa può essere evitata dalla presenza di un'atmosfera satura di vapore acqueo (cioè umidità relativa pari al 100%), dall'assenza di ventilazione dell'aria a contatto con il fluido e dal gradiente di temperatura tra il mezzo e l'atmosfera circostante[7].

Tutte le perturbazioni descritte sopra rappresentano il motivo principale per cui le acquisizioni MEA standard al di fuori degli incubatori cellulari vengono eseguite su un breve intervallo di tempo (ad esempio 10-30 minuti), preservando così l'affidabilità dei dati e la riproducibilità. Mentre questo rappresenta un metodo potente ed efficace per gli studi a tempo limitato (ad esempio l'effetto acuto di un farmaco), rappresenta un problema per le acquisizioni che richiedono un periodo prolungato[8]–[10]. Fino ad ora sono state proposte poche soluzioni per affrontare questo problema. Ad esempio, il campionamento dello stato di una cultura negli studi sullo sviluppo della rete tipicamente avviene una volta ogni pochi giorni. Studi di trattamenti farmacologici cronici misurano l'attività di rete dopo alcune ore o giorni di incubazione dopo il rilascio del farmaco[10]. Tuttavia, inevitabilmente, tutti questi approcci portano con sé rischi, come infezioni della cultura, perdita di continuità dei dati, informazioni mancanti e così via. Quindi, sembra che il modo più affidabile per preservare le condizioni ambientali e ottenere simultaneamente dati continui per un lungo periodo di tempo, sia eseguire registrazioni direttamente in un ambiente con parametri controllati[8], [10]. Questa considerazione ha portato alla diffusione di camere commerciali controllate per indagini di microscopia prolungate al di fuori di un incubatore cellulare (ad esempio Ibidi GmbH, Okolab srl). Anche questo approccio presenta aspetti delicati: in alcuni studi, i segnali MEA devono essere acquisiti dal dispositivo di registrazione parzialmente inserito nell'incubatore, condizione che impone ulteriori accorgimenti[7]. In base ai problemi descritti, una soluzione proposta consiste nell'implementare un sistema da banco che consenta di eseguire acquisizioni in uno spazio con parametri ambientali controllati, integrando al tempo stesso più piattaforme MEA. Molte soluzioni sono disponibili sul mercato: la maggior parte delle schede di acquisizione MEA sono dotate di una piastra riscaldata al di sotto del chip MEA per evitare shock termici alle cellule, controllati tramite un circuito di feedback. Al fine di compensare l'evaporazione media e quindi stabilizzare l'osmolarità, è comune utilizzare cappucci personalizzati, integranti un collegamento a tubi per la perfusione[5]. Tuttavia, le capsule/camere chiuse sopra il MEA richiedono lo spostamento del cappuccio e la somministrazione diretta nel terreno, esponendo così il mezzo di coltura all'aria ambientale. Questo è un problema specialmente per gli esperimenti farmacologici cronici, in cui un requisito vincolante è che l'operazione di stimolazione del farmaco non

esponga le cellule al rischio di infezione, il che indurrebbe attività artefatta durante l'esperimento[10]. In alternativa alle soluzioni sopra descritte, sono state introdotte alcune camere stand-alone personalizzate. La temperatura in tali camere può essere mantenuta con riscaldatori integrati nella parte superiore o circostante la camera, consentendo un'omogeneità spaziale della temperatura, consentendole inoltre di raggiungere valori più elevati. Infine, poiché la maggior parte delle configurazioni sono progettate per singoli esperimenti MEA, potrebbero non essere pratici e facili da gestire se usati per registrare simultaneamente da più di un chip MEA, che è fondamentale per abbreviare i tempi sperimentali e migliorare la comparabilità dei dati di diverse culture[10]. In alternativa, le configurazioni che ricorrono alla perfusione media richiederebbero la connessione costante di apparecchiature di perfusione a ciascun MEA[12]–[14]. Queste disposizioni complicano le operazioni sperimentali e ostacolano l'accessibilità e la maneggevolezza del setup, specialmente in caso di MEA multipli.

Per ovviare a tutte le problematiche descritte, in questo lavoro sono stati sviluppati l'assemblaggio e la validazione di una camera di coltura cellulare e di registrazione multi-MEA da banco precedentemente sviluppata[13]. Mentre il primo prototipo aveva fornito una registrazione ininterrotta prolungata esemplare di una coltura su MEA, la sua riproducibilità e applicabilità in diversi scenari (ad es. diversi tipi di colture, setup sperimentali, ecc.) deve ancora essere valutata[15]. Questo passaggio è obbligatorio per trasformare un prototipo sperimentale integrato in un dispositivo testato che possa essere adottato in diversi contesti. In particolare, qui presentiamo (1) la validazione del sistema di registrazione MEA accoppiato alla camera, (2) test del sistema di controllo che regola i parametri ambientali attraverso una serie di sensori e controllori di retroazione e (3) esperimenti neurofisiologici condotti su colture cellulari (es. neuroni ippocampali, cellule neuronali iPS), mirate ad estrapolare caratteristiche significative dell'attività neuronale, descrivendo il comportamento delle cellule all'interno della camera da banco[8], [10], [14].

II. MATERLIALI E METODI

A. Descrizione del Setup

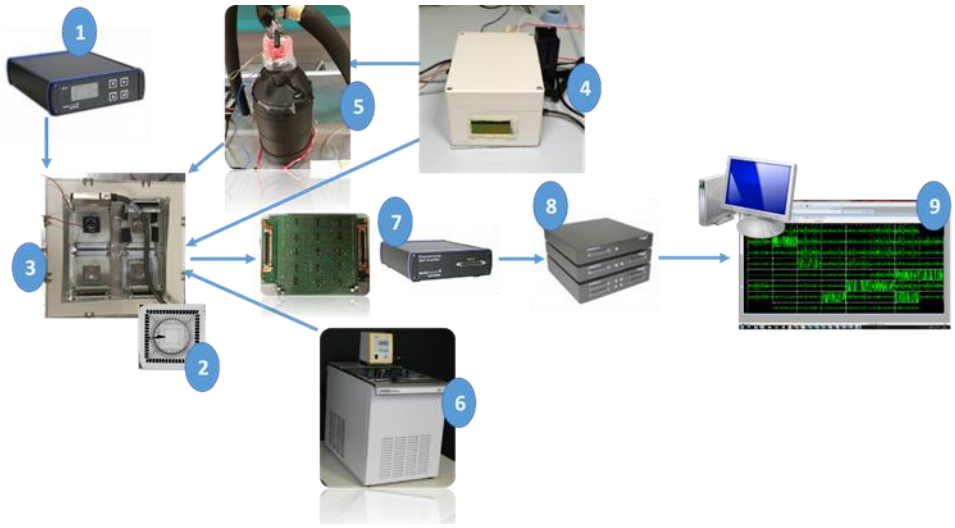

Figura 1 Setup sperimentale:
(1) Controller termico;
(2) chip MEA;
(3) Camera di coltura;
(4) Unità di controllo;
(5) Sistema di perfusione dell'aria;
(6) Termostato;
(7) Filter Amplifiers (FA);
(8) Sistemi di acquisizione dati;
(9) Piattaforma MC_Rack.

La configurazione sperimentale qui sviluppata include: (1) Controller termico MCS TC02 (MCS, Multichannel Systems GmbH); (2) chip MEA; (3) Camera di coltura e schede di pre-amplificazione; (4) Unità di controllo: regolatore dei parametri ambientali; (5) Sistema di perfusione dell'aria; (6) Termostato: regolatore di temperatura basato su flusso d'acqua; (7) Filter Amplifiers (FA): FA64 (MCS), Custom e PGA: 64-channel filter amplifier (MCS), con impostazioni di guadagno e filtro programmabili; (8) Sistemi di acquisizione dati: USB-ME128-System e USB-ME64-System (MCS); (9) piattaforma MC_Rack. La camera è composta da lastre in metacrilato di polietilene (PMMA) ed è stata dimensionata per ospitare 4 MEA contemporaneamente. Gli scomparti sulla piastra superiore sono progettati per scopi multipli (iniettori, alloggiamento dei sensori, ecc.). Fissato alla parte superiore della camera, c'è un set di quattro schede di acquisizione[11]. Ognuna di esse è composta da una serie di 60 pin d'oro, che trasferiscono il segnale a un sistema di pre-amplificazione. In base alle diverse esigenze, sono stati sviluppati amplificatori con guadagni diversi[11].

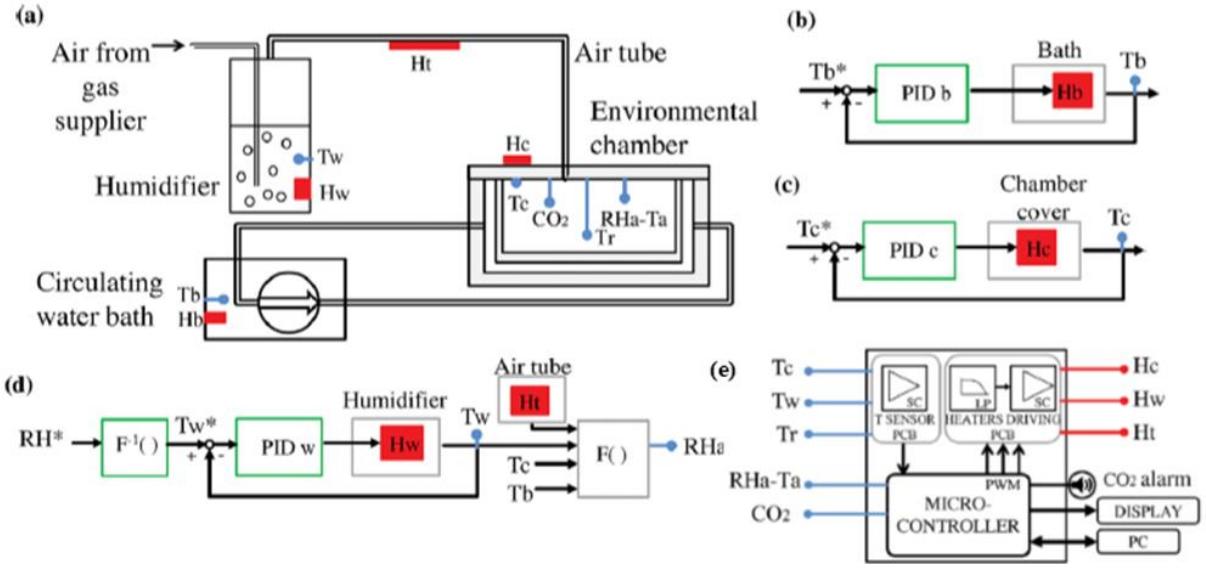

Figura 2 Sistema di controllo di parametri ambientali.
a) Rappresentazione schematica del sistema di controllo dell'ambiente accoppiato alla camera. Punti blu: sensori; rettangoli rossi: elementi riscaldanti.
b) Schema del controllo della temperatura. Tb *, Tr * = set point. I parametri sintonizzati per ottenere il profilo di temperatura desiderato si riferiscono al controller esterno (blocco verde).
c) Schema del controllo feedback della temperatura interna del pannello superiore (Tc). Tc * = set point. Questo sistema previene la formazione di umidità nella parte inferiore del coperchioo della camera attraverso un filo riscaldante posto su di essa (Hc).
d) Schema di controllo per ottenere il livello di UR desiderato nella camera (RHa). Un filo riscaldante (Hw) controllato tramite sistema PID (in verde) ed un filo riscaldante all'interno del tubo che immette l'aria (Ht) riscaldano l'aria umidificata alla temperatura desiderata.
e) Schema dell'unità di controllo accoppiata alla camera, contenente PCB personalizzata per l'elaborazione del segnale di temperatura, un microcontrollore e una PCB che pilota elementi riscaldanti attraverso segnali PWM (pulse-width modulated).
Adattato da [11] (Regalia et al. 2016)

Il controllore dei parametri ambientali deve mantenere valori specifici di temperatura, umidità relativa e concentrazione di CO_2 all'interno del bioreattore, al fine di assicurare la sopravvivenza cellulare. In particolare, nel caso di colture di neuroni ippocampali usate nei trial di questo lavoro, la letteratura suggerisce range di valori ottimali: temperatura: 36-38 ° C, UR> 90%, CO_2: 4,5-5% [9]. La *Fig.2* mostra uno schema dell'intero sistema, che indica la posizione di ciascun sensore (in blu) e dell'attuatore (in rosso) integrati nella configurazione. Per riprodurre un'umidità relativa elevata e stabile (RH) nella camera, è stato progettato un modulo di umidificazione e riscaldamento. Un cilindro da 10L/150bar fornisce una miscela di gas (11,99% O_2-5,04% CO_2) con una pressione pari a circa 180 mmHg all'interno di una bottiglia riempita con 450 ml di acqua Salf sterilizzata, mediante un tubo rigido. Questa bottiglia contiene un riscaldatore (Hb) regolato da un controller PID. Questa configurazione diventa un umidificatore d'aria personalizzato, che fornisce il flusso d'aria alla camera attraverso un tubo di silicone isolato termicamente riscaldato con un filo di Nickel-Cromo. La temperatura dell'acqua dell'umidificatore [Tw] viene misurata mediante una termoresistenza Pt100 ad immersione [Tw] e regolata da un riscaldatore Nickel-Chrome (Hw) in base ad un controllo PID. Vengono sfruttate altre due fonti di calore: acqua riscaldata che riempie la cavità tra la scatola interna e quella esterna, fatta circolare e temperata da una pompa commerciale (E360, Lauda GmbH) dotata di una sonda Pt100 [Tb] e di un filo nichel-cromo (Hc) accoppiato alla piastra superiore della camera. Questo cavo è collegato al controller termico MCS TC02 che consente di regolare la temperatura della piastra superiore grazie a una sonda Pt100 posta sotto la piastra superiore [Tc]. Questo aiuta anche ad evitare la formazione di umidità sotto la piastra superiore, che potrebbe contaminare le colture cellulari. Nella camera è integrato un sensore digitale di temperatura e umidità [RHa e Ta] (SHT75, Sensirion Inc.). RHa dipende dal valore di Tb, Tc, Tw e dalla potenza erogata al riscaldatore del tubo dell'aria [Ht] [blocco F ()]. Un sensore di CO_2 digitale a infrarossi miniaturizzato [COZIR Probe, Gas Sensing Solutions Ltd., CO_2 *in Fig.2* monitora il livello di CO_2. L'unità di controllo (*Fig.1*) ospita un microcontrollore (scheda Arduino Due, Arduino) e un circuito stampato personalizzato. Il microcontrollore legge gli input dai sensori, visualizza i parametri ambientali e fornisce uscite di controllo che pilotano i riscaldatori e un altoparlante per l'allarme del livello di CO_2. Attraverso la comunicazione USB, i parametri ambientali vengono registrati su un computer per il monitoraggio remoto in tempo reale.

B. Validazione del Sistema di controllo ambientale

Una volta configurato ogni sensore, è stato eseguito un test a lungo termine (circa 26 ore) sui tre parametri principali. Per ogni parametro ambientale, vengono calcolati il valore minimo, il massimo, la media e la deviazione standard (SD) delle misurazioni complete. Quindi, in queste condizioni stabilizzate, abbiamo testato il mantenimento del terreno nel quale le cellule studiate devono essere immerse per fornire loro nutrienti.

C. Validazione del sistema di registrazione MEA

Per verificare la qualità dei segnali MEA attraverso l'intero percorso di acquisizione, sono stati condotti una serie di test. Questi consistevano in una registrazione di uno o cinque minuti per tutte e tre le schede (indicate in figura con il loro rispettivo guadagno), con un generatore di segnale MEA (MEA-SG) e successivamente con un chip riempito con soluzione fisiologica (PBS). Quindi, le stesse registrazioni sono state ripetute con un setup commerciale (Benchmark), al fine di ottenere un dataset utile per un confronto (Fig.3).
Dopo le acquisizioni, il segnale è stato analizzato. Per l'acquisizione e la registrazione è stato utilizzato il software MC_Rack. Per quanto riguarda i test condotti utilizzando il Signal generator, l'analisi quantitativa del segnale è calcolata in MATLAB R2016b attraverso un algoritmo ad hoc di estrazione delle caratteristiche si spiking e bursting[14]. Dopo il filtraggio del segnale digitale (300 Hz-3kHz, filtro Butterworth del secondo ordine), il rapporto segnale-rumore (SNR) degli elettrodi di accensione viene calcolato come il rapporto tra le ampiezze picco-picco dei picchi mediante la deviazione standard del segnale calcolato nei primi 500 ms[14]. È quindi possibile, per ottenere un confronto in termini di specificità e sensibilità, estrapolare misure statistiche delle prestazioni di un test di classificazione binaria (funzione di classificazione). Una volta ottenuti tutti i dati necessari, abbiamo confrontato il segnale di riferimento e quelli prodotti dal setup sperimentale.
La parte qualitativa dell'analisi è stata effettuata direttamente grazie alla modalità replay MC_Rack. Nello specifico, l'analisi qualitativa si è focalizzata sul confronto tra benchmark e set-up sperimentale in termini di ampiezza della banda di rumore, ampiezza del picco e parametri estratti. La seconda parte di test ha coinvolto un chip MEA riempito con soluzione salina (PBS). Le registrazioni sono state acquisite in un ambiente simile a quelle di un incubatore, al fine di verificare come l'umidità, la temperatura e la CO_2 influenzano il comportamento degli elettrodi. Come dimostrato in questo lavoro, anche durante esperimenti biologici, tali fattori non influenzano in modo significativo alcun componente della catena di acquisizione elettronica.

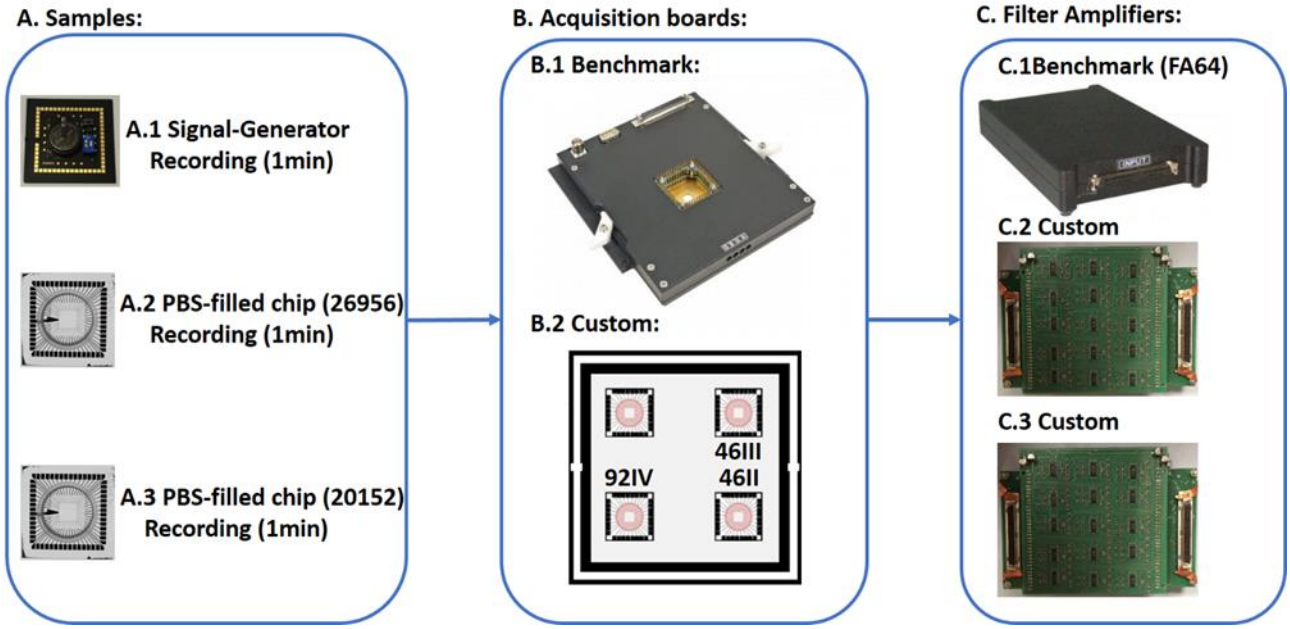

Figura 3 Schema riassuntivo del protocollo per la validazione di acquisizioni eseguite in parallelo. Nel primo pannello (A) è descritta l'attrezzatura utilizzata per convalidare il sistema. Il secondo pannello (B) mostra la scheda di pre-amplificazione commerciale (Benchmark) e la camera di coltura personalizzata con le tre schede utilizzate, ciascuna indicata con il suo guadagno (ad esempio 46, 92). Il terzo pannello (C) mostra il Benchmark ed i Filter Amplifier personalizzati (FA) utilizzati in questo lavoro.

D. Prove neurofisiologiche

Le cellule scelte per gli studi neurofisiologici sono neuroni ippocampali da embrioni prenatali di topo (E18), ampiamente utilizzati nelle registrazioni MEA[13], [17]. La manipolazione degli animali è stata eseguita in conformità con le linee guida del San Raffaele Scientific Institute e con un protocollo IACUC numero 694 approvato. Le acquisizioni sono state ripetute a 12 giorni *in-vitro* (DIV) e 18 DIV. Al fine di isolare e studiare come ciascuno dei fattori di variabilità influenzi l'analisi dell'attività neuronale, sono stati sviluppati e applicati diversi protocolli di acquisizione durante gli studi fisiologici. Innanzitutto sono state eseguite le acquisizioni benchmark. Uno degli scopi principali delle registrazioni di riferimento è il monitoraggio dell'attività delle colture durante diversi giorni *in-vitro* e l'impostazione di uno standard per le registrazioni personalizzate nella stessa finestra temporale. Al fine di confrontare benchmark e custom setup, sono state eseguite più acquisizioni di chip in parallelo. Viene eseguita una pre-elaborazione eseguita con MC_Rack. Uno dei suoi strumenti consiste nel personalizzare il rilevamento spike selezionando il fattore per il quale moltiplicare la deviazione standard (SD), a seconda della distribuzione del rumore. Questo rappresenta uno strumento utile in caso di picchi spuri che non siano biologici. Per isolare e studiare questo fattore di variabilità computazionale abbiamo analizzato le registrazioni su un singolo chip e nello stesso intervallo di tempo con il sistema di riferimento ed una scheda sperimentale. Quindi, utilizzando MC_Rack, abbiamo analizzato i dati utilizzando le stesse soglie eccetto la SD. I timestamp così ottenuti sono stati utilizzati nell'algoritmo di MATLAB per l'estrazione di parametri. Un altro test è stato eseguito per confrontare l'attività delle cellule con diversi DIV. Per una migliore comprensione dell'attività di rete, una volta applicato il rilevamento degli spike a tutti i canali MEA, è possibile osservare su grafici di tipo raster, un'immagine della distribuzione spazio-temporale dell'attività neuronale durante l'esperimento.

III. RISULTATI

A. Convalida del setup sperimentale

Nella *Tabella I* è possibile apprezzare una varianza molto bassa di tutti i valori durante l'acquisizione, garantendo un ambiente adatto alle cellule anche in caso di esperimenti a lungo termine. Abbiamo monitorato un tasso di evaporazione del terreno di coltura inferiore al 15% al giorno.

Per quanto riguarda il test condotto con il MEA-SG, è possibile apprezzare le somiglianze tra il benchmark e il sistema sperimentale, sia in termini di parametri di rilevamento degli spike (*Tabella II*) che di ampiezza e forma del segnale *(Fig.5-6)*. Rispetto al sistema di riferimento, tutte e tre le schede mostrano un comportamento costante e prevedibile. In dettaglio, la scheda con un fattore di amplificazione più elevato sembra presentare un numero leggermente superiore di artefatti che è possibile identificare anche sul segnale mediato nell'analisi della Power Spectral Density (PSD). Inoltre, è possibile notare la stessa quantità di rumore di fondo e la stessa forma dei picchi generati dal MEA-SG. In generale, una presenza uniforme di picchi nella PSD può essere vista intorno alle stesse frequenze (10^3 Hz). La variabilità dell'ampiezza dipende dagli accoppiamenti della scheda-FA e dal rapporto di scalabilità eseguito da MC_Rack. Non ci sono canali che sono costantemente inutilizzabili, in termini di grande rumore o nessun segnale.

Tabella I ANALISI DEI PARAMETRI AMBIENTALI

	Min	***Max***	***Media± SD***
T [°C]	36,65	36,98	36,81±0,08
CO_2 %	4,78	5,67	5,23 ± 0,23
Rh %	97,87	98,91	98,25 ± 0,25

Tabella II TEST MEA-SG: PARAMETRI SPIKE DETECTION

	TPR	***SPC***	***PPV***	***ACC***	***AR***	***AS***	***SW***	***NE***	***SNR***
Benchmark	0,9	1	1	0,97	0,001	8,3	0,001	1,3	4,2
Custom	0,9	0,97	0,96	0,94	0,3	9,5	0,001	1.1	6,3

Confronto in termini di funzioni di classificazione e parametri per la spike detection tra due esempi esplicativi di benchmark setup e custom setup con signal generator. TPR: Sensitività; SPC: Specificità; PPV: Precisione; ACC: Accuratezza; AR: Amplitude Rate; AS: Amplitude Ratio; SW: Spike Width; NE: Noise Esteem.

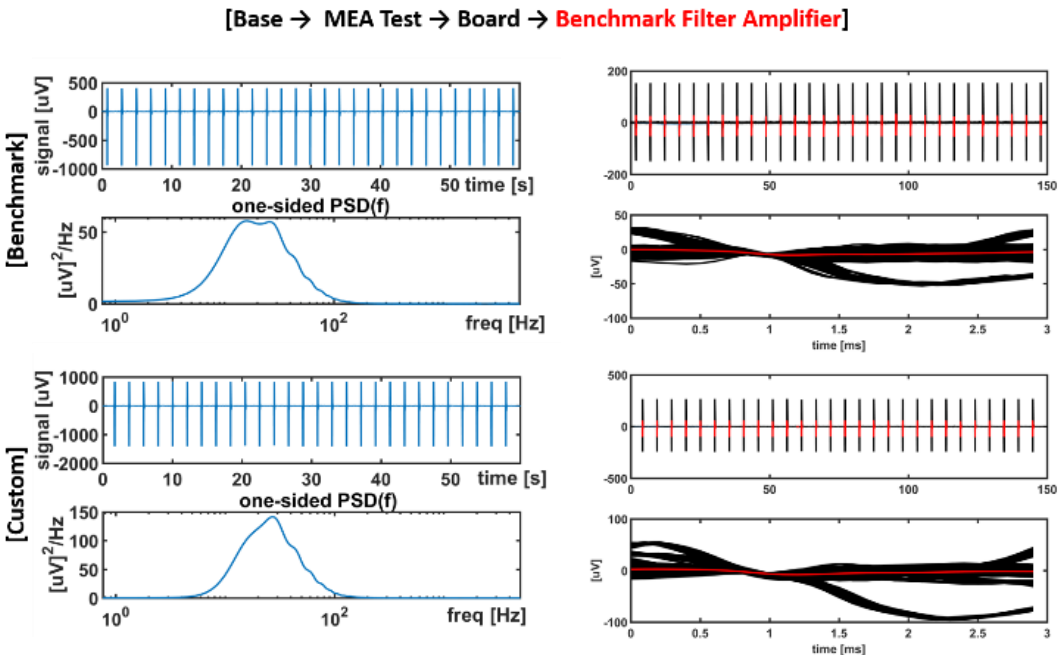

Figura 4 Confronto tra PSD e forme d'onda degli spike tra Benchmark e sistema Custom con un FA commerciale (Benchmark), con signal generator. La prima riga mostra il segnale medio (a sinistra) e il picco rilevato (a destra). La seconda riga mostra le forme d'onda PSD (a sinistra) e spike (a destra). Le forme d'onda rilevate come picchi (EPSP) sono evidenziate in rosso.

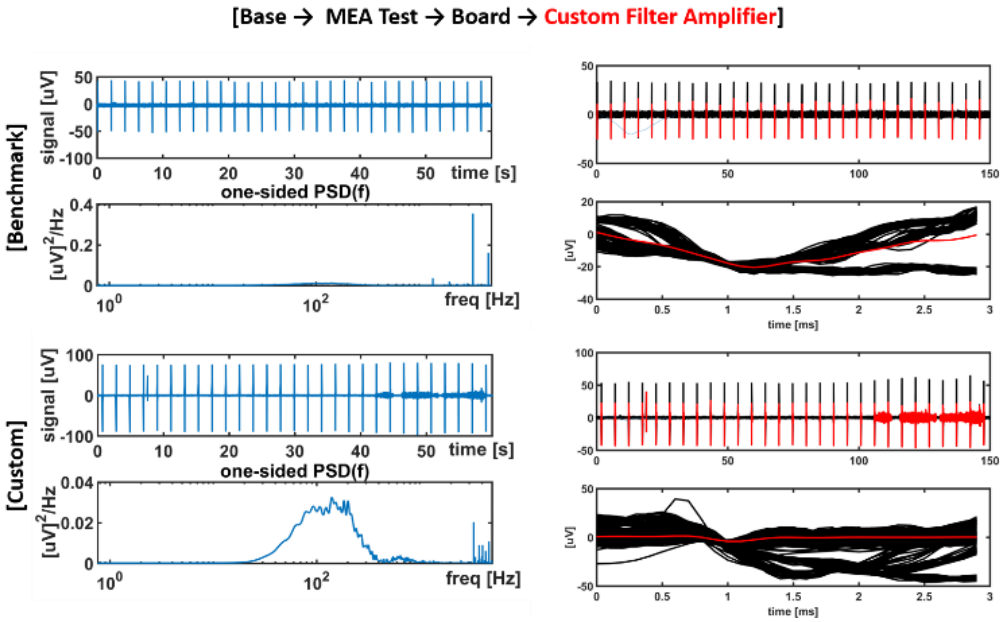

Figura 5 Confronto tra PSD e forme d'onda degli spike. Trad Benchmark e sistema Custom con una FA custom. La prima riga mostra il segnale medio (a sinistra) e il picco rilevato (a destra), con signal generator. La seconda riga mostra le forme d'onda PSD (a sinistra) e spike (a destra). Le forme d'onda rilevate come picchi (EPSP) sono evidenziate in rosso.

B. Prove neurofisiologiche

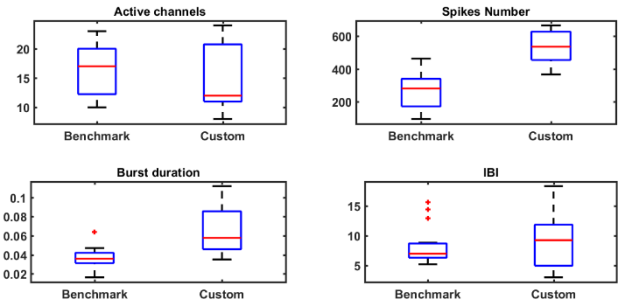

Figura 6 12DIV. Box plots rappresentanti parametri significativi di spiking and bursting. Popolazione di 15 campioni corrisponenti a 15 bins (1 bin = 1 minute). (IBI: Inter Burst Frequencies)

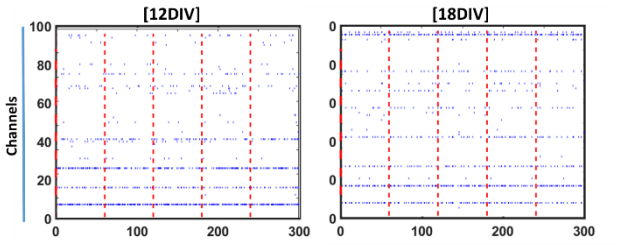

Figura 7 Raster plots rappresentanti tasso di firing medio a 12 e 18 DIV, in acquisizioni di 5 minuti. Tempo espresso in secondi sull'asse orizzontale; canali della scheda sull'asse verticale.

Riportiamo alcune caratteristiche significative estratte durante i trial neurofisiologici condotti su colture di neuroni ippocampali (E18). Durante tutte le registrazioni, il pc e la piattaforma utilizzati si sono dimostrati in grado di eseguire più acquisizioni in parallelo con ottime prestazioni. Questo tipo di approccio è stato reso possibile grazie all'utilizzo simultaneo di tre Filter Amplifiers. Le schede di pre-amplificazione non hanno riscontrato alcuna forma di interazione tra di loro, né hanno risentito delle particolari condizioni di umidità e temperatura.

Per un confronto tra la configurazione personalizzata e quella di riferimento, riportiamo alcune caratteristiche significative di spiking e bursting che mantengono i loro valori statistici di entrambi i sistemi. Riportiamo i boxplot, che rappresentano i valori delle caratteristiche misurate in ciascun minuto per un'acquisizione di 15 minuti della stessa coltura (Fig.6). È possibile notare alcuni valori anomali, molti dei quali nella rappresentazione di Inter Burst Frequencies. Per quanto riguarda le differenze del secondo quartile, tra benchmark e setup personalizzati, è ragionevole affermare che vi è un impatto influente del fattore di variabilità biologico nel confronto. Secondo la letteratura, infatti, a 12 DIV è comune registrare attività di spike[17]. Tuttavia, è possibile notare un comportamento elettrofisiologico oscillante delle reti neuronali. In ogni caso, l'intervallo in cui si trovano la maggior parte dei valori è lo stesso in entrambi i casi.

In Fig.7 è possibile osservare una rappresentazione tramite Rasterplot della distribuzione spazio-temporale dell'attività neuronale durante l'esperimento. Ogni grafico rappresenta 5 minuti (scala temporale rappresentata su assi verticali) e intervalli da un minuto sono indicati con linee verticali tratteggiate rosse. Sugli assi orizzontali sono rappresentati i canali della scheda. Le acquisizioni vengono eseguite a 12 e 18 DIV. È possibile notare un'attività elevata nelle prime righe (corrispondenti ai canali da 12 a 40), costante durante tutta l'acquisizione. L'attività è ridotta a 18 DIV, alternando periodi di spiking a silenzio.

Concludendo, riportiamo *i p-values*, ottenuti con test non parametrico di Wilcoxon, per una robusta analisi statistica. Il test viene eseguito sia per un confronto tra benchmark e setup personalizzato, sia per acquisizioni eseguite a diversi DIV, con un confronto tra quattro caratteristiche significative. Per il confronto tra diversi DIV, è possibile notare un valore di $p > 0,05$ per tutte le caratteristiche, ad eccezione della Durata dei Burst. Per quanto riguarda i confronti tra le diverse schede personalizzate, la maggior parte dei test restituisce $p < 0,05$, suggerendo valori di mediana diversi tra le diverse schede. Nei confronti tra sistema di riferimento e schede personalizzate, il test di Wilcoxon conferma differenze nei parametri analizzati estratti con diverse schede custom.

Per spiegare il diverso comportamento di un singolo chip, con all'interno la medesima coltura cellulare, tra due acquisizioni eseguite in una ristretta finestra temporale, quattro classi principali di fattori di variabilità sono state identificate durante gli studi. Fattori di variabilità biologica racchiudono tutti i cambiamenti dovuti all'attività elettrofisiologica intrinseca del neurone. I fattori ambientali influenzano l'attività dei neuroni: come dimostrato in diversi studi, i cambiamenti di concentrazione di CO_2, temperatura, umidità, pH e così via alterano il comportamento cellulare[1], [2]. I fattori legati all'hardware includono tutte le differenze in termini

di dispositivi elettronici che influiscono sull'attività di spiking e bursting. I fattori di variabilità computazionale tengono conto di tutte le soglie modificabili e delle impostazioni scelte durante l'analisi.

Per riportare un esempio di quest'ultimo fattore, come già esposto è possibile personalizzare il rilevamento degli spike selezionando il fattore per il quale moltiplicare la deviazione standard (5 * SD o 7 * SD). Tuttavia, lo studio dei parametri di attività spiking e bursting estrapolati con questi due diversi valori ha dimostrato che l'adozione di un fattore più alto compromette la sensibilità del rilevamento degli spike. È chiaramente possibile apprezzare un'invarianza nel rilevamento degli spike utilizzando il sistema benchmark nei due casi. Ciò è dovuto al fatto che viene rivelata un'ampiezza di banda del rumore più sottile, in particolare durante i primi 500ms, quando l'algoritmo calcola la deviazione standard per il rilevamento. Al contrario, nel test condotto con una scheda sperimentale, vi è una drastica riduzione in termini di rilevamento degli spike. Sebbene l'ampiezza del rumore si trovi su un intervallo accettabile (meno di ± 20µV), è superiore a quella del benchmark, quindi le ampiezze del picco non sono abbastanza elevate da costituire una deviazione sufficiente dalla larghezza di banda del rumore bianco. Questo inconveniente si riflette anche nei grafici raster, in cui il tasso medio di attività ottiene una significativa riduzione.

Per quanto riguarda le prove condotte su cellule di tipo iPS nella loro prima fase di sviluppo, abbiamo eseguito inizialmente delle acquisizioni con il setup benchmark. Innanzitutto, è stato possibile rilevare attività elettrofisiologica solo grazie alla piccola banda di rumore del setup di riferimento MCS. Tale scarsa attività si è manifestata con ampiezza ridotta rispetto alle registrazioni eseguite su neuroni. Con l'adozione della scheda pre-amplificazione personalizzata, la leggera attività neurofisiologica è stata coperta dalla banda di rumore, annullando ogni possibilità di analisi quantitativa. Per quanto riguarda le acquisizioni eseguite ad uno stato di maturazione avanzata (25DIV), il sistema sperimentale si è dimostrato in grado di monitorare l'attività neurofisiologica nelle cellule di tipo iPS neuron-like (Fig.8). La differenza mostrata nei risultati tra il numero di spike rilevato dal modello commerciale di riferimento e quelli rilevati dal sistema personalizzato sono dovuti allo stato di deterioramento della coltura cellulare. Ciò suggerisce una revisione ed un miglioramento del protocollo di manutenzione delle colture, ad esempio per quanto riguarda i parametri dell'incubatore o il ciclo di cambio del terreno di coltura.

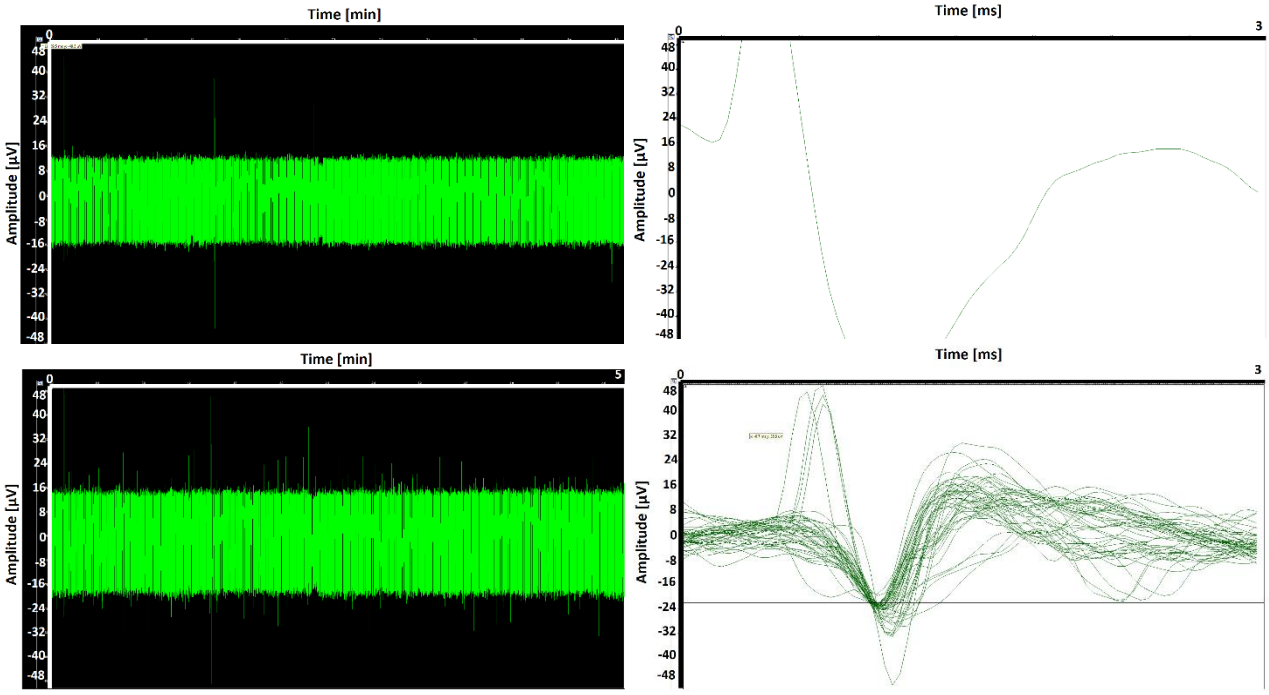

Figura 8 Setup sperimentale (custom). Pannelli superiori: attività sul canale 66 monitorata durante acquisizione di colture cellulari di cellule di tipo iPS (14DIV). Pannelli inferiori: attività sul canale 36 monitorata durante acquisizione di colture cellulari di cellule di tipo iPS (25DIV). Finestra del segnale Longterm (sinistra), finestra Waveform (destra). Da analisi MC_Rack.

IV. CONCLUSIONI

In questo lavoro, abbiamo migliorato e validato un sistema da banco, che integra un sistema di monitoraggio del controllo ambientale ed un sistema di registrazione multi-MEA, migliorando efficacemente le sue prestazioni e perfezionando la sua capacità di eseguire più registrazioni in parallelo (formato multi-MEA). Questo tipo di approccio è stato reso possibile grazie all'utilizzo simultaneo di tre amplificatori di filtro. Ciascuno di essi ha dimostrato di essere associabile a qualsiasi scheda di pre-amplificazione, anche se alcuni accoppiamenti hanno dimostrato di agire meglio nell'acquisire segnali.

Dopo la validazione del sistema di acquisizione e del sistema di controllo dei parametri ambientali, la sperimentazione condotta su neuroni ippocampali ha evidenziato numerosi vantaggi del sistema sperimentale. Tale setup, evitando movimenti non necessari dagli incubatori al sistema di acquisizione, riduce fortemente le perturbazioni dannose per le colture neuronali. Inoltre, sono state estrapolate informazioni significative sull'attività della rete neuronale, che si sono rivelate utili per definire protocolli per efficienti studi biologici e farmacologici.

L'approccio con il modello commerciale MEA (Benchmark) ha dimostrato la necessità di miglioramenti per questo tipo di tecnologia nel monitoraggio dell'attività di cellule iPS di tipo neuron-like nella loro prima fase di sviluppo. Con le acquisizioni eseguite in uno stato di crescita avanzata, il sistema da banco si è dimostrato in grado di monitorare l'attività neurofisiologica delle cellule. La differenza mostrata nei risultati tra il numero di spike rilevato dal modello di riferimento e quelli rilevati dal sistema personalizzato sono dovuti allo stato di deterioramento della coltura. Questo suggerisce un necessario miglioramento del protocollo di manutenzione, ad esempio per quanto riguarda il cambiamento del terreno di coltura.

Per quanto riguarda la prima parte del differenziamento delle cellule iPS ti tipo neuron-like, una rilevazione di attività scarsa e con bassa ampiezza di spike è stata resa possibile solo grazie alla ridotta banda di rumore del sistema Benchmark MCS. Inoltre, il protocollo adottato per la differenziazione di hiPSc richiede una diversa concentrazione di O_2 rispetto a quella adottata durante le prove neurofisiologiche classiche. Per questo motivo, se si intende utilizzare il sistema MEA personalizzato per monitorare questo primo passaggio nello sviluppo dei neuroni, è necessario calibrarlo correttamente, installando bombole con una diversa concentrazione di O_2 e impostando il sistema PID per raggiungere i valori desiderati. Quindi, questa calibrazione deve essere cambiata quando i neuroni passano al secondo stadio di maturazione.

In conclusione, i MEA sono una tecnologia ampiamente utilizzata in diversi studi e costituiscono un gruppo di strumenti sperimentali che promuovono una migliore comprensione del modo in cui il Sistema Nervoso elabora le informazioni in condizioni fisiologiche e patologiche. Attraverso una serie di test di validazione e test biologici multipli, questo lavoro evidenzia alcuni aspetti fondamentali che devono essere presi in considerazione durante lo sviluppo del sistema e l'analisi dei dati, al fine di ottenere la rappresentazione più affidabile delle caratteristiche elettrofisiologiche cellulari.

1. Introduction & State of the art

1.1. *In-vitro* neuroengineering

Neuroscience concerns the study of nervous system. This is divided into Central Nervous System (CNS) composed by brain and spinal cord, and Peripheral Nervous System (PSN), consisting of the nerves and ganglia outside the brain and spinal cord.

The fundamental element of the nervous system is the neuron. The complexity of the CNS and the PNS are due both to neuron numbers (~10^{11}) and the interconnections among them (~10^{14}), which allow some peculiar abilities in learning and in neural plasticity. Neurons are differentiated in various kinds (e.g. local interneuron, projection interneuron, motor neuron, sensory neuron, neuroendocrine cells). The generic neural cell is constituted by a cell body, including the cell nucleus, and two main extensions to receive and deliver electric impulses. There are both afferent (from periphery to CNS) and efferent (from CNS to periphery) neurons. Sensory neurons differ morphologically from the other kinds as their input extension is connected to specialized receptor cells (mechanoreceptor, photoreceptor, nociceptor etc.) by one input axon. Synapses, structures located on the dendrites or membrane of the neuron, are involved in signal exchanging between neurons. Neurons communicate with each other through biochemical signals. Neurotransmitters are molecules (amino acids, monoamines, peptides…) stocked in the pre-synaptic neuron. There exist both excitatory (e.g. acetylcholine, noradrenalin, glutamate) and inhibitory (e.g. dopamine, gamma aminobutyric acid, serotonin, endorphin) neurotransmitters. Apart from acetylcholine (present at the neuromuscular junction), neurotransmitters are mostly amines or amino acids. They are released in the space between synapses, perceived then by receptors in the post-synaptic neuron.

When the integral signal is strong enough, i.e. overcome a certain threshold, the neuron emits a signal electrically conveyed, called action potential (AP), running through the output axon. The output signal might be sent to another synapse, and might activate other neurons. Each neuron can contact up to several thousand other neurons. There are both excitatory and inhibitory effects of the connections. Excitatory connections contribute positively in increasing the summation of the integral signal. Conversely, inhibitory connections decrease the integral effect. Synapses are constantly modified by neuronal interaction.

The boundary of the neuron, the *cell membrane*, has a voltage difference, also called *membrane potential*, between the inside and outside. The membrane has a very small thickness (70 - 150 Angstrom) with a very high capacity (1μF/cm^2). It is impermeable to proteins but under certain conditions, it is permeable to potassium (K^+), sodium (Na^+) and chloride (Cl^-) ions. At rest, that is to say with no firing impulse, sodium and potassium ions are mainly confined to the membrane outside and inside, respectively. The permeability is controlled by ion channels located in between the two membrane boundaries. The closure and the aperture of the ion channels are voltage and time dependent. The restriction of sodium ions outside the membrane is determined by the Na^+ ion channel that is almost closed

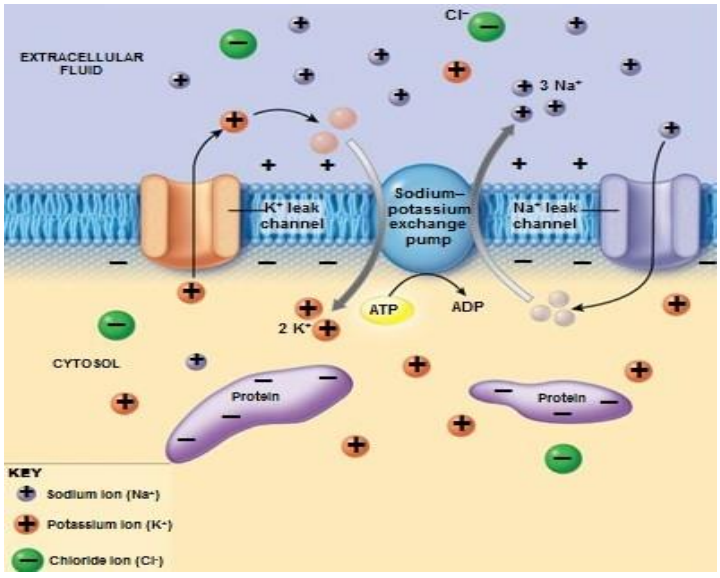

Figure 1.1 Cellular membrane model

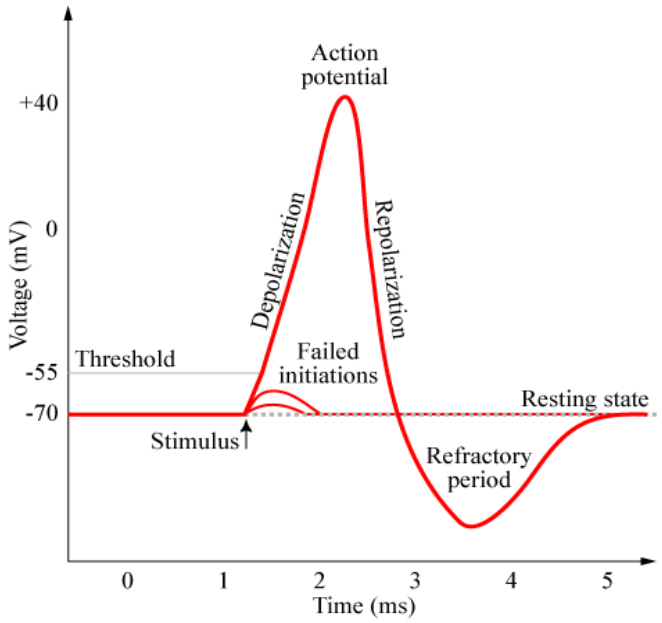

Figure 1.2 Action Potential

at rest. At this *rest* condition, the membrane potential ($V_m = V_{in} - V_{out}$) is negative (about -70mV) and mostly determined by potassium Nernst potential, i.e. the voltage difference due to the concentration gradient across the membrane (about -90mV). However, in this condition, the membrane permeability to potassium ions is about 50-100 times higher to that one sodium ions, i.e. the potassium ion channel is not completely closed to the gradient concentration and potassium channels are greater in number with respect to sodium channels. The sodium-potassium pump is an active biochemical mechanism, additional to ion channels, which requires energy supply (ATP-ADP) to activate and guarantees to keep such a voltage difference at the membrane boundaries. At rest, the membrane is said to be *polarized*. The active state of the excitable cell is in correspondence of generating the action potential. The neuron activation requires a stimulus able to induce a sufficient membrane depolarization over a predetermined voltage. Overcoming such a threshold makes the depolarization completely autonomous. Depolarization involves the increase of the membrane permeability to the sodium ions (NA^+ ion channel opening), which move from the outside toward the inside. This mechanism makes the membrane voltage growing rapidly towards the sodium concentration gradient voltage (Na^+ Nernst potential about +55mV). The membrane has thus a positive voltage inside and a negative voltage outside. Very quickly, the sodium channel closes and the potassium channel opens allowing the potassium ions to rapidly diffuse out. The cell returns to be positive on the outside and negative on the inside. This is called *re-polarization phase*. Locally, the voltage decreases towards the Nernst potential of the potassium even overcoming the rest potential (*hyperpolarization*). Meanwhile, the sodium ions move along the inside to an adjacent area causing a slight change in the polarity of the membrane. The polarity change causes the adjacent closed sodium channel to open. Again, sodium ions move in increasing local polarity inducing soon a closure of the sodium channel. This way the action potential is travelling along the membrane. The potassium channel is activated to restore the negative polarity inside the cell again. The sodium potassium pump push back from inside to outside sodium ions and push in from outside to inside potassium ions restabilising the rest potential distribution. This repeated mechanism along the axon membrane delivers the neural spike from cell body to axon terminals.

Measurements about the features of single spike, in a non-myelinated neuron, lead to estimate a duration of few milliseconds and a traveling speed of about 25 m/s. However, this last value depends on axon diameter and myelinated fibres. In a myelinated fibre, the spike traveling speed is typically tenfold with respect the speed in the axon with no myelin sheet. Due to absolute refractory period, the frequency cannot overcome some hundred Hz with a minimum frequency of about few Hz. Basically, we can assume that the spike duration is about 5ms.The neural computation is highly parallel with a single neural transmission being about few bits of equivalent information. Knowledge in the brain is thus distributed throughout neural connections.

Neuroscience studies represent a deep source of knowledge for many engineering fields. Neuroengineering, in particular, focuses on how to represent brain abilities (memory, learning, reasoning, and computing), in order to apply them to several areas such as:

- Classification functions
- Input/output mapping
- Function learning
- Control models
- Artificial memories
- Input synthesis
- Data dimensional reduction

Besides, a better comprehension of the nervous system could help understanding pathologies correlated and developing drugs, in order to reduce their side-effects and to act more specifically[18][19].

Depending on the functional scale of the imaging investigation, there are many techniques, which use different chemical, physical and electrical properties of the section of system in analysis[20].

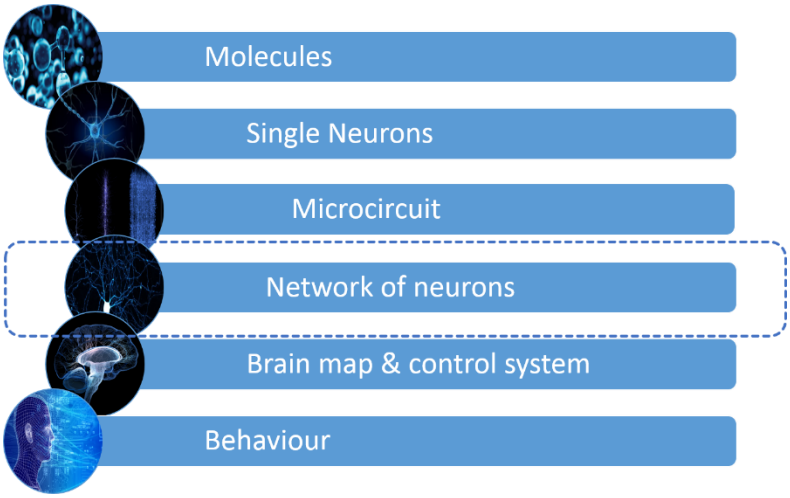

Figure 1.1 Functional scale of investigation

Neuron networks layer represents an optimal field of investigation. In fact, microbiological research has deeply investigated on the activity of single neurons and the interaction between them, putting the basis for the applied research at this level. More in detail, modern *in-vitro* techniques of imaging are widely applied and avoid all the flaws due to in-vivo experimentations, such as animals breeding or human subjects' management. Moreover, due to the huge number of cells in the brain and the high parallel activities, what is known by *in-vivo* experiments is very limited and concerns only a subsystem[20].

It is clear that *in-vitro* models require suitable technologies to interface with any biological system, in order to avoid perturbations and to reduce invasiveness as much as possible. While from a reading technological point of view, *in-vitro* methods are simpler than *in-vivo* ones, *in-vitro* models require solutions designed to mimic the physiological environment and to assure that networks developed *in-vitro* are behaving as *in-vivo* ones. Preparation of culture needs always to follow detailed validated protocols and often baseline behaviour needs to be tested before performing any specific experiment. Neurons are very delicate cells, and *in-vitro* neuronal culturing is quite challenging, especially for assuring cells nutrients and proper perfusion of medium, besides temperature, pH, humidity and so forth[21]. Culturing medium, for instance, plays an important role. Its change during culture growth is e a procedure that perturbs the neurons activity, but it is fundamental considering long term

experiments. The need for an aseptic environment also is a fundamental step in the course of the analysis[2].

1.2. MEA Technology

Electrophysiology applied to *in-vitro* tissues takes into account many approaches, which have to fulfil several requirements. One of them is the possibility to perform simultaneously both different recordings and stimulation on a high population of cells analysed. In fact, working most of the time on signals that are distorted, or covered, by noise, it is necessary to count on an elevated number of sources, allowing to reduce distortions and to improve SNR (Signal-to-Noise Ratio)[1]. From a quantitative point of view, a monitoring system must be able to detect the transmembrane potential in the relevant cell-physiological range of −80 to +30 mV, detect subthreshold potentials such as excitatory and inhibitory synaptic potentials with amplitudes in the range of ±0.5–10 mV with a rise time less than 1ms and a slow decay time of 100–1000ms. It has also to be able to record membrane oscillations in the range of ±5 mV at frequencies from 1 to 50 Hz, record APs with amplitudes of ~100 mV and duration in the range starting from 1ms up to 500ms, in the case of recordings from cardiomyocytes.
Resuming, the setup must be capable to catch transmembrane potential of a neuron and to detect a spike or a burst occurrence. Simultaneous records are also useful to perform a statistical evaluation and sorting of the data required.
An adequate technology must be capable to perform both a targeted stimulation, for instance in a very specific area, and a simultaneous one to a population of hundreds of neurons. This specificity represents, for instance, a powerful tool in studying transmembrane receptors and ion channels.
Another requirement for the instruments of investigation is the capability to perform long-term acquisitions, in the order of days but even months. This allows to test the long end effects of a treatment or a drug, for instance, but also to obtain more data during a single acquisition of a culture.
One of the most used techniques used in the study of cellular action potential is the so-called *Patch Clamp*. Through an electrode, introduced by a glass micropipette inside the cell membrane, it is possible to investigate the single cell properties and its activity. This is a kind of intracellular recording, which has as fundamental advantage an optimal electrical coupling between the cell and the electrode, thus providing an accurate readout of the entire dynamic range of voltages generated by cells without distorting the readout over time. This method has allowed neurophysiologists to study, just to make few examples, receptors sensitivity, ion-cell gating and to create several neuron models. However, the use of sharp or patch microelectrodes is limited to individual neurons as steering of the electrode tips into target cells requires the use of bulky micromanipulators. Besides, the duration of intracellular recording sessions is limited by mechanical and biophysical instabilities.

In general, the traditional intracellular electrophysiology has some advantages:

- ✓ The locally, well identified cause-effect link is perfectly known;
- ✓ There is a correspondence between morphology and function;
- ✓ Good SNR and dynamic response.

From the other side, there are some drawbacks as well:

- × It is invasive and therefore it perturbs the neuron which dies just after the measure;
- × The spatial resolution is linked to the number of clamps that are placed on the neural culture. The positioning must be done at the microscope, and it is not possible to place more than one or two clamps. Investigation at the network level is not possible with this method;
- × There is an intrinsic biophysical and mechanical instability, which prevents to prolong experiments over few hours.

Multi Electrode Arrays, or Micro Electrode Arrays (M*EA*) represent the solution to most of the limitations described before. With that, in fact, it is possible to record, amplify, and analyse signals from biological samples *in-vitro*, adding the great benefit of collecting data in a continuous-time window. MEA-Systems are used to record from brain or cardiac slices, neuronal or cardiac cultures, *ex-vivo* retina, cell lines or stem cells[1].
MEAs are devices that contain multiple plates or shanks through which neural signals are obtained or delivered, essentially serving as neural interfaces that connect neurons to electronic circuitry. They are based on substrate-integrated matrices of electrodes for the recording of extracellular activity. MEAs could be used both *in-vivo*, thanks to an implantable form, and *in-vitro*.
The obtained measure is an extracellular measure with respect to a reference electrode, thus a voltage difference is measured. It should be noted that each electrode does not correspond to a single neuron. MEA has a spatial resolution that corresponds to a cluster of neurons.
As stated, one of the main advantages of this method is the possibility to perform extracellular recording of the cellular electrophysiological activity. The extracellular space, in fact, is conductive and its resistance is very low. According to the voltage divider rule, the voltage recorded is quite small: $V_{extra} = V_{in} \frac{R_{extra}}{R_{extra}+R_{intra}}$

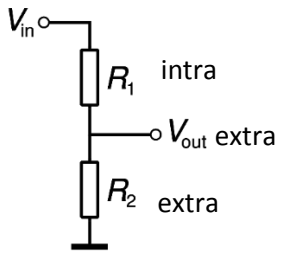

Figure 1.2 Voltage divider model

The characteristics of the extracellular signal depend on many factors, one of them is the relative position between the signal source and the electrode, which determines the shape of the AP recorded. The recorded signal is also affected by the membrane properties, the culturing medium between the cell and the electrode, the electrode pad and so forth. All of them act as capacitors, which entail a strong attenuation of the signal and also a filtering of high frequency[1].

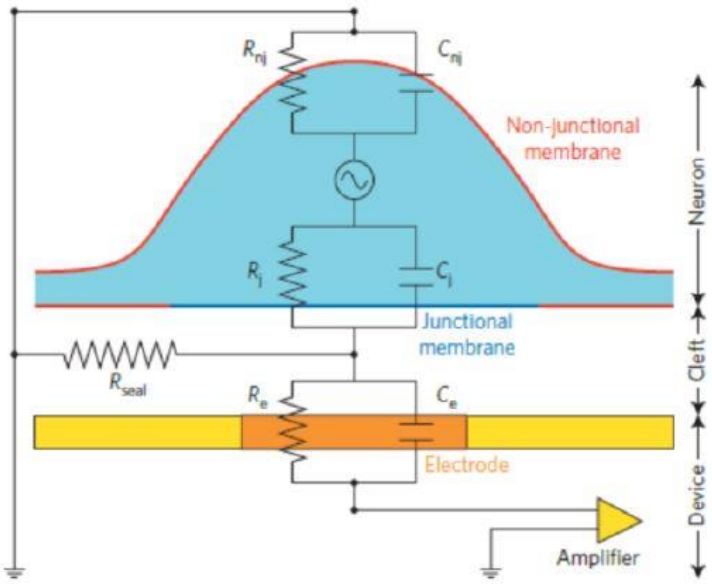

Figure 1.3 Cell-Electrode coupling (electrical model)

Schematic layout depicted (*Fig.1.5*) represents the spatial relationships between a neuron and a substrate-integrated electrode and the analogue passive electrical circuit. The cell body of a neuron (light blue) resides on a sensing electrode (orange) integrated in the culture substrate (yellow). The electrode is coupled to an amplifier (yellow). A cleft filled by the culturing media (ionic solution) interposes between the cell membrane and the electrode–substrate. The neurons plasma membrane is subdivided into two: the part that faces the electrode (blue) is defined as the *junctional membrane* and is represented by

the junctional membrane resistance (R_j) and the junctional membrane conductance (C_j). The junctional membrane can be a portion of the entire cell surface, up to approximately 50% in cells that flatten while adhering strongly to substrate-integrated sensing pads. This percentage depends on the geometry of pads, the adhesion characteristics and the morphology of the cell. The rest of the membrane, defined as the *non-junctional* membrane (red), faces the bathing solution and the culture substrate. The non-junctional resistance (Rnj) and the non-junctional capacitance (Cnj) represent this part of the membrane. The physiological solution within the cleft generates the seal resistance (R_{seal}) to ground. The electrode resistance and capacitance (Re and Ce, respectively) represent the electrode (orange) impedance. The electrode can be a passive element or a transistor. For simulation purposes of APs or intracellular current injections, current can be injected into the analogue cell-circuit in-between R_{nj} and R_j. Under physiological conditions, current is generated by transient changes in the membrane conductance[1].

According to the Ohm's law, it is necessary to reduce the junctional membrane resistance, in order to improve the electrical coupling between neuron and electrode. For this reason, sharp electrodes are used, in order to increase the size of an electrode in contact with the neuron (*Fig.1.6*). The standard type of MEA chip comes in a pattern of 8x8 or 6x10 electrodes. Electrodes are typically composed of indium tin oxide (ITO) or titanium and have diameters between 10 and 30μm. These arrays are normally used for single-cell cultures or acute brain slices[22][23], [9].

In case of recording in-vitro slices, one major issue in order to obtain quality signals concerns that electrodes and tissue must be in close contact with one another. The perforated MEA design applies negative pressure to openings in the substrate so that tissue slices can be positioned on the electrodes to enhance contact and recorded signals.

A different approach to lower the electrode impedance is by modification of the interface material, for example by using carbon nanotubes, or by modification of the structure of the electrodes, with for example gold nanopillars or nanocavities. However, increasing the electrodes' size brings to a reduction of the spatial resolution of the MEA.

To check the quality of the electrical coupling between the electrode and the cell, it is computed the ratio between the maximal voltages reordered by the device and the maximal voltage generated by an excitable cell. The coupling depends on the working frequency too[23].

After the acquisition, signals collected by the MEA system need to be filtered, in order to delete background noise and to permit the extraction of spike's and burst's time[24]. Subsequently, collected a complete dataset for spiking and bursting, through specific algorithms it is possible to extract features and to perform a clustering based on them.

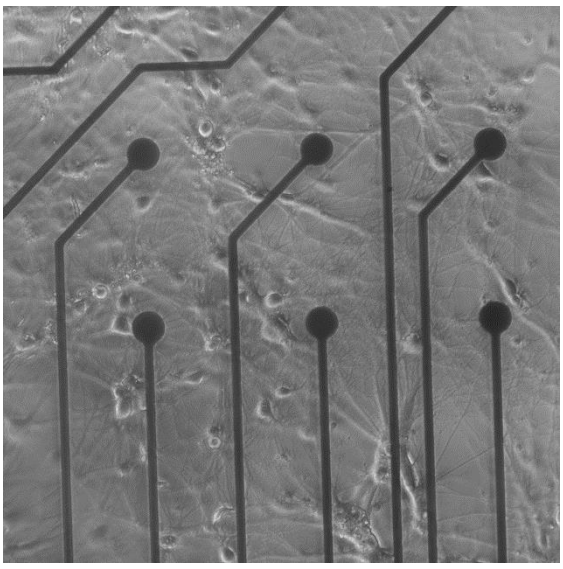

Figure 1.4 Example of electrodes for neuronal recording (MEA microscope imaging)

Assuming that environmental conditions are kept constant, each neuron of the culture fires with the same spike shape for all the time of the acquisition. In this way, the algorithms are able to identify and fix different templates, cluster them and link to a source, building a spatial resolution map of the chip. However, with this kind of technology is not possible to link the templates to the network morphology.

If two cells are afferent to the same electrode, which is a common case in very proliferative cultures, they cover different areas of the electrode. Even if the neurons cover the same electrode area, their spike

waveforms are different because of their different ion channel density, for instance. In this way, the algorithms for the spike sorting and clustering is able to discern between two different neurons acquired by the same electrode[25], [14].
Nevertheless, there are some drawbacks regarding MEAs technology. One of them is the low selectivity during stimulation experiments. In fact, the medium in which cells are is conductive, so it is necessary to confine the stimulus in order to strike a specific target. Microfluidic solutions are being studied to bypass this issue. Another defect regards the so-called *dark neurons:* when a neuron fires, it could have been triggered by:

- An endogenous mechanism;
- Cessation of an inhibition;
- Right summation of excitatory inputs.

With extracellular approaches, it is impossible to infer which mechanism has triggered the firing, so an intracellular approach is required.

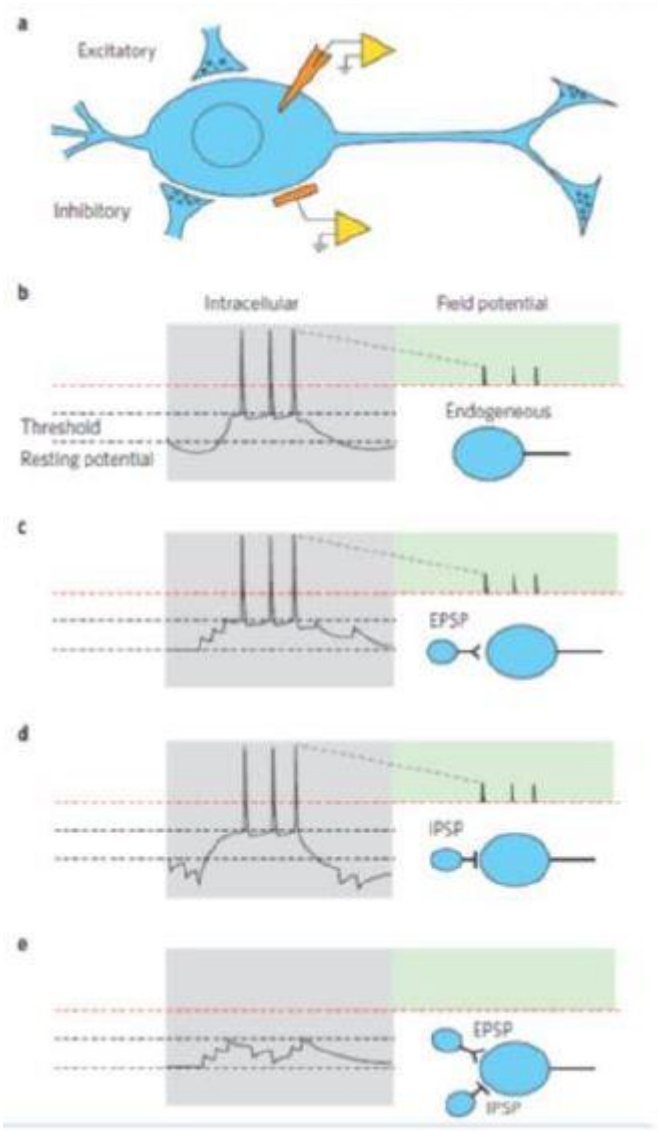

Figure 1.5 Neurons spiking activity

Here described in *Fig.1.7*, a neuron (blue) receives an excitatory and an inhibitory synaptic input in a subthreshold and supra-threshold electrophysiological activity of the neuron is recorded by an intracellular (upper orange electrode) and an extracellular (lower orange electrode) electrode. The intracellular recordings are shown in the left panels of b–e, and the corresponding extracellular recordings are shown in the right panels (green background). In b, a neuron endogenously generates a train of APs (of approximately Δ100 mV) by depolarization of the membrane potential from the resting value of approximately −80 mV (bottom dashed line) reaching a threshold level to fire APs (middle dashed line) at about −50 mV, and then the membrane potential endogenously repolarizes[1].
The extracellular electrode picks up the Field Potentials (FP) generated by the APs (marked by vertical lines and green background). Note that the recorded FP amplitudes range between 0.01 and 1 mV, and are not drawn to scale. The attenuation factor (1/100 to 1/1000) is so large that subthreshold potentials generated by individual neurons cannot be recorded. Thus, the extracellular electrode is practically 'blind' to the subthreshold events (grey background, below the red dashed line). In c and d, the very same pattern of APs firing is generated by excitatory (c) and inhibitory (d) synaptic inputs. Whereas in c summation of excitatory synaptic potentials depolarizes the neuron to reach the firing level, and the neuron stops firing when

the barrage of the excitatory inputs stops (leading to membrane repolarization), in d the train of APs is generated by dis-inhibition (the cessation of the barrage of inhibitory synaptic inputs). The significant differences in these mechanisms (b–d) cannot be detected by the extracellular electrode. Furthermore, unless an individual neuron is firing APs, synaptic inputs are not 'visible' to the extracellular electrodes at all (e). In this example, the extracellular electrode does not detect the presence of a neuron that receives a barrage of excitatory and inhibitory synaptic inputs. These inputs may be of significant importance to the functioning of the neuronal circuit[1].
Recapping, the main advantages of MEA systems are:

- ✓ Large scale acquisitions;
- ✓ Editability of local properties and study of the impact on the entire network;
- ✓ Long-time recordings, with high temporal resolution;

The drawbacks, on the other hand, are:

- × Low correspondence between morphology and function;
- × Low spatial resolution;
- × Low selectivity in stimulation;
- × Absence of records about subthreshold potentials (low SNR): dark neurons.

1.3. Incubators for environmental conditions control

Environmental conditions play a fundamental role in every physiological mechanism and, more in general, in physical and chemical processes within a living being. For instance, regarding mammalian cells the temperature range must be found between 36 and 38 °C, otherwise the risk of cell damage unto apoptosis increases. In particular, there are studies [2] showing that hyperthermia represents a more dangerous condition than lower temperatures (up to 36 to 15°C) exposition.
From the point of view of electrophysiology, environmental changings become much more relevant. In fact, even if slight and low increasing or decreasing in temperature could not alter the viability of cells, they surely lead to an alteration of electrical behaviour of excitable cells [26]. Several studies show that temperature influences basic neuronal properties such as single ion channel conductance, membrane input resistance, action potential amplitude, duration and propagation speed of action potential and synaptic transmission[2], [27], [28]. Cooling has been found to reversibly depolarize the membrane potential and increase the input resistance as well as the amplitude and duration of action potentials in hippocampal and cortical neurons [28]. Furthermore, decreasing temperature reduces the clearance of the excitatory neurotransmitter glutamate from the synaptic cleft and diminishes the excitatory postsynaptic current (EPSC) amplitude. Accordingly, it was observed that both synaptic activity and spontaneous bursting and synchronized activity decrease when lowering temperature [3], [29]. Conversely, it was reported that warning up to 41°C results in depolarization and increase in excitability in hippocampal neurons [30]and that changes in synaptic responses are reversible until up to 43°C [31].
For these reasons, cells managing and movements in labs, for instance among incubators, acquisition setups and imaging setups become a critical issue during the work. Another aspect that has to be taken into consideration is the condition of the medium where the cells are immersed. It is always a good practice to bring it to a physiological temperature (36-38°C) before putting it into contact with biological samples.
Regarding culture medium, pH is fundamental, too. It is possible to obtain mammalian cell cultures with best growth characteristics and viability if the pH is within a narrow range of 7.1 to 7.5 centered around the physiological pH of 7.3 [32], [4]. Decreasing the pH of the medium inhibits growth and production of proteins and alters cell metabolism, with lethal values below 6.8 [21]. Alkaline values also decrease cell viability, up to a lethal value around 8.5[4].

One of the most efficacious methods to keep under control culture pH consists in controlling CO_2 concentration inside the sample. In fact, bicarbonate anions dissolved in medium represent a buffering system similar to that found in human blood. Specifically, the pH is stabilized to the 7.3-7.5 range when the CO_2 percentage in the incubator is regulated between 4.5 and 5.5 % (Henderson-Hasselbach equation). However, for several manipulations it is mandatory to expose the sample to room air, in which CO_2 concentration is about 0.05%. Bicarbonate then leaves the medium as gaseous CO_2 and the pH drifts to non-physiological values in 10 minutes, reaching a detrimental lethal value after around 60 minutes [4], [33] if it is not re-equilibrated. Therefore, exposition time becomes another key factor in samples handling (e.g. pH drops from 8.5 to 7.5 in around 60 minutes) [4]. Because of pH upward drift at room air, MEA experiments can provide reliable data about the culture electrophysiological state throughout a limited time window of about 10 minutes, before the onset of negative influences on culture physiology due to the increase of pH. For instance, it was observed that spontaneous firing incidence in hippocampal slices transiently increases due to alkalosis of the bicarbonate buffered medium at ambient CO_2 levels, before being eventually suppressed if the pH reaches lethal values. When CO_2 concentration returned to 5% after 30 minutes at ambient level, a transient activity peak was observed before pH re-equilibrated to the physiological range [6].

Even if culture medium exchange represents a stress factor for cultures, it is important to follow up every step of cells growth [7]. Indeed, with culture maturation neurons become metabolically more active, leading to an increasing of excretion of acids (e.g. lactic and carbonic acids), resulting in an increase of extracellular pH [25]. During culture maintenance in 5% CO_2 incubators, neuronal cultures might also experience acidification of the medium (i.e. pH lower than the physiological range). If this can't be balanced by the bicarbonate buffer system (e.g. due to a high cell number or too low buffer concentration), the medium can get too much acid.

The third factor that must be considered for culture survival and electrophysiological activity stationarity is osmolarity [34]. Standard cell culture conditions result in an increase of extracellular salt concentration over time, and thus hyperosmolarity, due to medium evaporation [4], [6]. Evaporation can be avoided through an atmosphere saturated with water vapour (i.e. relative humidity equal to 100%), the absence of air ventilation in contact with the medium and temperature gradient between the medium and the surrounding atmosphere [7]. However, even if cell culture incubators guarantee a high relative humidity level (>90 %) to slow down evaporation, this value is not equal to 100%, thus a minimal evaporation is present. Moreover, as soon as the incubator door is opened, dry air enters the incubator and it takes quite a long time to recover a high humidity level after door enclosure [4], when evaporation is accelerated. The ventilation employed to achieve uniformity in temperature and gas composition may also accelerate evaporation inside a closed incubator. The operation of medium exchange permits to attenuate the osmolarity increase, but not to cancel it. Because the osmolarity of the medium increases over time due to water evaporation, the remaining half of the medium in the culture container presents a higher osmolarity than the freshly added medium. Therefore, osmolarity increases slowly over time even when a percentage of the medium is regularly replaced.

Electrophysiological effects may take place if the osmolarity change alters the concentrations of the ions involved in the generation of the resting and action potentials. Concerning direct effects on signalling, high osmolarity might cause voltage changes in amplitude or time course.

Besides hyperosmolarity, one common cause of neuron death is infection by mold, microbes or air pathogens[4]. Indeed, the warm and humid environment found in incubators is ideal for the proliferation of mold, especially in the water containers used to humidify the air. Infection could occur also from the influx of room air from door openings. Moreover, when cultures are brought out of the incubator for experiments and manipulations, they are put at a further risk of infections. This

risk is even more enhanced in the case of MEA experiments, which require moving the cells repeatedly from the incubator and the experimental setup throughout culturing. Clearly, cellular dysfunction provoked by culture infection results in altered and eventually suppressed neuronal electrical activity.
Finally, the culture handling imposes to transfer the cells from the incubator to the workbench and vice-versa. If the cells are exposed to an excessive turbulence of the medium they might be torn from the substrate, and thus it is important to carry the cultures at a careful pace, which on the other hand stretches the time window under non-physiological conditions. Moreover, mechanical perturbations were shown to transiently affect activity patterns, inducing synchronization of activity among different sites of the network [16]. Thus, recordings during the first few minutes (e.g. 5 minutes) after culture repositioning in the setup represent artefactual activity.
All the perturbations described above represent the main reason why standard MEA acquisitions are performed on a short time interval (e.g. 10-30 minutes), thus preserving data reproducibility and comparability between different cultures subjected to the same experimental protocol. Whereas this represent a powerful and effective method for temporally restricted studies (e.g. acute effect of a drug), this is a limit for acquisitions requiring a long-time window:

- studies of forms of neuronal plasticity at cellular or synaptic loci induced or expressed over many hours or days [10];
- studies of synaptic structures tenacity and remodelling, which are visible only over behaviourally relevant time scales [35];
- studies of dynamics of neuronal excitability over extended timescales;
- studies of neuronal network activity evolution during culture development [36];
- studies of axonal regeneration;
- effects of chronic consequences (i.e. after several hours or days) of the exposure to drugs;
- pharmacological experiments to obtain concentration-response curves adding sequentially increasing doses of a compound;

Until now, it has been tried to get around the obstacle. For example, studies of network development typically sample the state of a culture one every few days [16], [36]. Studies of chronic pharmacological treatments measure the network activity after some hours or days of incubation after the drug delivery [37]. However, unavoidably all those approaches bring with them serious risks, such as culture infection, lost in data continuity and so forth.
Then, it seems that the most reliable way to preserve environmental conditions and simultaneously getting continuous data for an extended period of time, is to perform recordings directly inside an environmental parameters controlled area [16], [10], [38].
In the biotechnology field, environmental devices for prolonged investigations outside a cell incubator were first developed for microscopy imaging and patch clamp experiments. Prototypes of environmental chambers first appeared in the 1950s and since the 1980s several systems improving cell survival have been developed. Temperature controlled bath chambers were designed to provide an accurate and uniform heating during live cell imaging and patch clamp experiments [3]. Devices for the control of the gaseous environment and for the improvement of the bicarbonate–carbon dioxide buffer system, which aimed at pH maintenance, were also proposed. These works eventually lead to the diffusion of commercial climate-controlled chambers for prolonged microscopy investigations outside a cell incubator (e.g. Ibidi GmbH, Okolab srl). Even this approach presents

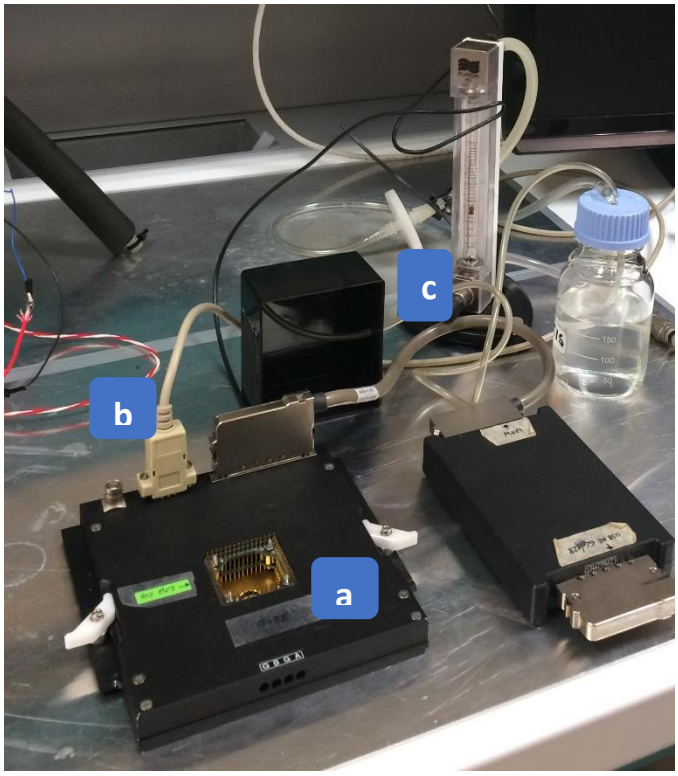

Figure 1.6 Commercial MEA Setup (Benchmark)

tricky aspects, as in some studies MEA signals must be acquired from the recording device put inside the incubator [7]. A common limitation for performing recordings inside the incubator is the humid environment, which causes electrical shorts, changes in component properties, and destruction of materials commonly used in electronic devices. Finally, sterility becomes very challenging for any exogenous component introduced within an incubator.

According to the described issues, a proposed solution is to implement bench-top systems that allow to perform, in an environmental controlled space, acquisitions thanks to integrate, multiple MEA platforms[39]. Actually, many solutions are available on the market: most of MEA acquisition boards are equipped with a heated-plate below the MEA (*Fig. 1.8.a*) to avoid thermal shock to the cells, controlled via an electronic feedback loop (*Fig. 1.8.b*). The simplest and currently widely adopted solution by MEA users is represented by the use of membranes made of materials selectively permeable to oxygen and carbon dioxide and relatively impermeable to water vapour, like fluorinated ethylene–propylene [4] or polydimethylsiloxane[34]. They efficiently prevent contamination and slow down evaporation without hindering the exchange of vital gases from the atmosphere with the medium. To further extend the duration of bench-top experiments, researchers resorted to the utilization of a glass lid sealed with parafilm over the MEA or to small caps/chambers confined around the MEAs including a connection for the flow of a conditioned air mixture (dry or humidified) in contact with the medium. The latter can be a built-in-house modified inverted Petri dish or ad-hoc designed tool [19]. In order to compensate for medium evaporation and thus stabilize osmolarity, the use of custom-designed caps including connection to tubes for medium perfusion [35]or the addition of small volumes of water at predefined time points during experiments have been reported in the literature [40], [41], alternative to the aeration of medium surface with humidified air. However, closed caps/chambers over the MEA require to move the cap and directly pipetting in the medium, thus exposing culture medium to lab air [19]. This represents an issue especially for chronic pharmacological experiments, where a binding requirement is that the operation of drug stimulation does not expose cells to infection risk, which would induce artefactual activity throughout the chronic experiment.

Alternatively to cap-shaped solutions fitted with the MEA housing of commercial pre-amplifiers, few custom-designed stand-alone chambers have been introduced [18], [42], [5], representing important steps in literature. Being independent on the MEA head-stage, the temperature in such chambers can be maintained with heaters integrated in the top or surrounding the chamber[42], allowing higher temperature spatial homogeneity. A rough solution, used in the course of this work for benchmark acquisitions, is to put a cover over the board with a stream of air with suitable gas mixture (*Fig.1. 8.c*).

Finally, since most of the setups are designed for single MEA experiments, they may not be practical and easy to handle if used to record simultaneously from more than one MEA chip, which is

fundamental to shorten experimental time and improve comparability of data from different cultures [40]. For instance, small chambers/caps each confined around each MEA, would require the reproduction of the desired gaseous atmosphere confined over each chip[19]. On the other hand, setups resorting to medium perfusion would require the constant connection of perfusion equipment to each MEA[35]. These arrangements likely complicate the experimental operations and hinder accessibility and handiness of the setup.
This work is based on a bench-top system, whose main components have been developed in the course of different projects [13], [15], based on the data provided by long-term MEA acquisitions experiments [35]. The setup includes a prolonged, continuous and parallel MEA acquisition board with a bench-top platform, developing a stand-alone experimental platform integrated in the same device, with the following features:

- house neuronal cultures on MEAs in a compact chamber on the lab bench, so to ease its integration with other devices needed to perform experiments (e.g., pumps, microscopes, stimulators), without hindering accessibility or requiring a specific location in the laboratory setting;
- provide opportunities for parallel operation to enhance the throughput of MEA experiments, thus shortening experimental timescales and improving data comparability;
- reproduce and stabilize environmental conditions identical to canonical *in-vitro* culture maintenance conditions, in order not to alter the appearance of spontaneous network activity;
- integrate multiple sensors to provide an automatic and remote monitor and control of environment, minimizing the operator intervention;
- Keep permanently the cultures connected to the recording equipment also during chemical manipulations, in order to avoid stress and artefacts due to culture handling for medium exchange or compound addition and to reduce the infection risk during these operations.

1.4. iPS neuron-like cells

In studies related to the nervous system, there are different grades of complexity of the system analysed. First, *single neurons* could be monitored, before their growth. If they are placed in a suitable environment, they continue to grow and start to form connections. In this case, it is possible to obtain networks that have characteristics very similar to those that would have developed *in-vivo*.
Another type of structure that could be monitored with *in-vitro* approaches are *neural tissue slices*. With this method, the network is developed *in-vivo* and then can be sectioned to be put in a monitoring system. The technical problems here are that dead neurons at the boundaries can be sources of noise and that the biological networks have a complexity that often goes beyond the actual biological sample.
Another kind of subject used in CNS and PNS studies and therapies are induced Pluripotent Stem (iPS) cells that, in the last decades, have shown a hopeful prospective in research[43].

Totipotent embryonic stem cells (ESCs) can give rise to differentiated and specialized cells with restricted developmental potential. At some point, the specialized cells no longer differentiate or dedifferentiate, and this state has been referred to as terminal differentiation. The process of terminal differentiation has been thought to be an irreversible process. In contrast to this long-held view, key transcription factors, retroviral-mediated, can convert (reprogram) somatic cells, such as fibroblasts, into iPS cells. Examples of these factors are *Klf4, c-Myc, Nanog, Oct4, and Sox2* [44]. A retrovirus is an RNA virus that uses an enzyme, *reverse transcriptase*, to replicate in a host cell and subsequently produce DNA from its RNA genome. This DNA incorporates into the host's genome, allowing the virus to replicate as part of the host cell's DNA. The additive activities of these transcription factors were thought to be necessary and sufficient to reprogram human or mouse somatic cells to iPS cells[45]. In addition to these classical transcription factors described by the Yamanaka and Thomson groups[46], additional transcription factors and miRNAs and small molecules have been added to the list. Accordingly, a combination of two or three transcription factors (often called Yamanaka factors) may be sufficient to reprogram fibroblast cells into human or mouse iPS cells. For example, in some cell types, Oct4 and Sox2 might be sufficient to establish an iPS cell line, while in others, Sox2 is dispensable[47]. It is apparently clear that Oct4 occupies the upstream position in terms of its ability to reprogram somatic cells, while other Yamanaka factors are required for developmental differentiation events downstream of Oct4[46]. More recently, forced expression of the transcription factors Sall4, Nanog, Esrrb, and Lin28 in mouse fibroblast cells have been shown to generate high-quality iPS cells. The mechanisms of differentiation in iPS and ES cells could differ from those of various iPS cells derived from different somatic cells, but their similarities and differences have not been precisely delineated. Currently, the underlying mechanisms of iPS generation remain an area of great interest.

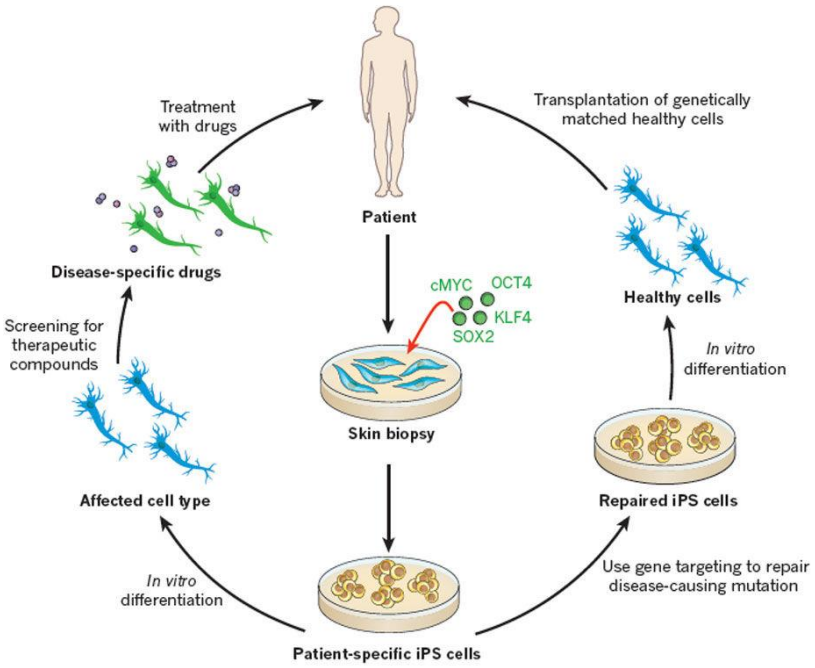

Figure 1.7 iPS cells application. Adapted from [44]

Referring to *Fig.1.9*, once obtained iPS cells from a specific subject, they could be used in gene targeting to repair forms of mutations that cause diseases. Once repaired, the healthy cells can be differentiated *in-vitro* and transplanted inside the patient. Otherwise, another application for iPS cells concerns personalized drug screening: affected cells are treated *in-vitro* with specific compounds that will bring to a patient/disease specific drug[43].

Relatively to this work, particular attention has been paid to iPS cell differentiated to neuron-like cells[43]. The paramount advantage of this approach is to have patient specific neuron-like culture by a skin biopsy. However, a lot of effort is still needed to really prove that these neuron-like cells are effectively "neuron-like". This represents, for instance, a very hopeful way to develop new treatments for neuro-degenerative pathologies, like Parkinson. In this case, it is mandatory to check if gene mutations that carry on that specific pathology, are transmitted to iPS cells.

1.5. Aim of the work

All the steps of this work are finalized to the development and validation of an experimental set-up, based on the results of previous works [13], [48].
The first aim regards the development of a control unit that regulates several environmental parameters through a set of sensors and a feedback loop. Particular attention is paid to efficiency in achievement and maintenance of optimal conditions for cell cultures inside a custom bioreactor.
The second aim regards exactly the development of the culture chamber. More precisely, improvements are made enhancing the capacity to perform long-term and parallel (i.e. multi MEA format) recordings. Starting from a first prototype, an experimental trial is conducted, performing recordings of known cells on custom setup and a commercial one (Multi Channel Systems Gmbh), which is used as benchmark. These experiments allow to determine critical parameters for the validation of a second improved prototype.
Once assembled the second bioreactor prototype, a series of tests are conducted in order to verify the correct behaviour and the efficiency of the system related to signal acquisitions. These tests involve electronic devices that simulates neuron electrical behaviour, and a calibration step with standard MEA chips filled with a buffer solution commonly used for *in-vitro* biological research (PBS).
We assembled the entire setup, composed mainly of:

- Bioreactor;
- Environmental controllers;
- Electronic chain for signal acquisition;

and we performed all the procedures to receive biological samples (e.g. sterilizations). Then we validated the environmental condition control system in the setup during long-time experiments, while monitoring the behaviour of biological materials put into the setup (e.g. culture medium evaporation rate, osmolarity, etc.).
Once proved the capability of the setup to support cultures, neurophysiological trials are conducted on known cells (e.g. hippocampal neurons). These trials are useful both to determine electrophysiological features inferable from the recordings, and to check the cells behaviour inside the bench-top system, also through imaging techniques to verify the cell's status after their stay.
Finally, neurophysiological trials were conducted on iPS neuron-like cells. Through the application of different algorithms [14] meaningful features are extrapolated, which show the behaviour of the iPS cells cultivated in the bioreactor, following their evolution during subsequent days *in-vitro* (DIV).
In conclusion, in this work, we have improved and validated a bench-top system, which integrates an environmental control monitoring system and a multi-MEA recording system, effectively enhancing its performance and improving its capability to perform multiple recordings in parallel (i.e. multi-MEA format). The setup, preventing unnecessary movements from incubators to acquisition system, strongly reduces detrimental perturbations of neuronal activities. Besides, meaningful information about neuronal network activity has been extrapolated, turning to be helpful to define protocols for efficient biological and pharmacological studies. Through a series of validation tests and multiple biological trials, this work highlights some fundamental aspects that must be taken into account during both system development and data analysis, in order to get the most reliable representation of cellular electrophysiological features. These perspectives could in principle assure very important advances in neurophysiological and neuropharmacological studies.

2. Materials & Methods

2.1. MEA Benchmark Setup

The MEA commercial setup (*Fig.2.1*) is composed of:

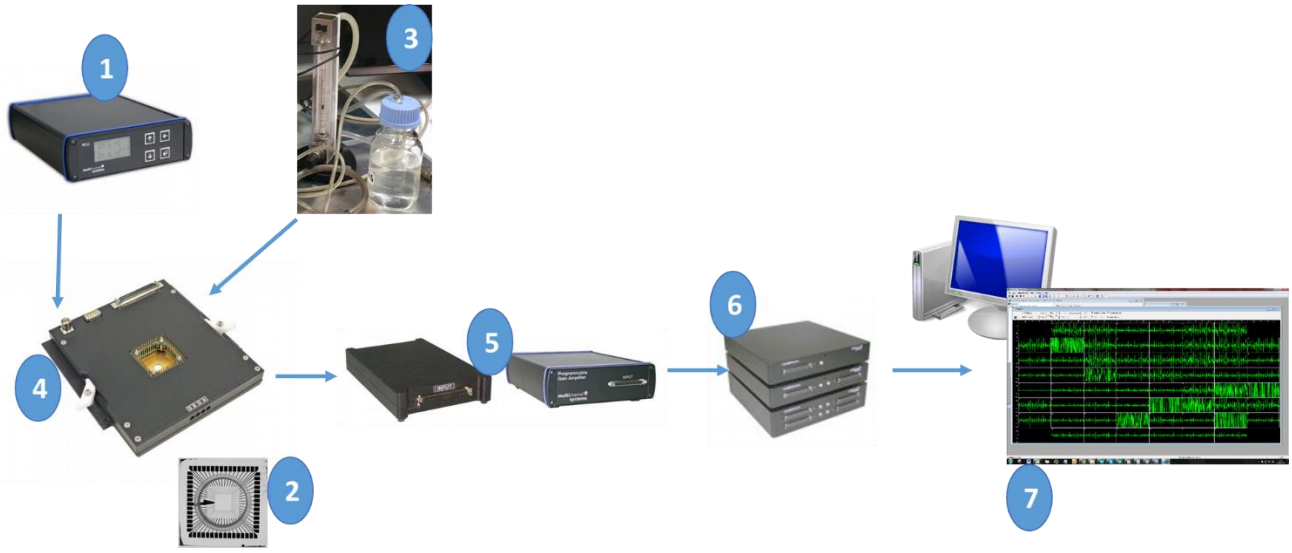

Figure 2.1 Benchmark MEA acquisition setup

During this work, the commercial setup used to set a benchmark is been the one sold by MultiChannel System MCS GmbH. In particular, it is composed of :

1. Thermal controller TC02: it brings, through a PID system, a plate under the acquisition board to a constant temperature, suitable for the cell survival;
2. Acquisition MCS MEA1060 pre-amplifier board (Gain=55);
3. Setup for basic environmental parameters control: through a dome, it is flowed a flux of air with a priori known parameters;
4. Substrate integrated matrices of electrodes, in which cultured cells are plated (Standard 60MEA Chip);
5. Filter Amplifiers:
    - FA64 Filter Amplifier (Gain=20);
    - PGA: 64-channel filter amplifier with programmable gain and filter settings;
6. Data acquisition systems: analog/digital board converting analog signals in digital data streams in real time:
    - USB-ME128-System: (2x64 channels);
    - USB-ME64-System (1x64 channels);
7. Software application MC_Rack: acquisition and registration.

For this work, both in commercial reference and in custom setup, it has been used Standard 60MEA200/10iR-ITO chips, sold by Multichannel System. The chip is composed of a base made of glass, 60 electrodes made of titanium nitride (TiN) connected by tracks to contact pads, entirely made of ITO (Indium Tin Oxide) and titanium. Of these 60 electrodes, 59 are recording electrodes, whereas one is an internal reference electrode (iR). The electrode impedance is 30-50kΩ for 30µm diameter electrodes, whereas is 250 - 400kΩ for 10µm diameter electrodes [49].

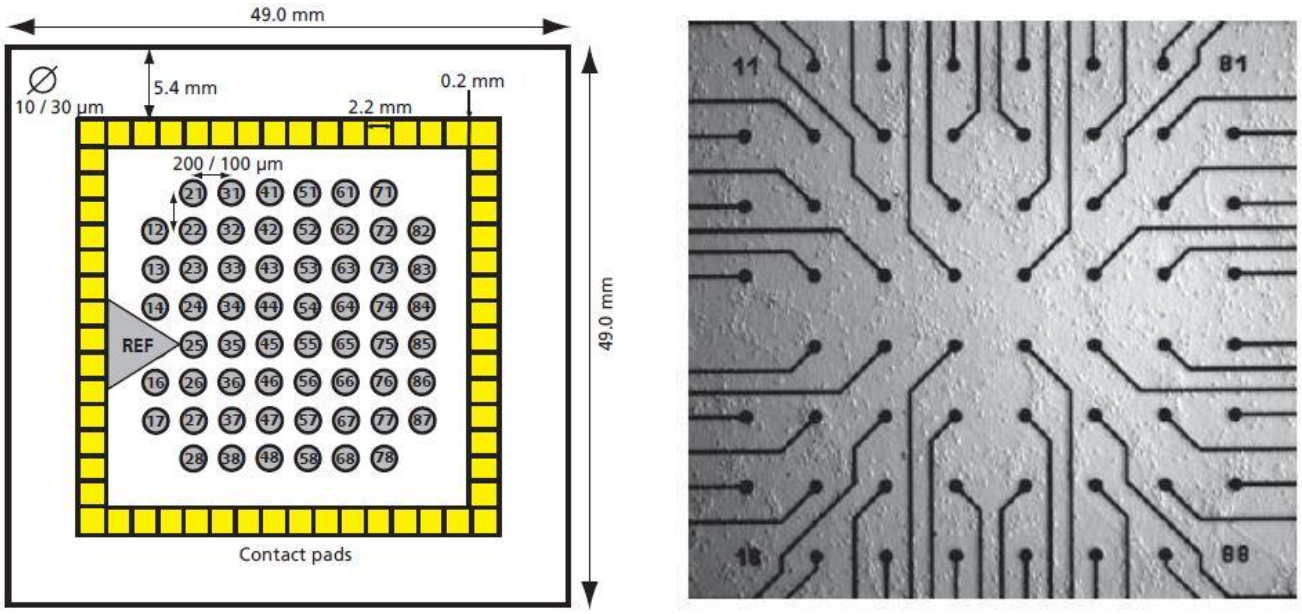

Figure 2.2 MEA chip pin map (left) and microscope electrodes image (right)

2.2. Software & algorithms

2.2.1. MC_Rack platform

The platform used in the course of this work is MC_Rack®, sold by Multichannel System©. This software allows both to record data and to compute an initial analysis on the signals acquired. Combined with the hardware, it forms a complete data acquisition system for measuring extracellular activities of excitable cells, *in-vitro* and *in-vivo* (https://www.multichannelsystems.com/software/mc-rack).

Regarding data acquisition phase, the software offers many settings in order to regulate the signal recorded, as well as the possibility to check the signal in real time thanks to different kinds of display (long term, waveform etc.).

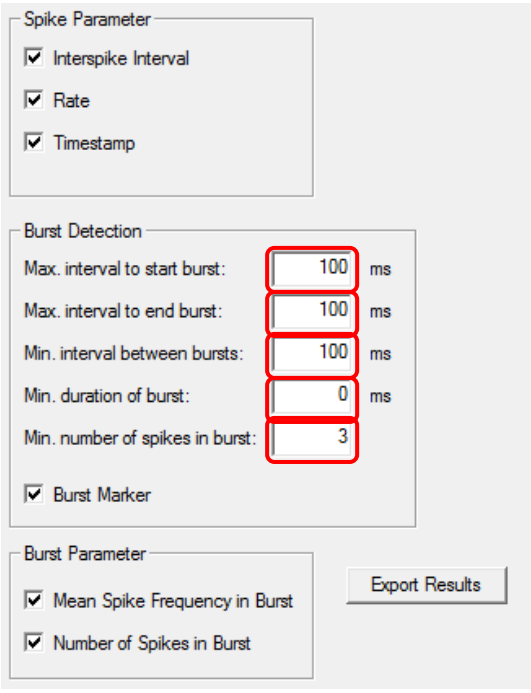

Figure 2.3 MC_Rack spike sorter window

After that, it is possible to analyse the recording saved in *.mcd* format. First, it is necessary to configure the analyser, depending on the signal. For this aim, MC_Rack offers different filters, averagers, spike sorters and so on *[Fig. 2.4]*. For this work, two *second order Butterworth filters* are used: one high pass with cut-off frequency at 300Hz, and a low pass with cut-off frequency at 3000Hz. Then, it is present a *spike sorter [Fig. 2.4.1]*, which is able to detect and classify spiking and bursting activity and to discriminate them from noises. In particular, it computes a threshold of white-noise band, considering the first 500ms of the signal recorded and allows to modify the threshold for any channel, considering the output shown in the display. The operator can set an automatic threshold or a manual one, depending on the kind of disturbances present on the channels: electrical noise (wide band noise), bad coupling (flat line) and so on. It is also possible to

change, for a single channel, the standard deviation needed to differ a relevant signal amplitude from background (in this case, 5 or 7 SD).

The *Spike analyzers tool* offers the possibility to select which spike parameter has to be saved, setting characteristic values found in literature[16], [10] *[Fig. 2.5]*.

In the standard window analyser used are present different displays too. Each of them is divided into 60 windows that correspond to a different channel *[Fig.2.4.2]:*

2. *Longterm display*: while the recording is replayed, it is possible to monitor the signal shape and to estimate important parameters such as white noise band amplitude, disturbances eventually present or monitoring spiking activity *[Fig. 2.4.a]*. The operator can set different amplitude and time scales, depending on the nature of his experiment (signal acquired, duration of the experiment…);
3. *Waveform display:* it shows the waveform of signal detected, and allows the operator to understand its nature (*Fig.2.4.3:* window-*b* electrical disturbances, window-*c* spike shape). It is important to note that the right waveform will not be necessarily the same of an action potential *(Fig. 2.4.c).* Spike amplitude and width will depend on the relative position with the electrode that will detect it.
4. *Timestamp display:* it shows in the time domain the instant in which the software detects a spike. It allows then to save this distribution, enriched by many signal's characteristics, in a *.dat* format file. This file extension will be used in MATLAB analysis of spiking and bursting activity. Otherwise, it is possible to convert these files in *.MAT* format (one file per channel) in order to apply several algorithms for technical analysis (e.g. SNR, PSD…). [1]

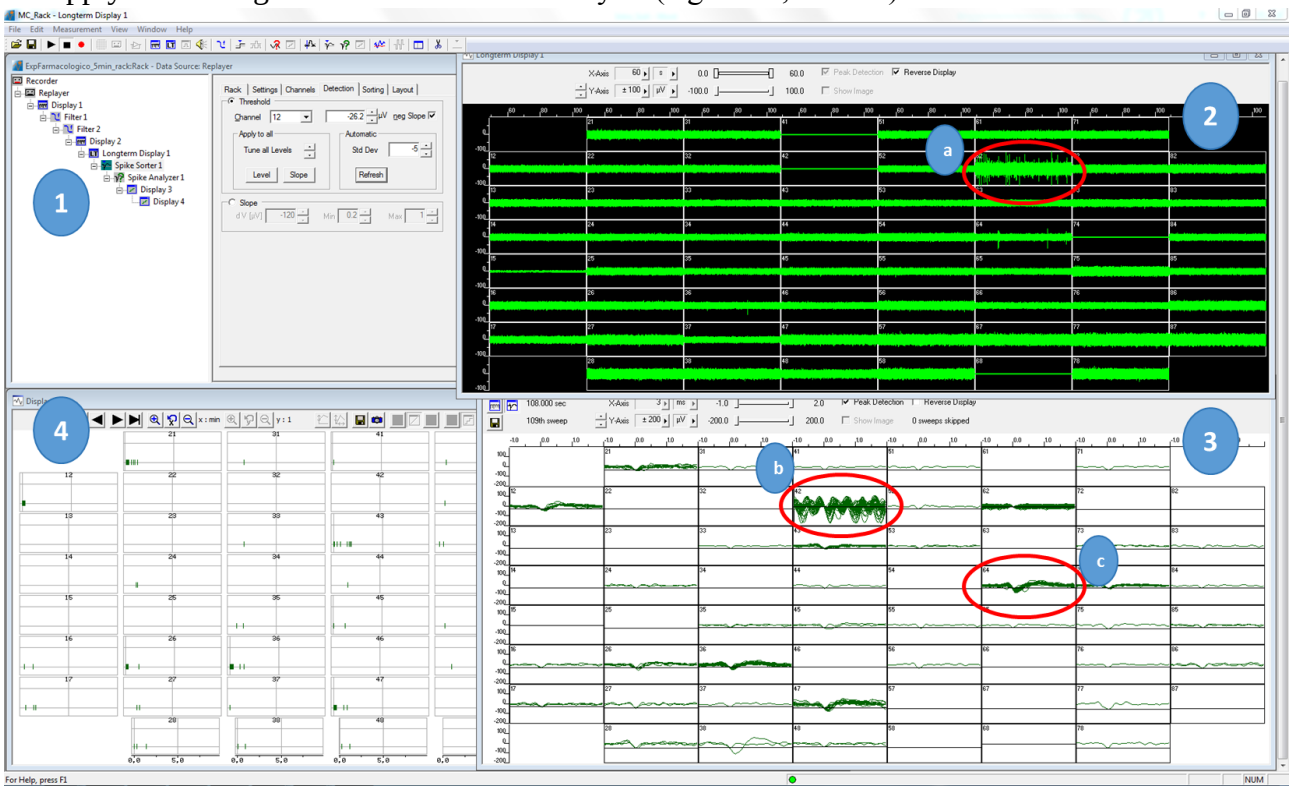

Figure 2.4 MC_Rack Replayer

[1] Prof. Dr. Ulrich Egert from the university in Freiburg, Germany, has designed the MEATools (www.brainworks.uni-freiburg.de) based on MATLAB for analysing MC_Rack data files recorded from MEAs. [MC_Rack Manual-april release (p 172)].

2.2.2. Algorithms for data analysis

According to literature[50], here is a list of most significant parameters that allow classifying the spiking and bursting activity of neuronal cells (the values used in the course of this work are expressed in brackets):

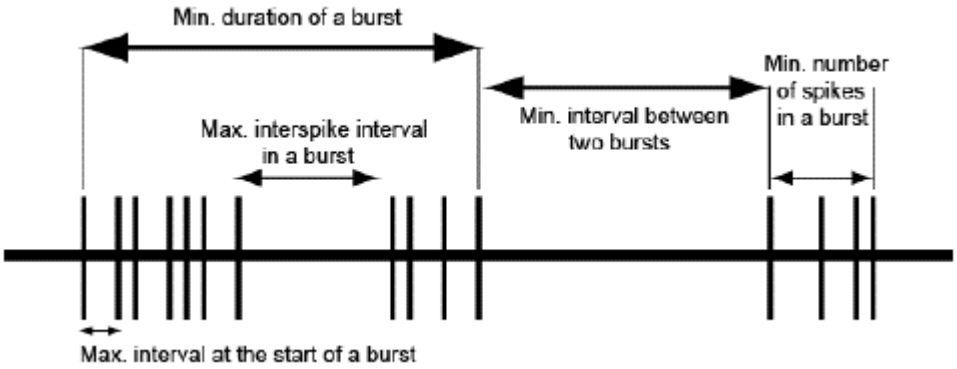

Figure 2.5 Spiking and bursting parameters [48]

- **Max. Interval to start bursts** maximum interspike interval to start the burst (100ms);
- **Max. Interval to end bursts** maximum interspike interval to end the burst (100ms);
- **Min. Interval between bursts**: minimum interspike interval between two bursts (100ms);
- **Min. duration of burst:** minimum burst duration (0ms);
- **Min. number of spikes in burst:** minimum number of spikes in a burst (3).

After saving Timestamps from MC_Rack, they have to be imported in Matlab for the Spiking and Bursting features extraction:

Spiking activity parameters:

1. **N_active_channles:** number of channels with activity greater than 0.03Hz, which is more than 10 spikes in 5 minutes.[51] ;
2. **Maximum_spike:** number of spikes in the channel with maximum activity;
3. **N_spike_total:** total spikes number per registration;
4. **Spike_mean:** average spikes number, considering all the channels involved;
5. **N_spike_mean_act:** average spikes number, considering only the active channels;

Bursting activity parameters:

6. **Percentage_bursting_ch:** percentage of electrodes that show burst activity, compared with the number of active channels.
7. **M_number_burst:** average number of bursts per channel, considering only those channels that have at least 2 bursts [36];
8. **M_duration_burst:** average duration of the burst (s);
9. **M_IBI:** Inter Burst average Interval (s);
10. **M_spike_burst:** average number of spikes per burst;
11. **M_spike_burst_percentage:** percentage of spikes in the burst compared to the total spike number;
12. **M_spike_noburst_percentage:** percentage of random spikes (out of bursts) compared with the total spike number;
13. **M_bursting_rate:** average bursting rate, i.e. number of bursts in 5 minutes (burst / minute);
14. **M_IB_frequency:** Intra Burst frequency (spikes / second);

Network bursting (NB) activity parameters:

15. **NB_numelectrodes:** average number of channels involved in the network burst, compared with the number of active channels;
16. **NB_duration:** average duration of network burst (s);
17. **NB_spike:** average number of spikes involved in network burst;
18. **NB_spike_percentage:** percentage of number of spikes in the NB with respect to the number of total spikes;
19. **noNB_spike_percentage:** percentage of random spikes (out of NB) percentage with respect to total spike number;
20. **INB_frequency:** Intra frequency NB (spikes / s);
21. **NB_bursting_rate:** network burst number in 5 minutes (burst / min).

Once Matlab returns the matrix that gathers each of these values computed for any bin, it is necessary to copy it inside a template excel file. In here, there are spiking and bursting parameters grouped by chip number and bin (e.g. 1 minute long). Besides, there are reported meaningful information about the acquisitions, as well as graphs showing a comparison between mean values.

2.3. Starting prototypal culture chamber

The MEA custom bench-top system (*Fig. 2.6*) is composed of:

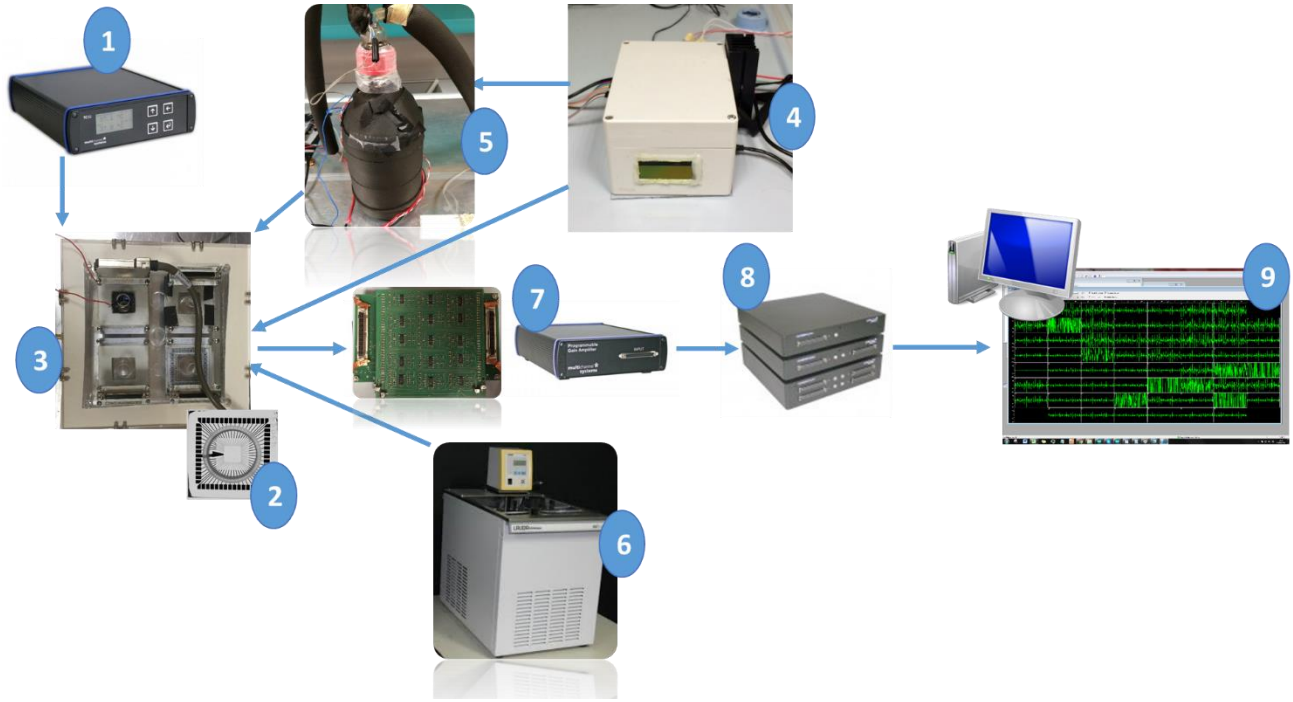

Figure 2.6 Custom bench-top setup: (1) TC02 thermal controller; (2) MEA chip; (3) Culture chamber;(4) Control Unit; (5) Air perfusion system;(6) Thermostat; (7) Filter Amplifiers (FA);(8) Data acquisition systems;
(9) MC_Rack platform.

1. **MCS TC02**
2. **MEA chip**
3. **Culture chamber & Pre-amplification boards**
4. **Control Unit:** environmental parameters controller
5. **Air perfusion system**
6. **Thermostat:** water flow based temperature controller
7. **Filter Amplifiers:**
    a. FA64 Filter Amplifier
    b. Custom Filter Amplifiers
    c. PGA
8. **Data acquisition systems**
    a. USB-ME128-System
    b. USB-ME64-System
9. **MC_Rack platform**

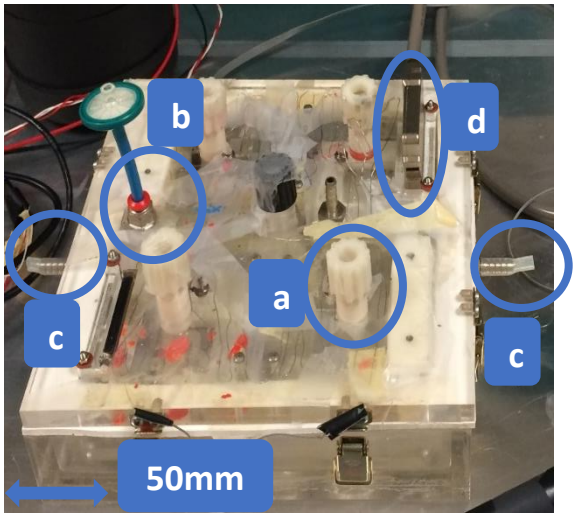

Figure 2.7 First prototypal culture chamber

A 4-MEA chamber is composed of plates made of Poly-Methil-Metacrilate (PMMA), chosen for its high optical transparency and good thermal insulation[15]. The chamber is composed of an external box, an internal box, and a top cover plate. PMMA plates have been glued with a biocompatible glue (*Wacker Chemie AG*). The chamber consists of an outer and an inner box, which are separated by a watertight cavity filled with water and covered by a top plate. The size of the outer box is 180 mm x 180 mm, with a height of 45 mm. The inner box (150mm x 150mm x 30mm) is leant on the outer one by means of four small backings. A 50 x 50 mm MEA housing and a well for the insertion of a temperature probe (Pt100) are provided inside, in symmetric positions with respect to the center to guarantee well reliability as reference *(Fig 2.7)*. A silicone membrane is located between the top plate and the boxes beneath, to guarantee the sealing of the closure, provided by means of eight small *Rolez* clamps.

The electrical connection between gold pins and the external adapter is allowed by means of three connectors, which pass through the top of the chamber. For this purpose, three openings are designed with *Pro-Engineer Wildfire*, manufactured using subtractive rapid prototyping (*Roland Modela MDX-40*) and sealed by means of a silicone glue (*Elastosil E43, Wacker Chemie AG*). The same milling machine is used to realize openings for the insertion of inverted microscope objectives beneath both the MEA housing and the reference well. The whole system can be sterilized with Ultra Violet rays or with Ethylene Oxide (EtOH).

Airtight openings for multiple purposes have been drilled with a numerical control milling machine (*Teknosan* srl) on the cover plate. The compartments are designed for:

a. Openings placed upon each board in order to allow eventual injections in the MEA chip or manipulations, without perturbing the chamber internal environment, assuring sterility and air tightness with pierce silicone membranes for needle insertion, and a *Parafilm* layer;
b. Air outlet with a top filter;
c. Inlet and outlet for tempered water circulation;
d. Slots for board connectors.

Fixed to the top of the chamber by screws, there is a set of four acquisition boards. Each of them is composed of an array of 60 golden pins, which transfer the signal to a pre-amplifier system (*Fig. 2.9*). The boards transmit the signal, through pin header connectors, to a custom adapter board, with

dimensions 76x115mm, placed on the top plate (*Fig. 2.8*). This board arranges pin signals in a 68-pin socket. Then the signal is conveyed to the Filter Amplifiers through a standard cable, exploited in recording devices from *Multi Channel Systems GmbH (MCS GmbH)*.
According to different needs, we developed amplifiers with different gains *(Fig. 22.10*), to obtain the right amplitude of the signal through the right matching with the external Filter Amplifiers[11].
Assuming that the spiking signal lies inside the hypothesized frequency range, it is possible to assume that the pre-amplifier will get a constant gain, in our case fixed at 46 or 92, without being corrupted by phase shifting[11].

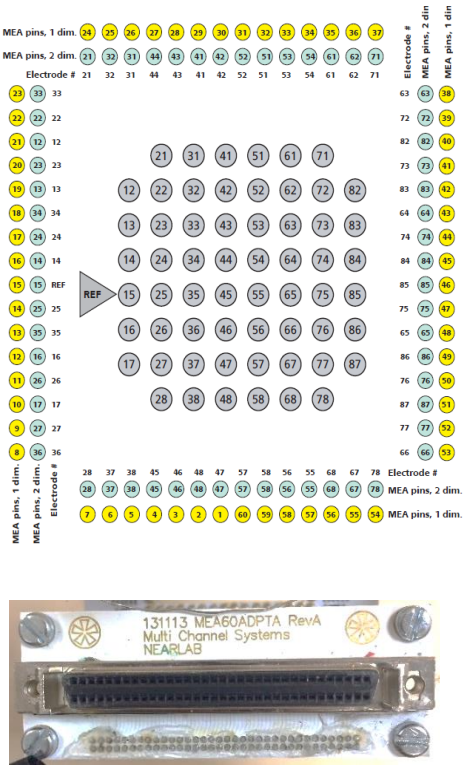

Figure 2.8 Adapter board

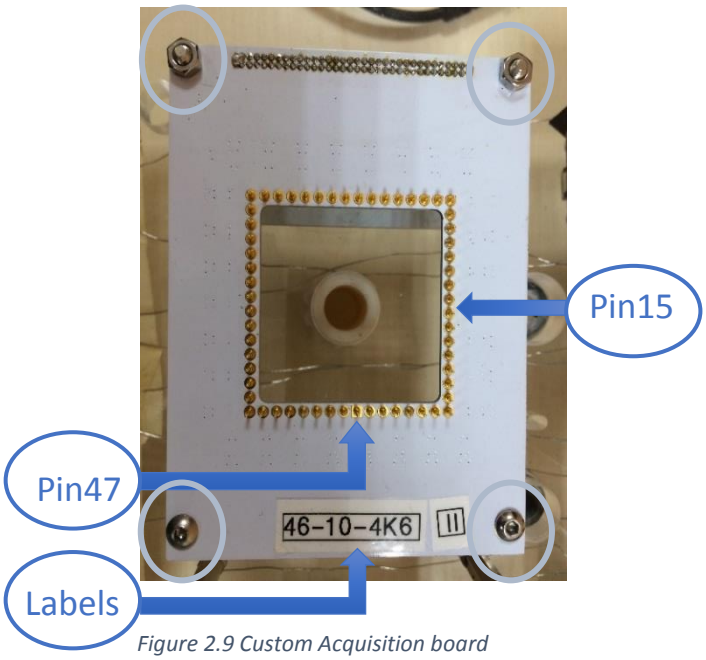

Figure 2.9 Custom Acquisition board

On the bottom of each board there is a label, resuming the main features:

46 → Gain
10 → Lower corner pass-band (10Hz)
4.6 → Upper corner pass-band (4,6KHz)
II → Board id number

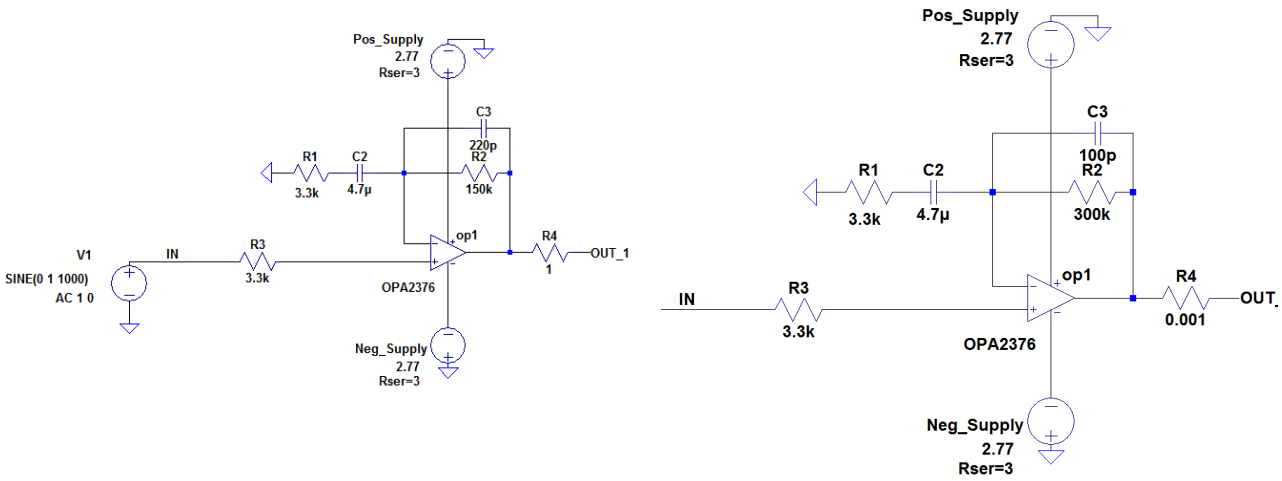

Figure 2.10 Pre-amplification board scheme

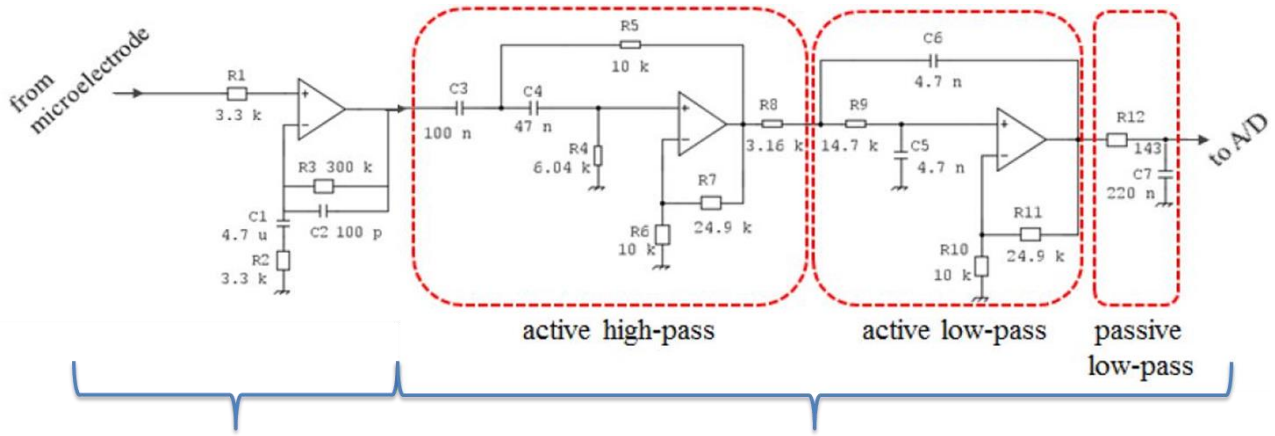

Pre-Amplifier:

$$Kpre - Amp = 1 + \frac{R_3}{R_2} = \begin{cases} 46 \\ 92 \end{cases}$$

Custom Filter Amplifier (FA):

$$K = 1 + \frac{R_7}{R_6} = 12$$

Figure 2.11 electrical scheme, starting from electrode, passing through pre-amplification board and Filter Amplifier, reaching ADC. The gains indicated (K) are in working frequencies condition. Adapted from [47]

2.4. Final prototypal culture chamber

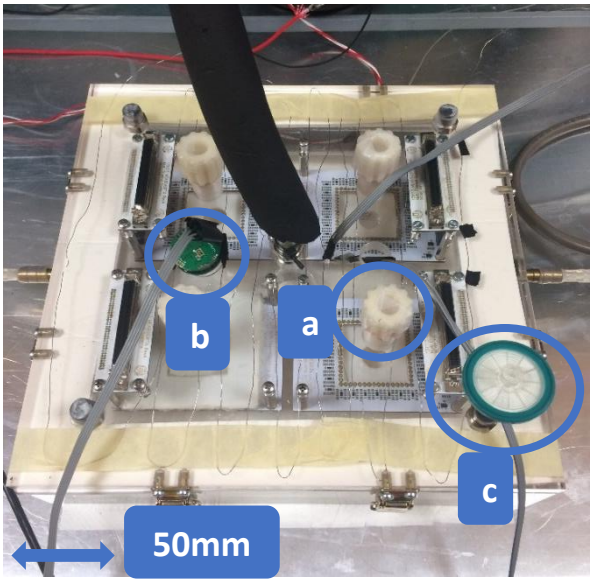

Figure 2.11 Final prototypal culture chamber

The second prototype of the bioreactor is slightly bigger than the first one *(Table I)*. This allows much space for holes on the top plate and a more precise distribution of the heating wire. As in the first chamber, there are holes upon every board for eventual injections and manipulations *(Fig. 2.11.a)*, sensor docks *(Fig. 2.11.b)* and an air outlet valve with a filter *(Fig. 2.12.c)*. We also improved the slots for the board connectors, in order to optimize the space and to reduce internal air losses. All the internal junctions of the new bioreactor have been sealed with an insulant glue (*Dow corning® 732 Multi-Purpose Sealant*), thus avoiding water infiltrations noticed during first environmental tests and thus obtaining a watertight space.

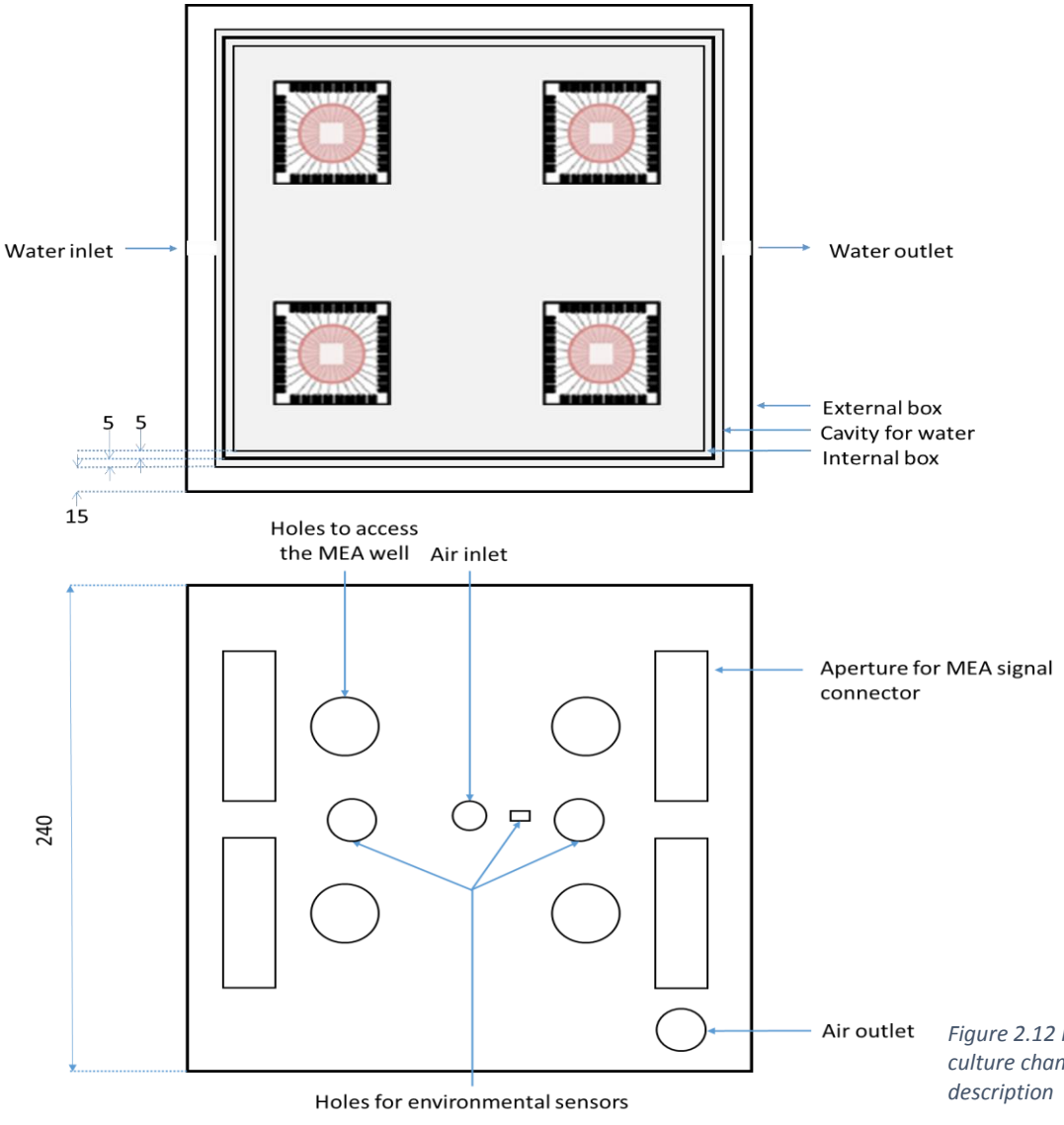

Figure 2.12 Final prototypal culture chamber inlets description

Table I FINAL PROTOTYPAL CULTURE CHAMBER DIMENSIONS

	BxWxH (mm)	Thickness (mm)
Internal box	190x190x30	5
External box	240x240x45	15
Cover	240x240x10	10

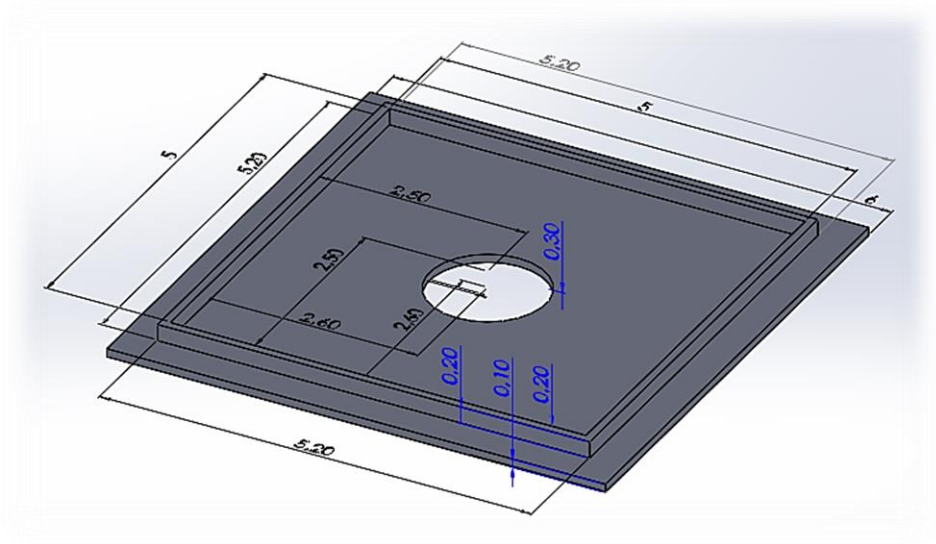

Figure 2.13 Support Base 3D model

One of the most common issues noticed during first acquisition trials, consisted in the difficulty in MEA chip positioning inside the bioreactor. Matching the board pins with the chip ITO electrodes could result very challenging, dealing with spots of much reduced dimensions (~1mm) and being the field of view hindered by the board's top plate. To solve this inconvenient, we designed a support base using *SolidWorks*®, a CAD program produced by *Dassault Systèmes*®. The base has been 3D-printed using polylactic acid (PLA), a biodegradable and bioactive thermoplastic aliphatic polyester chosen both for his common use in 3D printing and for being UV and EtOH resistant, fundamental characteristic in case of sterilization.

We printed a base for each board, and fixed them to the floor of the culture chamber with *Plasting*© *bondacryl CEMENT FIX 10HV*, in a position that allows the right coupling between pins and chip microelectrodes.

Any support is surrounded by four walls that confine the chip right under the board, and has a 1mm high elevation that improves the quality of coupling. Besides, a hole is present on bottom, allowing, eventually, the use of microscope imaging on chips, without removing them from the environment of the bioreactor.

After installing the acquisition boards on the new bioreactor, we made tests to verify that all the connections are correctly set. Matching the MEA System Manual grids of pin and electrodes with the custom maps, we stimulated every single pin of the pre- amplifier board with a function generator to

check the response on a MC_Rack live streaming monitor. In this way, the integrity of the path has been correctly verified starting from the board, through pin header connectors toward upper adapter on the top plate. Besides, we verified that the reference electrode is in short-circuit with the *gnd* pin of the filter amplifier.

2.5. Control unit

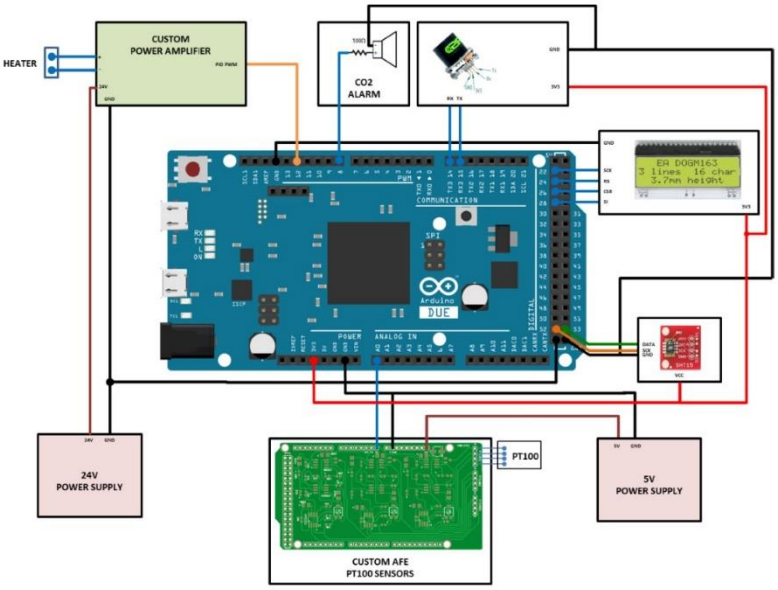

Figure 2.14 Control Unit scheme. Adapted from [11]

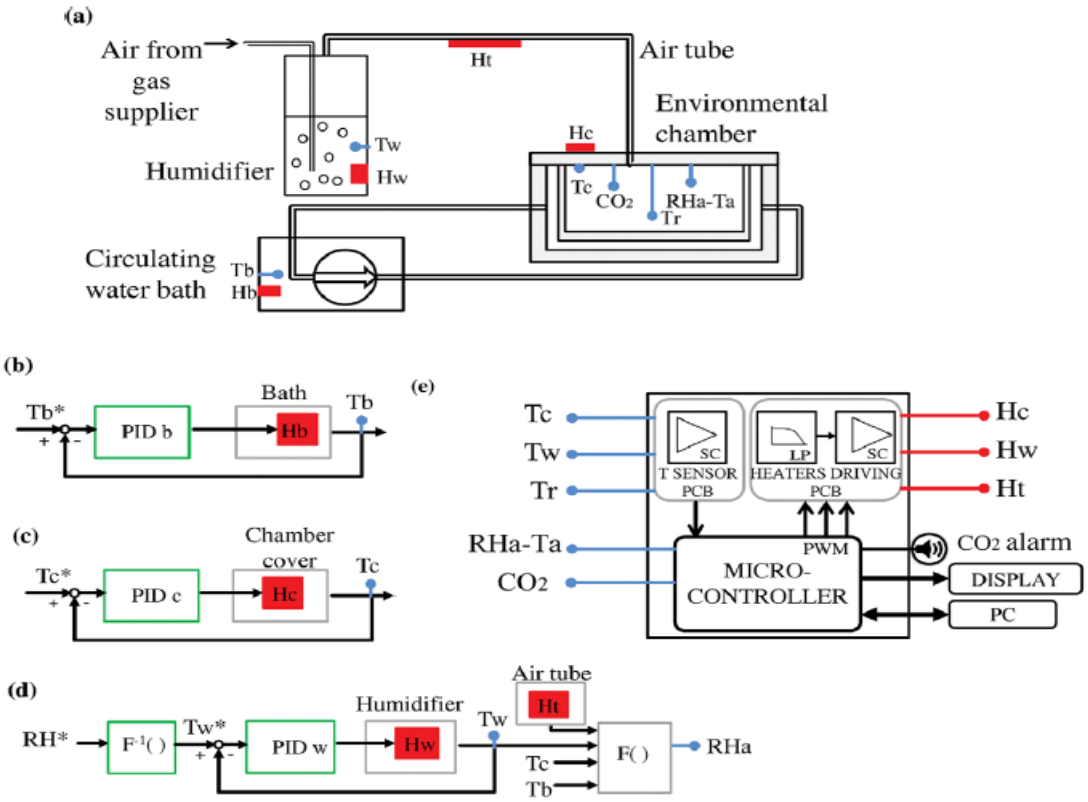

Figure 2.15 Configuration of the set-up. It shows the connections between the chamber, a circulating water bath which controls Tr (temperature of the reference well) by modulating Tb (temperature of the bath) and a humidifier module. In blue: environmental sensors. Adapted from [11]

According to data in literature, and referring to commercial incubators parameters, the environmental parameters controller must maintain specific values in temperature, relative humidity and carbon dioxide concentration inside the bioreactor, in order to assure cells survival. To reproduce a high and stable RH in the chamber, a humidifying and heating module has been devised. A 10L/150bar cylinder flows a mixture of gas (11.99% O_2-5.04% CO_2) with a pressure equal to approximately 180mmHg inside a bottle filled with 450ml sterilized *Salf* water, by means of a rigid tube. This bottle contains a heater (Hb) regulated by a PID controller. This setup becomes a custom air humidifier, formed by a glass filter candle, which delivers the air stream to the chamber through a thermally insulated silicone tube heated with a bounded Nickel–Chrome wire. The humidifier water temperature [Tw] is measured by an immersion Pt100 thermoresistance [Tw] and regulated by a Nickel-Chrome heater (Hw) according to a PID control law [13], [15].
During first tests on bottle's heater performances, we noticed a low capacity for the system to warm the water up to the desired value. To overcome this issue, the bottle is covered with a sheath, made with nitrile rubber, a synthetic rubber copolymer that is UV resistant and with an operating temperature range between -100°C and +140°C. In this way, it is possible to ensure a better thermal isolation of the bottle, which is now able to reach higher temperatures thanks to the heating wire, in a shorter time.
Two other heat sources are exploited: heated water filling the cavity between the internal and external box, circulated and tempered by a commercial pump (*E360, Lauda GmbH*) equipped with a Pt100 probe [Tb], and a Nickel–Chrome wire (Hc) coupled to the chamber top plate. This wire is connected to a MCS TC02 thermal controller, which allows to regulate the temperature of the wire and, consequently, of the top plate, thanks to a miniaturized Pt100 probe below the top plate [Tc]. This helps also to avoid moisture deposition beneath the top plate, which would contaminate the cell cultures.
The chamber has been also equipped with other environmental sensors and connected to equipment for monitoring and controlling the desired incubator-like atmosphere. The environmental parameters have been chosen according to literature (i.e., temperature: 36–38°C, RH >90%, CO_2: 4.5–5%), in order to assure to hippocampal neurons used in trials optimal chances of survival [9]. *Figure 2.15* shows a scheme of the whole system, indicating the position of each sensor (in blue) and actuator (in red) integrated in the setup. A miniaturized digital RH and temperature sensor [RHa and Ta] is integrated in the chamber (*SHT75, Sensirion* Inc.). RHa depends on the value of Tb, Tc, Tw, and the power delivered to the air tube heater [Ht] [block F()]. The CO_2 level is monitored by a miniaturized digital infra-red CO_2 sensor [*COZIR* Probe, Gas Sensing Solutions Ltd., CO_2 in *Fig.2.15*]. The custom-built control unit *[Fig. 2.14]* houses a microcontroller (*Arduino Due board, Arduino*) and a custom printed circuit. The microcontroller reads the inputs from the sensors, displays the environmental parameters, and provides control outputs that drive the heaters and a miniaturized loud speaker for CO_2 level alarm. Through USB communication, environmental parameters are sent to a computer. Here, with an *Arduino* platform-integrated serial monitor, the following parameters are plotted:

- Chamber temperature [°C]
- Relative humidity [%]
- CO_2 concentration [%]
- Air humidifier (bottle) temperature [°C]
- Heater PID power status (255 ON| 0 OFF)
- Bubbler set point (255 ON| 0 OFF)

2.5.1. Validation of the environmental control system

Once each sensor has been set, a long-time test on the three principal parameters is conducted. Three graphs in paragraph 3.1 (figures from *3.1 to 3.3*) show culture chamber temperature, expressed in °C, relative humidity (Rh) percentage, and Carbon Dioxide concentration, expressed in percentage, respectively.
On the horizontal axis, there is the time scale: considering that the Arduino algorithm plots a sample for each parameter every 5 seconds, and having conducted the registration for approximately 26 hours, there are:
(26 hours * 60 min * 60 s)/5~19246 samples.
Then, in these stabilized conditions, we tested the maintenance of the medium where the cells have to be plunged in order to supply them nutrients. We put on a chip 1ml of culturing medium, composed of:

- Neurobasal (48.25 ml);
- B-27 1 ml (50X Invitrogen, 0080085-SA);
- PEN/STREP 1%(0.5 ml);
- Glutamax 1mM (250µl) (Invitrogen, 200 mM, 35050-038)

and after placing it in the chamber with steady-state environmental parameters, the amount of fluid evaporated has been measured every 24 hours.

2.6. Validation of the MEA recording system

The set-up used for the tests includes:

1. Prototype culture chamber
2. Pre-amplifier boards:
   a. 46-10-4K6 II (46II)
   b. 46-10-4K6 III (46III)
   a. 92-10-4K8 IV (92IV)
3. MEA chip:
   a. 26956
   b. 20152
3. Commercial MEA 1060 amplifier (BB)
4. Commercial FA64 Filter amplifier
5. 2 Custom Filter Amplifiers (FA)
6. 2 Data acquisition systems:
   a. USB-ME64-System
   b. USB-ME128-System
7. MEA Signal Generator (60MEA-SG)

The abbreviation that indicates each board on the test schemata is reported in brackets.
For the acquisition and recording, MC_Rack software is used.
The gain settings are used for scaling and displaying the signals properly[2] .

[2] cf MC_Rack Manual, pp 38-40

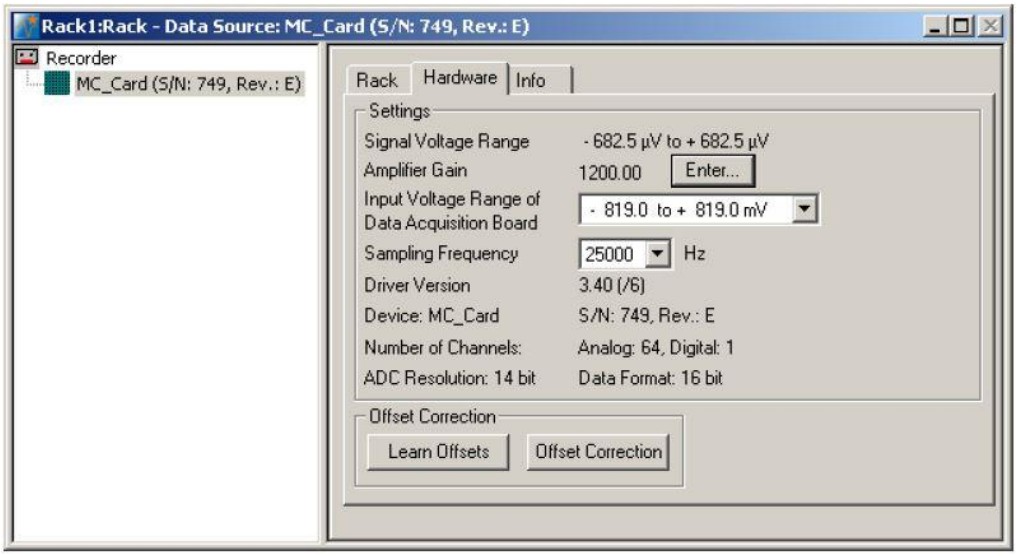

Figure 2.16 MC_Rack Recorder window. Gain for MC_Rack scaling: (Based on the combination used, you need to set the correct total gain in McRack to see the actual amplitude of the signal returned to the input pin).

Using gain values reported on paragraph 2.1, the commercial setup composed of filter amplifier FA64 and MEA 1060 pre-amplifier board, has a total gain equan to: 55*20=1100. Regarding configurations with custom components:

- Filter Amplifier (FA64) MCS=20
- Custom Filter Amplifier=12

- FA64 x 46= **920**
- FA64 x 92= **1840**
- Custom_FA x 46= **552**
- Custom_FA x 92= **1104**

2.6.1 Signal Generator (MEA-SG) test

Regarding the first test type, a signal generator is used. The 60MEA-Signal Generator, sold by Multi Channel System GmbH, can replace a MEA. The device has the same dimensions and contact pad layout as a Standard 60-channel MEA chip, and is compatible with all MEA 1060 amplifier types. The MEA-SG produces sine waves, or replays a variety of biological signals. These signals are fed into the MEA amplifier as analog signals. With this artificial data, it is possible to test the functionality of the hardware and software system, without the need for a biological sample on a real MEA chip[3]. In this case, a "hippocampal neuron spikes" configuration is used. Other parameters of the SG are:

Figure 2.17 60MEA_SG

- F_spiking= 0,5 Hz (30 spikes in 60s);
- Spike shape: EPSP (Excitatory Post Synaptic Potential);
- Spike amplitude (measured with FA_MCS + Benchmark board MCS) = ~77 µV.

[3] Cf MEA_Signal-Generator_Manual, p.8

To get a correct display of the signal, the SG and the setup must have a common reference ground. For the commercial Filter Amplifier FA64, the reference ground has been fixed to the setup ground through a wire connected to a screw of the pre-amplification board, which is connected to the system ground too. Regarding the Custom Filter Amplifiers, the two grounds have been connected through the pin *gnd* of the FA boards *(Fig. 2.18).*

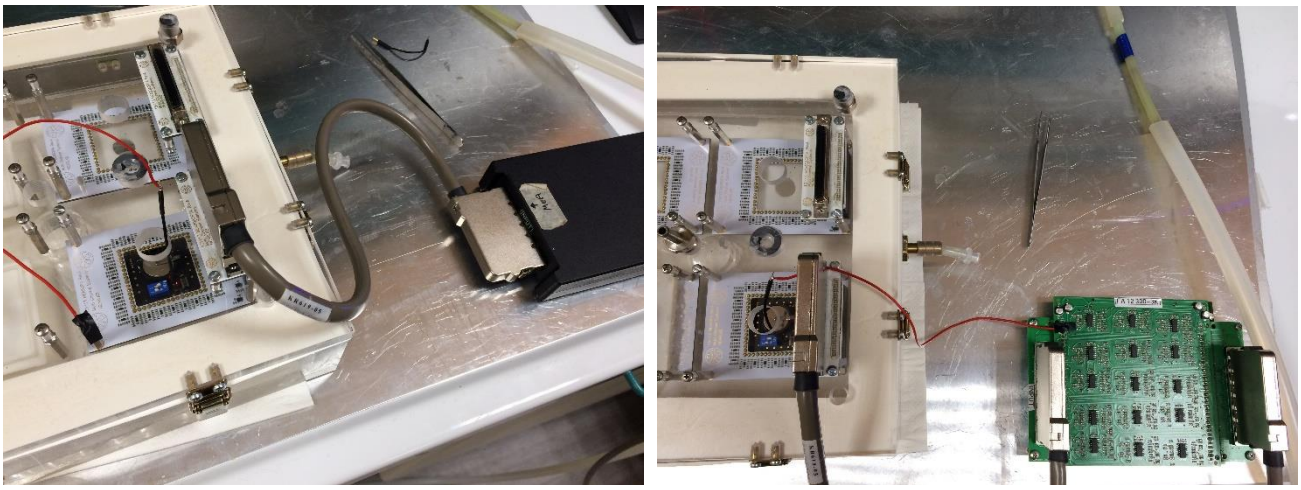

Figure 2.18 SG grounding: with commercial FA (left) and custom FA (right)

Using the commercial set-up, a reference set of recordings is acquired. First, a one-minute long recording is performed with the commercial acquisition board, repeating the test, for each sample, with a different Filter Amplifier. The rest of the signal acquisition pathway is the same as in the experimental case.
Then, we performed acquisitions with the custom set-up inside the culture chamber.

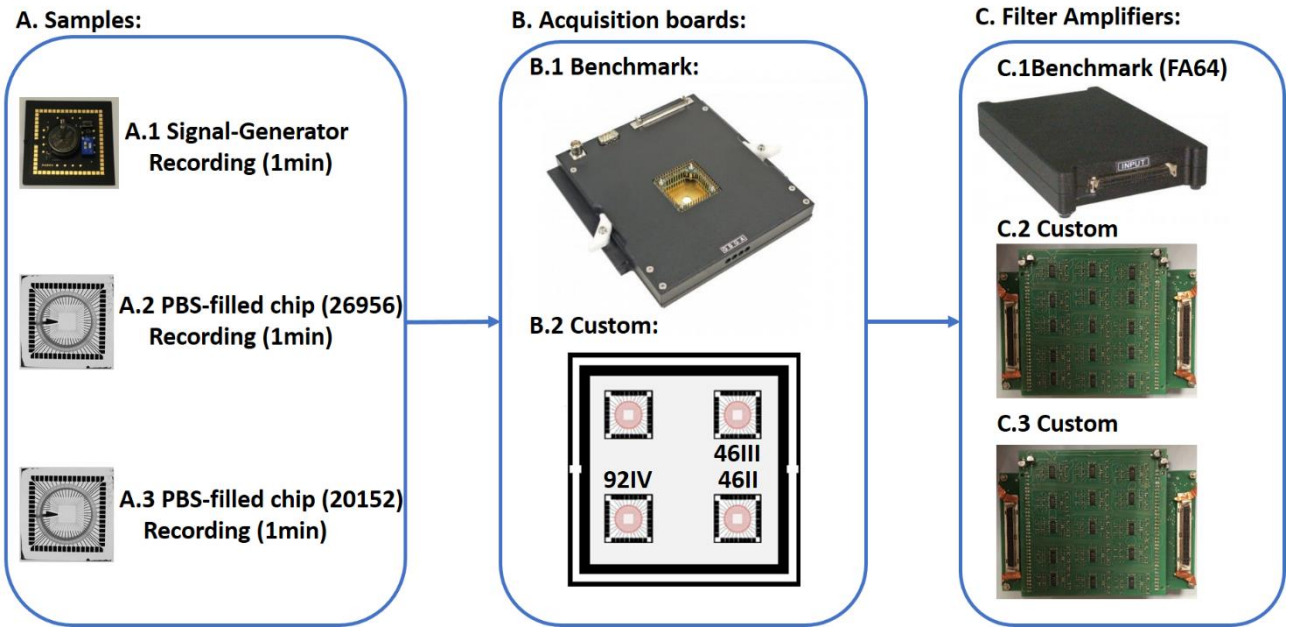

Figure 2.19 Validation Test protocol. Three samples are used to test simultaneously three custom boards of the bioreactor. . In the first panel (A) is described the equipment used for validating the setup. The second panel (B) shows the commercial pre-amplification board (Benchmark) and the custom culture chamber with the three boards used, each one indicated with its gain (eg. 46, 92). The third panel (C) shows the Benchmark and the custom Filter Amplifiers (FA) used in this work.

To test the possibility to make acquisitions in parallel, these two kinds of test are performed at the same time with different boards, using both USB-ME64-System and USB-ME128-System for the data acquisition[4]. Unlike the benchmark case, the three Filter Amplifiers available are used simultaneously, one per each acquisition board, repeating the acquisition in order to get all the couplings between boards and FA possible. The entire acquisition protocol is recapped in *Fig. 2.19.* It describes how to obtain different acquisitions turning over the chips and the SG with all the boards, thus obtaining, for each coupling between boards and FA, a recording from SG and a recording from PBS-filled chips.

Once all the necessary data are obtained, we have performed an analysis to get a comparison between the benchmark signal and those produced by the custom set-up. The qualitative part of the analysis is done directly thanks to MC_Rack replay mode.

Specifically, qualitative analysis focuses on:

- Comparison between benchmark and custom set-up noise band amplitude;
- Comparison between benchmark and custom set-up spike amplitude;
- Comparison between benchmark and custom set-up parameters extracted;

First, it is useful to extract a truth table regarding fake spikes correctly detected, to do a comparison with the custom setup in specificity and sensitivity. With the following features:

- True Positive (TP): spikes generated by 60MEA-SG. On a time-window of one minute, with a frequency of 0.5Hz, max[TP]=30;
- True Negative (TN): time instants in which spikes are correctly absent. On a time-window of one minute, with a frequency of 0.5Hz, max[TN]=30;
- False Positive (FP): spikes wrongly detected, i.e. spikes which are not generated by 60MEA-SG;
- False Negative (FN): spikes wrongly absent, i.e. spikes which are generated by 60MEA-SG but not detected by the acquisition system.

It is then possible to extrapolate statistical measures of the performance of a binary classification test (classification function):

- *Sensitivity* (true positive rate) measures the proportion of positives that are correctly identified as such;
- *Specificity* (true negative rate) measures the proportion of negatives that are correctly identified as such;
- *Precision* (positive predictive value) is a description of random errors, a measure of statistical variability;
- *Accuracy* (trueness) is a description of systematic errors, a measure of statistical bias;

The statistical measures are calculated as follows:

$$\text{Sensitivity (TPR)} = \frac{TP}{TP + FN} \qquad \text{Specificity (SPC)} = \frac{TN}{TP + FN}$$

$$\text{Precision (PPV)} = \frac{TP}{TP + FP} \qquad \text{Accuracy (ACC)} = \frac{TP + TN}{TP + FP + TN + FN}$$

To check the quality of the signal through the entire pathway, a series of tests have been conducted on the chamber. These tests consisted in a one or five-minute-long recording for all the four boards,

[4] Cf USB-ME64-System_Datasheet, USB-ME128-System_Datasheet

once with a MEA signal generator and then with a chip filled with a physiological solution. Then, the same recordings are repeated with a commercial pre-amplifier, in order to obtain a benchmark useful for a comparison. After the acquisitions, the signals generated are analysed first qualitatively and then quantitatively.

The quantitative analysis of the signals is computed thanks to the algorithms for MATLAB, developed in previous works [14], [10].

First, it is necessary to convert MC_Rack files (.mcd file format) in files that can be read by MATLAB (.mat file format)[1].

After extracting a single file per channel with the recording saved in .mat extension. Then, quantitative analysis involves MATLAB scripts for Root Mean Square (RMS) estimation, assuming Gaussian noise. A sampling frequency equal to 25KHz is used. The algorithm follows the following steps:

1. Peak-to-peak value estimation and RMS starting from a noisy signal, computed on a 10ms time window;
2. Power Spectral Density (PSD) area computation for RMS estimation, using Bartlett method;
3. Cutting bandwidth from 48 Hz to 52 Hz, in order to avoid disturbances due to AC from energy suppliers;

The second set of scripts are used to estimate Signal-to-noise ratio (SNR) per each channel.

This protocol for the evaluation of signal quality has been applied before and after the installation of the support bases inside the culture chamber.

The tests are grouped according to the Filter Amplifiers used during the acquisition:

- Benchmark (Multichannel System MCS): FA64;
- First Custom Filter;
- Second Custom Filter.

For each one the following groups we show:

- MC_Rack total acquisition window;
- Single channel window;
- PSD analysis averaged over 60 channels;
- Window of the reference channel 15;
- PSD analysis of the channel 15.

Each screen shows four windows, one for each pre-amplification board.

Subsequently a Signal-to-Noise Ratio analysis has been performed.

After digital signal filtering (300 Hz-3kHz, Butterworth 2nd order), spikes are detected comparing voltage values with a threshold appointed to -5 times the standard deviation of signal computed in the first 500ms of recording. Then, the SNR of firing electrodes is computed as the ratio of the peak-to-peak amplitudes of spikes by the standard deviation of signal computed over the first 500ms[48].

In *Table V* we report meaningful outputs obtained from algorithm of analysis of the SNR:

- Amplitude ratio: ratio, in absolute value, of the maximum value on the minimum;
- Amplitude spikes: difference between the maximum value and the minimum;
- Spike width: difference, in absolute value, between the spike instants divided the sampling frequency (10KHz);
- Noise esteem: $\sqrt{\frac{1}{\frac{f_s}{2}*\sum y^2}}$;
- SNR= $20 * \log\left(\frac{\text{Amplitude\_spikes}}{6*\text{Noise\_esteem}}\right)$

The first four rows are the benchmark acquisitions (BB). In case of missing values, the algorithm reports *NaN*.
We show spike waveform representations grouped for Filter Amplifier used in test (red in labels). In the upper part, there are recordings with spiking activity spotted with red lines, whereas in the lower part we show the fake spike waveforms detected by the algorithm with a red line indicating the average value respect the noise amplitude.

2.6.2 PBS- filled chip qualitative test

The second testing part involves a MEA chip filled with Phosphate-buffered saline (PBS). Its uses include substance dilution and cell container rinsing, and thanks to its ions concentration, it has a good conductivity and helps the impedance adapting between cells and electrodes. In fact, its resistivity is $\rho \approx 66 \Omega cm$, equivalent to silicon doped with 10^{14} cm^{-3}. The entire acquisition protocol is recapped in *Fig. 2.19.*
During the test conducted with the PBS-filled MEA chip, the recordings are acquired in an incubator-like environment, in order to check how the humidity, temperature and CO_2 influence the electrodes' behavior. We checked even the parallelism performance of the setup, through the three Filter Amplifiers and the analog-to-digital converters available, to ensure the system's ability to execute multiple acquisitions.

2.7.Neurophysiological trials

2.7.1. Preparation of the bench top system

In order to guarantee optimal conditions of the bench-top system's parts that hosting the MEA chips, a sterilization protocol has been developed. First, the inner part of the culture chamber is filled with 75% ethanol. The same diluted solution is used to plunge all the plastic and metal parts (air valves, injection inlets, chip bases etc.), which are removable from the setup. These can be dry heated (110°C, ~3h), whereas the culture chamber is dried with a hood, because PMMA is not suitable for dry heating. Then, all the components are exposed to UV light overnight. Regarding the fluidic parts, the water-bath flows a 0.1% bleach solution overnight through the entire pathway (water-bath→ pipes→ bioreactor cavity). The same bleach solution is used to clean the components that constitutes the humidifying and heating module.
Once completed the sterilization procedures, the water bath is filled with bi-distilled water 0.05% bleach, whereas the humidifier's bottle is filled with *Salf* water.

2.7.2. Preparation of the hippocampal neural cells culture

The cells chosen for the neurophysiological trials are hippocampal neurons from mouse prenatal embryos (E18), widely used in MEA recordings[25], [17]. Animal handling have been performed in accordance with San Raffaele Scientific Institute guidelines and with an approved IACUC protocol number 694.

Regarding the plating protocol, it is briefly resumed[48]:

1. Day 1:
   - Plating medium, 1mL [2h];
   - PBS washing;
   - Poly-L-Lysine (400 µL) [Overnight]
2. Day 2:
   - Dispose Poly-L-Lysine;
   - PBS washing;
   - Plating medium, 1mL [Few hours]
3. Day 3: (0 DIV)
   - Plating cells [idle 4h];
   - Check adhesion;
   - Dispose Plating medium;
   - Culturing medium

The MEA chips have been set submitting them to a plasma treatment and dry heating them at 110°C for few hours.
The acquisitions have been repeated at 12 DIV (*Days In Vitro*) and 18 DIV.

2.7.3. MC_Rack acquisition and analysis

First, the benchmark acquisitions are performed. The setup and methods used are described in paragraph 2.1 (*Fig.* 2.1). After positioning the chip in the commercial (Benchmark) board and putting the dome with the airflow above it, there are 10 minutes of waiting time to let the cells reaching stationary conditions. Then three recordings are performed, each of them 5 minutes long, reaching 15 minutes long acquisitions.
The benchmark acquisitions have multiple aims. First, checking chip quality: it has been checked the noise bandwidth of all the channels, verifying that its range is below ±20µV. Besides, it has be assured the right grounding of reference pin 15, showing the flatness of its bandwidth in all the chips. Then, it is important to identify the ratio of working channels, assuring the availability of at least the 80% of electrodes, i.e. at least 48 on 60 channels.
The second aim of benchmark recordings is monitoring cultures activity during different days in vitro and setting a standard for the custom registrations in the same time window.
Once all the chips have been verified with the commercial board, the custom setup is used for the registrations. The environmental features described in literature for a better cellular survival are quite different respect to the air parameters (O_2~21%, CO_2~0.04%) [2], [4]. In order to reach and maintain stationary conditions and to test all the custom boards with the entire chip set at disposition, the protocol described in *Fig. 2.20* is applied:

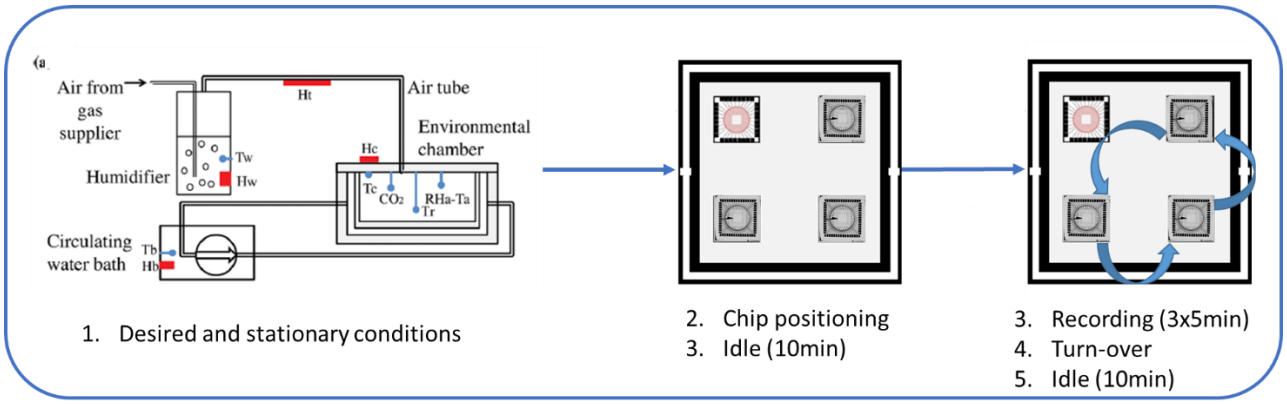

Figure 2.20 Neurophysiological trial acquisition protocol.

For each chip placement, in order to compare benchmark and custom setups, multiple acquisitions of chips have been performed in parallel. This protocol increases considerably the time interval between benchmark acquisitions and the custom one. However, it is necessary because it allows to check the capability of the setup to acquire from three different sources, as well as the performance of the PC under stress. Besides, with this approach it is possible to check if the three boards interfere with each other. During all the recordings, the machine used (Windows 7 desktop computer - Intel® Core™ i5-2500 - 3.3GHz CPUs, 4GB RAM,) has proved capable of performing multiple acquisitions with good performances, and the boards did not present any form of interfence among them. In order to isolate and study how each one of the variability factors influences the analysis of neuronal activity, several acquisition protocols have been developed and applied during physiological trials.

A pre-processing performed with MC_Rack is carried out. One of its tools consists in customizing the spike detection selecting the factor for which multiplying the standard deviation (SD) for thresholding, depending on the distribution of noise. This represents a useful tool in case of spurious spikes that are not biological. In order to demonstrate if the spikes recorded in the custom board are real or spurious, i.e. generated by a non-biological noise source, there are many options. One of them is to inject in the culture a voltage dependent sodium channels inhibitor with tetrodotoxin, to see if the activity stops after the injection. Another way is to study the waveform recorded by the software and to check if reflect the behaviour of an action potential. To isolate and study this computational variability factor we have analyzed the recordings on a single chip and in the same time interval with the benchmark system and a custom board. Then, using MC_Rack, we analyzed the data using the same thresholds except the SD. The timestamps so obtained have been used in the MATLAB algorithm for features parameter, thus obtaining different comparable values.

Another test is performed to compare cells activity at different DIVs. For a better comprehension of the network activity, once spike detection is applied to the all MEA channels, it is possible to observe a picture of the spatio-temporal distribution of spiking neuronal activity throughout the experiment, referred to as raster plot.

For each parameter, we report different mean values in a template. Among all the features described before, in paragraph 2.2.2, we have selected seven particularly meaningful:

- Active channels
- Spikes number
- Bursting percentage
- Inter Burst Frequency (IBI)
- Network Bursting (NB) rate
- NB duration
- Burst duration

After reporting their values and means during the acquisition, we have analysed four of them using boxplots, in order to look for correlations and differences between custom and setup outputs, different days *in-vitro* and different threshold used during analysis.

A Wilcoxon matched pair test computation has been integrated in the analysis[48] [52]. The MATLAB function *ranksum* returns the p-value of a two-sided Wilcoxon rank sum test. R*anksum* tests the null hypothesis that data are samples from continuous distributions with equal medians, against the alternative that they are not. The test assumes that the two samples are independent. This test is equivalent to a Mann-Whitney U-test. *Ranksum* also returns a logical value indicating the test decision. The result h = 1 indicates a rejection of the null hypothesis, and h = 0 indicates a failure to reject the null hypothesis at the 5% significance level[5]. This means that p-value lesser than 0.05 indicates that *ranksum* rejects the null hypothesis of equal medians at the default 5% significance level. The tests performed with custom setup have as filter amplifier the commercial FA64, in order to guarantee the comparison only among pre-amplification boards.

Finally, through a 5x differential interference contrast image (DIC), photos of the substrate have been acquired, in order to check the status of the cells after their stay inside the bioreactor. This step is also useful to check any correlation between recorded activity and cell population inside the chip.

[5] Cf. https://it.mathworks.com/help/stats/ranksum.html

2.7.4 iPS trial

The final part of neurophysiological trials regards the study of human induced pluripotent stem cells (hiPSc) with MEA technology approach. The cells involved in this part are developed thorugh a differentiation and maturation process created with the protocol described in [53]. The process is divided into two main phases: the first one, which is 14 DIV long, consists in a differentiation process of the cells. According to the protocol, during the early stage of differentiation the cells need to be maintained inside an environment with 5% O_2 and 5% of CO_2, which are different conditions of typical cell incubators. The second phase, instead, runs until 26 DIV, and consists in a maturation process through growth factors administration [53]. According to *Meneghini et. al.*, in brief:

hiPSCs are detached with dispase (Thermo Fisher Scientific Life Sciences) and cultured as embryoid bodies (EBs) in EB medium. On day 4, EBs are plated on Matrigel-coated chips and grown in EB medium supplemented with NOGGIN (250 ng/ml)[53]. All cultures are 14 DIV, corresponding to the first phase of the protocol: the differentiation process. In *Table II* we report a list of three chips used. It includes cell type, i.e. specific treatements applied during differentiation, and source:

Table II iPS CELLS CHARACTERIZATION

Chip	Type	Source
25041	8#+	Patient-Correct
26957	WT-SAN5	Normal Donor
19155	FMLD-31	Patient

In order to perform the most accurate analysis, given the observed electrophysiological activity during a preliminary acquisition with the benchmark setup, we have chosen a higher scale on the windows used. During the MC_Rack first analysis stage, for the longterm acquisition windows, we have used a ±50 µV scale in an intervalof 5 min. For waveform windows, we have used ±100 µV in a range of 3ms. We report some meaningful screenshots in paragraph 3.3.4. Regarding thresholds parameters for the spike detection, a standard deviation factor of 5*SD has been used. With lower values (4.5*SD) the systems acquires also noise waveforms generating artifacts, whereas with higher values (6*SD) no activity is detected.

Besides, a comparison in terms of SNR has been performed, with the same MATLAB script described in paragraph 2.6, regarding acquisition system validation. The comparison has involved the same channel of one chip for benchmark and custom systems. Channel 66 has been chosen for its constant electrophysiological activity, proved by the waveforms registered with the commercial board.

More acquisitions have been performed at later DIVs, to check if maturation process leads to recognizable activity.

Furthermore, through a 5x differential interference contrast image (DIC), photos of the substrate have been acquired, in order to check any correlation between cells population and distribution with their electrophysiological activity and features registered.

3. Results

We present as results different meaningful outcomes of the validation tests conducted on the bioreactor, grouped into environmental tests, acquisition system tests and neurophysiological trials. In the environmental tests, we demonstrate that the bench-top system is capable to set and maintain stable vital conditions for the entire period of a long-term study. Regarding the acquisition system tests, we present a rich set of acquisitions, conducted both with the Signal Generator and with PBS-filled chips, with all the possible couplings between boards and filters. The quality of the signal, and its comparison with the benchmark system, are described in term of Power Spectral Density, Signal-to-Noise Ratio and waveforms acquired. To conclude, all the boards have been used for trials on hippocampal neural cells and hiPSc. These last tests include also a description of different variability factors that influence the analysis of the neurological activity. For each of these factors, it has been developed an approach of analysis, which allows to isolate and to study its impact on the features extracted from a cell-culture.

3.1. Validation of the environmental control system

In this paragraph the values of three main environmental parameters during a long-term test (26 hours) are shown, which demonstrate that their optimal ranges are kept for all the period with negligible oscillations. Minimum value, maximum value, mean and standard deviation of each environmental parameter are summarized in *Table III*. In it, it is possible to appreciate a very low variance of all values throughout the acquisition, assuring a suitable environment for cells even in case of long-term experiments. Regarding the evaporation test with the medium, we monitored an evaporation rate less than 15% per day. This quite high value is probably due to a non-optimal sealing of the inlets. Anyway, we have decided to overcome this issue with the adoption of improved PDMS caps, which have guaranteed an optimal sealing during biological trials.

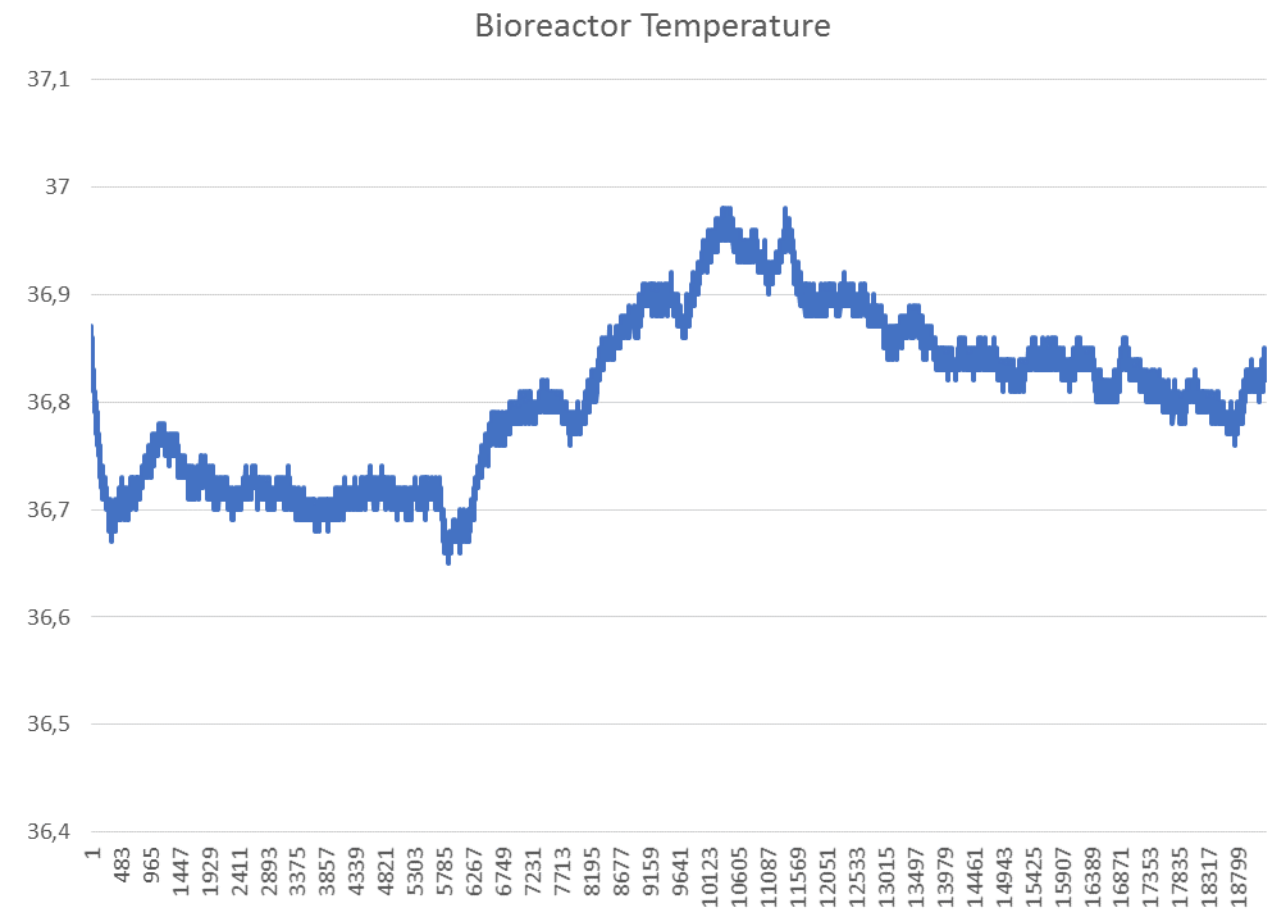

Figure 3.1 Temperature values inside bioreactor for 26 hours monitoring. Sampling frequency= 0.2 Hz

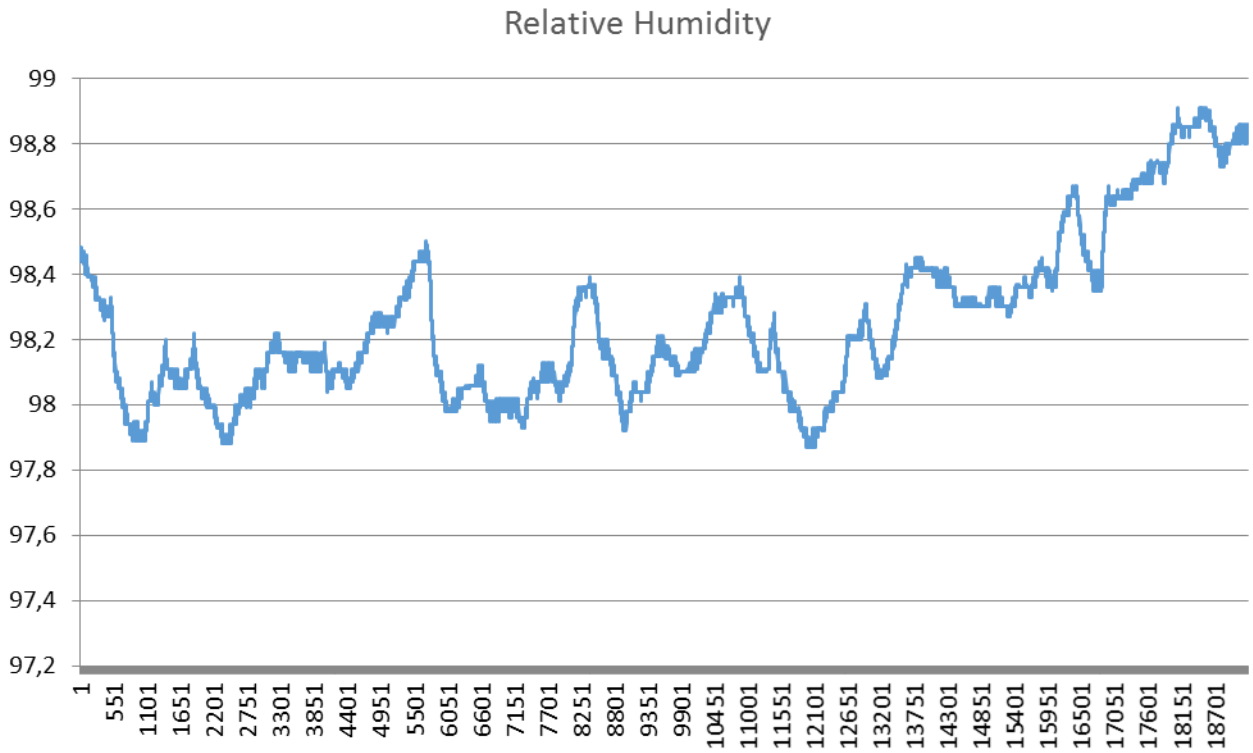

Figure 3.2 Relative humidity values inside bioreactor for 26 hours monitoring. Sampling frequency= 0.2 Hz

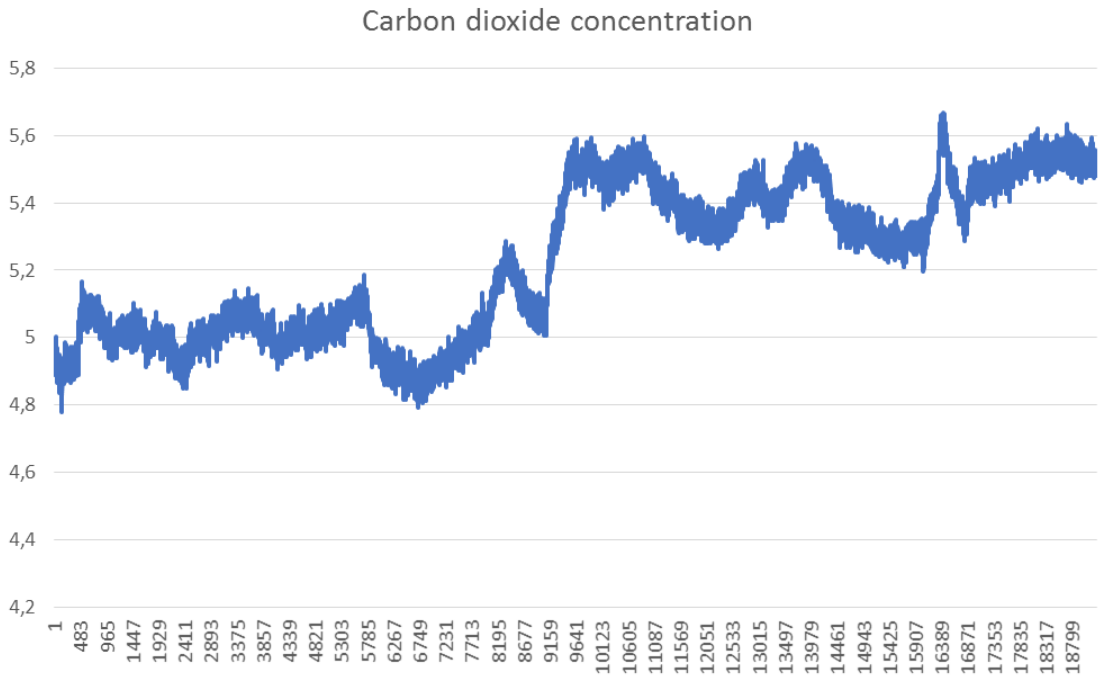

Figure 3.3 CO_2 concentration values inside bioreactor for 26 hours monitoring. Sampling frequency= 0.2 Hz

Table III ENVIRONMENTAL PARAMETER ANALYSIS

Environmental Parameters	min	max	Mean	Std Deviation
T [°C]	36,65	36,98	36,81	0,08
CO_2 %	4,781	5,669	5,23	0,23
Rh %	97,87	98,91	98,25	0,29

3.2. Setup validation

3.2.1. Signal Generator (MEA-SG) test

Table IV SPIKE DETECTION STATISTICAL MEASURES

Truth table	TP	TN	FP	FN	Sensitivity	Specificity	Precision	Accuracy
Dummy_BB_BF	26	34	0	2	0,93	1	1	0,97
Dummy_BB_FF	30	30	0	0	1	1	1	1
Dummy_BB_SF	30	30	0	0	1	1	1	1
Dummy_46II_BF	30	30	0	0	1	1	1	1
Dummy_46II_FF	27	33	1	3	0,9	0,97	0,96	0,94
Dummy_46II_SF	30	30	0	0	1	1	1	1
Dummy_46III_BF	30	30	0	0	1	1	1	1
Dummy_46III_FF	27	33	0	3	0,9	1	1	0,95
Dummy_46III_SF	1	59	1	1	0,5	0,98	0,5	0,97
Dummy_92IV_BF	30	30	0	0	1	1	1	1
Dummy_92IV_FF	27	33	1	3	0,9	0,97	0,96	0,94
Dummy_92IV_SF	29	31	1	1	0,97	0,97	0,97	0,97

Table IIII Statistical values extrapolated during the SG test. In the first column is described the components of the acquisition system during the single test: BB (Benchmark Board), BF (Benchmark Filter), FF (First Custom Filter), SF (Second Custom Filter).

Regarding the test conducted with the MEA-SG, it is possible between the benchmark and the custom system in terms of spike detection parameters (*Table IV).* Subsequently, we also report *Table V* to appreciate the similarities in signal amplitude and shape. Compared to the benchmark system, all the three boards show a constant and predictable behaviour. These results are shown in figures from *3.4* to *3.10*. In this paragraph we report only the most significative windows; a complete set of test screenshots is reported in Appendix at the end of this thesis.

For each board-FA coupling (described on the top of the figure) we show:

- Long-term windows comparison;
- Single channel comparison;
- PSD comparison;
- Reference channel 15 comparison;
- Spike detection and waveform comparison.

At the top of each block of figures, it is reported a brief description of the system used to perform each acquisition. Each of them is performed with the new printed support (Base) installed on the bottom of the bioreactor. Then, it is indicated the sequence until the type of Filter Amplifier used, written in red. Each panel, in the upper left, has the abbreviation of the pre-amplification board used. Longterm windows are reported with the same scale, to better compare the spike generated in respect to the basal band:

- Longterm window: ±100µV x 60s;

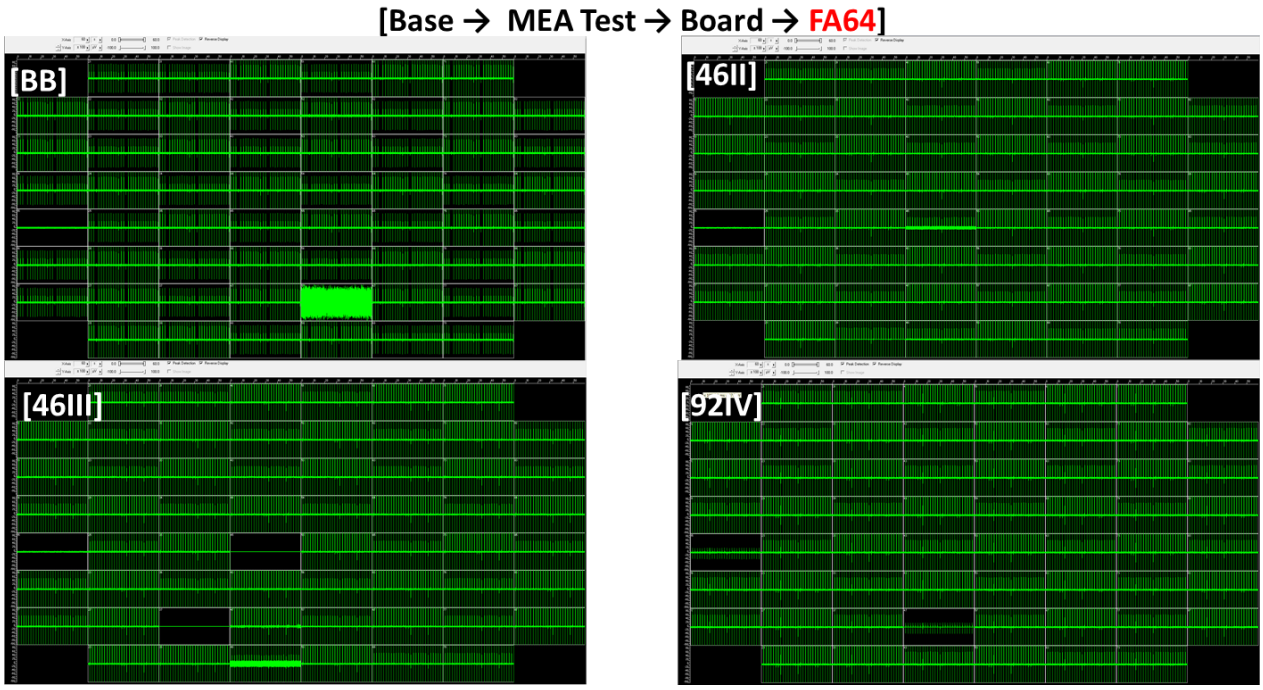

Figure 3.4 Signal Generator Test. MC_Rack long term acquisition window. Benchmark board (BB) coupled with FA64 Filter Amplifier, consistutes the reference system.

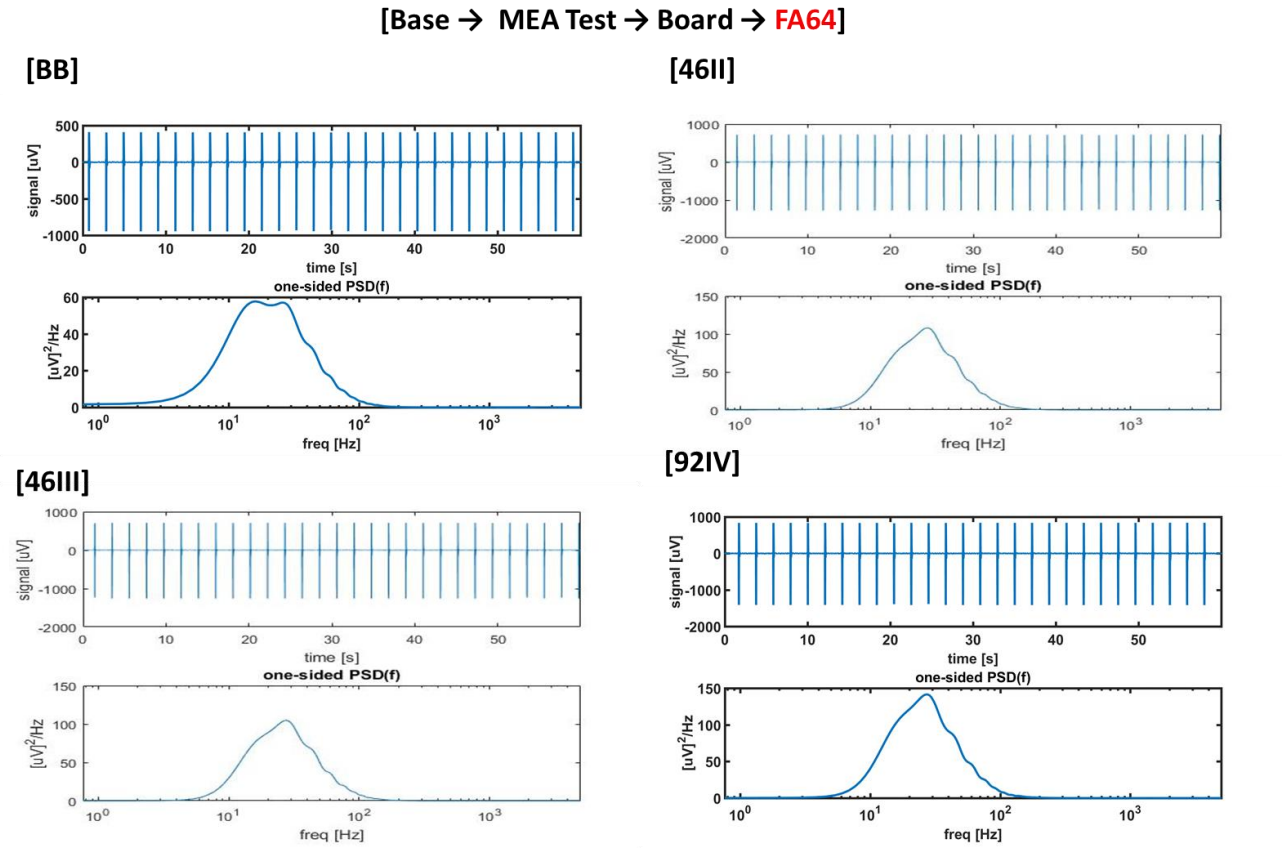

Figure 3.5 Signal Generator Test. PSD analysis averaged over 60 channels. Benchmark board (BB) coupled with FA64 Filter Amplifier, consistutes the reference system.

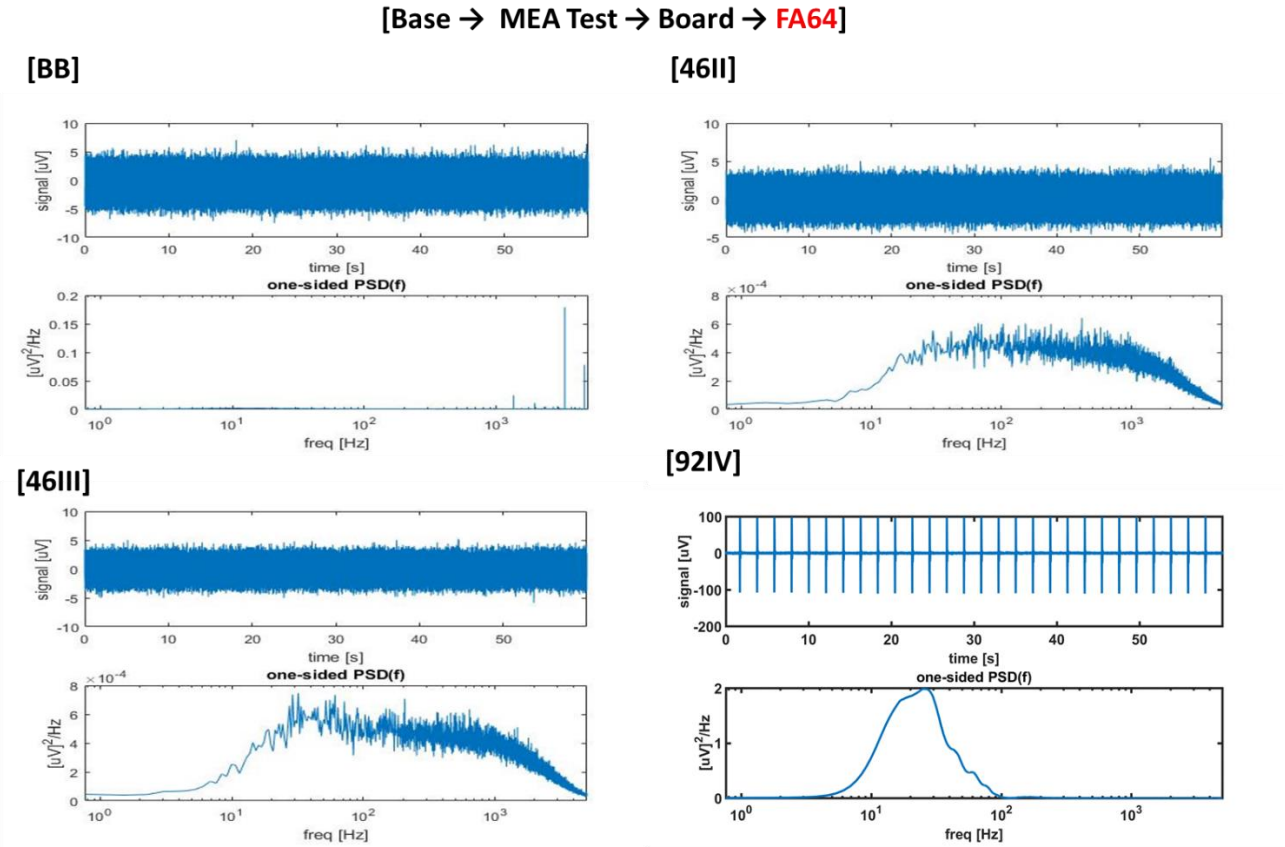

Figure 3.6 Signal Generator Test. PSD analysis on reference channel 15. Benchmark board (BB) coupled with FA64 Filter Amplifier, consistutes the reference system.

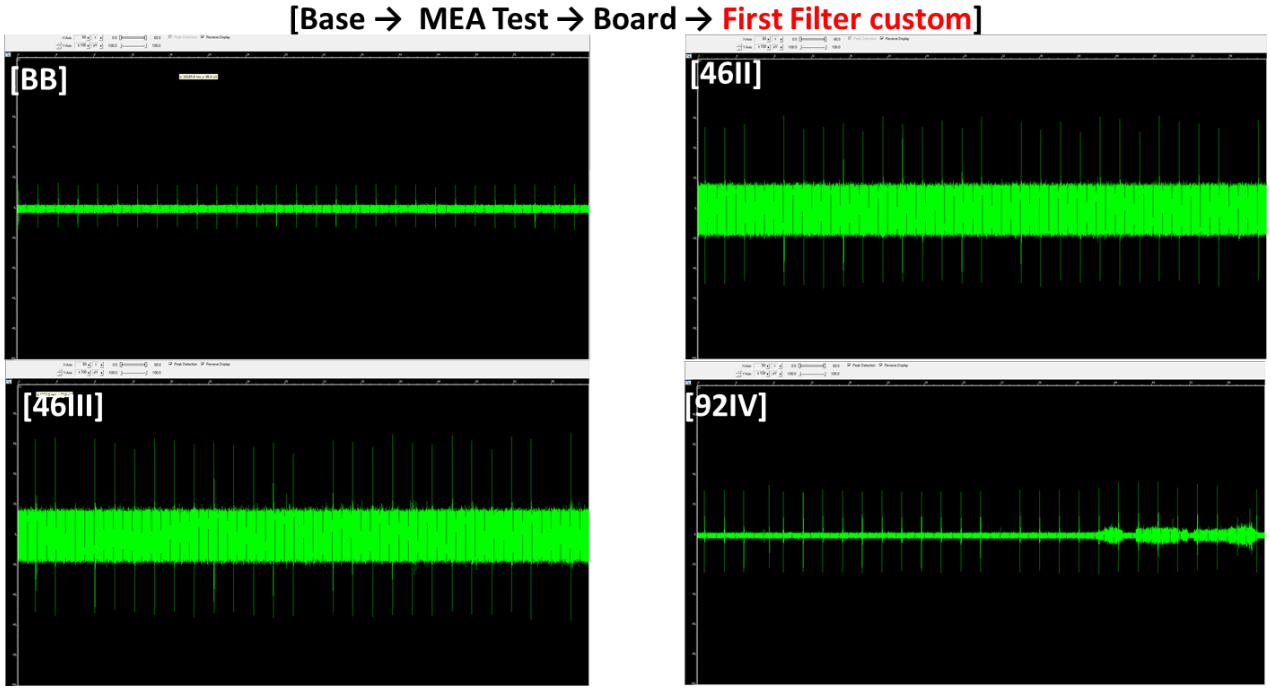

Figure 3.7 Signal Generator Test. Single channel window.

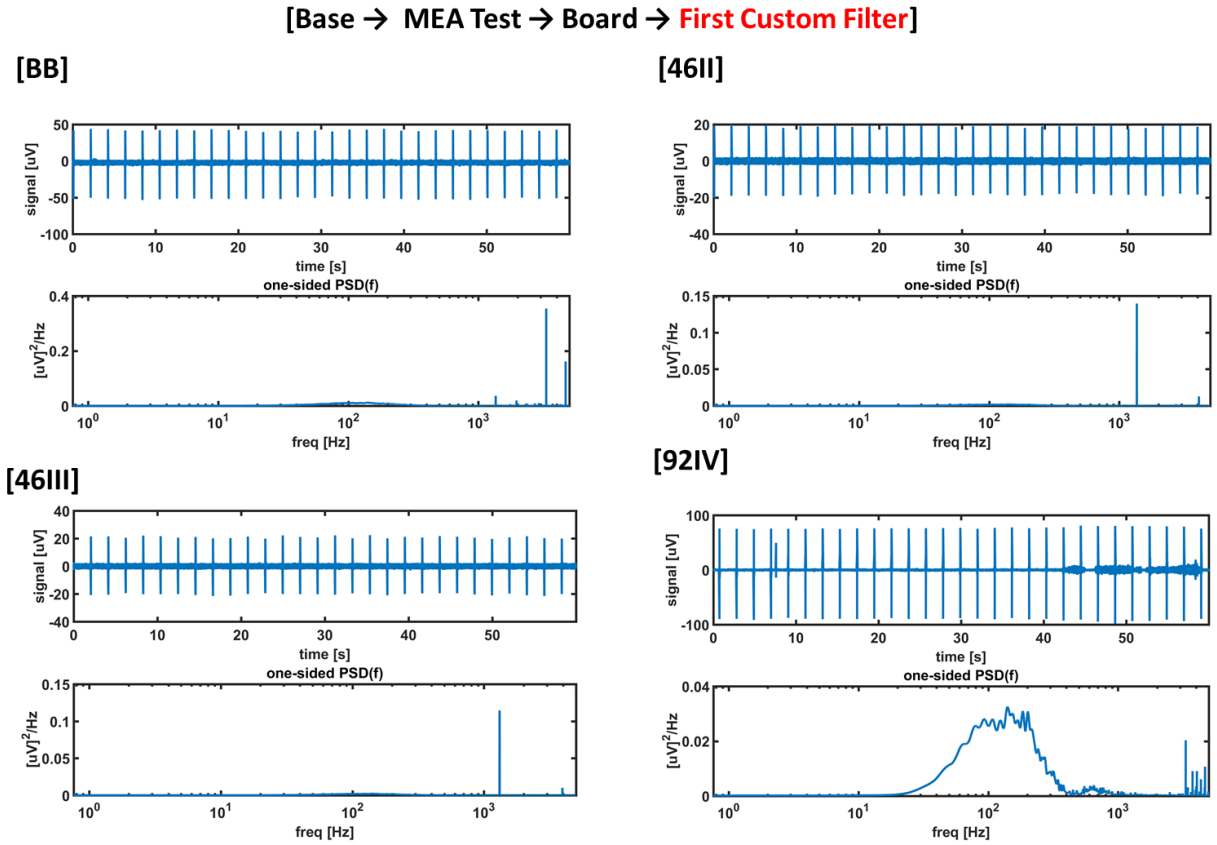

Figure 3.8 Signal Generator Test. PSD analysis averaged over 60 channels

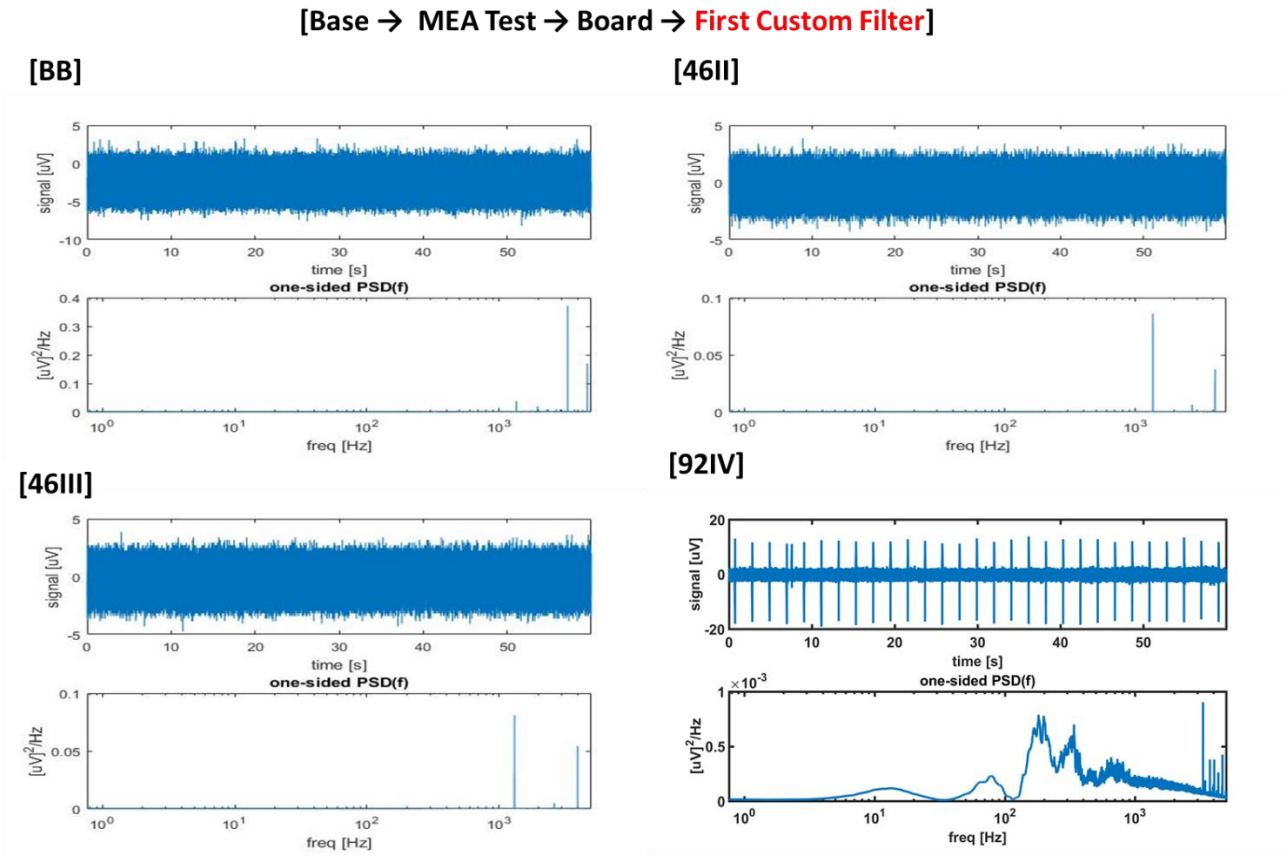

Figure 3.9 Signal Generator Test. PSD analysis on reference channel 15

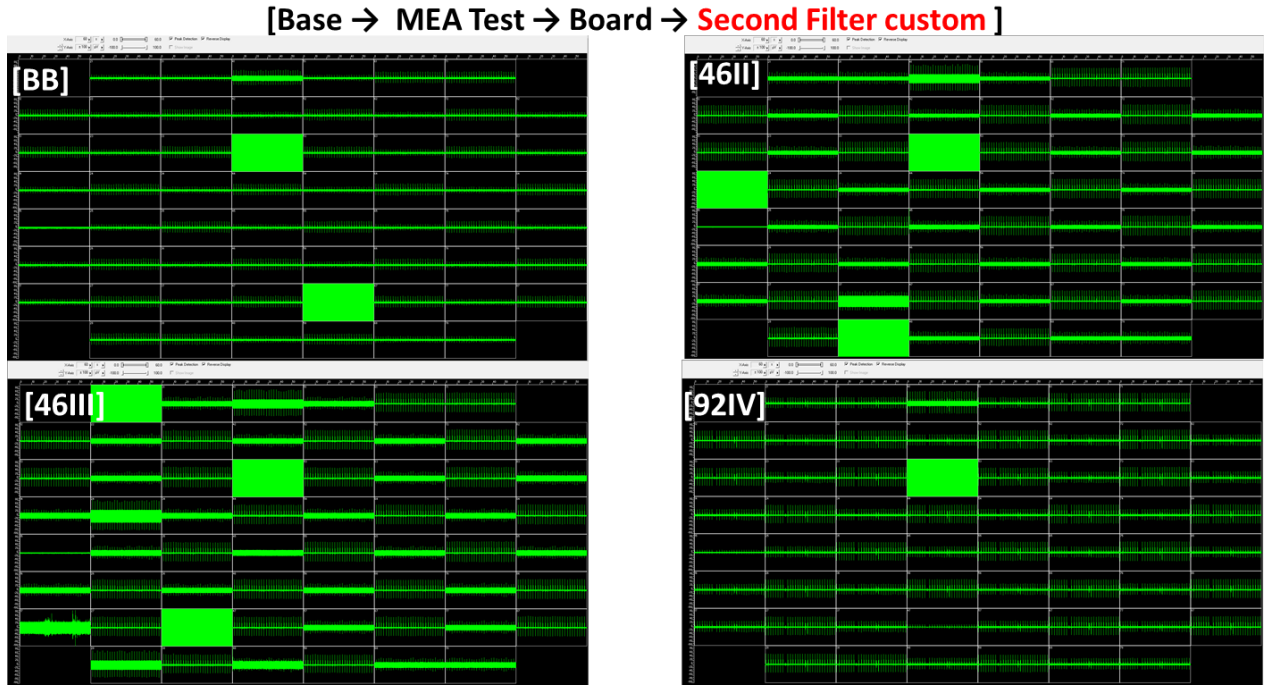

Figure 3.10 Signal Generator Test. MC_Rack long term acquisition window

It is possible to appreciate the similarities between the benchmark and the custom systems, both in terms of signal amplitude and shape. Regarding the test conducted with the signal generator, it is possible to note same amount of background noise, and the same shape of spikes generated by the MEA-SG.
However, there are remarkable differences among the various couplings. For instance, board 92IV presents an interference on ground pin (15), which seems to record the signal coming from the other channels, albeit at reduced amplitudes *(Fig.3.6-3.9)*. In general, a uniform presence of peaks in the PSD can be seen in the neighbourhood of the same frequencies (~10^3Hz). The amplitude variability depends on the couplings among boards and FAs and the scalability ratio performed by MC_Rack. There are not channels that are constantly unusable, in terms of large noise or no signal. The disturbances found during the test acquisitions on some channels are transitory. In detail, 92-10-4K8 IV board seems to present a slightly higher number of artefacts, probably due to its higher amplification factor, that is possible to note even on the signal depicted in the PSD analysis (*Fig. 3.8-3.9*).

Compared to the other two FAs, the Second Custom Filter Amplifier exhibits lower performances, both in terms of broad spectral density and reduced SNR. An exception is the coupling with the board 92IV (*Fig. 10*). In detail, board with higher amplification factor seems to exhibit a slightly higher number of artefacts that is possible to identify even on the signal averaged in the PSD analysis. Besides, it is possible to note same amount of background noise, and the same shape of spikes generated by the MEA-SG.

All channels have a white noise band with amplitude minus than ± 20μV.

Regarding the SNR analysis, we show the results gathered in *Table V* and in schemes depicted in Fig. *3.11 and 3.12*.

Table V SPIKE DETECTION PARAMETERS

SNR analysis	Amplitude ratio	Amplitude spikes	Spike width	Noise esteem	SNR	Channel
Dummy_BB_BF	0,0011	8,27	1,00E-03	1,30	4,20	12
Dummy_BB_FF	0,0614	21,42	0,0012	3,28	1,98	12
Dummy_BB_SF	0,4973	24,88	0,0018	1,47	7,45	12
Dummy_46II_BF	0,3262	0,27	0,0011	0,97	6,97	12
Dummy_46II_FF	NaN	NaN	NaN	11,69	-2,71	66
Dummy_46II_SF	0,3036	18,19	9,00E-04	4,73	-1,26	17
Dummy_46III_BF	0,2944	9,53	0,0011	1,08	6,26	12
Dummy_46III_FF	0,2538	43,21	1,00E-03	11,22	-2,47	12
Dummy_46III_SF	0,6893	17,35	1,00E-03	1,35	7,62	33
Dummy_92IV_BF	0,3092	10,42	1,00E-03	1,06	7,23	12
Dummy_92IV_FF	0,3203	5,41	4,00E-04	0,68	6,28	12
Dummy_92IV_SF	0,3555	7,92	9,00E-04	0,74	7,22	12

Table V SNR e Spike detection values extrapolated during the SG test. In the first column is described the components of the acquisition system during the single test: BB (Benchmark Board), BF (Benchmark Filter), FF (First Custom Filter), SF (Second Custom Filter).

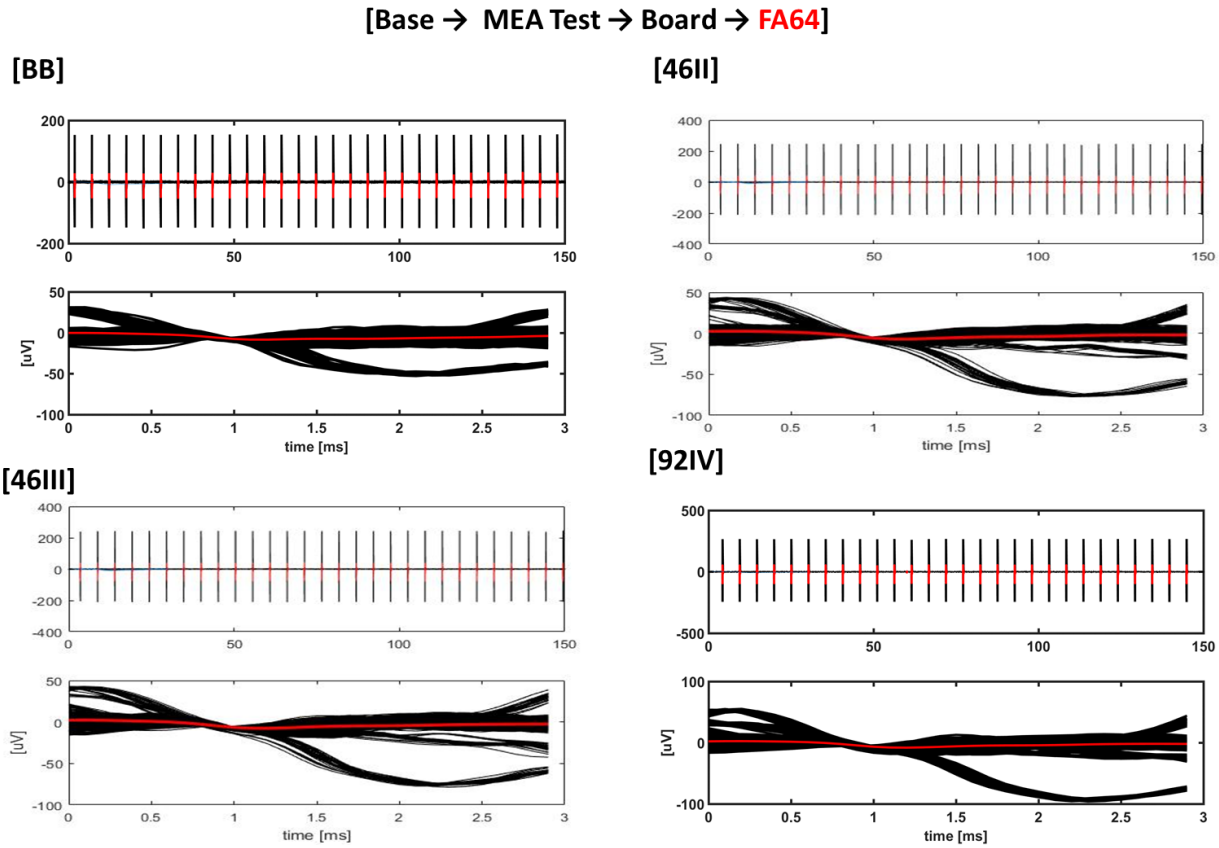

Figure 3.11 Signal Generator Test. Comparison between Spike waveforms. The first row in each panel shows averaged signal and spikes detected (in red). The second row shows spike waveforms. Waveforms detected as spikes (EPSP) are highlighted in red over signal representations.

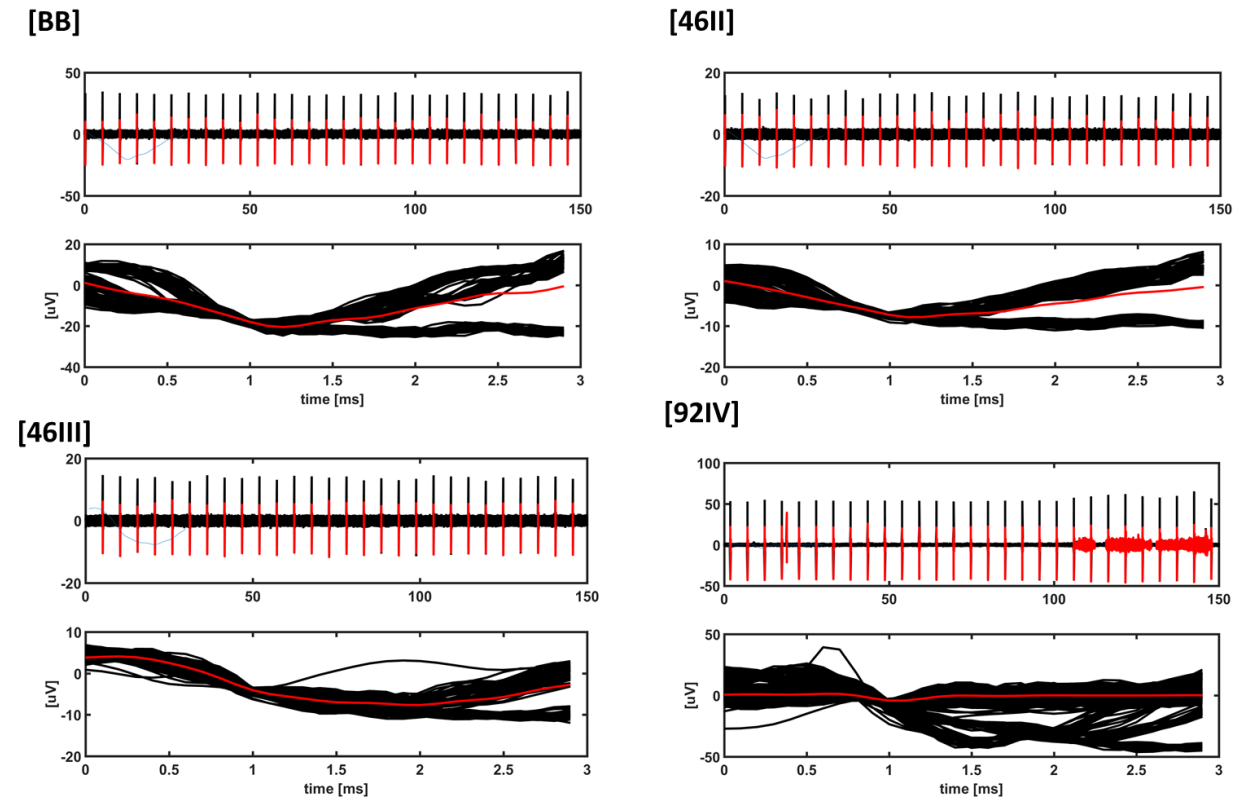

Figure 3.12 Signal Generator Test. Comparison between Spike waveforms. The first row in each panel shows averaged signal and spikes detected (in red). The second row shows spike waveforms. Waveforms detected as spikes (EPSP) are highlighted in red over signal representations.

In the presence of negative SNR values (cf. Dummy_46II_FF, Dummy_46II_SF, Dummy_46III_FF), the algorithm detected only waveforms with negative peaks respect to the noise band.

3.2.2 PBS-filled chip qualitative test

Regarding the acquisition conducted with the PBS-filled MEA chip, shown in *Fig. 3.13-3.14*, it is clear how the background noise (assumable as a white noise) level of the two systems is quite the same, included in a range of ±20 µV.

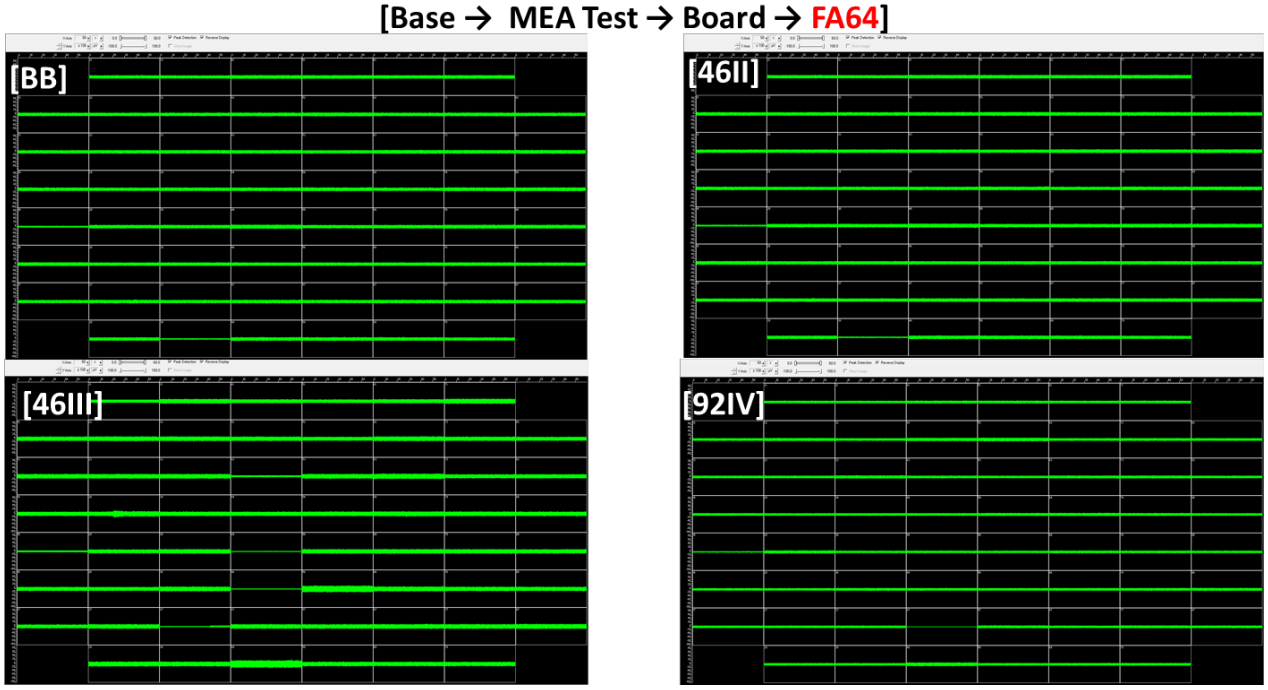

Figure 3.13 PBS-filled chip test. MC_Rack long term acquisition window

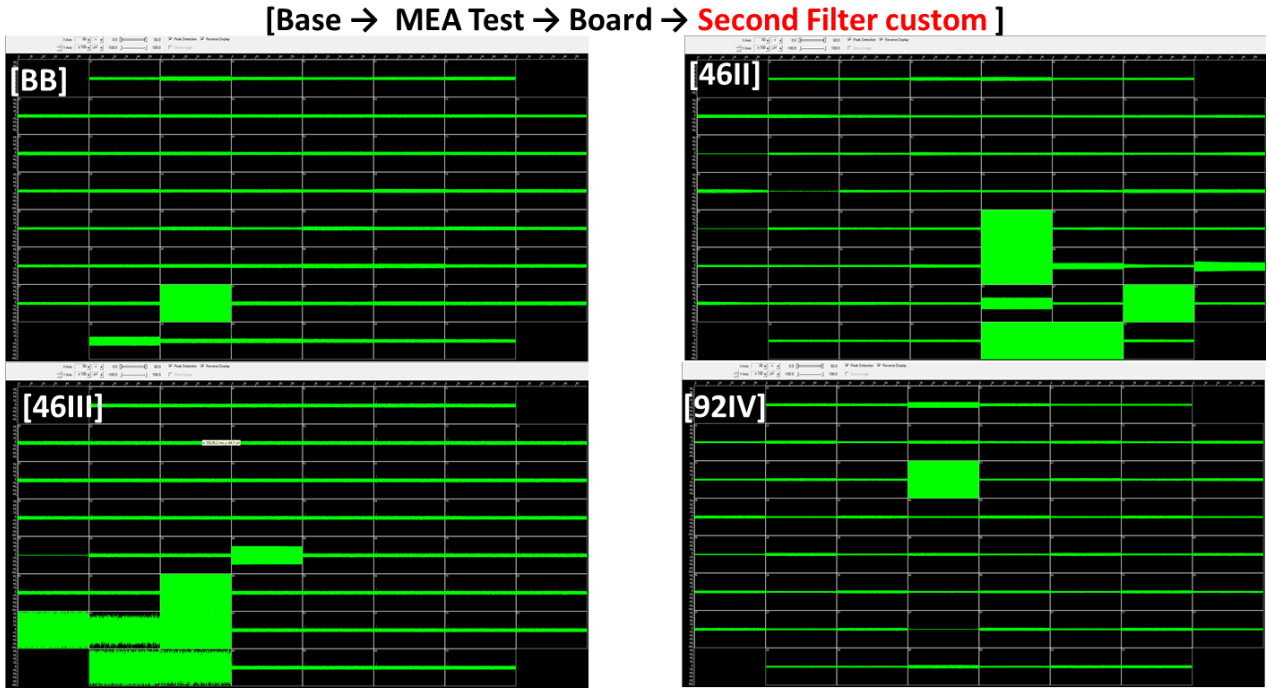

Figure 3.14 PBS-filled chip test. MC_Rack long term acquisition window

The second custom filter continues to have a performance that is worse than the other ones, even due to the presence of large noise band. The board 92IV constitutes an exception (*Fig. 3.14*).
There are not channels that are constantly disturbed. The anomalies found during the test phase on some channels are transitory. All channels have a white noise band with amplitude less than ±10μV.

3.3. Neurophysiological trials

In this paragraph, we report some meaningful features extracted during neurophysiological trials on cultures of hippocampal neurons from mouse prenatal embryos (E18). According to literature [13], [17], 12DIV is a common time step for the onset of recordable spiking activity. However, it is possible to note an oscillating electrophysiological behaviour of the firing cells. During all the recordings, the machine used has proved capable of performing multiple acquisitions with good performances, and the boards did not present any form of interaction among them. This kind of approach has been made possible thanks to the use of three Filter Amplifiers simultaneously. Each of them has been proved to be couplable with any pre-amplification board, even if some couplings have been proved to act better in acquiring signals (e.g. board 92IV with custom Second Filter, cf. paragraph 3.2). Environmental factors, such as humidity or temperature, does not influence drastically any component of the electronic acquisition chain put into the bioreactor.

3.3.1. Analysis of hippocampal neuron activity after 12 days in-vitro

For a comparison between custom and benchmark setup, we report meaningful spiking and bursting features, among them selected, that preserve their statistical values both in the benchmark recording setup and in the custom one, reported in box plots (*Fig. 3.19-3.20*). It is possible to appreciate few outliers, most of them in the representation of Inter Burst Frequencies. Regarding the second quartile, i.e. the median, shifting between benchmark and custom setups, it is reasonable to assert that there is an influent impact of the culture behaviour in the comparison. Anyway, the range in which most of the values lies is the same in both cases.

For each feature, we also reported different mean values, averaged on 15 bin (each bin is one minute long) (*Fig. 3.16 and 3.18*). Each bar of the histogram represents a meaningful feature, computed using different chips and boards (cf. legend). There are depicted error bars too, representing standard deviation of the population.

In *Table VI* are reported p-values obtained with the Wilcoxon test performed between different couples of acquisition systems, using two different chips. In the first six rows are reported comparisons among different custom boards, in terms of four meaningful features selected. Most of the tests returns $p<0.05$, suggesting different median values among different custom boards. From the sixth to the eleventh row, there are comparisons between benchmark system and custom boards. In general, Wilcoxon test applied to chip 26954 return predominantly $p>0.05$, suggesting a more stable behaviour of the neuronal network developed in this case. Resuming, for the features selected the test highlights equal medians at the default 5% significance level between custom and benchmark setup. This trend can be monitored also from the graphs representing the features during the acquisition time (*Fig.3.15-3.17*). In detail, the board that scores the best values with both chips is the 46III.

Table VI P-VALUES ANALYSIS FOR BENCHMARK AND CUSTOM BOARDS

Board code	Active channels p-value	Spikes Number p-value	Burst duration p-value	IBI p-value
26007_46II_46III	0,002	0,281	0,081	0,062
26007_46II_92IV	0,084	0,000	0,016	0,184
26007_46III_92IV	0,063	0,010	0,002	0,245
26954_46II_46III	0,883	0,000	0,300	0,042
26954_46II_92IV	0,000	0,000	0,006	0,000
26954_46III_92IV	0,008	0,000	0,245	0,002
26007_46II_BB	0,000	0,000	0,000	0,426
26007_46III_BB	0,002	0,000	0,000	0,426
26007_92IV_BB	0,000	0,000	0,000	0,645
26954_46II_BB	0,062	0,062	0,004	0,009
26954_46III_BB	0,252	0,000	0,001	0,836
26954_92IV_BB	0,000	0,004	0,000	0,001

Table VI In the first column we report the chip used for the acquisition and the two boards compared

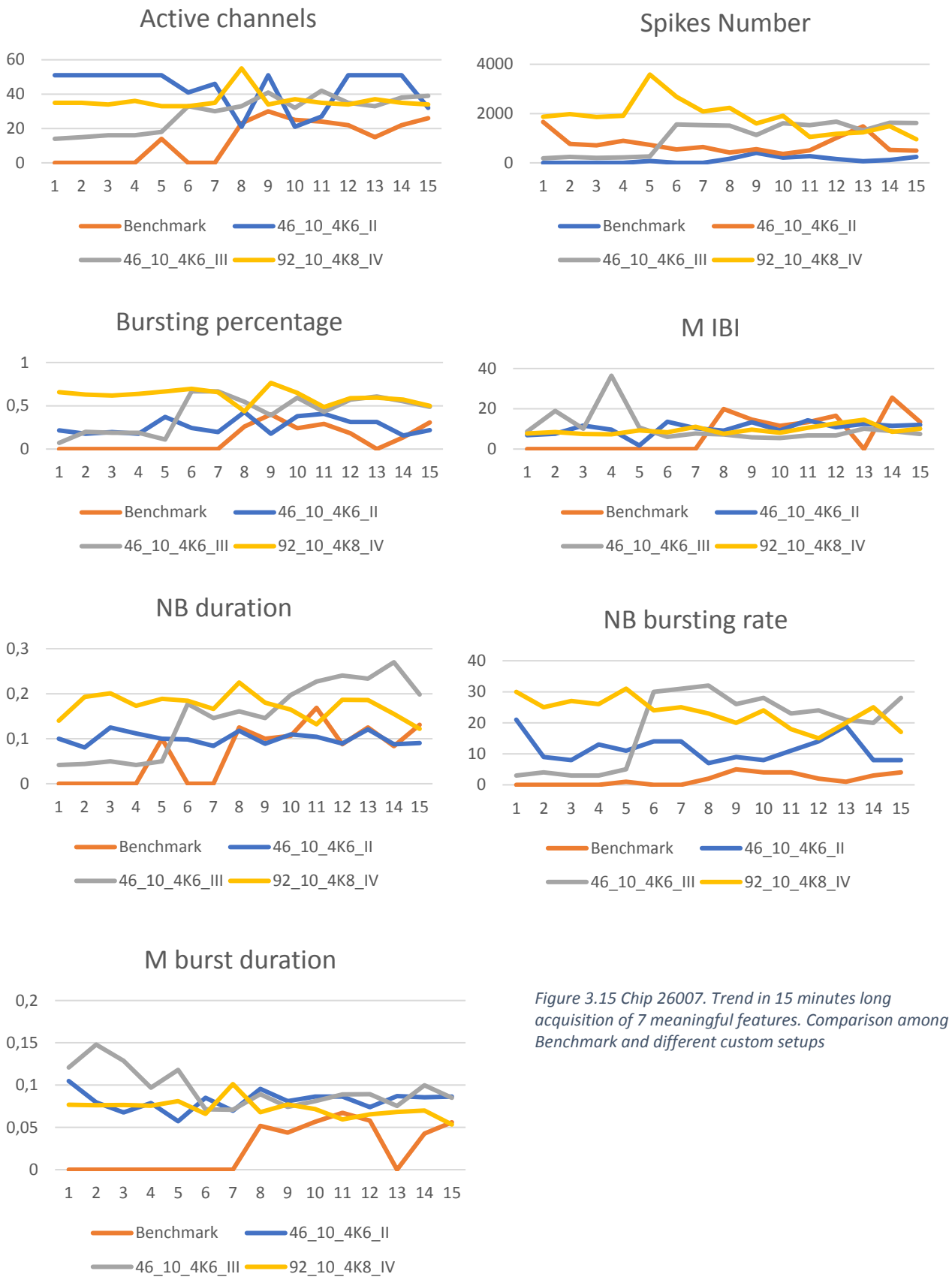

Figure 3.15 Chip 26007. Trend in 15 minutes long acquisition of 7 meaningful features. Comparison among Benchmark and different custom setups

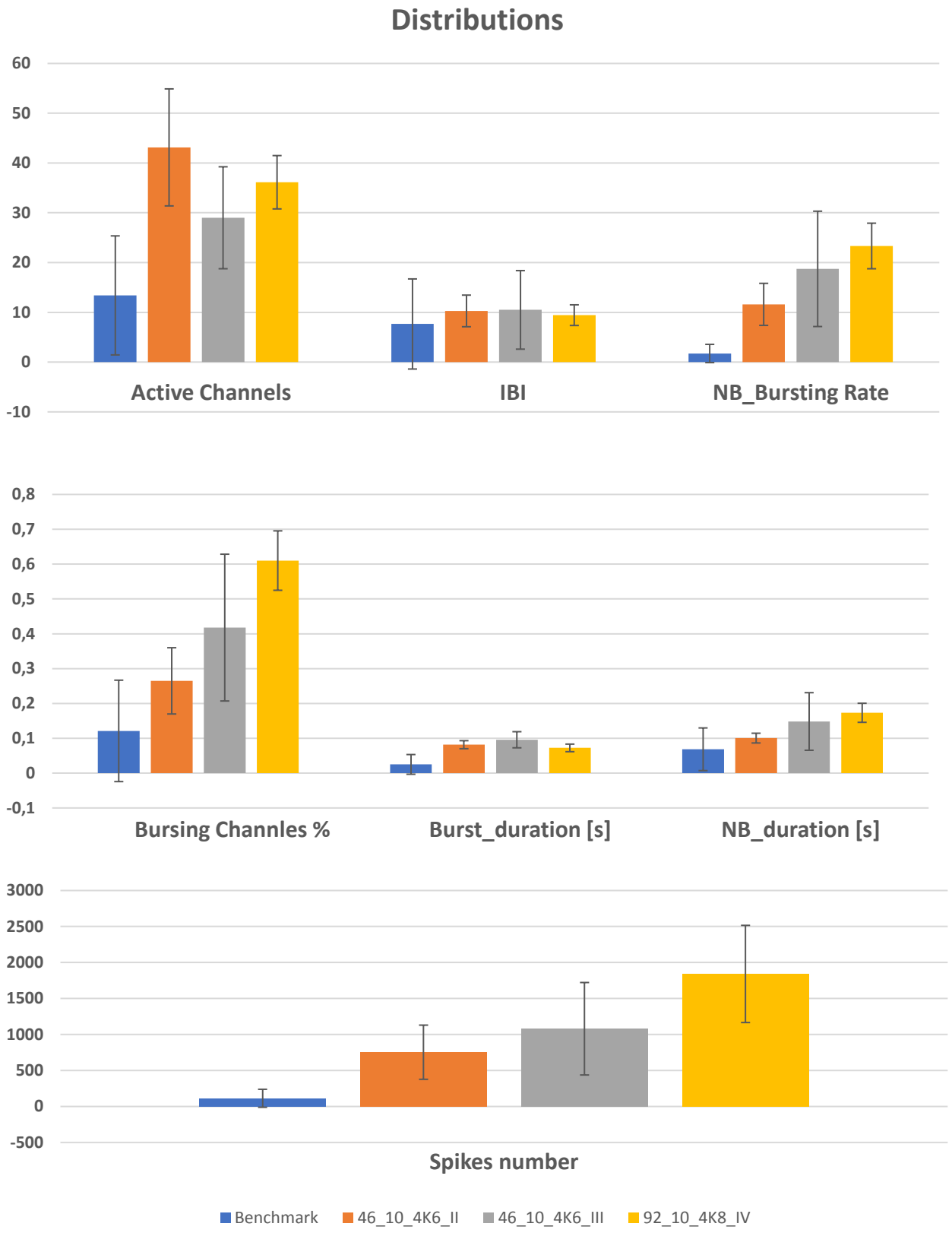

Figure 3.16 Chip 26007. Mean values reported for 15-minutes long acquisition, both in benchmark and different custom boards.

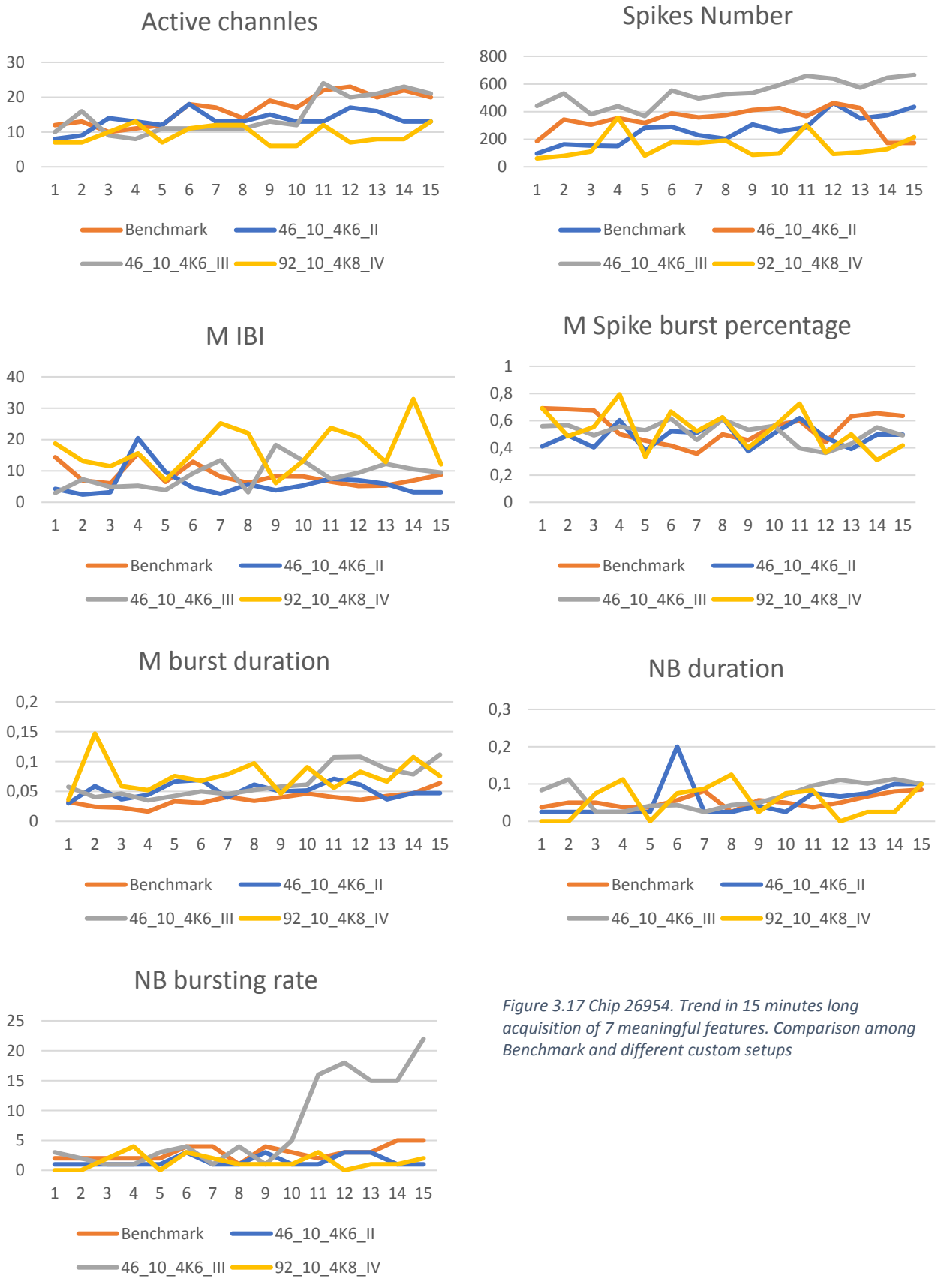

Figure 3.17 Chip 26954. Trend in 15 minutes long acquisition of 7 meaningful features. Comparison among Benchmark and different custom setups

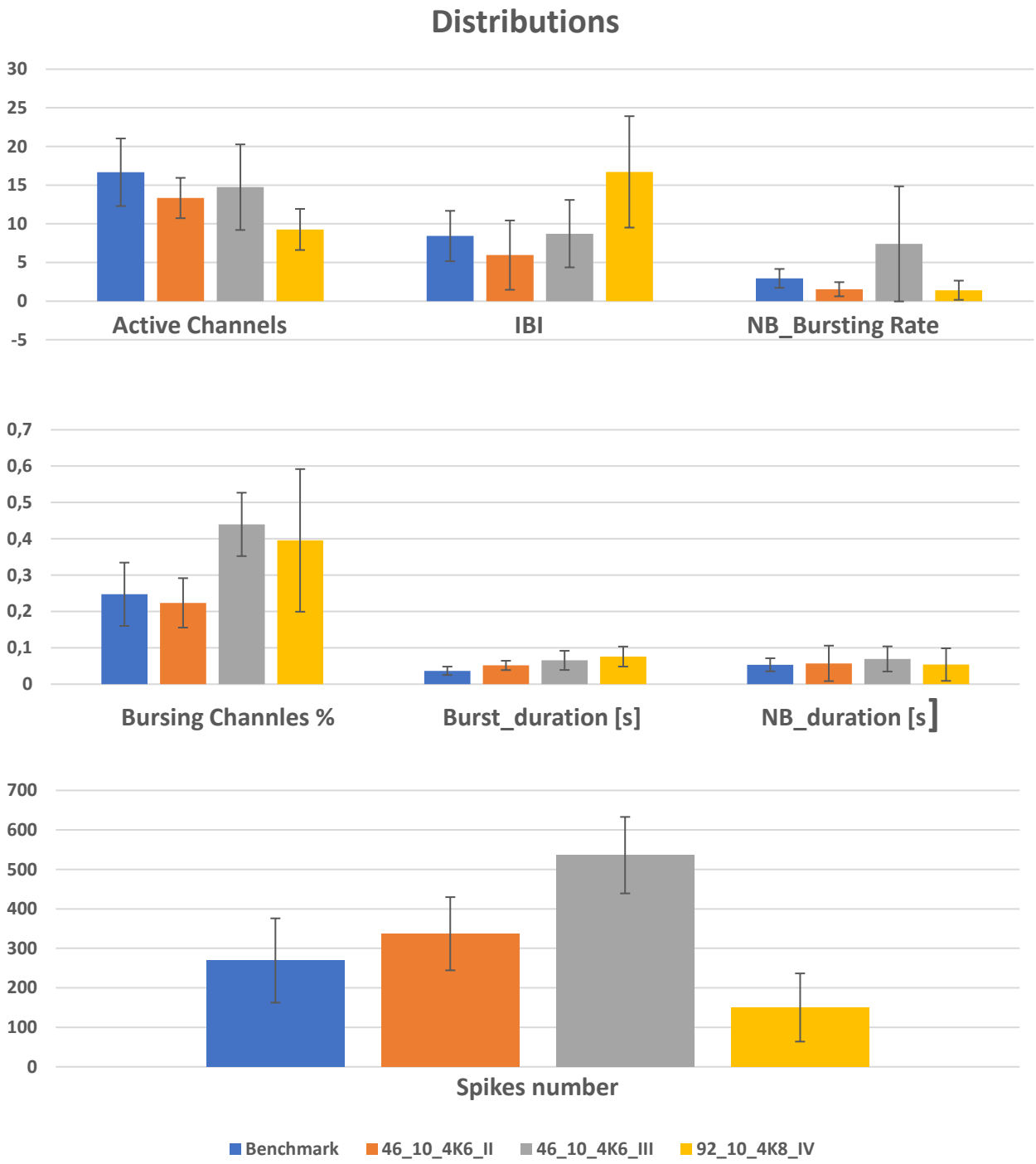

Figure 3.18 Chip 26954. Mean values reported for 15-minutes long acquisition, both in benchmark and different custom boards.

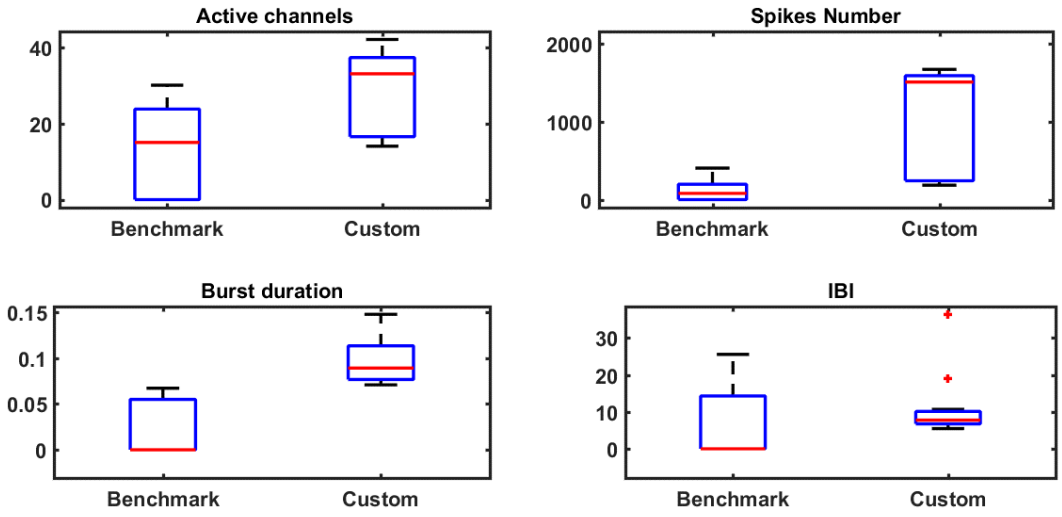

Figure 3.19 Box plots representing meaningful spiking and bursting features comparison between benchmark and custom (46III) boards. Population of 15 samples corresponding to bins (1 bin = 1 minute). Chip 26007.

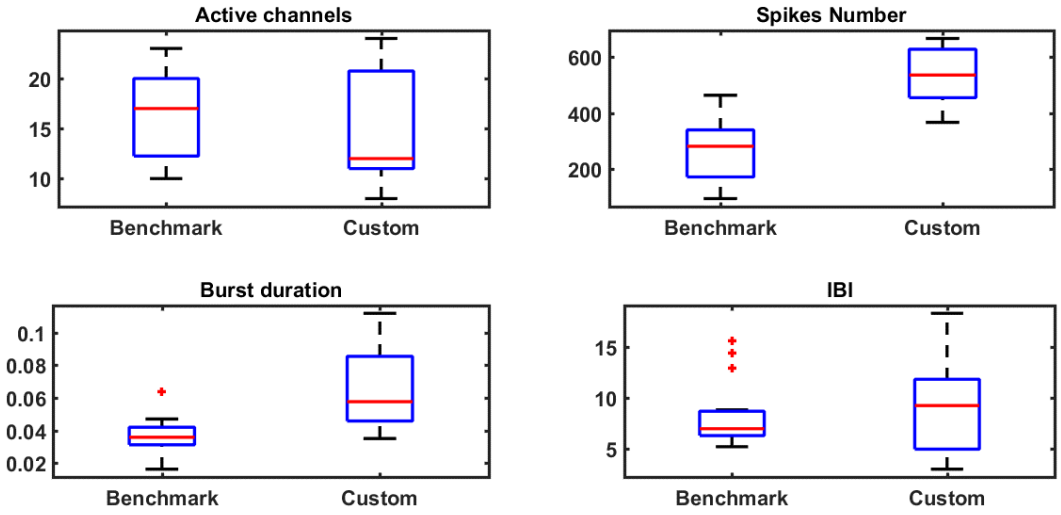

Figure 3.20 Box plots representing meaningful spiking and bursting features comparison between benchmark and custom (46III) boards. Population of 15 samples corresponding to bins (1 bin = 1 minute). Chip 26954.

For a better comprehension of the network activity, once spike detection is applied to the all MEA channels, it is possible to observe a picture of the spatio-temporal distribution of spiking neuronal activity throughout the experiment, referred to as raster plot (*Fig. 3.22*). Each plot is 5-minute-long (time scale depicted on vertical axes), and the single 1-minute-long bins are indicated with red dashed vertical lines. On horizontal axes the channels are depicted. With raster plots, it is possible to qualitatively observe that firing rate and the rate of synchronized firing across channels overall are strengthened from the start to the end of the monitoring period. Observing the first row of three scatter plots, which describes the mean firing rate computed on the recording with the benchmark system, it

is possible to note a low activity of cells, slowly increasing at the end of the acquisition. The activity is quite different in the custom acquisitions (cf. long-term acquisition windows, *Fig.3.21*), where it is possible to appreciate an increased activity and the presence of bursts too.

As shown, the firing sites are not strictly the same over time, but rather activity at some electrodes (especially in the lower half of the graph) displayed an irregular occurrence, alternating firing and silent periods. It is possible to observe a proper response of the cell culture with the custom setup.

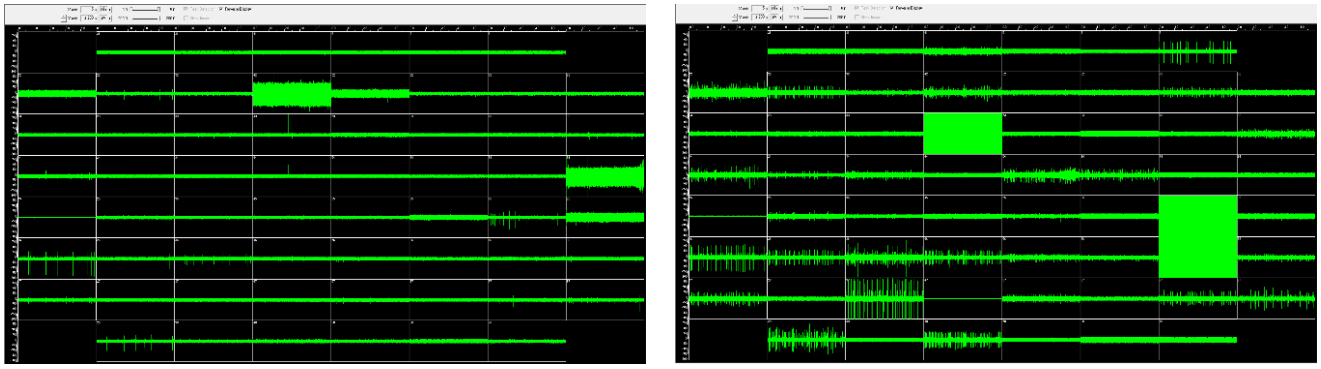

Figure 3.21 Chip 26007. Benchmark acquisition (left) and Custom 92IV (right).

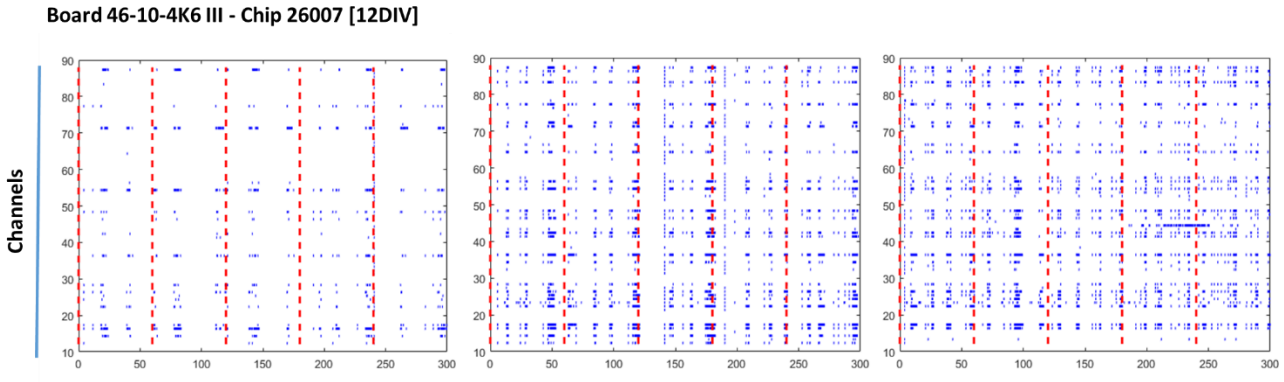

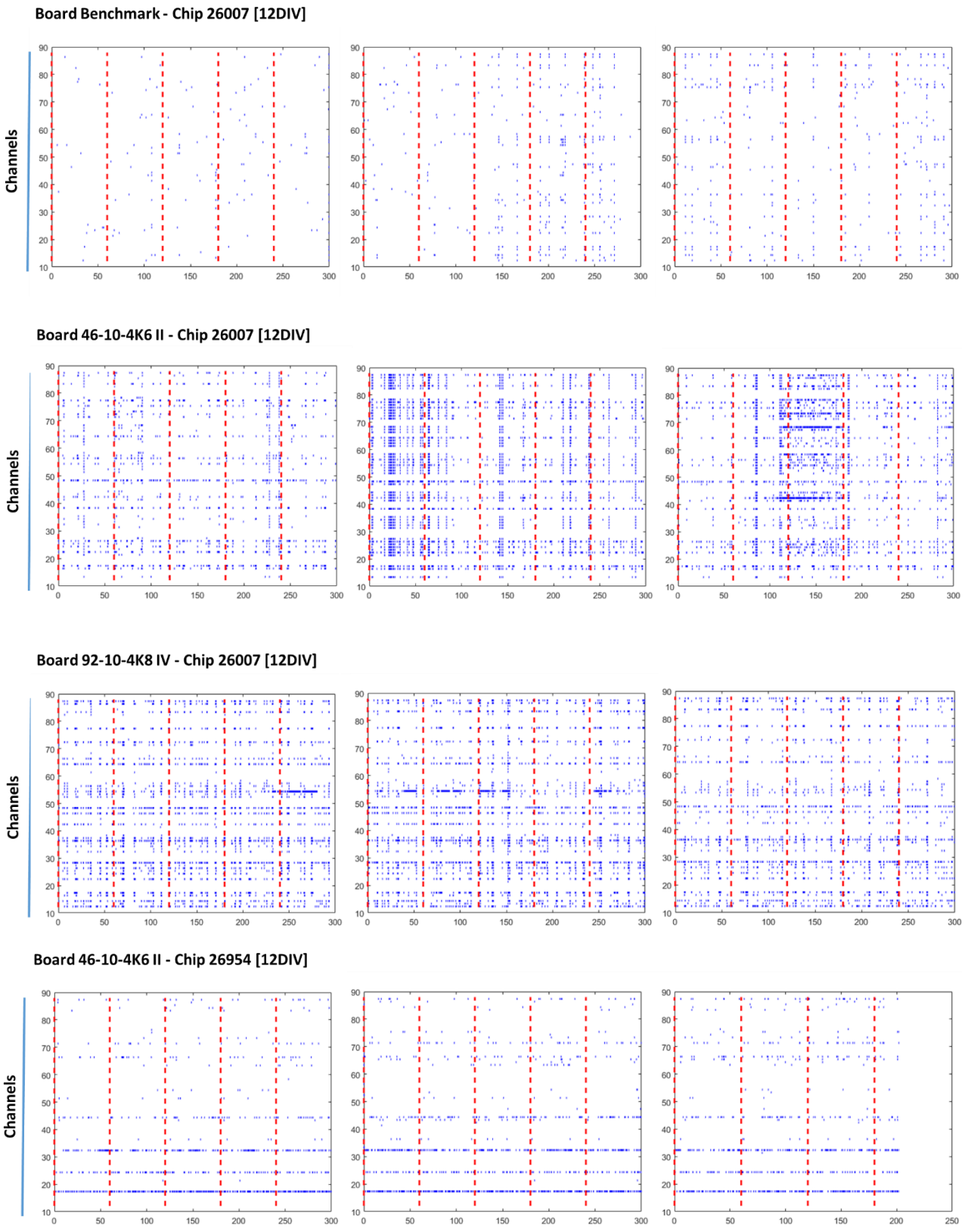

Figure 3.22 Raster plots representing mean firing rate. 3x 5 min acquisition windows. Time expressend in seconds on horizontal axis, board channels on vertical axis. Boards, chip used and DIV indicated in labels above each plot.

3.3.2. Analysis of hippocampal neuron activity after 18 days in-vitro

Finally, *Fig. 3.23* show recordings at 18 DIV, computed on the recording with the custom system. Focusing on chip 26954 comparison between different DIVs, it is possible to note a high activity in the first rows from the bottom of the plot at 12 DIV, which is constant along all the acquisition. The activity is quite different at 18 DIV, where it is possible to appreciate an activity reduction, alternating firing and silent periods. Another comparison between 12 and 18 DIV activity is depicted on boxplots in *Fig.3.24-3.25*, obtained from the same culture chip (26954) with custom setup. Specifically the acquisition board (46II) used is the same in both cases, in order to reduce as much as possible the hardware-related variability factor. Besides the qualities described above about the custom benchtop system, it is possible to note different variations, in long term activity, among different features. For instance, Active channels and Spikes number lie in the same narrowed range both in 12 and in 18 DIV. On the contrary, there in an increasing in Burst Duration and in IBI feature, probably due to culture maturation.

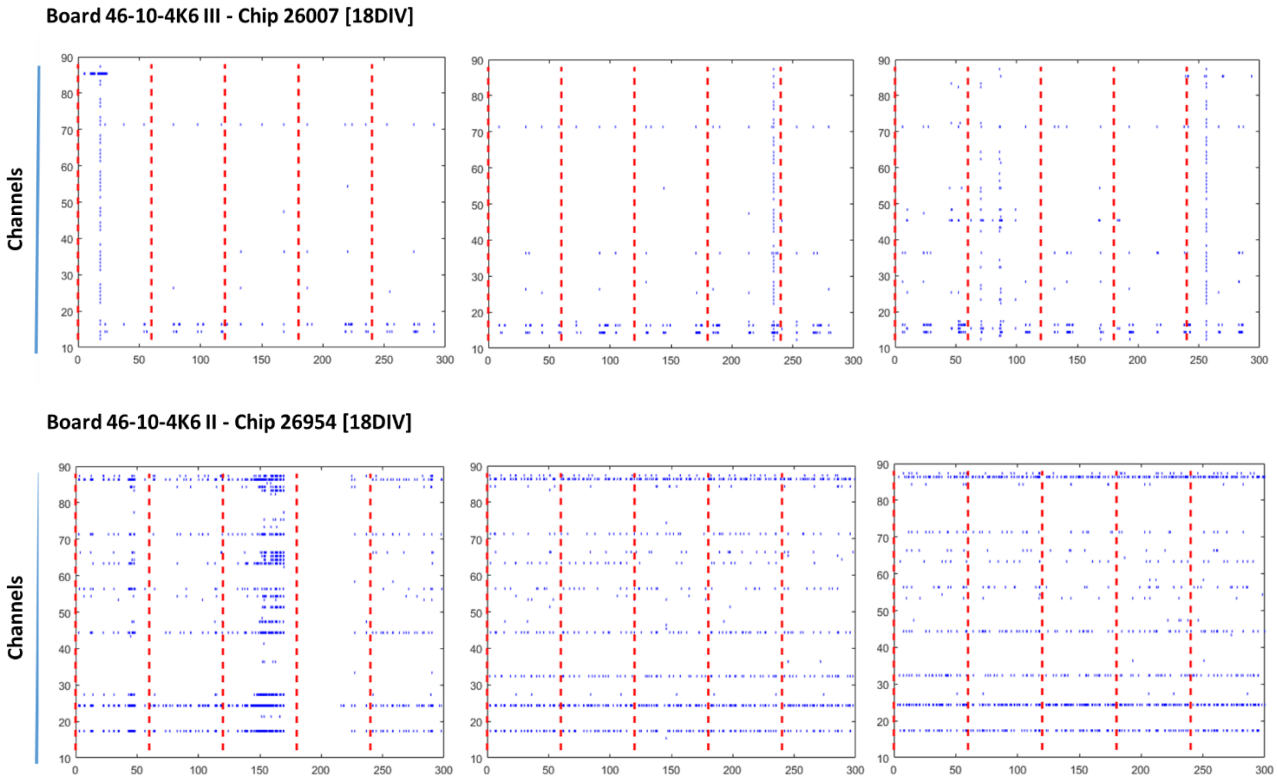

Figure 3.23 Raster plots representing mean firing rate. 3x 5 min acquisition windows. Time expressend in seconds on horizontal axis, board channels on vertical axis. Boards, chip used and DIV indicated in labels above each plot.

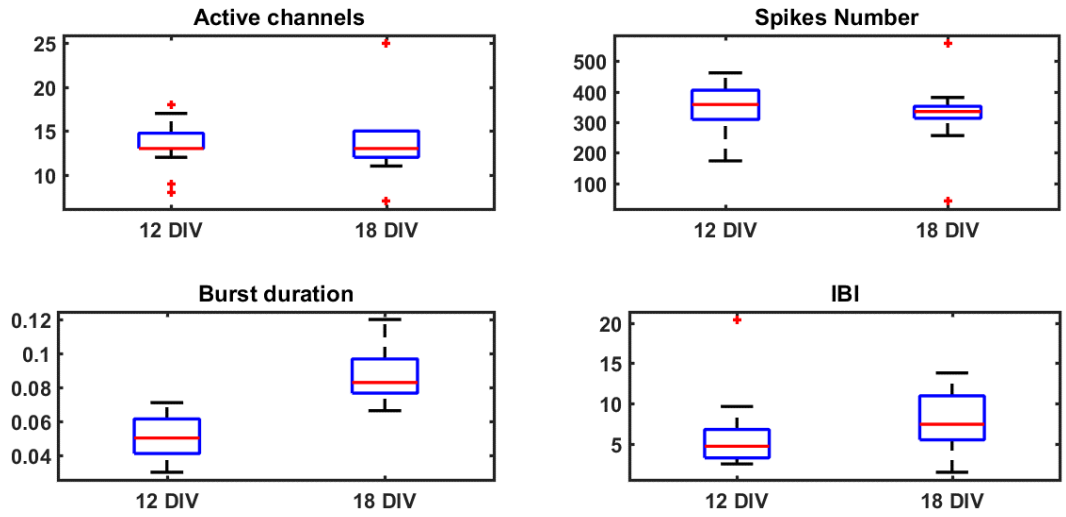

Figure 3.24 Chip 26954. Box plots representing meaningful spiking and bursting features, at 12 and 18 DIV. Population of 15 samples corresponding to bins (1 bin = 1 minute). Acquisition comparison performed both days with custom board 46II.

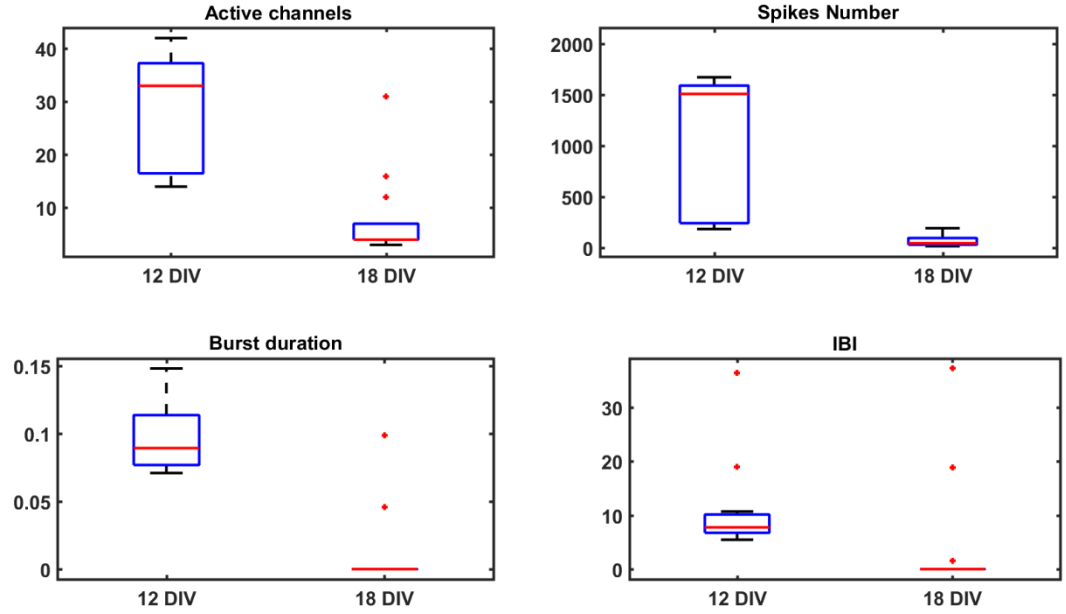

Figure 3.25 Chip 26007. Box plots representing meaningful spiking and bursting features, at 12 and 18 DIV. Population of 15 samples corresponding to bins (1 bin = 1 minute). Acquisition comparison performed both days with custom board 46III.

To conclude, in T*able VII* we report p-values, obtained with Wilcoxon non- parametric test, for a robust statistical analysis. They regard the two DIV acquisitions, with a comparison among the four features reported previously in the boxplots. Regarding culture in chip 26954, it is possible to note $p>0.05$ for all the features selected, except for the Burst Duration. This means a smaller variation in terms of medians for the features selected, except for burst duration, which results having a median value higher at 18 DIV. A longer duration of the bursts is related to a better organization of the neuronal network even after few days growth. Regarding the culture contained in chip 26007, it shows $h=1$ ($p<0.05$) for all the features in exam. Looking at the boxplots, it is possible to appreciate a drastic decreasing in all values, with the presence of few outliers. This trend can be ascribed to a degeneration

of the culture, probably jeopardized during the operations of maintenance, culturing medium changings or environment impairment. The same decreased activity is clearly appreciable on the Raster plots (*Fig.3.23*).

Table VII P-VALUES ANALYSIS FOR 12 AND 18 DIV ACTIVITY COMPARISON

p-values	Active channels	Spikes Number	Burst duration	IBI
26954_12_18	0,579	0,281	0	0,068
26007_12_18	0	0,0001	0,0002	0,0003

Table VII In the first column are reported the chip used for the acquisition.

3.3.3. Analysis of the variability factors

Within the current work, we have observed considerable changes in features extracted during the various trials, even on recordings performed on a single chip in a restricted time window. In order to explain this phenomenon, four main classes of variability factors have been identified during trials:

- **Biological** variability factors enclose all changings due to intrinsic electrophysiological activity of the neuron;
- **Environmental** factors influence neuron activity: as demonstrated in several studies changes in CO_2 concentration, temperature, humidity, pH and so on alter the neuron's behaviour [2], [4];
- **Hardware-related** factors include all the differences in terms of electronic devices that affect spiking and bursting activity;
- **Computational** variability factors take into account all the editable thresholds and settings chosen during analysis.

Referring to variability factors described above, the culture's behaviour shown during the trials could be explained because of these elements. First, referring to biological variability factor, the neuronal network could have behaved differently during different tests, even if the time interval is short. In detail, referring to the benchmark acquisition, the neural activity shown in the analysis is slightly lower than the one obtained with the experimental setup.

Regarding environmental variability factors, a controlled environment, with ideal parameters set, could allow the cells to increase their activity. This is clearly demonstrated by performing an acquisition, in a close time window, of the same chip both within the environmental-controlled benchtop system and within the only commercial acquisition boards, without any environmental parameter controlled.
About hardware-related variability factor, a higher gain of the first stage of pre-amplifier in the custom board could make it more sensitive to electrophysiological activity, which is a good point unless different hypersensitive electrodes record the same neuron spiking, altering and making an overestimation of the spiking activity. This point can be inferred comparing acquisitions performed with board with gain equal to 92 and the ones with gain equal to 46.

We report a clear example of computational variability factor. In order to demonstrate if the spikes recorded in the custom board are real or spurious, we have chosen to study the waveform recorded by the software and to check if it reflects the behaviour of an action potential. Referring to the acquisition aboard, the spike sorter detected the typical forms of an AP (*Fig. 3.26*).

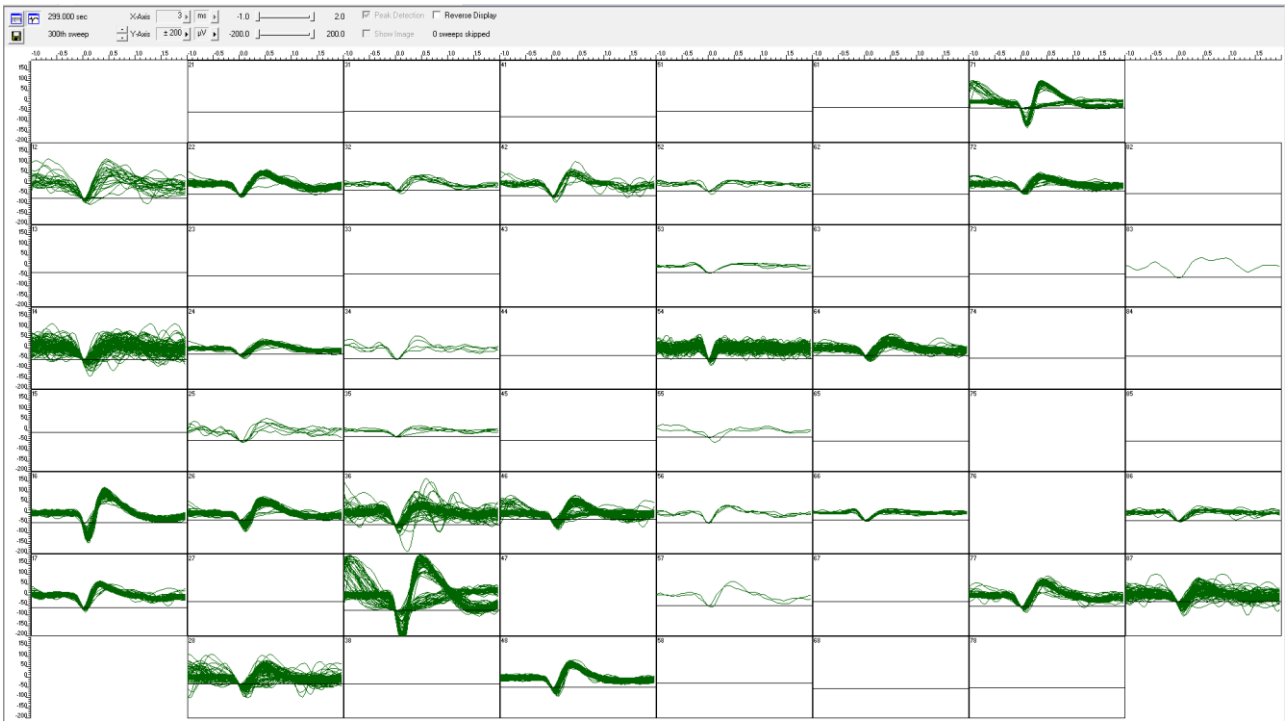

*Figure 3.26 MC_Rack waveform analysis window. Chip 26007, board 92IV, Custom Filter Amplifier, 7*SD.*

As stated (cf. chapter 2.2.1), it is possible to customize the spike detection selecting the factor for which multiplying the standard deviation. This represents a useful tool in case of spurious spikes that are not biological but are due, for instance, to the electrical network or to an accidental movement of the setup. For this work, 5*SD or 7*SD have been used. However, studying spiking and bursting activity parameters extrapolated with these two different values has shown that adopting a higher factor compromises the sensitivity of the spike detection. For each feature selected for the neurophysiological activity study, we have reported different mean values, averaged on 15 bin (each bin is one minute long) (*Fig. 3.3.27-3.28*). Each bar of the histogram represents a meaningful feature, computed using different chips, board for acquisition system, and standard deviation multiplication factor (SD) chosen for the spike detection (cf. legend). It is clearly possible to appreciate an invariance in spike detection using the benchmark system in the two cases. This is because a thinner noise bandwidth is revealed, in particular during the first 500ms, when the algorithm computes the standard deviation for the detection.

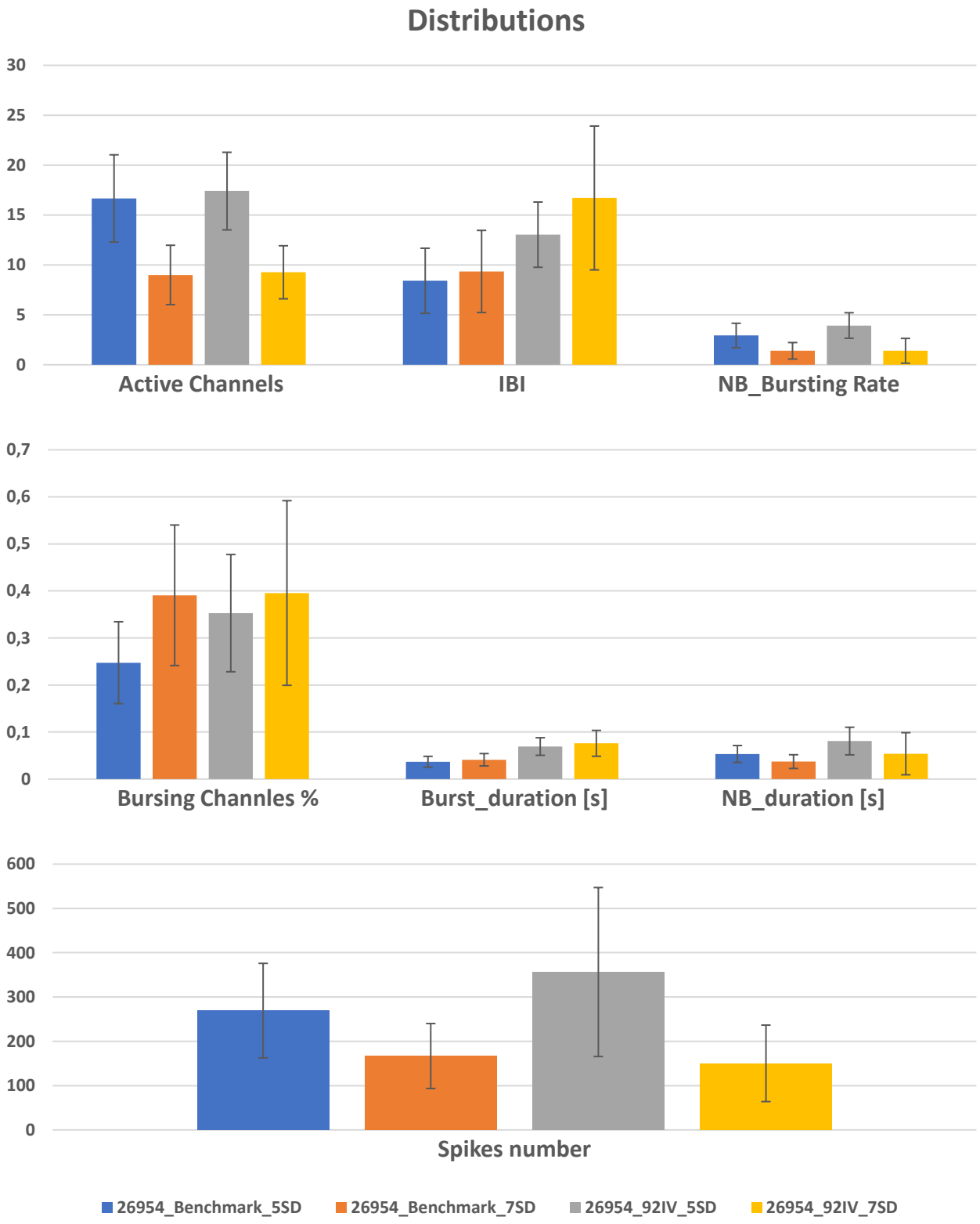

Figure 3.27 Mean values comparison among different boards and different SD factors. On the legend: chip used, board type, SD factor.

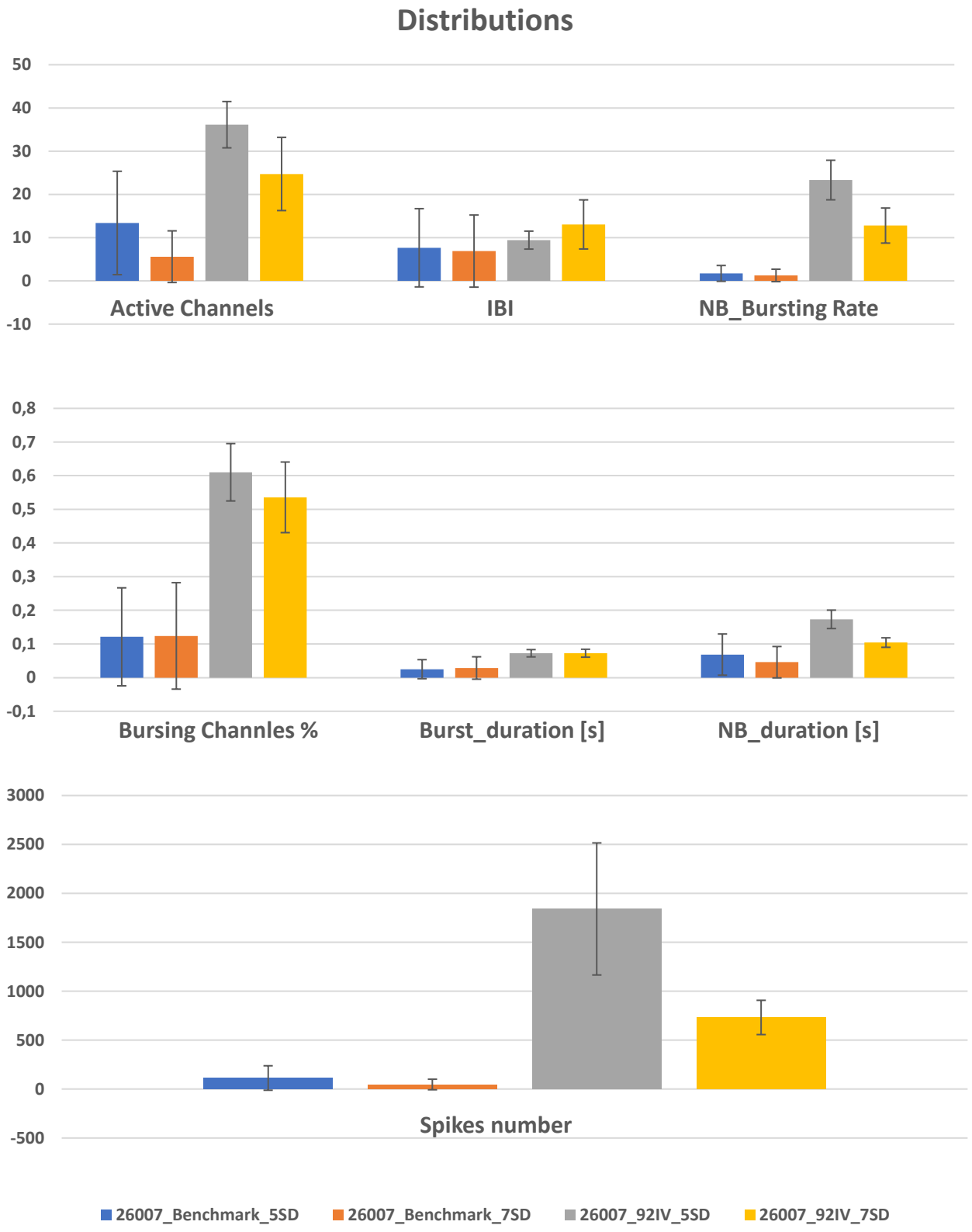

Figure 3.28 Mean values comparison among different boards and different SD factors. On the legend: chip used, board type, SD factor.

On the contrary, on the test conducted with a custom board there is a drastic reduction in terms of spike detection.

Although the noise amplitude lies on an acceptable range (minus than ±20µV), it is higher than the benchmark one, so the spike amplitudes are not high enough to constitute a sufficient deviation from the white-noise bandwidth. This drawback is reflected also in the raster plots (*Fig. 3.30*), where the mean firing rate gets a significant reduction.

We also report four features in the two cases, maintaining all the parameters fixed except for the SD multiplying factor. In the first two groups of boxplots (F*ig.3.31*), representing benchmark data, it is possible to note lower values in Active Channels and Spike Numbers computed with 7*SD, whereas the values of Burst Duration and IBI remain constant. The patterns change in case of custom board (92IV): in fact, in the last group it is clearly reported a decrease in Active Channels and Spikes Number detected with 7*SD analysis, as well as an increase in Burst duration and IBI, even if the median value remains constant in both cases.

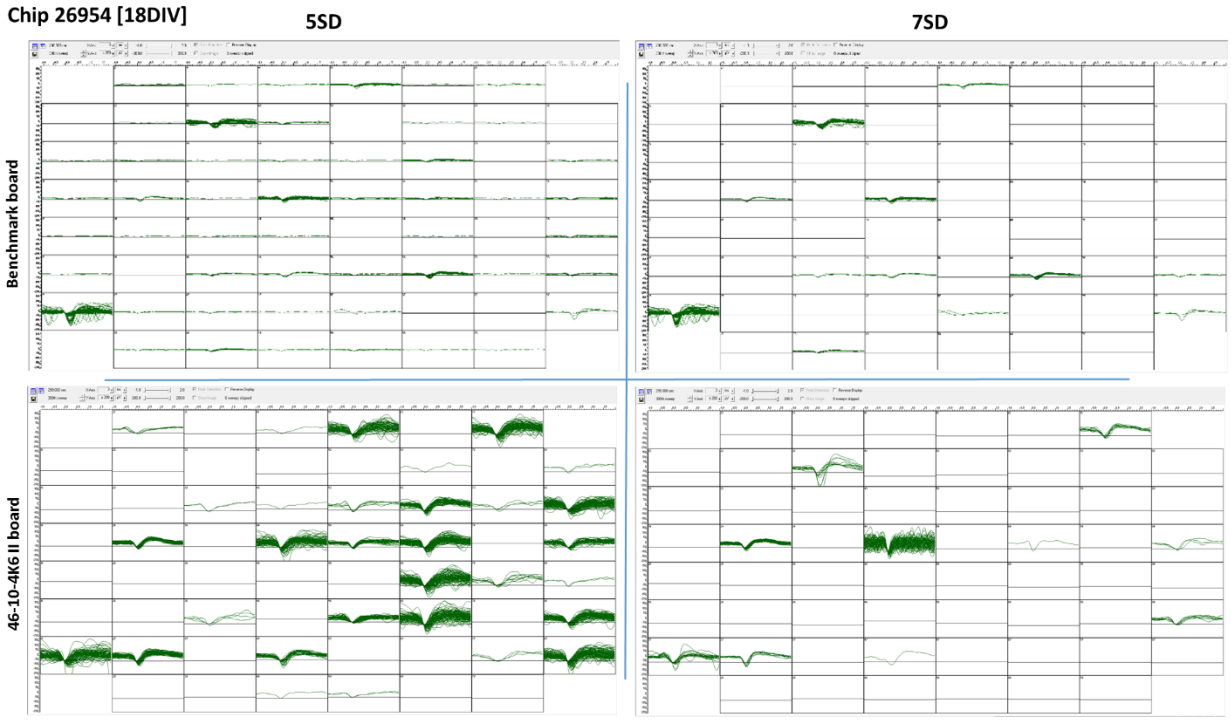

*Figure 3.29 MC_Rack waveform analysis window comparison between different boards, at 5*SD and 7*SD. Upper panels: Benchmark board. Lower panels: (46II) board.*

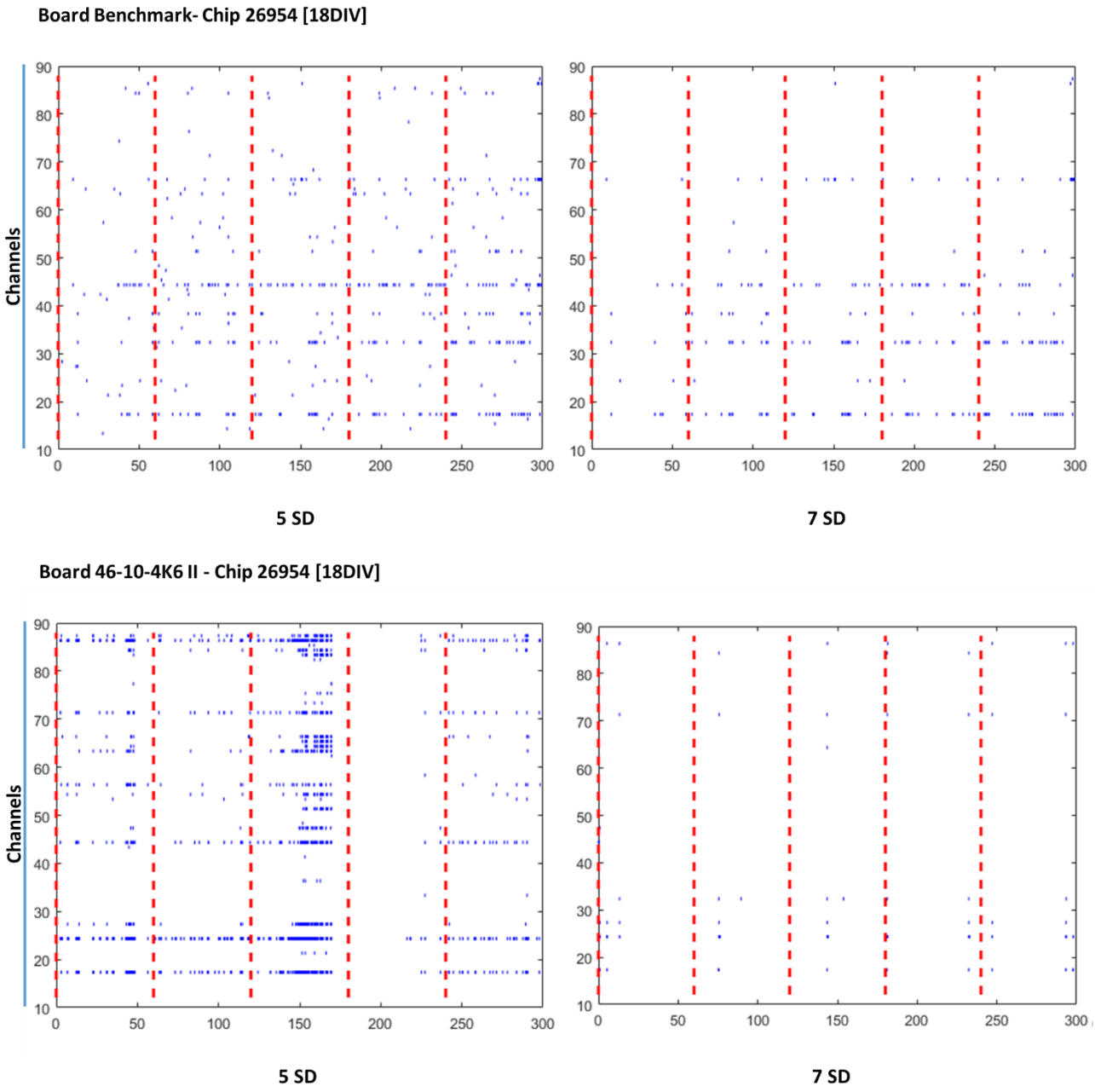

*Figure 3.30 Raster plots representing mean firing rate. Comparison with benchmark and custom setup at 5*SD and 7*SD*

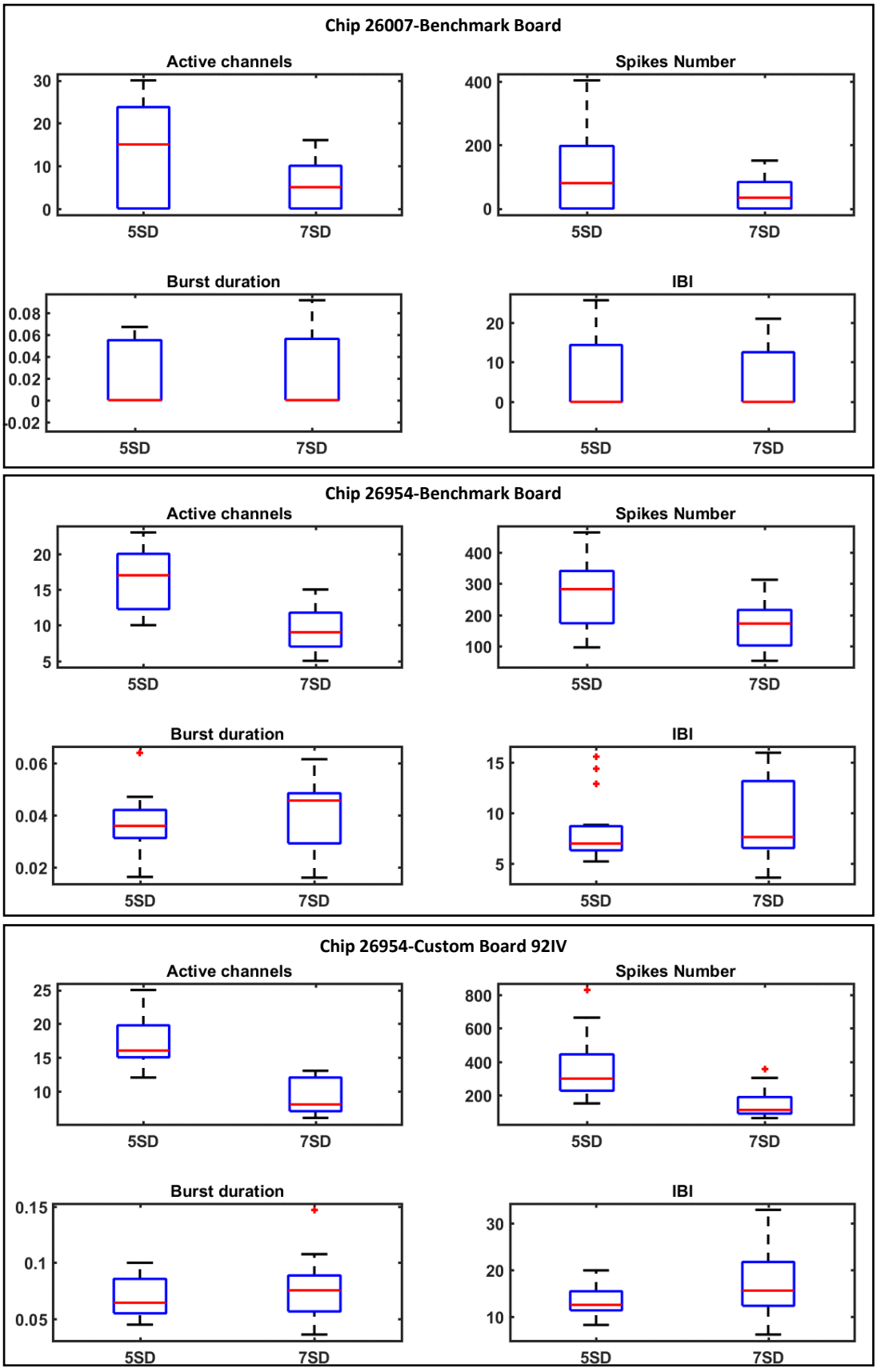

*Figure 3.31 Box plots representing meaningful spiking and bursting features, at 5*SD and 7*SD. Population of 15 samples corresponding to bins (1 bin = 1 minute).*

3.3.4. iPS trial

Among the three chips used in the iPS trial, only chip 26957 presents activity during the entire acquisitions period. We report a comparison between a benchmark acquisition and one with the custom setup, both performed in a restricted time window, on this single chip. At 14DIV, considering the same channel (66) and assuming negligible the biological variability factor, the spiking activity can be considered similar between the 2 setups. However, the higher custom board noise bandwidth avoids MC_Rack platform to detect the same amount of waveforms (*Fig.3.32*). In this early stage of growth, in fact, spikes amplitude differs from noise bandwidth of few microvolts. Longterm and wafeform windows are reported with different scales, to better visualize the spiking activity with respect to the basal band:

- Longterm window: ±50µV x 5min;
- Wavefrom window: ±50µV x 3ms;

With the custom setup, on a basal band with amplitude of about ±16µV, spiking activity has an amplitude range unclear in this phase of pre-processing.With the commercial (Benchmark) setup, on a basal band with amplitude of about ±8µV, spiking activity has an amplitude of about 16 µV.

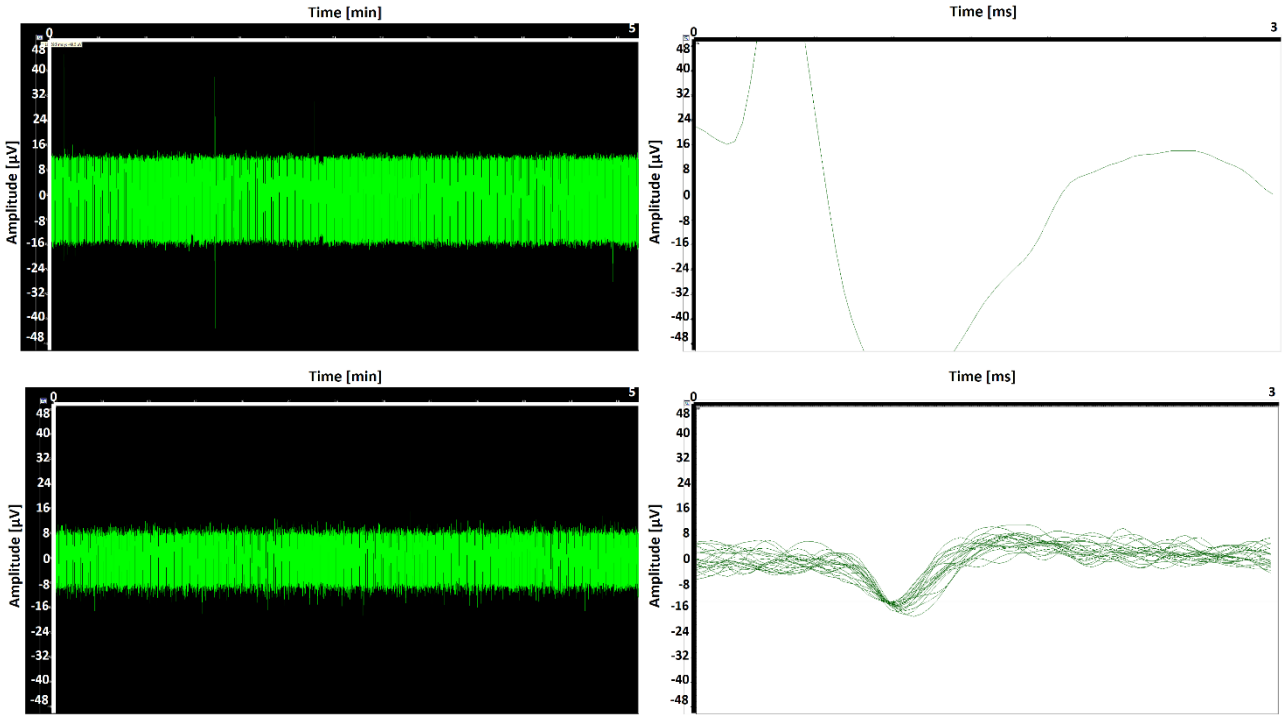

Figure 3.32 14 DIV. Custom board (upper panels), Benchmark board (lower panels). Channel 66 activity monitored during acquisition of chip 26957 with hiPSc culture: Longterm window (Left), Waveform window (right)

Then, at 25 DIV, spikes amplitude is higher, thus allowing the custom system (i.e. board 46II with custom Filter Amplifier) to detect activity, even if lower than benchmark (*Fig. 3.33*). We have now focused on single channel 36, because it is the only who preserved high spiking activity. Longterm and wafeform windows are reported with the same scale values used at 14 DIV. With the custom setup, on a basal band with amplitude of about ±16µV, spiking activity has an amplitude range between 20µV and 50µV. With the commercial setup, on a basal band with amplitude of about ±10µV, spiking activity has an amplitude range between 24 µV and 50 µV.

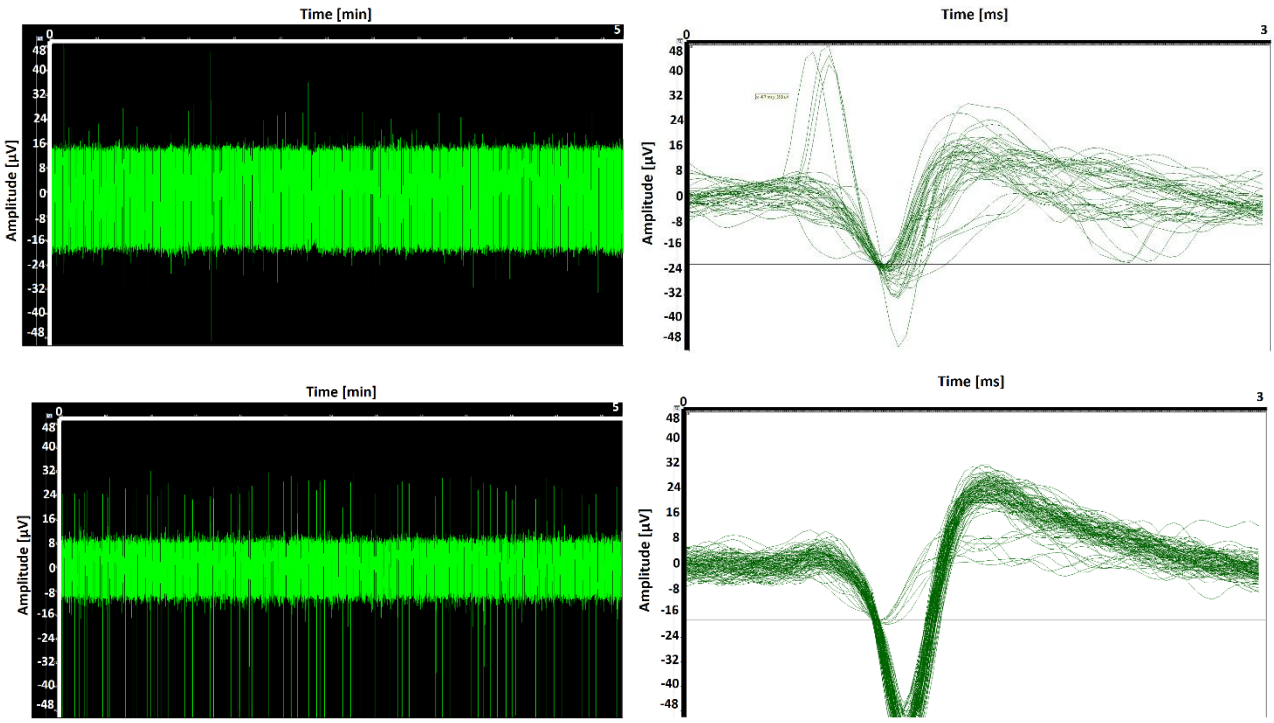

Figure 3.33 25 DIV. Custom board (upper panels), Benchmark board (lower panels). Channel 36 activity monitored during acquisition of chip 26957 with hiPSc culture: Longterm window (Left), Waveform window (right)

Regarding SNR analysis, we first report in *TableVI* values that highlight the differences between benchmark and custom setups. At 14 DIV, most of custom values are absent (*NaN*), and the noise esteem is much higher respect to the benchmark system. At 25 DIV, most of values reported are similar. Then in F*ig.3.33*, we report the results of spike detection in MATLAB performed with the two systems. At 14 DIV, it is clear that spike rate detected (in figure in red) is higher using the commercial board with a smaller noise bandwidth, whereas in the custom one the activity detected is poorer. At 25 DIV, thanks to higher spikes amplitude value described in *Fig.3.45*, the difference between custom and benchmark setup is significantly reduced.

Table VI SNR ANALYSIS FOR BENCHMARK AND CUSTOM BOARDS

SNR analysis	Amplitude ratio	Amplitude spikes	Spike width	Noise esteem	SNR	Channel	DIV
26957_Benchmark	0,0432	21,8048	0,0014	2,8784	2,6497	66	14
26957_46II_FF	NaN	NaN	NaN	12,6544	2,1720	66	14
26957_Benchmark	0,4529	42,4472	0,0011	3,1575	5,1592	36	25
26957_46II_FF	0,4881	42,2370	0,0011	4,9815	4,3207	36	25

The chip used for the acquisition and the board used are reported in the first column.

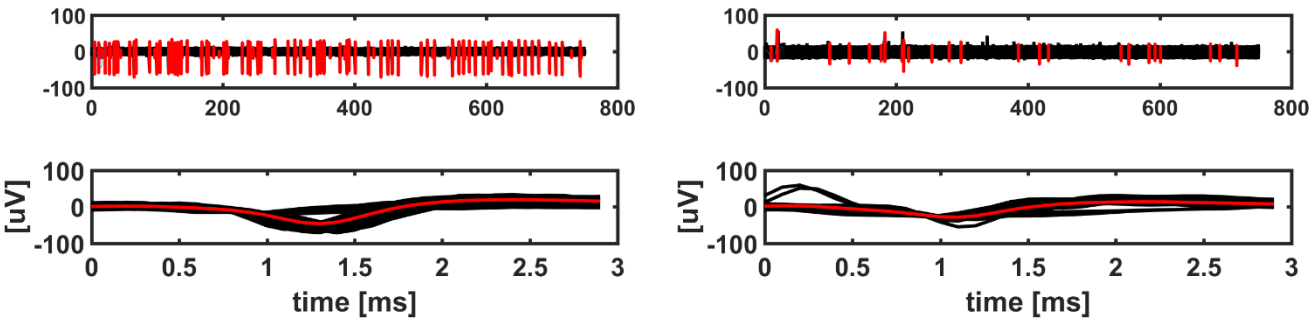

Figure 3.34 Chip 26957 (channel 36). Spike waveform detection comparison between Benchmark setup (left) and custom setup (right). Spike detected are red highlighted above the basal bandwidth. 24 DIV.

For the reasons described above, a quantitative analysis of the custom setup has been not possible before an adequate maturation level of the culture. Besides, according to the protocol adopted for hiPSc differentiation (cf. paragraph 2.7.4), during the early stage of differentiation the cells need to be maintained inside an environment with 5% O_2 and 5% of CO_2, which are different conditions of typical cell incubators. For this reason, if the custom MEA bench-top system need to be used in monitoring this first step in neurons development, it should be calibrated properly, both installing cylinders with a different O_2 concentration and setting the PID system in order to reach desired values. Even if this solution would not increase electrophysiological activity during the early stage, at least preserves the cultures environment condition during the period of stay inside the bioreactor.

At 25 DIV, in chip 26957, no bursting activity is detected neither with custom nor with benchmark setup. For this reason, we report in *Fig. 3.35* only spikes number computed by MATLAB algorithm in the benchmark and custom case, focusing only on channel 36.

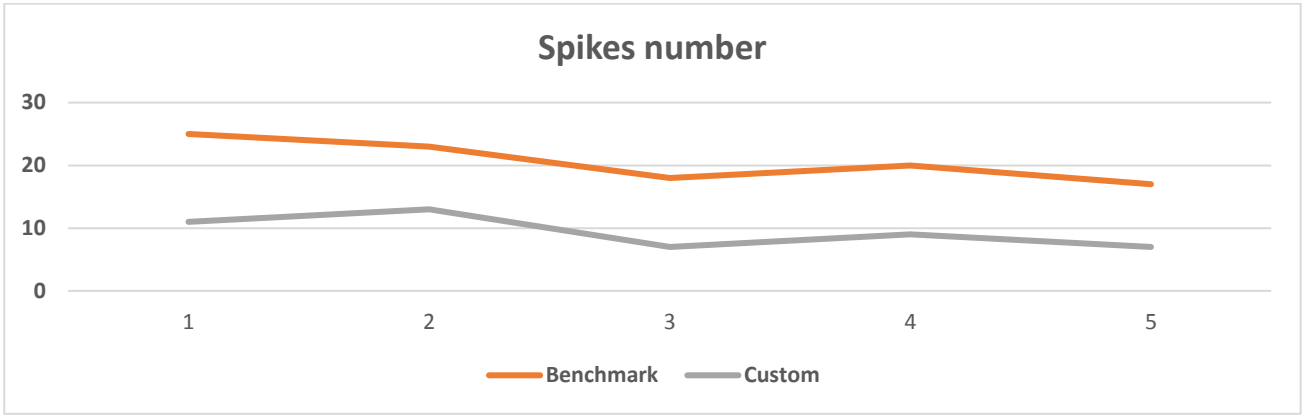

Figure 3.35 Chip 26957, Spikes number trend at 25 DIV comparison between custom and benchmark system. 5 minutes long recording.

3.3.5. Microscope imaging

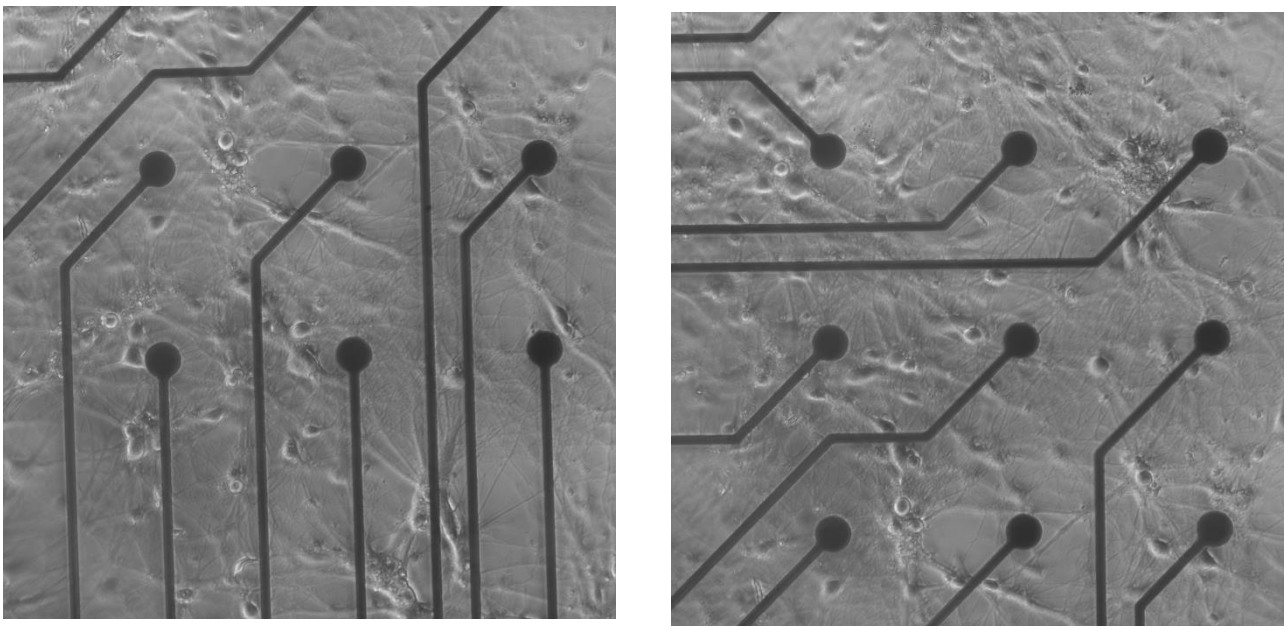

Figure 3.36 5x differential interference contrast image (DIC) of a neuronal network grown on MEA. 18 DIV.

To study the status of the cells after a long-term permanence inside the culture chamber, we analysed the neuronal network through microscope imaging and here report two representative 5x differential interference contrast image (DIC) of a neuronal network grown on MEA, at 18 DIV (*Fig. 3.36*). It is possible to note that the cells remain attached to the substrate, allowing the electrodes to better detect their activity, thus demonstrating the effectiveness of the plating protocol, too. The cells preserved their vitality, and a reduced presence of dead cells in suspension is detected.

We report in figures from *3.37 to 3.39* a set of photos of the chip's substrate, clearly showing cells distribution and population, at 14 DIV. As registered in previous studies [53], iPS cells differentiated in neurons forming clusters with a big concentration of axons, grouped into thick fibres. This behaviour is likely due to a non-proper adhesion. The clusters lead the neurons forming microcircuits, thus preventing the electrodes from detecting spiking with high amplitudes. In *Fig.3.38* we report chip 25041: it has a higher number of cells in respect to the other two ones. For this reason, the culturing medium is consumed more rapidly, provoking a lower pH, i.e. its environment is more acidic. It is reasonable to assert that these two effects, an environment with a lower pH and a higher cell density, can counterbalance each other, not changing the recorded neurophysiological activity in respect to chips with reduced population. Electrophysiological activity, in fact, is absent for pH<7.2 [34]. The reduced activity in chips with high populations has been demonstrated in previous studies [25], [14]. Besides preveting evaportation thanks to an adequate value of relative humidity, set by the environmental parameter control system, it is necessary to prepare the chips in order to guarantee the same amount of cells population. In this way, it is possible to maintain optimal pH values performing less changes of culturing medium during the period of long term acuisitions, and to guarantee well-distributed networks inside the chip.

Chip 26957 (*Fig. 3.39*), with monitored activity lasting until 25 DIV, presents a lower number of cell bodies. However, it has a well distributed network of interconnections among them.

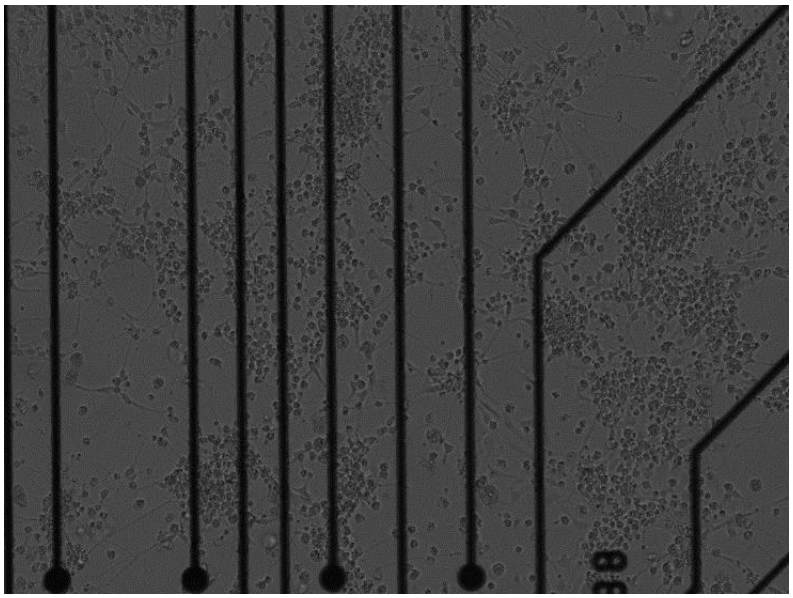

Figure 3.37 5x differential interference contrast image (DIC) of a neuronal network grown on MEA. (Chip 19155, 14DIV)

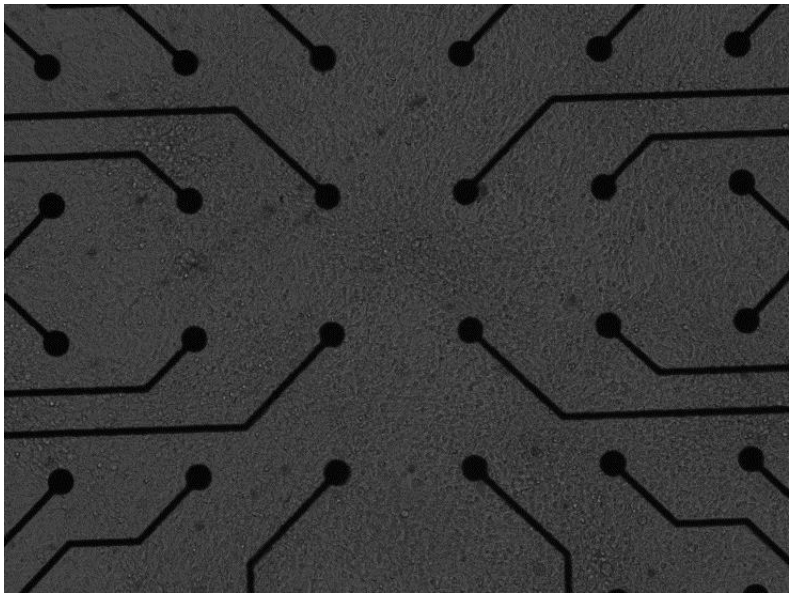

Figure 3.38 5x differential interference contrast image (DIC) of a neuronal network grown on MEA. (Chip 25041, 14DIV)

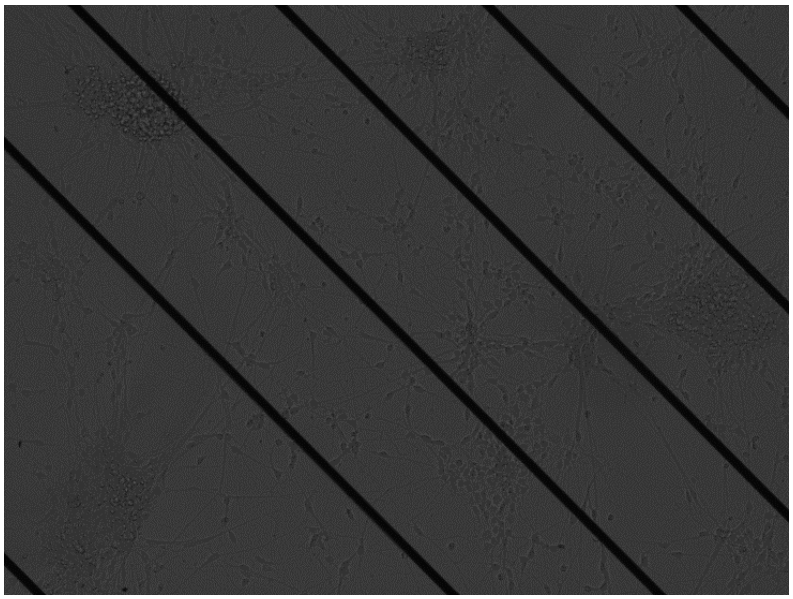

Figure 3.39 5x differential interference contrast image (DIC) of a neuronal network grown on MEA. (Chip 26957, 14DIV)

4. Discussion and Conclusion

In this work, we have improved and validated a bench-top system, which integrates an environmental control monitoring system and a multi-MEA recording system, effectively enhancing its performance and improving its capability to perform multiple recordings in parallel (i.e. multi-MEA format). During all the recordings, the setup used has proved capable of performing multiple acquisitions with good performances in parallel, and the boards did not present any form of interaction among them. This kind of approach has been made possible thanks to the use of three Filter Amplifiers simultaneously. Each of them has been proved combinable with any pre-amplification board, even if some couplings have been proved to act better in acquiring signals (e.g. board 92IV with custom Second Filter, cf. paragraph 3.2).

After the validation of the acquisition system and the environmental control system, the trial conducted on the hippocampal cells has highlighted several advantages of the personalized bench-top system. The setup, preventing unnecessary movements from incubators to acquisition system, strongly reduces detrimental perturbations of neuronal activities. Besides, meaningful information about neuronal network activity has been extrapolated, turning to be helpful to define protocols for efficient biological and pharmacological studies. During neurophysiological trials, it has been assumed that the neuronal network acts in a stationary way both in Benchmark and in custom case, and that neither environmental nor biological variability factors do not influence so significantly the mean firing rate in this acquisition protocol. An option to find if standard deviation editing alters the results *hiding* some activity with lower amplitude is to try repeating the analysis with lower factors respect to those present in literature. Unluckily, starting from a factor equal to 4.5 the software will recognize even small noise fluctuations as spikes, altering the result and preventing to adopt this test.

Regardin the iPS trials, the approach with the MEA Benchmark setup proved the need of improvements for this kind of technology in monitoring hiPSc activity in their first stage of development. With the acquisitions performed in an advanced growth state, the benchtop system has proved to be capable of monitoring neurophysiological activity in iPS neuron-like cells. The difference showed in the results between spikes number detected by the benchmark board and the ones detected by the custom system are due to the deterioration state of the cell culture. This suggest an improvement required with the maintenance protocol, for instance regarding the medium change.

Regarding the first stage of neuron-like cells differentiation, a detection of the poor and low-amplitude activity has been made possible only thanks to the reduced noise band of the MCS commercial setup. With the adoption of the custom pre-amplification board, the slight neurophysiological activity was covered by the noise bandwidth, preventing the possibility of quantitative analysis. Moreover, as stated in paragraph 2.7.4, the protocol adopted for the differentiation of hiPSc requires a different O_2 concentration respect to the one adopted during classical neurophysiological trials. For this reason, if the custom MEA bench-top system need to be used in monitoring this first step in neurons development, it should be calibrated properly, both installing cylinders with a different O_2 concentration and setting the PID system in order to reach desired values. Then, this calibration needs to be changed when the neurons switch to the second stage of maturation. Anyway, in the case of hiPSc study, the custom bench-top system should be adopted for monitoring the differentiation during an advanced maturation stage. If so, the effects of a stay inside an environment with different O_2 concentration for the reduced period of monitoring, should be considered as negligible as the period in which cells stay outside the incubator for culturing medium change.

We have also defined some critical points that could compromise the quality of recordings, as well as the stability of the internal environment of the bioreactor. For any of them, we report the solution adopted with eventual drawbacks, as well as outlooks for better implementations.

One of these problems faced during this work is represented by non-uniform heating of the culture chamber top-plate, leading to moisture making beneath the top-plate that could in turn contaminate the cultures. To partially overcome the moisture issue, on the top-plate of the second prototype chamber a wire made of the same material used in the first prototype has been installed. This configuration presents a more organized distribution respect to the previous one, as well as a better adherence to the top-plate thanks to a heat-resistance tape.

We tried to substitute Chrome-Nickel wire with a transparent conductive oxide panel (ITO) that could uniformly warm-up the surface. However, the thermal controller was unable to supply a sufficient amount of current in order to reach the desired temperature of the panel (~37°C) so another source of power has to be found.

The question of multiple sources recorded at the same time has been dealt using different Filter Amplifiers and performing multiple registrations from a PC. This approach, although has proved to be capable of performing simultaneous recordings without compromising PC performance in terms of speed, could generate some issues that compromise the signal quality. One of them is the use of multiple Filter Amplifiers, which represents unavoidably a hardware-related variability factor described in results. Working with parallel and long-time acquisitions, another critical aspect is the big amount of data produced, increasing the computational resources needed for acquisition and analysis.

A possible solution that can reduce the hardware variability factor related to multiple Filter Amplifiers and reduce the amount of data generated, is represented by the implementation of a MUX (Multiplexer) customized system put in the electronic chain just before one single Filter Amplifier. Besides, with a fixed time interval the multiplexer could switch among different pre-amplification boards, allowing to reduce the space required for multiple acquisitions. This step requires the development of a sampling system that avoids loss in terms of significant features and would represent an acceptable trade-off between temporal resolution and data collection optimization.

Dealing with pluripotent stem cells, in the last decades many approaches have been suggested to promote and improve their management and programmed differentiation. About that, another possible use of the bench-top system has been suggested in [54], where they prove that electro-magnetic fields (EMF) exposure induces epigenetic changes that promote efficient somatic cell reprogramming to pluripotency. The work has been conducted with the use of electro magnetized gold nanoparticles (AuNPs) that facilitate an efficient direct lineage reprogramming to induced dopamine neurons in-vitro and in-vivo, in the presence of specific EMF conditions. This technique could be used coupled with MEA technology, using as EMF vector the electrodes of MEA chips directly in contact with cells. Further, MEA recording could benefit from being coupled with optical methods for recording [55] or stimulation as well as with microfluidic devices[56], [57].

To conclude, MEAs are a widely used technology in several studies and constitute an establishment of experimental tools promoting a better understanding of the way the Nervous System processes information in physiological and pathological conditions. Through a series of validation tests and multiple biological trials, we demonstrate the capability of the personalized bench-top system to record long-term bioelectrical activity using simultaneously multiple acquisition boards, in a controlled environment that preserves cells survival and vitality. Besides, this work highlights some

fundamental aspects that must be taken into account during both system development and data analysis, in order to get the most reliable representation of cellular electrophysiological features. These perspectives could in principle assure very important advances in neurophysiological and neuropharmacological studies, but technology is still based on research prototypes of single labs. The utmost goal is to integrate all these new technological features in a new generation of devices capable to interrogate experimentally *in vitro* cultures so to study information processing in cultured networks.

Bibliography

[1] M. E. Spira and A. Hai, "Multi-electrode array technologies for neuroscience and cardiology," *Nat. Nanotechnol.*, vol. 8, no. 2, pp. 83–94, 2013.

[2] R. W. Joyner, "Temperature effects on neuronal elements.," *Fed. Proc.*, vol. 40, no. 14, pp. 2814–8, Dec. 1981.

[3] I. D. Forsythe and R. T. Coates, "A chamber for electrophysiological recording from cultured neurones allowing perfusion and temperature control.," *J. Neurosci. Methods*, vol. 25, no. 1, pp. 19–27, Aug. 1988.

[4] S. M. Potter and T. B. DeMarse, "A new approach to neural cell culture for long-term studies.," *J. Neurosci. Methods*, vol. 110, no. 1–2, pp. 17–24, Sep. 2001.

[5] A. W. Blau and C. M. Ziegler, "Prototype of a novel autonomous perfusion chamber for long-term culturing and in situ investigation of various cell types.," *J. Biochem. Biophys. Methods*, vol. 50, no. 1, pp. 15–27, Dec. 2001.

[6] K. Albus, U. Heinemann, and R. Kovács, "Network activity in hippocampal slice cultures revealed by long-term in vitro recordings," *J. Neurosci. Methods*, vol. 217, no. 1–2, pp. 1–8, Jul. 2013.

[7] C. M. Hales, J. D. Rolston, and S. M. Potter, "How to Culture, Record and Stimulate Neuronal Networks on Micro-electrode Arrays (MEAs)," *J. Vis. Exp.*, no. 39, May 2010.

[8] D. Wagenaar, T. B. DeMarse, and S. M. Potter, "MeaBench: A toolset for multi-electrode data acquisition and on-line analysis," in *Conference Proceedings. 2nd International IEEE EMBS Conference on Neural Engineering, 2005.*, pp. 518–521.

[9] X. Li, W. Zhou, S. Zeng, M. Liu, and Q. Luo, "Long-term recording on multi-electrode array reveals degraded inhibitory connection in neuronal network development," *Biosens. Bioelectron.*, vol. 22, no. 7, pp. 1538–1543, Feb. 2007.

[10] D. J. Bakkum, M. Radivojevic, U. Frey, F. Franke, A. Hierlemann, and H. Takahashi, "Parameters for burst detection.," *Front. Comput. Neurosci.*, vol. 7, p. 193, 2013.

[11] G. Regalia, E. Biffi, G. Ferrigno, and A. Pedrocchi, "A low-noise, modular, and versatile analog front-end intended for processing in vitro neuronal signals detected by microelectrode arrays," *Comput. Intell. Neurosci.*, vol. 2015, 2015.

[12] J. Kreutzer, L. Ylä-Outinen, A. J. Mäki, M. Ristola, S. Narkilahti, and P. Kallio, "Cell culture chamber with gas supply for prolonged recording of human neuronal cells on microelectrode array," *J. Neurosci. Methods*, vol. 280, pp. 27–35, 2017.

[13] E. Biffi *et al.*, "A novel environmental chamber for neuronal network multisite recordings,"

Biotechnol. Bioeng., vol. 109, no. 10, pp. 2553–2566, 2012.

[14] G. Regalia, S. Coelli, E. Biffi, G. Ferrigno, and A. Pedrocchi, "A Framework for the Comparative Assessment of Neuronal Spike Sorting Algorithms towards More Accurate Off-Line and On-Line Microelectrode Arrays Data Analysis," *Comput. Intell. Neurosci.*, vol. 2016, pp. 1–19, 2016.

[15] G. Regalia, E. Biffi, S. Achilli, G. Ferrigno, A. Menegon, and A. Pedrocchi, "Development of a bench-top device for parallel climate-controlled recordings of neuronal cultures activity with microelectrode arrays," *Biotechnol. Bioeng.*, vol. 113, no. 2, pp. 403–413, 2016.

[16] D. Wagenaar, J. Pine, and S. Potter, "An extremely rich repertoire of bursting patterns during the development of cortical cultures," *BMC Neurosci.*, vol. 7, no. 1, p. 11, Feb. 2006.

[17] E. Biffi, G. Regalia, A. Menegon, G. Ferrigno, and A. Pedrocchi, "The Influence of Neuronal Density and Maturation on Network Activity of Hippocampal Cell Cultures: A Methodological Study," *PLoS One*, vol. 8, no. 12, p. e83899, Dec. 2013.

[18] A. Gramowski *et al.*, "Functional screening of traditional antidepressants with primary cortical neuronal networks grown on multielectrode neurochips," *Eur. J. Neurosci.*, vol. 24, no. 2, pp. 455–465, Jul. 2006.

[19] A. Novellino *et al.*, "Development of Micro-Electrode Array Based Tests for Neurotoxicity: Assessment of Interlaboratory Reproducibility with Neuroactive Chemicals," *Front. Neuroeng.*, vol. 4, p. 4, 2011.

[20] S. R. Sinha and P. Saggau, "Optical Recording from Populations of Neurons in Brain Slices," *Mod. Tech. Neurosci. Res.*, pp. 459–486, 1999.

[21] V. M. deZengotita, R. Kimura, and W. M. Miller, "Effects of CO2 and osmolality on hybridoma cells: growth, metabolism and monoclonal antibody production.," *Cytotechnology*, vol. 28, no. 1/3, pp. 213–227, Nov. 1998.

[22] Multi Channel Systems MCS GmbH, "Extracellular recording with microelectrode arrays for all applications Overview MEA-System." pp. 1–16, 2015.

[23] Multichannel Systems, "Multichannel Systems User Manual." 2014.

[24] Multi Channel Systems GmbH, "MC_Rack Manual." 2012.

[25] R. de Ceglia *et al.*, "Down-sizing of neuronal network activity and density of presynaptic terminals by pathological acidosis are efficiently prevented by Diminazene Aceturate," *Brain. Behav. Immun.*, vol. 45, pp. 263–276, 2015.

[26] M. G. White *et al.*, "Cellular mechanisms of neuronal damage from hyperthermia," in *Progress in brain research*, vol. 162, 2007, pp. 347–371.

[27] S. M. Thompson, L. M. Masukawa, and D. A. Prince, "Temperature dependence of intrinsic membrane properties and synaptic potentials in hippocampal CA1 neurons in vitro.," *J. Neurosci.*, vol. 5, no. 3, pp. 817–24, Mar. 1985.

[28] E. de la Peña *et al.*, "The Influence of Cold Temperature on Cellular Excitability of Hippocampal Networks," *PLoS One*, vol. 7, no. 12, p. e52475, Dec. 2012.

[29] G. K. Motamedi *et al.*, "Termination of epileptiform activity by cooling in rat hippocampal slice epilepsy models," *Epilepsy Res.*, vol. 70, no. 2–3, pp. 200–210, Aug. 2006.

[30] J. A. Kim and B. W. Connors, "High temperatures alter physiological properties of pyramidal

cells and inhibitory interneurons in hippocampus," *Front. Cell. Neurosci.*, vol. 6, p. 27, 2012.

[31] S. Fujii, H. Sasaki, K. Ito, K. Kaneko, and H. Kato, "Temperature dependence of synaptic responses in guinea pig hippocampal CA1 neurons in vitro.," *Cell. Mol. Neurobiol.*, vol. 22, no. 4, pp. 379–91, Aug. 2002.

[32] M. S. Kallos, L. A. Behie, and A. L. Vescovi, "Extended serial passaging of mammalian neural stem cells in suspension bioreactors.," *Biotechnol. Bioeng.*, vol. 65, no. 5, pp. 589–99, Dec. 1999.

[33] D. Saalfrank *et al.*, "Incubator-independent cell-culture perfusion platform for continuous long-term microelectrode array electrophysiology and time-lapse imaging," *R. Soc. Open Sci.*, vol. 2, no. 6, p. 150031, Jun. 2015.

[34] A. Blau, T. Neumann, C. Ziegler, and F. Benfenati, "Replica-moulded polydimethylsiloxane culture vessel lids attenuate osmotic drift in long-term cell cultures.," *J. Biosci.*, vol. 34, no. 1, pp. 59–69, Mar. 2009.

[35] A. Minerbi, R. Kahana, L. Goldfeld, M. Kaufman, S. Marom, and N. E. Ziv, "Long-Term Relationships between Synaptic Tenacity, Synaptic Remodeling, and Network Activity," *PLoS Biol.*, vol. 7, no. 6, p. e1000136, Jun. 2009.

[36] M. Chiappalone, M. Bove, A. Vato, M. Tedesco, and S. Martinoia, "Dissociated cortical networks show spontaneously correlated activity patterns during in vitro development," *Brain Res.*, vol. 1093, no. 1, pp. 41–53, Jun. 2006.

[37] M. Frega *et al.*, "Cortical cultures coupled to Micro-Electrode Arrays: A novel approach to perform in vitro excitotoxicity testing," *Neurotoxicol. Teratol.*, vol. 34, no. 1, pp. 116–127, Jan. 2012.

[38] Y. Mukai, T. Shiina, and Y. Jimbo, "Continuous monitoring of developmental activity changes in cultured cortical networks," *Electr. Eng. Japan*, vol. 145, no. 4, pp. 28–37, Dec. 2003.

[39] S. Petronis, M. Stangegaard, C. B. V. Christensen, and M. Dufva, "Transparent polymeric cell culture chip with integrated temperature control and uniform media perfusion.," *Biotechniques*, vol. 40, no. 3, pp. 368–76, Mar. 2006.

[40] A. F. M. Johnstone, G. W. Gross, D. G. Weiss, O. H.-U. Schroeder, A. Gramowski, and T. J. Shafer, "Microelectrode arrays: A physiologically based neurotoxicity testing platform for the 21st century☆," *Neurotoxicology*, vol. 31, no. 4, pp. 331–350, Aug. 2010.

[41] M. I. Ham, L. M. Bettencourt, F. D. McDaniel, and G. W. Gross, "Spontaneous coordinated activity in cultured networks: Analysis of multiple ignition sites, primary circuits, and burst phase delay distributions," *J. Comput. Neurosci.*, vol. 24, no. 3, pp. 346–357, 2008.

[42] J. J. Pancrazio *et al.*, "A portable microelectrode array recording system incorporating cultured neuronal networks for neurotoxin detection.," *Biosens. Bioelectron.*, vol. 18, no. 11, pp. 1339–47, Oct. 2003.

[43] "The Promise of Induced Pluripotent Stem Cells (iPSCs) | stemcells.nih.gov." [Online]. Available: https://stemcells.nih.gov/info/Regenerative_Medicine/2006Chapter10.htm. [Accessed: 13-Mar-2018].

[44] "Pluripotent Stem Cells, iPs cells | Learn Science at Scitable." [Online]. Available: https://www.nature.com/scitable/topicpage/turning-somatic-cells-into-pluripotent-stem-cells-14431451. [Accessed: 13-Mar-2018].

[45] I. Chatterjee, F. Li, E. E. Kohler, J. Rehman, A. B. Malik, and K. K. Wary, "Induced Pluripotent Stem (iPS) Cell Culture Methods and Induction of Differentiation into Endothelial Cells.," *Methods Mol. Biol.*, vol. 1357, pp. 311–27, 2016.

[46] B. Goldman, "Embryonic Stem Cells 2.0," *Nat. Reports Stem Cells*, May 2008.

[47] J. Yu *et al.*, "Induced Pluripotent Stem Cell Lines Derived from Human Somatic Cells," *Science (80-.).*, vol. 318, no. 5858, pp. 1917–1920, Dec. 2007.

[48] G. Regalia, "In vitro electrophysiological studies of neuronal networks: a novel device for reliable, prolonged and high throughput microelectrode array experiments superv," 2014.

[49] "USB-ME-System Manual."

[50] C. R. Legendy and M. Salcman, "Bursts and recurrences of bursts in the spike trains of spontaneously active striate cortex neurons," *J. Neurophysiol.*, vol. 53, no. 4, pp. 926–939, Apr. 1985.

[51] D. Eytan and S. Marom, "Dynamics and Effective Topology Underlying Synchronization in Networks of Cortical Neurons," *J. Neurosci.*, vol. 26, no. 33, pp. 8465–8476, Aug. 2006.

[52] E. Chah, V. Hok, A. Della-Chiesa, J. J. H. Miller, S. M. O'Mara, and R. B. Reilly, "Automated spike sorting algorithmbased on Laplacian eigenmaps and *k* -means clustering," *J. Neural Eng.*, vol. 8, no. 1, p. 16006, Feb. 2011.

[53] V. Meneghini *et al.*, "Generation of Human Induced Pluripotent Stem Cell-Derived Bona Fide Neural Stem Cells for Ex Vivo Gene Therapy of Metachromatic Leukodystrophy," *Stem Cells Transl. Med.*, vol. 6, no. 2, pp. 352–368, 2017.

[54] J. Yoo *et al.*, "Electromagnetized gold nanoparticles mediate direct lineage reprogramming into induced dopamine neurons in vivo for Parkinson's disease therapy," *Nat. Nanotechnol.*, vol. 12, no. 10, pp. 1006–1014, 2017.

[55] D. Ghezzi, A. Menegon, A. Pedrocchi, F. Valtorta, and G. Ferrigno, "A Micro-Electrode Array device coupled to a laser-based system for the local stimulation of neurons by optical release of glutamate," *J. Neurosci. Methods*, vol. 175, no. 1, pp. 70–78, Oct. 2008.

[56] E. Biffi *et al.*, "A microfluidic platform for controlled biochemical stimulation of twin neuronal networks," *Biomicrofluidics*, vol. 6, no. 2, p. 24106, Jun. 2012.

[57] E. Biffi, A. Menegon, F. Piraino, A. Pedrocchi, G. B. Fiore, and M. Rasponi, "Validation of long-term primary neuronal cultures and network activity through the integration of reversibly bonded microbioreactors and MEA substrates," *Biotechnol. Bioeng.*, vol. 109, no. 1, pp. 166–175, Jan. 2012.

Appendix

We report a complete set of validations performed for the Signal Generator test (Appendix A) and for PBS-filled chip test (Appendix B). We show screenshots acquired from MC_Rack replay and analysis software, then PSD and waveform analysis performed with MATLAB script. Details and discussions are reported in *Results* paragraph 3.2.

A. Signal Generator test

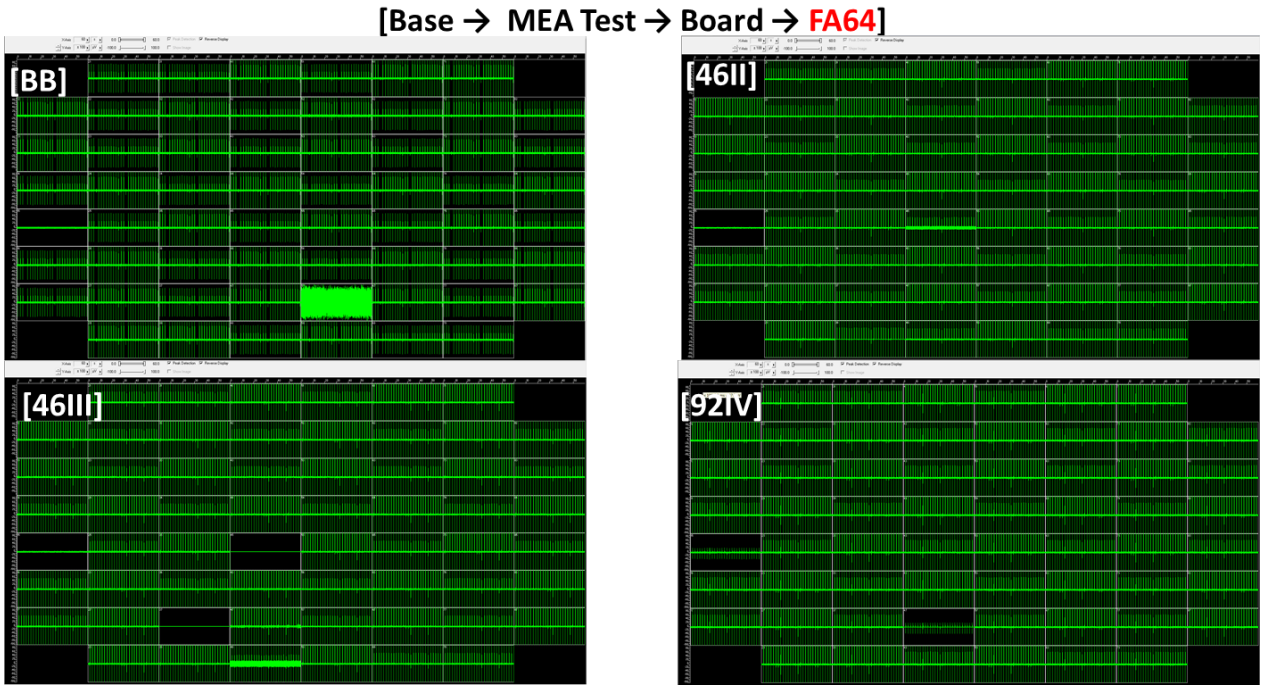

Figure A.1 Signal Generator Test. MC_Rack long term acquisition window

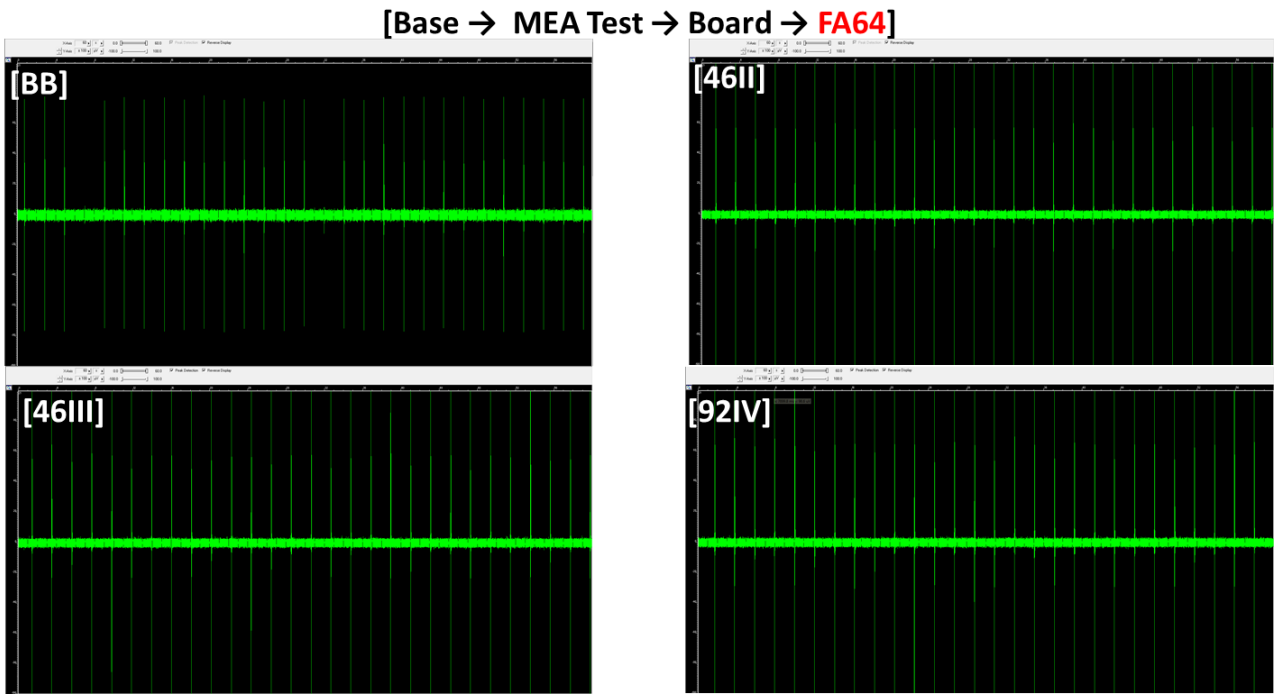

Figure A.2 Signal Generator Test. Single channel window

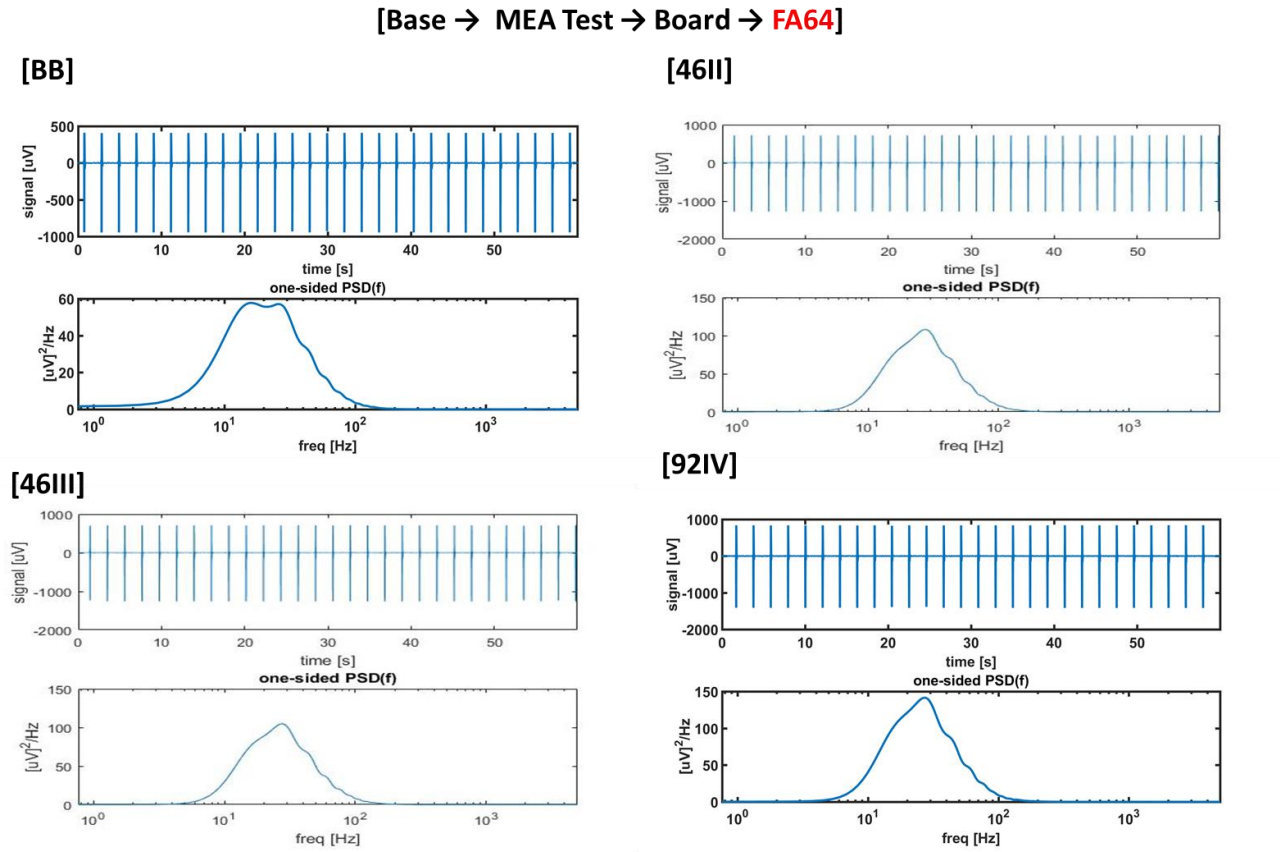

Figure A.3 Signal Generator Test. PSD analysis averaged over 60 channels

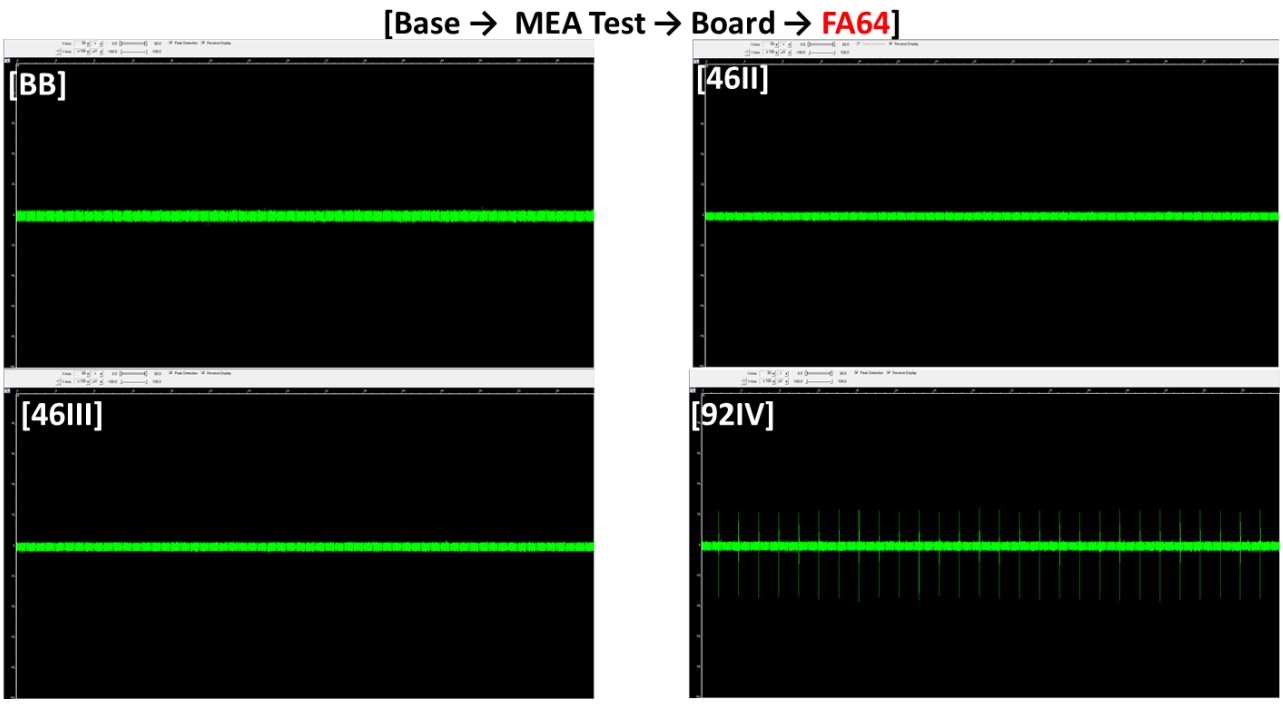

Figure A.4 Signal Generator Test. Reference channel 15 window

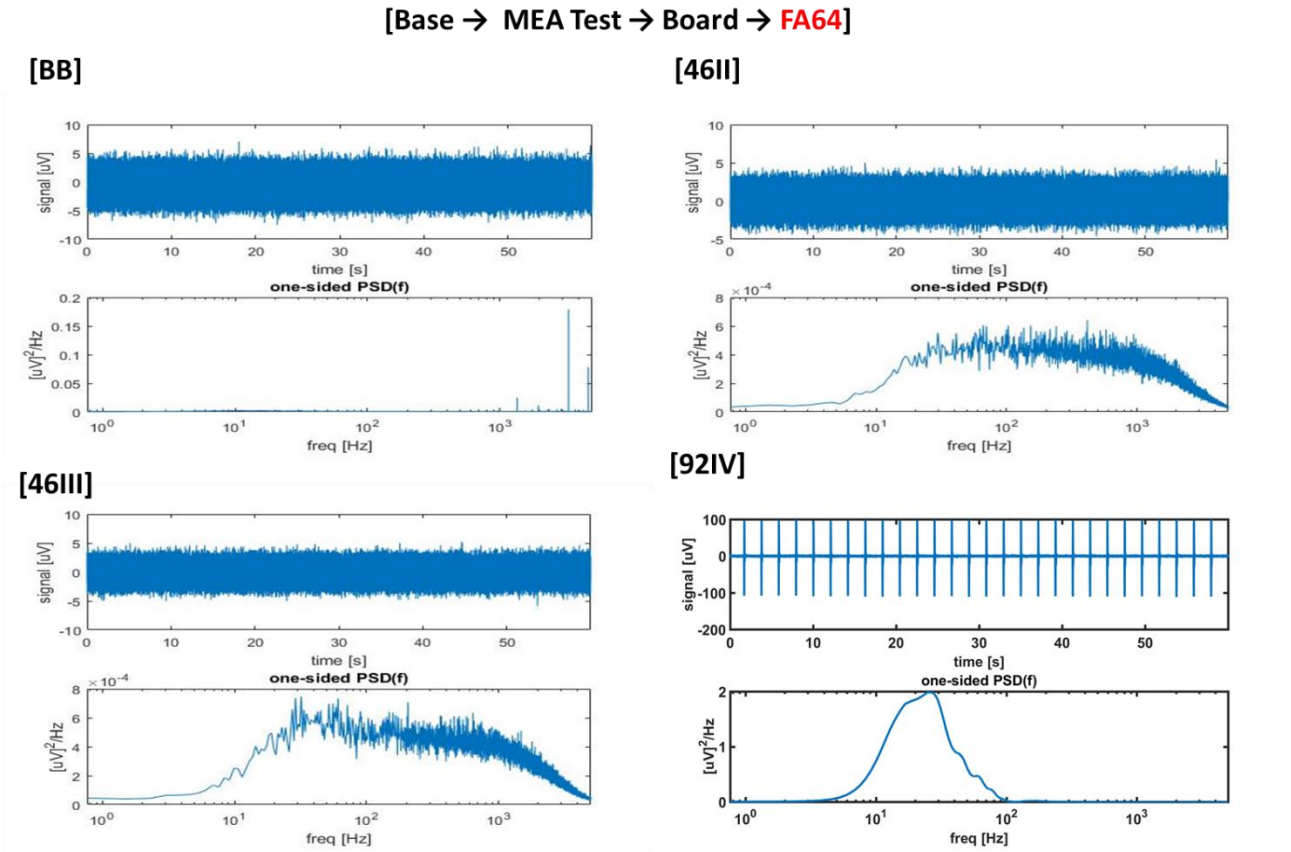

Figure A.5 Signal Generator Test. PSD analysis on reference channel 15

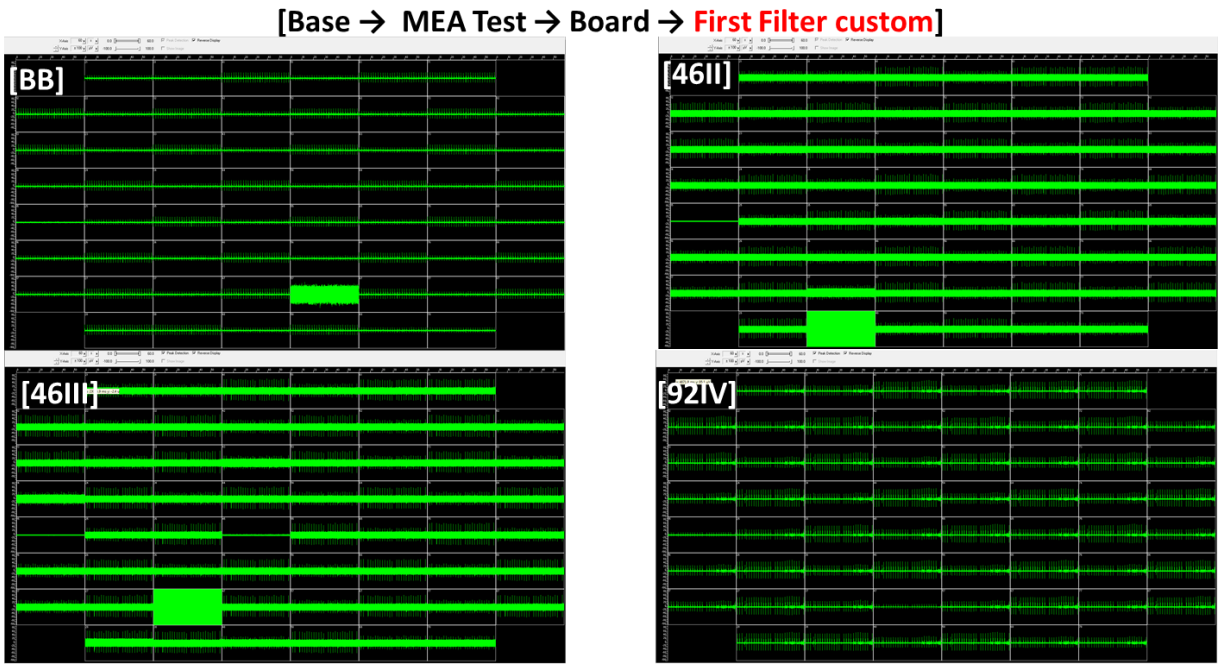

Figure A.6 Signal Generator Test. MC_Rack long term acquisition window

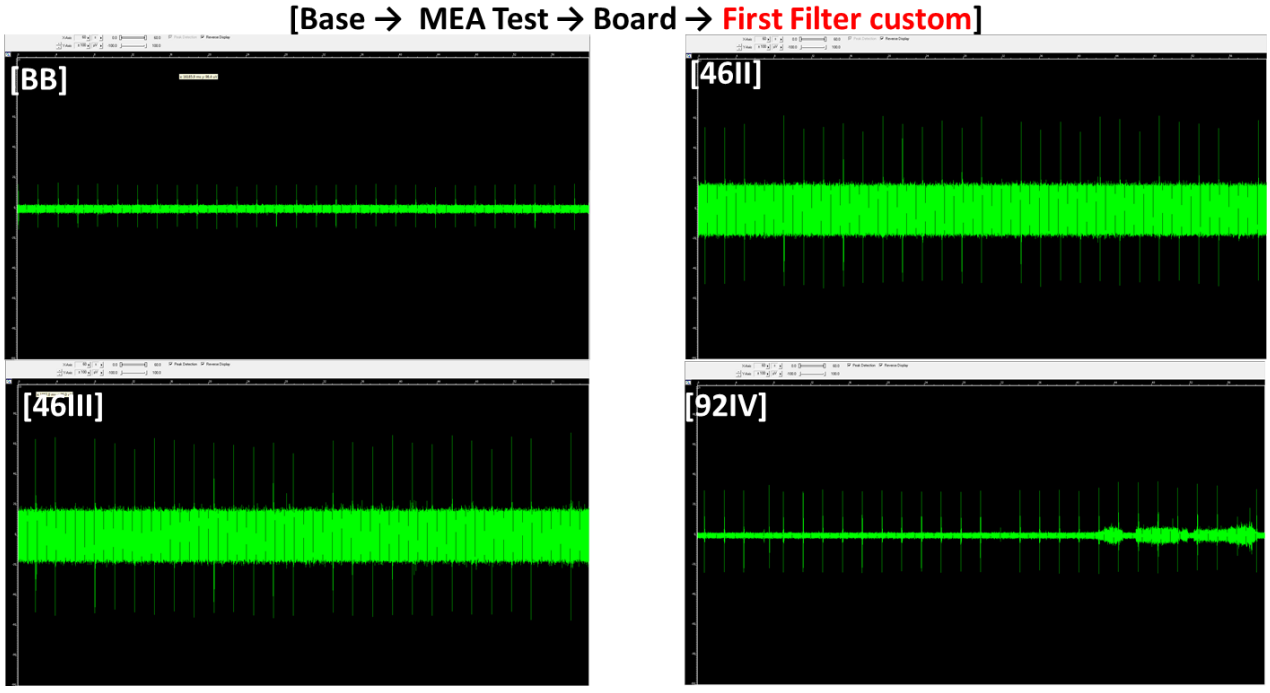

Figure A.7 Signal Generator Test. Single channel window

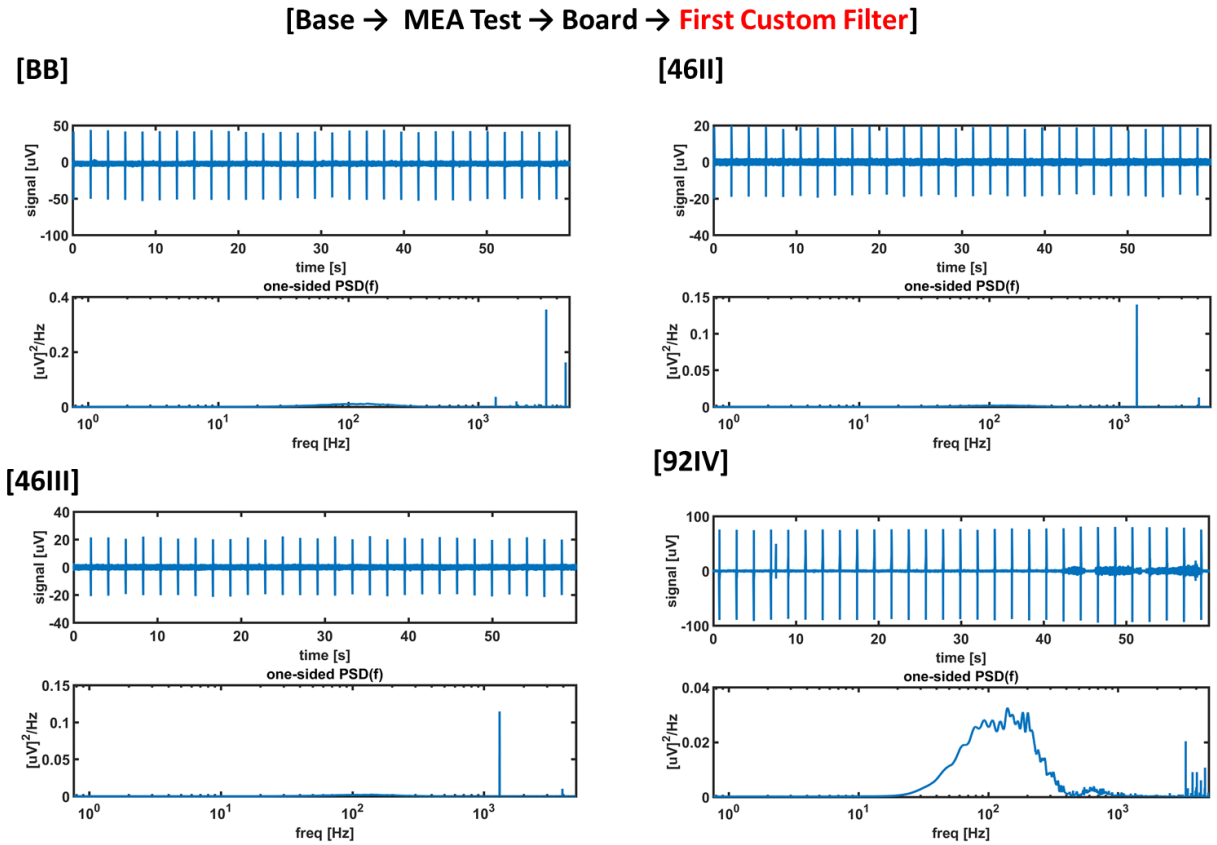

Figure A.8 Signal Generator Test. PSD analysis averaged over 60 channels

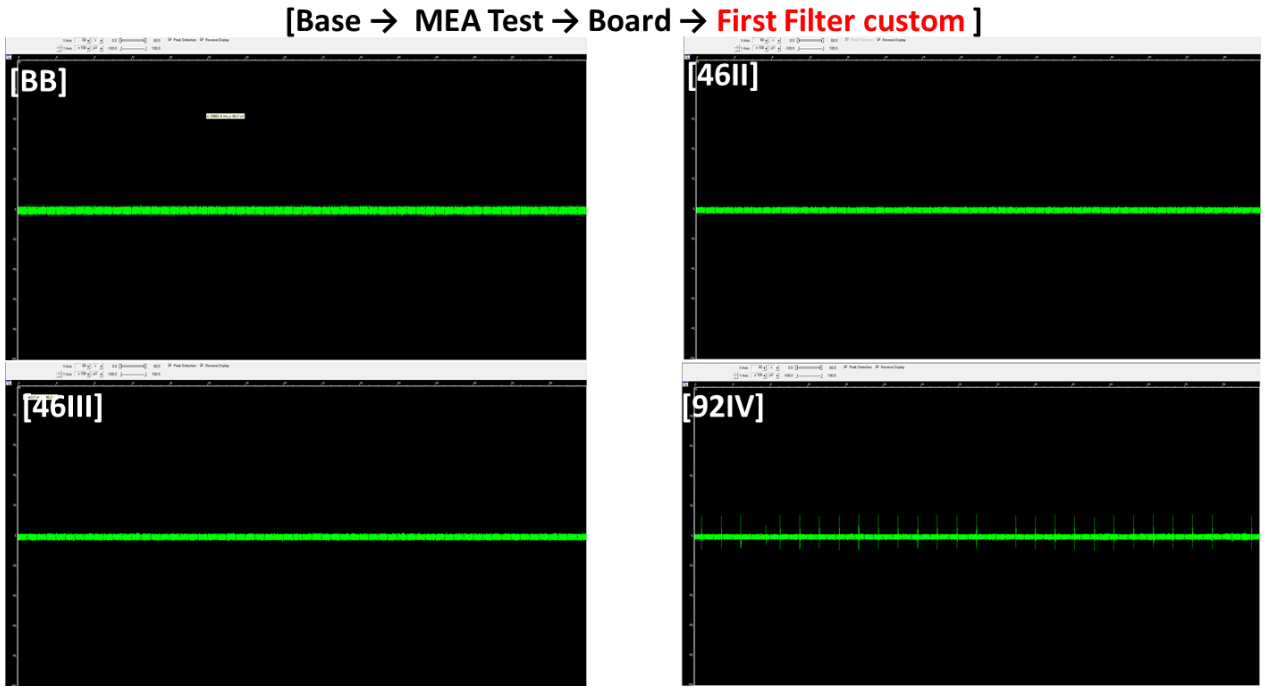

Figure A.9 Signal Generator Test. Reference channel 15 window

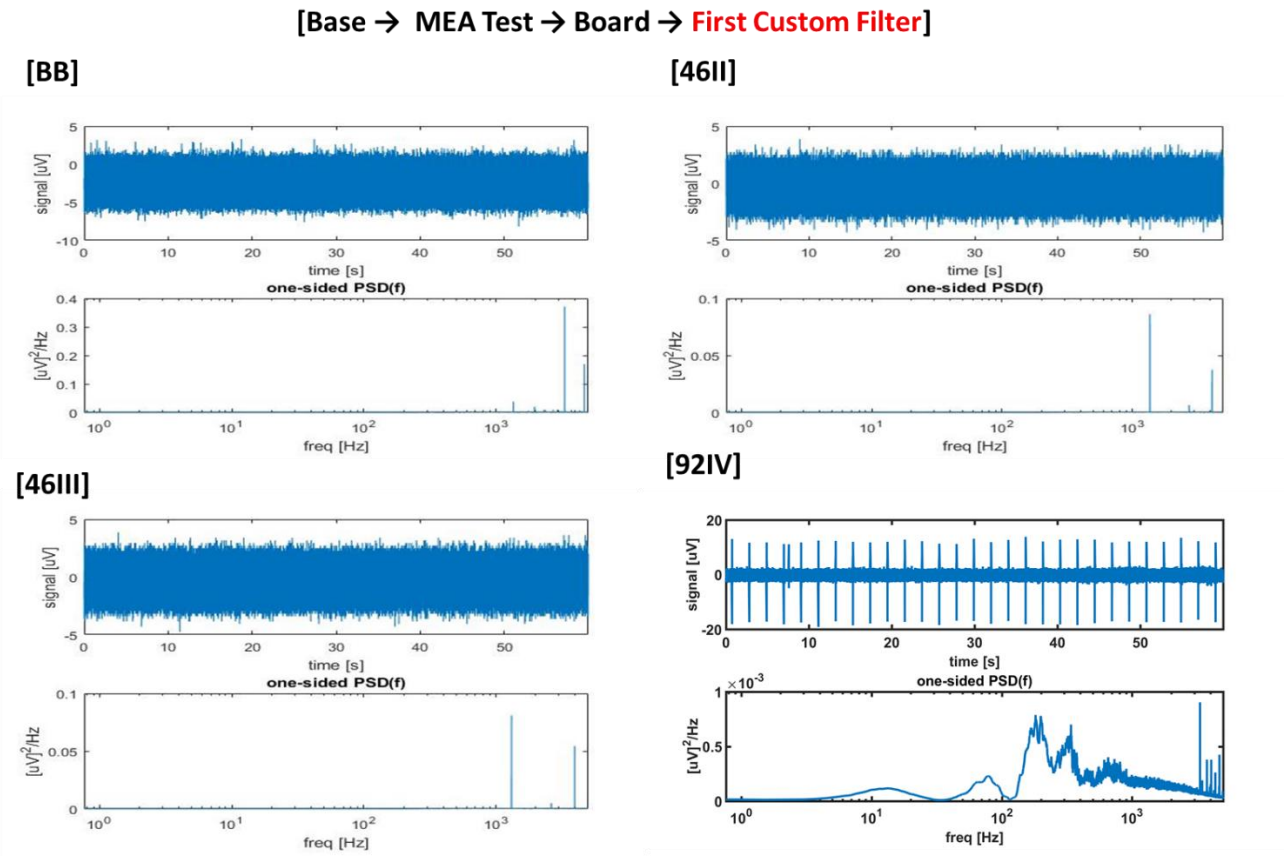

Figure A.10 Signal Generator Test. PSD analysis on reference channel 15

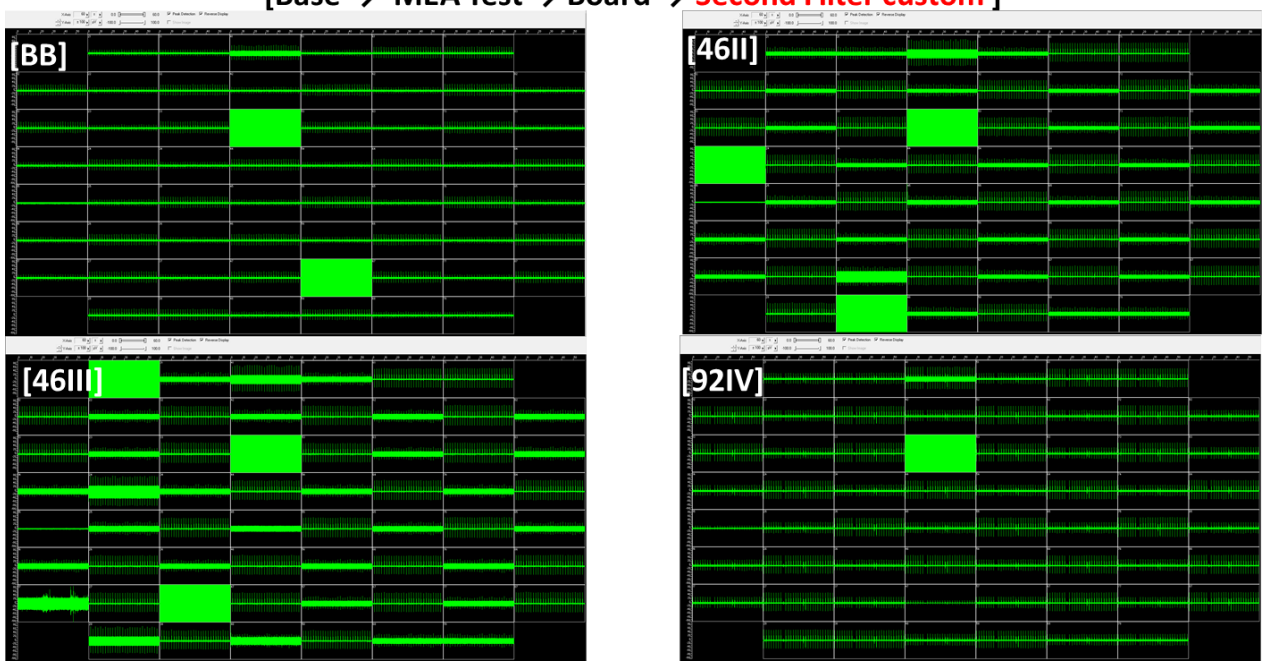

Figure A.11 Signal Generator Test. MC_Rack long term acquisition window

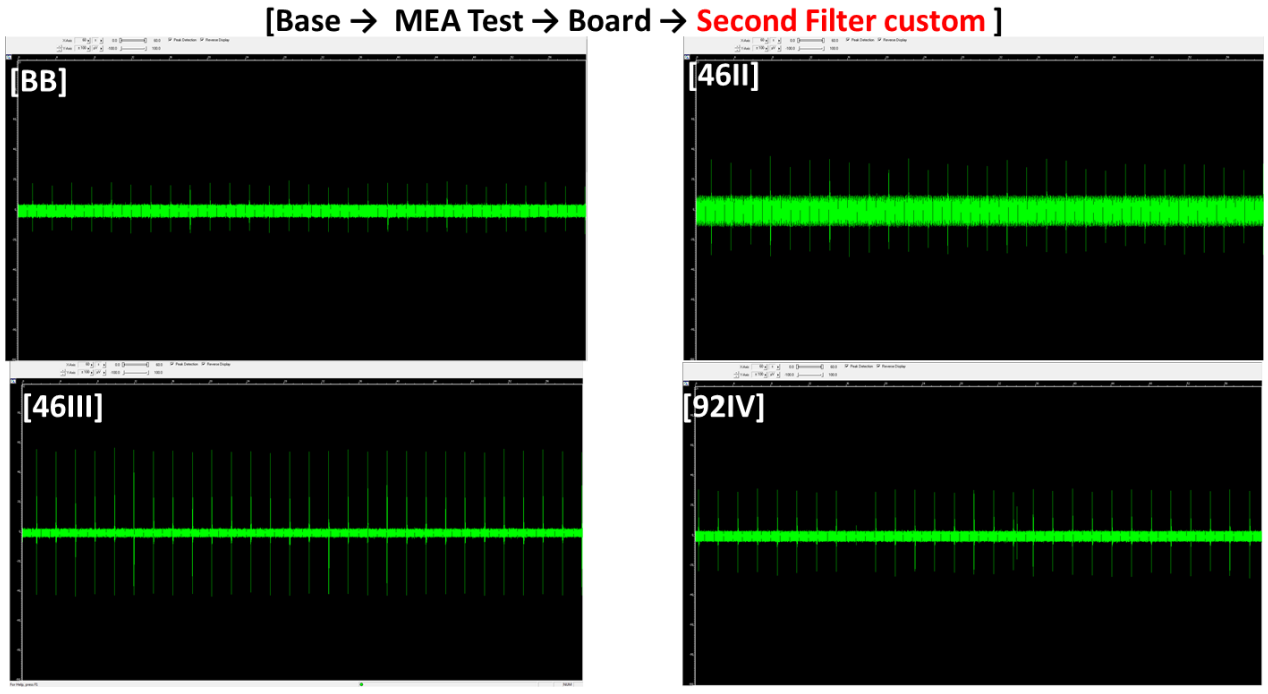

Figure A.12 Signal Generator Test. Single channel window

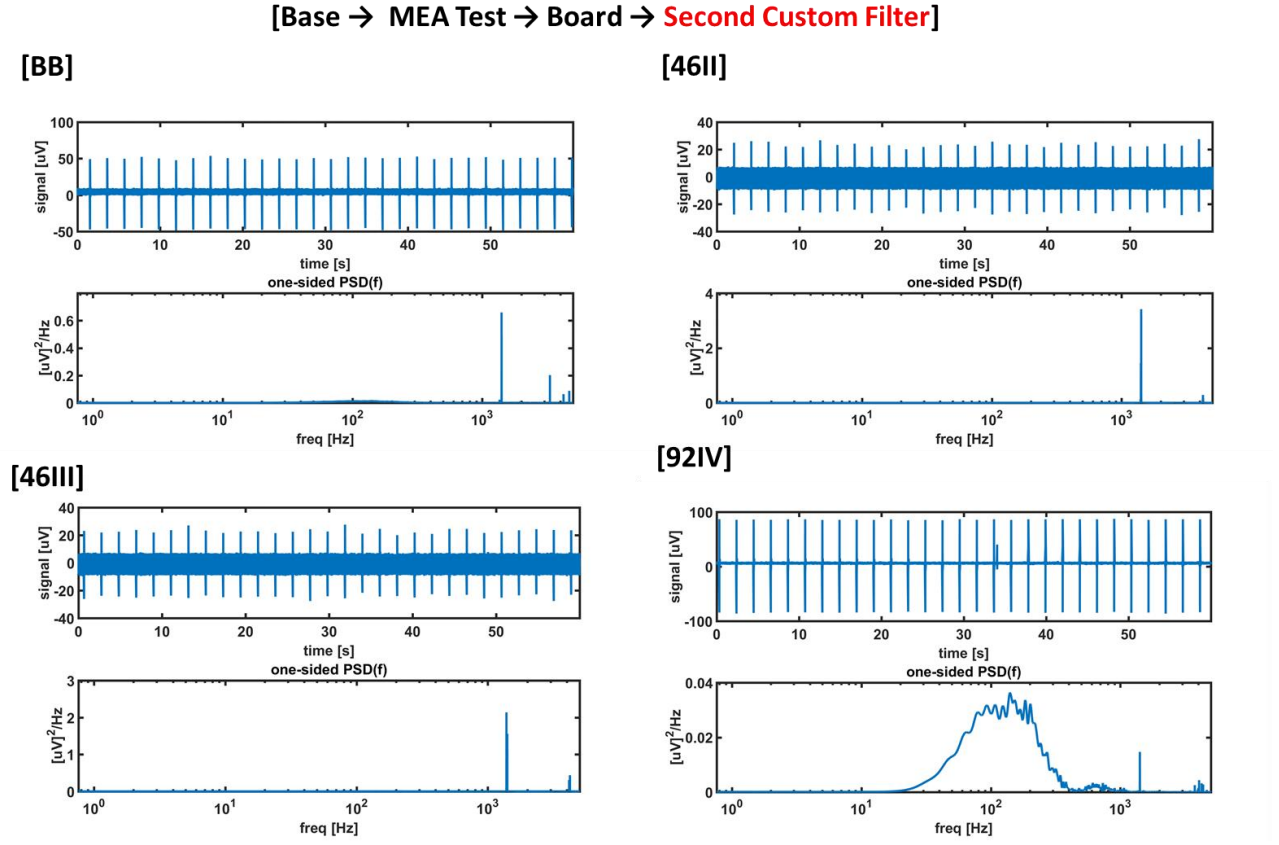

Figure A.13 Signal Generator Test. PSD analysis averaged over 60 channels

[Base → MEA Test → Board → Second Filter custom]

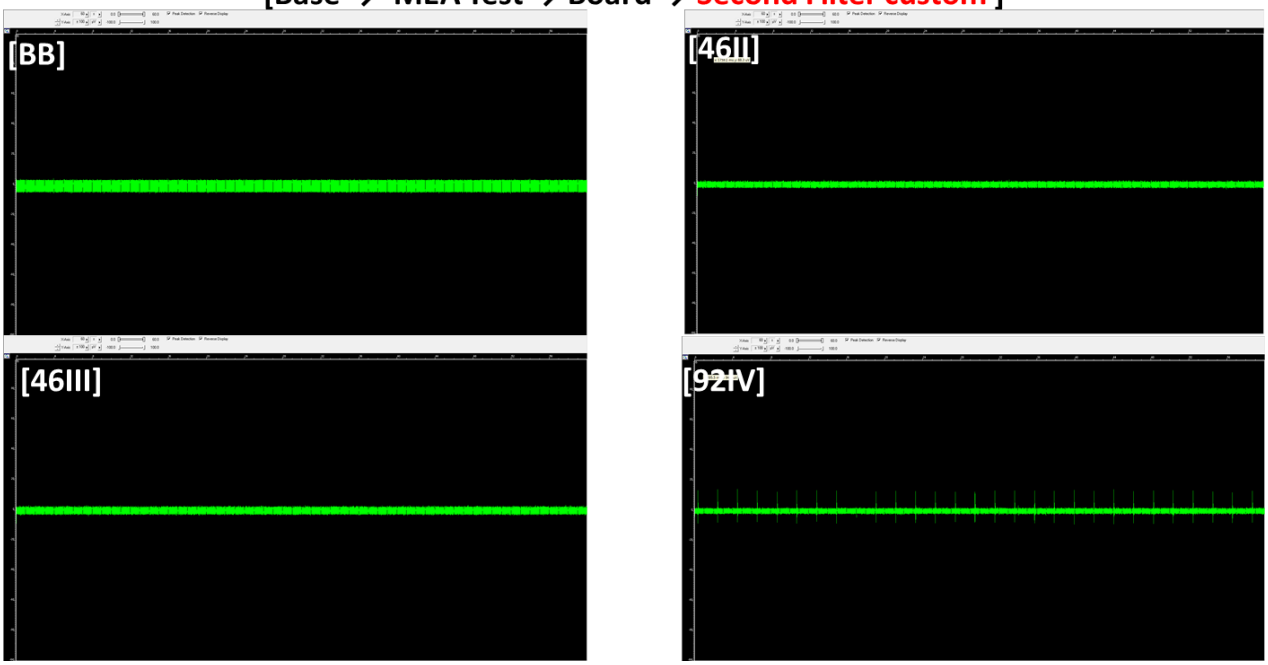

Figure A.14 Signal Generator Test. Reference channel 15 window

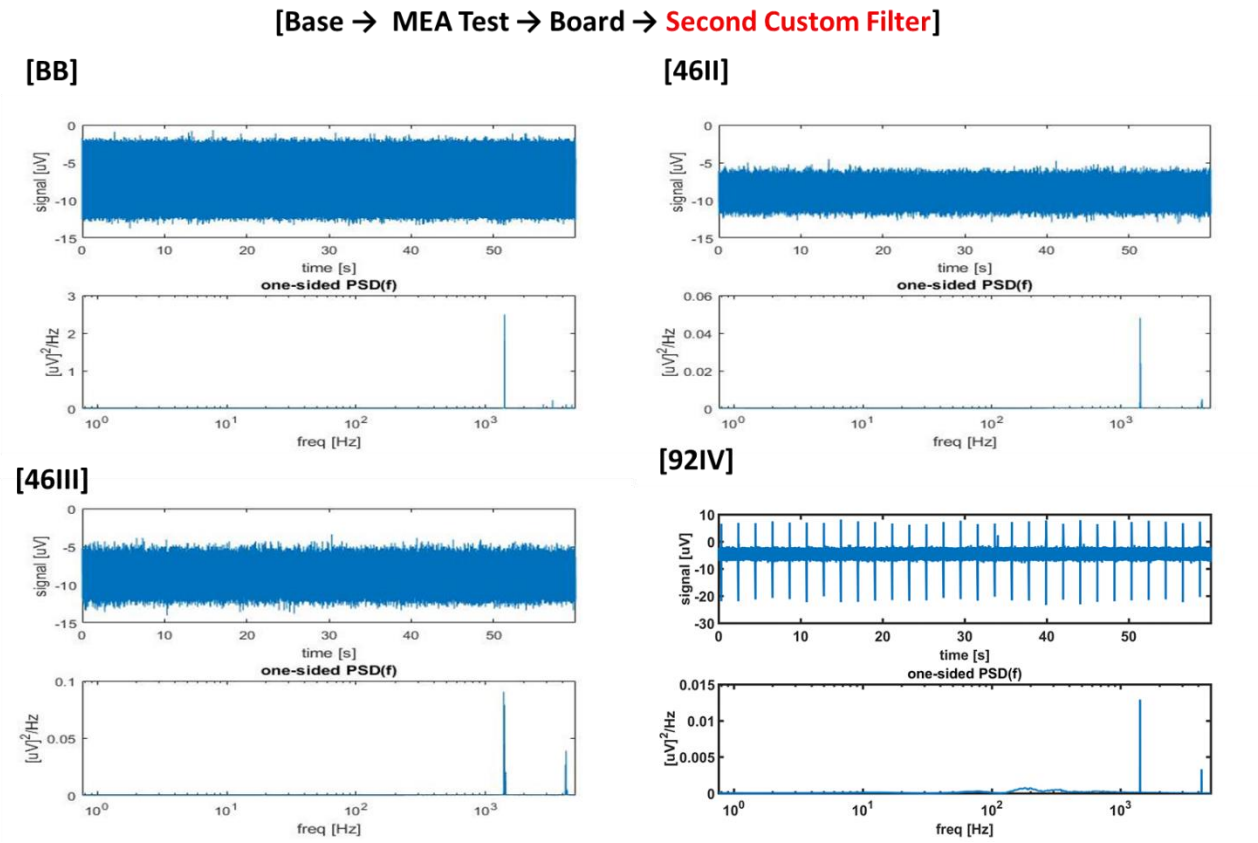

Figure A.15 Signal Generator Test. PSD analysis on reference channel 15

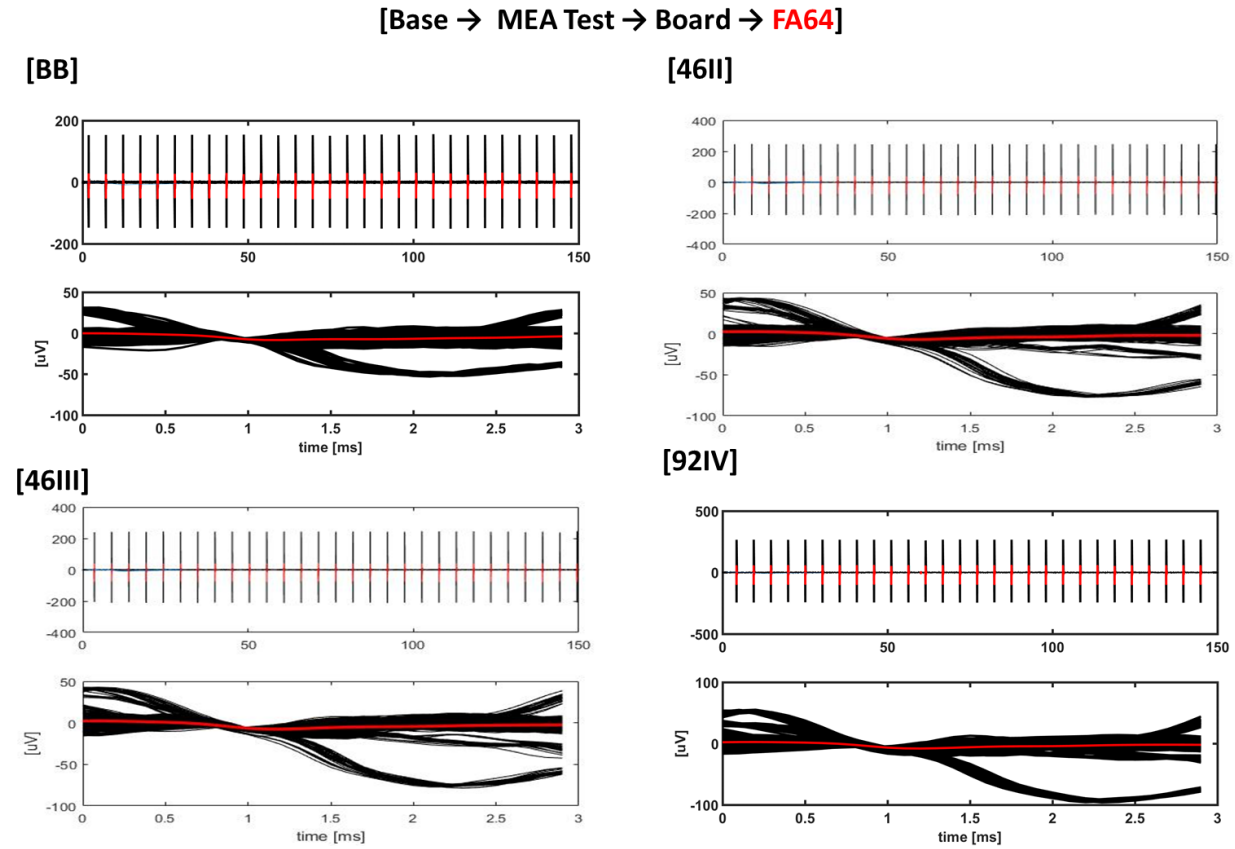

Figure A.16 Signal Generator Test. Comparison between Spike waveforms. The first row in each panel shows averaged signal and spikes detected (in red). The second row shows spike waveforms. Waveforms detected as spikes (EPSP) are highlighted in red over signal representations.

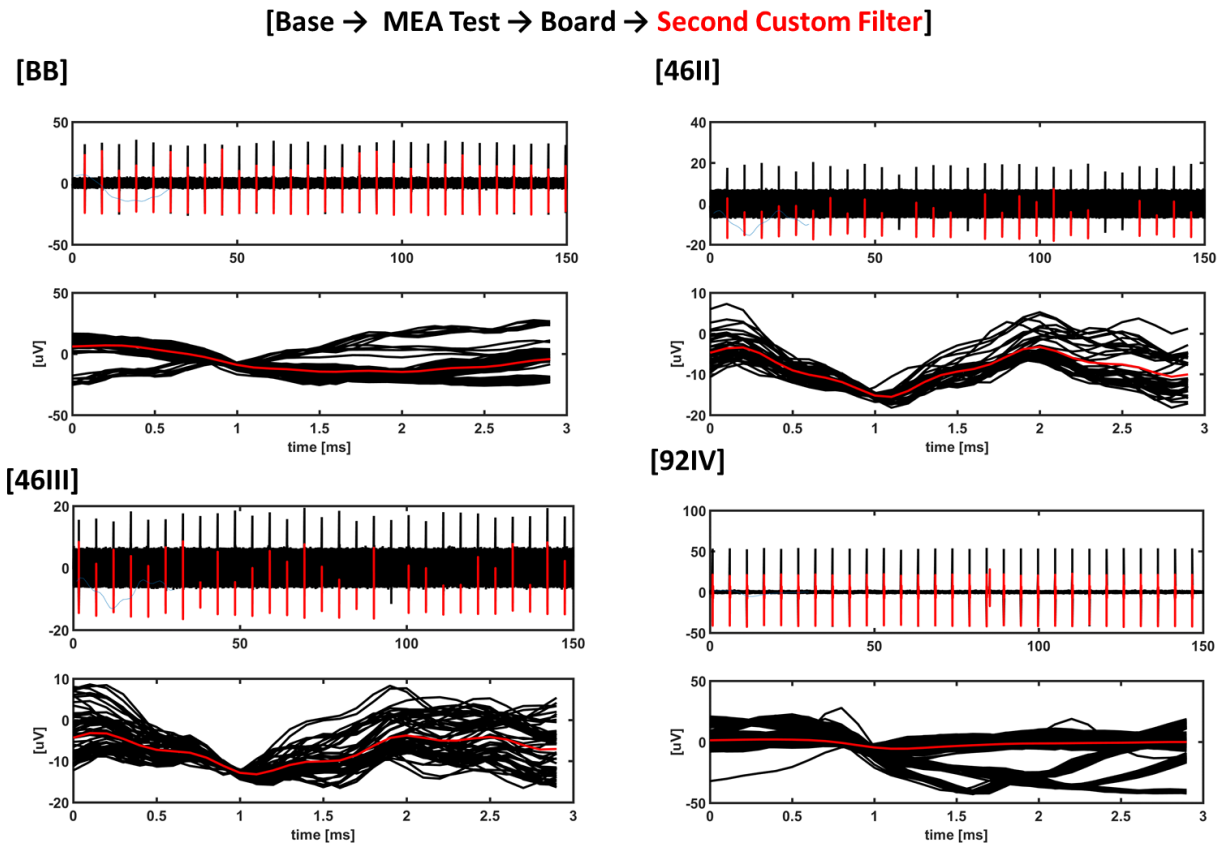

Figure A.17 Signal Generator Test. Comparison between Spike waveforms. The first row in each panel shows averaged signal and spikes detected (in red). The second row shows spike waveforms. Waveforms detected as spikes (EPSP) are highlighted in red over signal representations.

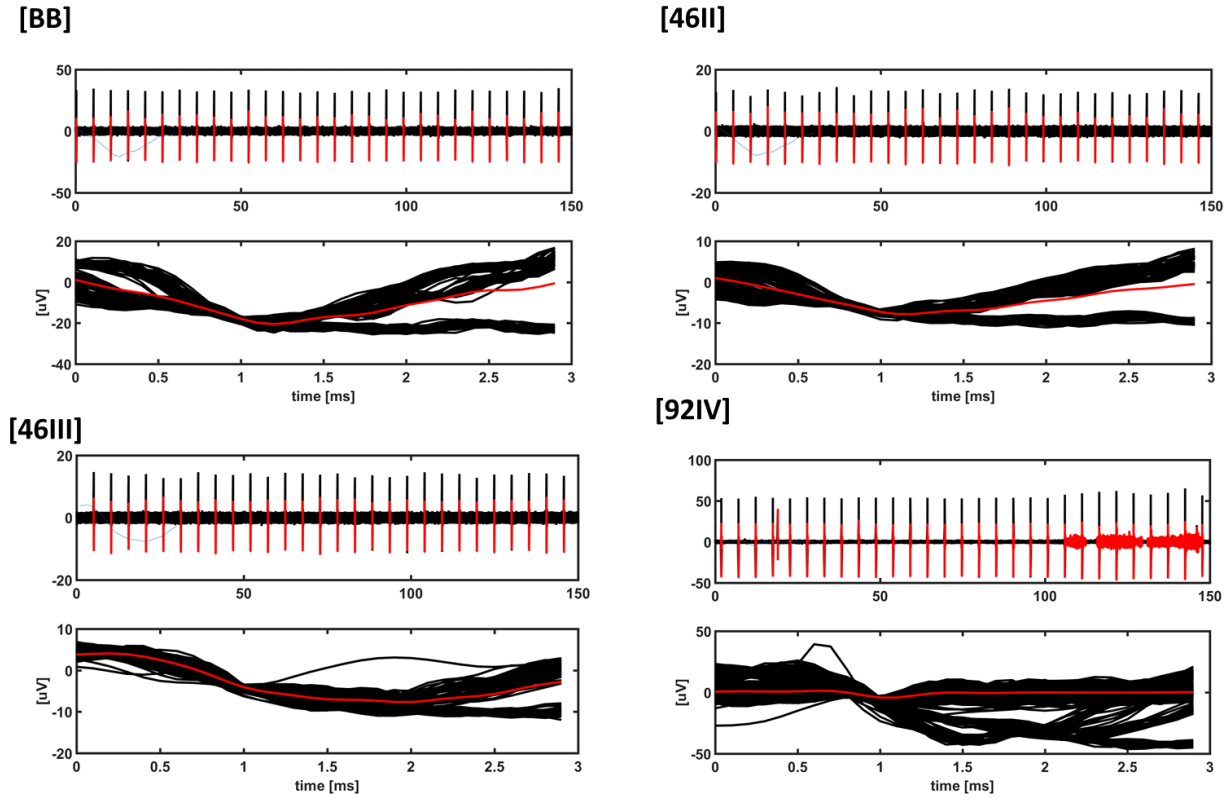

Figure A.18 Signal Generator Test. Comparison between Spike waveforms. The first row in each panel shows averaged signal and spikes detected (in red). The second row shows spike waveforms. Waveforms detected as spikes (EPSP) are highlighted in red over signal representations.

B. PBS-filled chip test

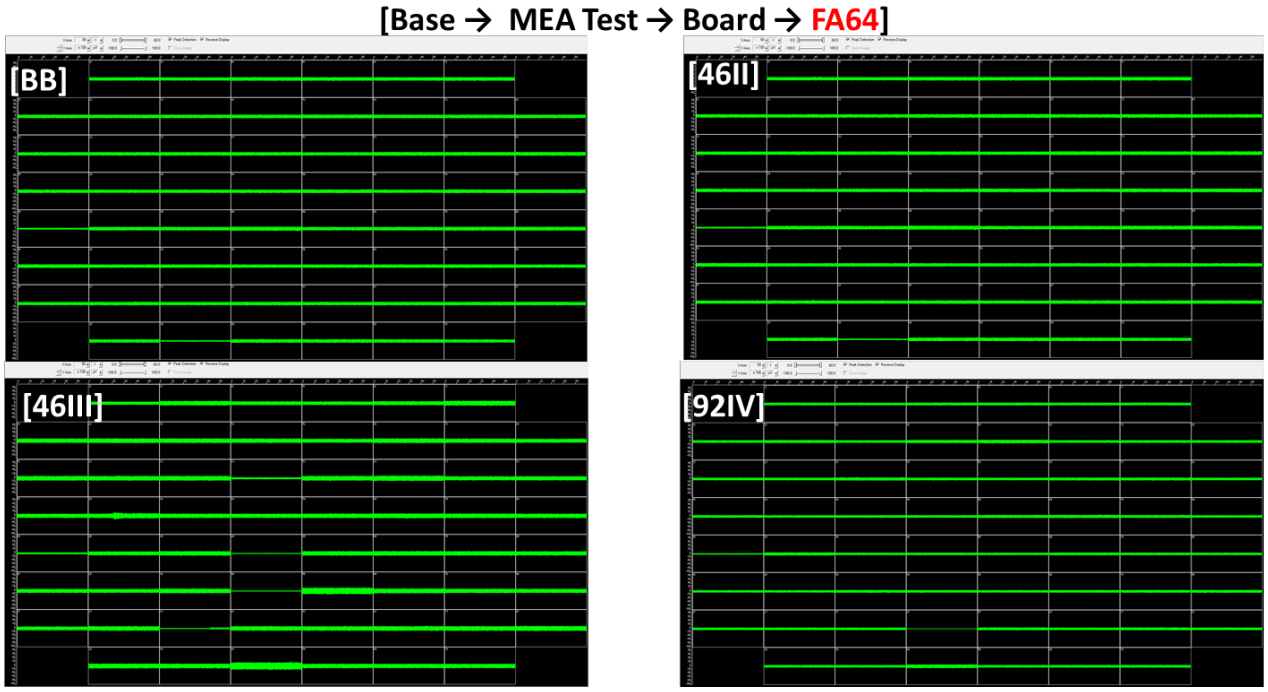

Figure B.1 PBS-filled chip test. MC_Rack long term acquisition window

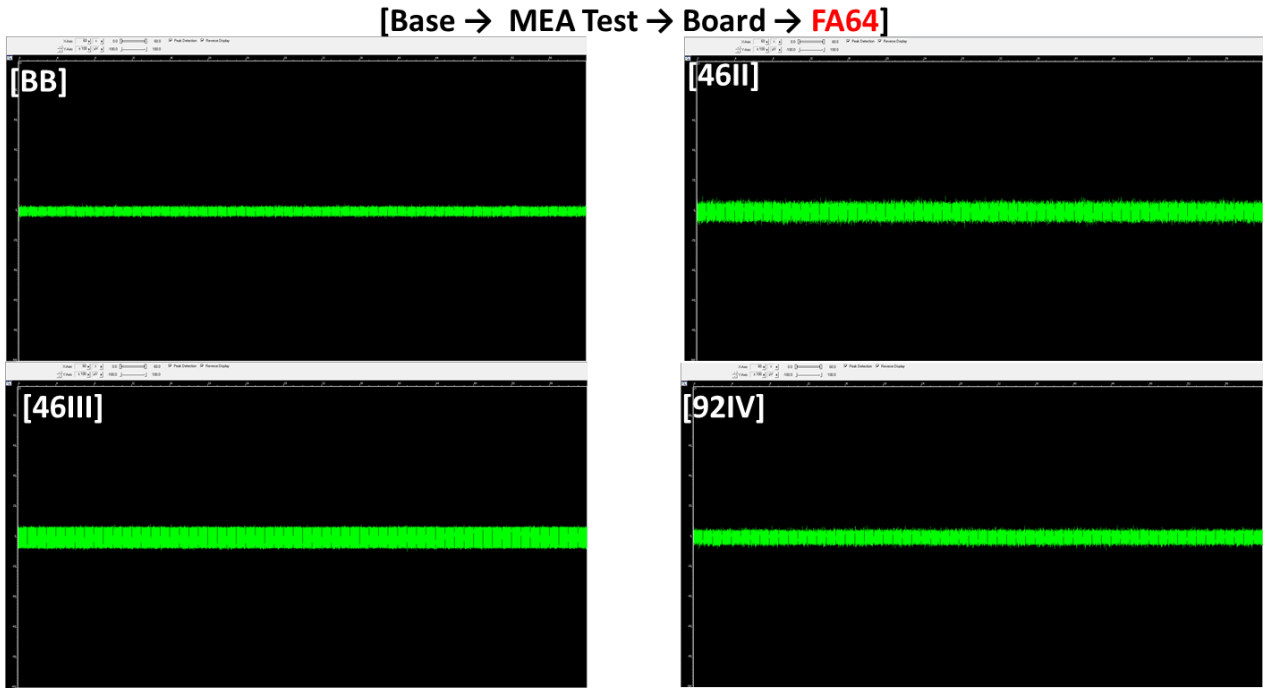

Figure B.2 PBS-filled chip test. Single channel window

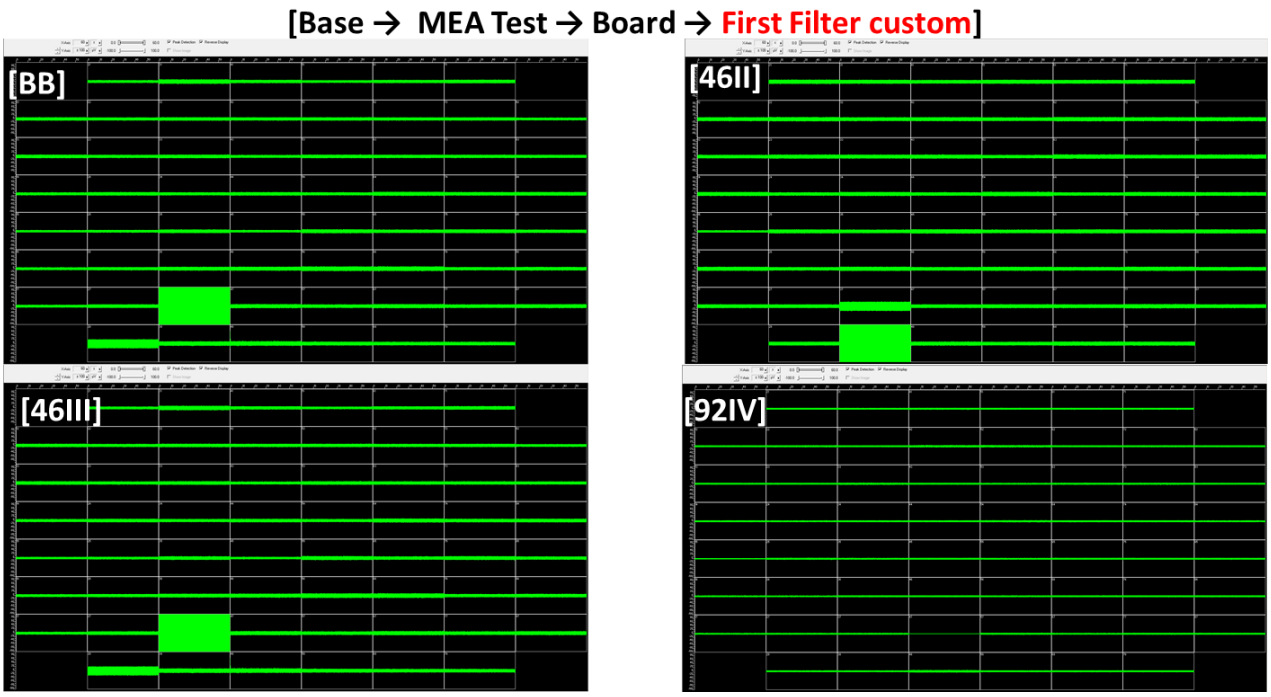

Figure B.3 PBS-filled chip test. MC_Rack long term acquisition window

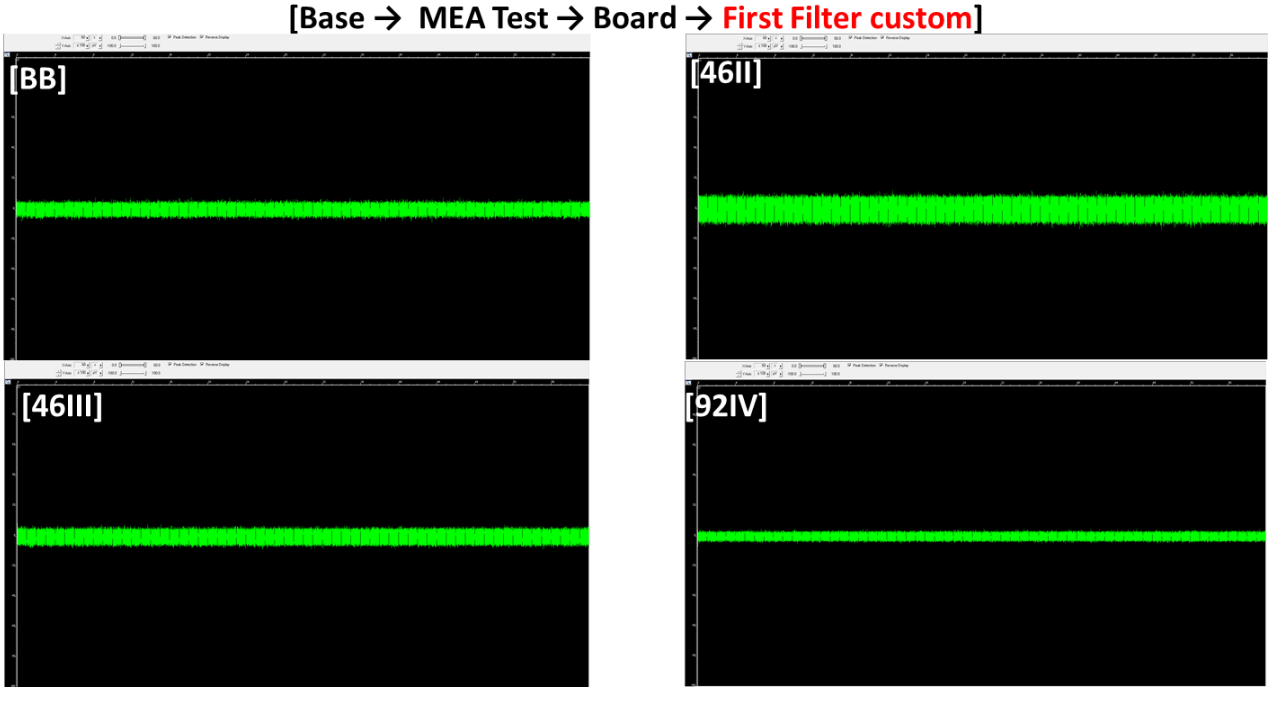

Figure B.4 PBS-filled chip test. Single channel window

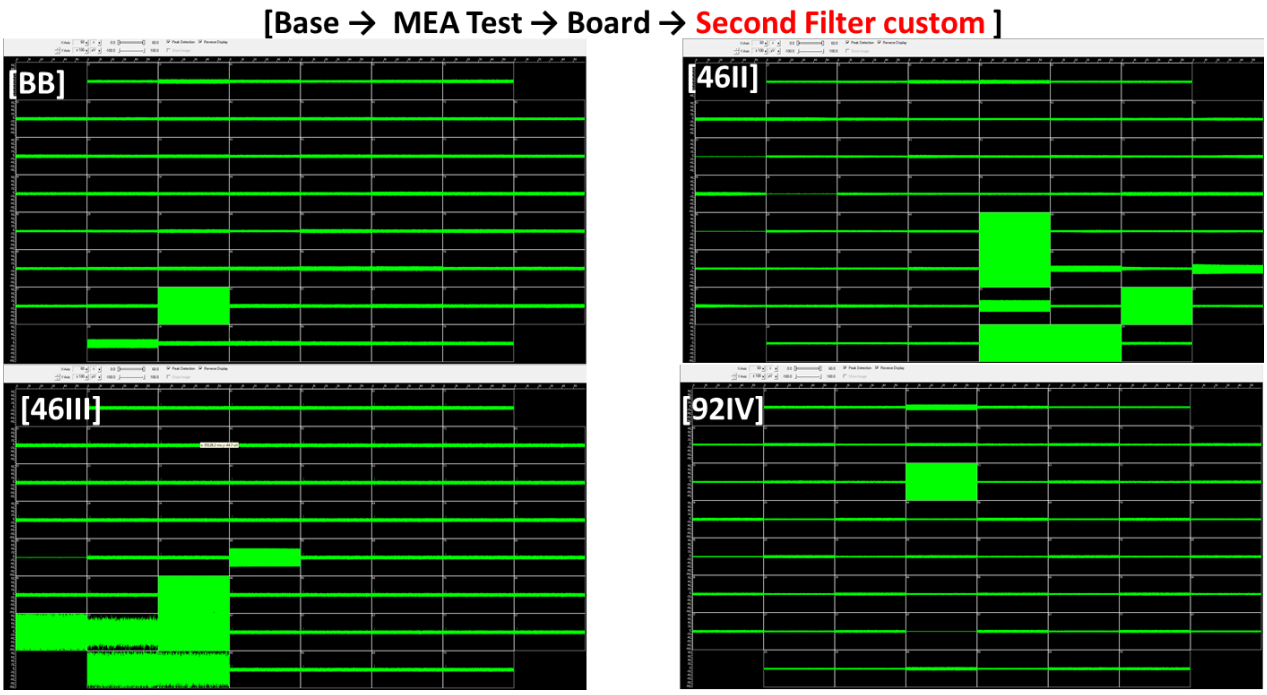

Figure B.5 PBS-filled chip test. MC_Rack long term acquisition window

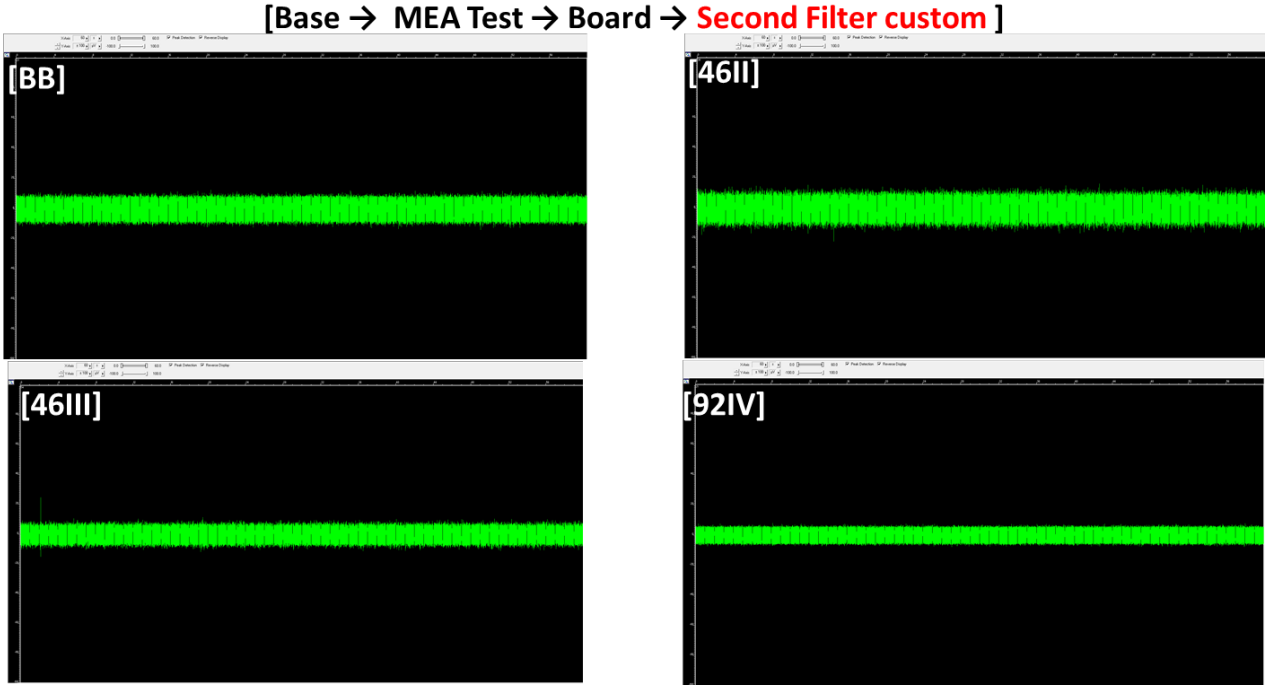

Figure B.6 PBS-filled chip test. Single channel window